1990

Anatomical and Neurochemical Organization of Medullary and Parabrachial Efferents to the Amygdala in the Rat

Andrea M. Zardetto-Smith
Loyola University Chicago

ANATOMICAL AND NEUROCHEMICAL ORGANIZATION OF MEDULLARY AND PARABRACHIAL EFFERENTS TO THE AMYGDALA IN THE RAT

BY

Andrea M. Zardetto-Smith

A Dissertation Submitted to the Faculty of the Graduate School of Loyola University of Chicago in Partial Fulfillment of the Requirements for the Degree of Doctor of Philosophy

January

1990

DEDICATION

To Bob and Kendra,
"you color my world with love"

ACKNOWLEDGEMENTS

I would like to thank my advisor, Dr. Thackery Gray, for the opportunity to work in his laboratory, and for encouraging me to inter-interact more with my colleagues, advice which led me to get involved in the Graduate Student Council and Medical Center administrative committees. I would also like to thank Debra Magnuson, for her technical expertise, her critical advice and comments, her patience in teaching me protocols and methodology, and her ability to straighten out my crooked lines, and most of all, for her friendship. Also, thanks to Joseph Costello and Rashel Piechowski, for their help in the lab, and to Sue Ming Yang, for all her help in preparing slides, photos and posters. I am also indebted to present and past members of our departmental administrative staff, Rosemarie Sarno, Judy Maples, Genevieve Fitzgibbons, and Maryann Trofimuk for their assistance in preparing documents and cutting through university red tape in times of need. I am also grateful for the help and advice of my committeee members: Dr. Castro, Dr. Neafsey, Dr. Wurster, and Dr. Saper. In addition to guiding my dissertation work, they each taught me something different and valuable about the philosophy of neuroscience, and science in general. Also, I would like to thank Dr. Martin Cassell and Dr. Margaret Moga for their help in navigating the cytoarchitecture of the central nucleus and bed nucleus, and for their helpful criticisms in preparing the figures for that particular study.

It would not have been possible to complete the courses and research required for the Ph.D. degree without the support, help, and camaraderie of my fellow graduate students. Terry McGarvey and Lori Kus were invaluble sources of help in typing references and copying

figures. I would also like to thank Dr. Catania, Dr. Karczmar, Dr. Chuldzinski, Dee Miller, Mary Rhey, and Mary Kroeger, for their efforts many times in helping me to cope with several personal difficulties, as well as the difficulties encountered by graduate students at LUMC. I am grateful to many of my professors for their teaching and the examples they set as scientists, particularly Dr. O'Morchoe, Dr. LaVelle, Dr. Sturtevant and Dr. Wezeman. I am especially grateful to Dr. Persky, for his friendship, his willingness to offer his resources whenever I needed them, his concern for graduate students, and the lessons he imparted in organization and dedication to teaching and research.

Finally, my accomplishments would not have been possible without the love and support of my family and friends. Most of all, I have my daughter Kendra and my husband Bob to thank for their unconditional love and sacrifices for me so that I might fulfill this dream.

VITA

The author, Andrea Marie Zardetto-Smith, was born on October 25, 1956 in Passaic, New Jersey to Ernest and Lorraine Zardetto. Her secondary education was received at Clifton High School in Clifton, New Jersey, from which she graduated in June of 1974. In September 1974, she entered the College of Saint Elizabeth and graduated "With Highest Honor" with a Bachelor of Science degree in Biology in May, 1978. In October of 1978 she entered Loyola University Graduate School where she was granted a Loyola University Basic Science Fellowship in the Department of Physiology. She received the degree of Master of Science in Physiology in January, 1983. While completing her degree, she was employed as a Research Biologist in the Cardiovascular/Renal Pharmacology-Antihypertension Program at G.D. Searle in Skokie, Illinois from May, 1981 until July, 1983.

In August of 1983, she entered the Department of Anatomy of the Graduate School of Loyola University of Chicago. While in the department she was the recipient of the Loyola University Basic Science Fellowship from 1984 to 1988. Along with her advisor, Dr. Thackery S. Gray, she received a Basic Science Research Grant from Loyola University Stritch School of Medicine in 1985 and in 1987 was awarded a Grant-in-Aid to Research from Sigma Xi. In May 1986 she won first place in the 16th Annual Sigma Xi Graduate Research Forum, and third place at the 18th Annual Forum in May, 1988. She also taught in the gross anatomy and neuroscience medical school courses. In 1984 she was elected into Sigma Xi, The Scientific Research Society, and in 1985 was induced into Alpha Sigma Nu National Jesuit Honor Society. Additionally, she served as President of the Graduate Student Council at the

Medical Center from 1985 to 1987, and was the graduate student representative to a variety of medical school committees, including the Committee on Student Life, President's Council, Library Committee, Student Health Committee, and Building Committee. She also served as Chairperson and Co-Chairperson of the Annual St. Albert's Day Celebration from 1984-1986.

Membership in professional societies includes Sigma Xi, the American Association of Anatomists, the Society for Neuroscience, and the Association for Women in Science. Her community and civic activities have included the teen program at St. Margaret Mary Church in Lisle, the National Association for Women in Construction (Aurora Chapter), and the National Endometriosis Association. She has also served as a Judge of Election for DuPage County, and currently serves as a precinct committeeperson for the Democratic party in Lisle township.

Andrea has been awarded a fellowship from the Cardiovascular Institute at the University of Iowa, Iowa City. She will begin an electrophysiological and anatomical study of the organum vasculosum lamina terminalis under the supervision of Dr. A. Kim Johnson in the Department of Psychology in June, 1989.

The author is married to Robert L. Smith and they are the proud parents of a beautiful two-year-old girl, Kendra Marie.

TABLE OF CONTENTS

LIST OF TABLES

LIST OF FIGURES

CHAPTER IV:

CHAPTER V:

ABBREVIATIONS

NUCLEI AND TRACTS

3V	third ventricle
4V	fourth ventricle
10	dorsal motor nucleus of the vagus
12	hypoglossal nucleus
ac	anterior commissure
ACo	anterior cortical amygdaloid nucleus
AMPO	anterior medial preoptic nucleus
AVPO	anteroventral proptic nucleus
AP	area postrema
ARC	arcuate nucleus
BL	basolateral amygdaloid nucleus
BM	basomedial amygdaloid nucleus
BST	bed nucleus of the stria terminalis and subnuclei
AL	anterior lateral subnucleus
AM	anterior medial subnucleus
DL	dorsal lateral subnucleus
IM	intermediate subnucleus
JXC	juxtacapsular subnucleus
PD	posterior dorsal subnucleus
PI	posterior intermediate subnucleus
PL	posterior lateral subnucleus
PM	posterior medial subnucleus
PO	preoptic subnucleus

PS	parastrial nucleus
SC	supracapsular subnucleus
VL	ventral lateral subnucleus
VM	ventral medial subnucleus

CeA	central nucleus of the amygdala and subdivisions
CeL	lateral
CeLC	lateral capsular
CeM	medial
CeV	ventral

Cu	cuneate nucleus
DM	dorsomedial hypothalamic nucleus
DMX	dorsal motor nucleus of the vagus
ECu	external cuneate nucleus
ex	external capsule
f	fornix
gr	gracile fasiculus
GR	gracile nucleus
I	intercalated amygdaloid nuclei
ic	internal capsule
La	lateral amygdaloid nucleus
LRt	lateral reticular nucleus
LPgi	lateral paragigantocellular nucleus
mlf	medial longitudinal fasciculus
MnPO	median preoptic nucleus
MPOA	medial preoptic area

NTS	nucleus of the solitary tract
ot	optic tract
PB	parabrachial nucleus of the pons
PeF-LH	perifornical-lateral hypothalamic area
py	pyramidal tract
PVNp	hypothalamic paraventricular nucleus-parvocellular
PVNm	hypothalamic paraventricular nucleus-magnocellular
PV	paraventricularthalamic nucleus
RC	retrochiasmatic area
SFO	subfornical organ
SHy	septohypothalamic nucleus
SP5C	spinal trigeminal nucleus, caudal
SP5I	spinal trigeminal nucleus, interpolar
spc	superior cerebellar peduncle
st	stria terminalis
SO	supraoptic nucleus
SolC	commissural nucleus of the solitary tract
SolM	medial nucleus of the solitary tract
SolL	lateral nucleus of the solitary tract
ts	solitary tract
VLM	ventrolateral medulla
RVL	rostral VLM
CVL	caudal VLM

ANATOMICAL TRACERS/TECHNIQUES/REAGENTS

FB	fast blue
FG	Fluoro-Gold
DAB	diaminobenzidine
GO	glucose oxidase
HRP	horseradish peroxidase
PHA-L	*Phaseolus vulgaris* leucoagglutinin
PBS	phosphate buffered saline
PBS-tx	phosphate buffered saline triton-X

PEPTIDES AND CATECHOLAMINERGIC BIOSYNTHETIC ENZYMES

BOM	bombesin
CGRP	calcitonin gene-related peptide
CRF	corticotropin relaesing factor
ENK	enkephalin (met)
NPY	neuropeptide Y
NT	neurotensin
PNMT	phenylethanolamine-N-methyltransferase
Sub P	substance P
SS	somatostatin
TH	tyrosine hydroxylase

CHAPTER I

SPECIFIC AIMS

Introduction. The amygdaloid complex has been implicated in the control of the endocrine and autonomic components of various adaptive behaviors. The central nucleus (CeA) is a distinctive area within the amygdaloid complex because of its multiple, reciprocal connections with other brain nuclei that are important in the regulation of autonomic function (for recent reviews, see Price et al., '87; Gray et al., '89). As part of the limbic system, one function of the amygdala may be the monitoring of environmental stimuli in order to detect those stimuli to which appropriate adaptive visceral responses are required. The CeA, in particular, is thought to be one part of the neural circuitry that integrates the somatic and visceral responses during various behaviors (e.g., fear, anger, flight, orientation, and the defense reaction). It has also been suggested that the CeA plays a role in emotion and memory formation, as well as in mediating autonomic and neuroendocrine responses to certain stressful environmental conditions.

Sensory feedback from the viscera is an integral feature of autonomic regulation of peripheral organ systems, such as the cardiovascular, respiratory, and gastrointestinal systems. The afferent limb of autonomic reflexes, conveying the current status of the viscera to the central nervous system controller, can strongly modulate effector function (Caleresu et al., '81) to maintain or restore homeostasis (Kupfermann, '82). For example, arterial baroreceptors can modify both sympathetic and parasympathetic discharge

to the heart (Downing, '81). In the rat, the nucleus of the solitary tract (where peripheral sensory afferents first terminate) projects directly to the CeA, representing one route by which interoceptive information may be relayed to the forebrain from peripheral receptors. Afferent information may also be transmitted to the CeA via the parabrachial nucleus of the pons. In species such as the cat where a direct pathway from the nucleus of the solitary tract to the CeA has not been demonstrated, the parabrachial nucleus may serve as a major relay nucleus for visceral feedback ascending to the telencephalon (Cechetto and Calaresu, '85). An efferent projection from the ventrolateral medulla, another brainstem autonomic-related area, may also provide a visceral input to the CeA that possibly is important in the control of vasomotor tone and vasopressin release.

Previous studies provided the basic evidence for the existence of efferents from the medulla and parabrachial nucleus to the CeA. In general, the purpose of the studies comprising this dissertation were to provide data concerning the anatomical and neurochemical organization of these pathways, hopefully aiding in the establishment of an anatomical framework for future functionally-oriented investigations. As studies in animal models have linked the CeA to the development or expression of several pathologies in which autonomic function is altered or impaired, possibly as the result of changes in visceral afferent feedback (e.g., hypertension), the results presented within this dissertation may ultimately contribute to the understanding of the mechanisms which underlie the normal and pathological functioning of these regions.

Specific objectives. In general, the studies in this dissertation employed anatomical techniques to examine the organization

and neurochemical content of medullary and parabrachial afferent pathways to the CeA. The specific objectives of this research are:

1. To describe the topographic organization of efferents from the nucleus of the solitary tract to the CeA and its related forebrain nucleus, the bed nucleus of the stria terminalis, using an anterograde tracer, Phaseolus vulgaris leucoagglutinin (PHA-L).

2. To examine the catecholamine and/or neuropeptide identity of efferents from the nucleus of the solitary tract to the CeA, using the combined retrograde tracer/immunocytochemical technique.

3. To examine the neuropeptide identity of efferents from the parabrachial nucleus of the pons to the CeA, using the combined rtetrograde tracer/immunocytochemical technique.

4. As during the course of experiments 2 and 3, retrograde label was noted to be present in the ventrolateral medulla in areas approximating the known location of the A1/C1 catecholaminergic groups, this study examined the neurochemical identity of CeA afferents from this area.

5. In material prepared for experiment 1 using the PHA-L technique, a direct projection from the nucleus of the solitary tract to the subfornical organ was noted. Since this pathway has not been previously demonstrated, and may be significant in cardiovascular and hydromineral regulation, this finding is discussed as a separate study.

Research animals for these experiments were acquired in

accordance with the guidelines published in the National Institutes of Health Guide for the Care and Use of Laboratory Animals (National Institutes of Health Publication No. 85-23, Revised 1985). Experiments were conducted as per the principles outlined in the Guidelines for the Use of Animals in Neuroscience Research as stated by the Society for Neuroscience.

CHAPTER II

REVIEW OF RELATED LITERATURE: THE CENTRAL NUCLEUS OF THE AMYGDALA

Phylogeny. In the course of his landmark studies on the evolution of the forebrain, Herrick ('22) described a structure in cyclostomes homologous to the mammalian amygdaloid complex as the lateral olfactory area. This region becomes considerably more differentiated in the amphibian telencephalon. An unspecialized cell mass, termed by Herrick ('33) the nucleus dorsolateralis amygdalae, is present and is composed of a specific amygdaloid neuropil. The amygdaloid nuclear group is slightly more developed in the frog and appears in pear-shaped form, but earlier workers called the region the epistriatum (Kappers et al., '36). The amygdaloid complex in reptiles is formed by an infolding of the pallidal gray from the edge of the piriform lobe cortex. Johnston ('23) suggested this be termed the amygdaloid ridge. The differentia-differentiation of this amygdaloid area varies in different reptiles. The area may appear as a definite ridge or band of cells directly continuous with the piriform lobe complex. Or, it may be present as a group of lateral cells, and groups of more densely placed cells (suggesting a ridge arrangement) constituting its more medial and periventricular portion (Kappers et al., '46). Because of its position, the largest and most centrally located part of the amygdaloid area in reptiles was designated the central nucleus of the amygdala (CeA) by Johnston ('23). He felt it was central also in the sense of being the oldest part around which the other members of the amygdaloid

complex came to be grouped.

The form relations of the amygdaloid complex in mammals varies with general changes in the morphology of the telencephalon (De Vries, '10; Johnston, '23). The amygdaloid nuclei in marsupials lie in the floor of the temporal horn of the ventricle, while in higher mammals, they occupy a position in its rostral wall. Johnston ('23) observed that in passing from lower to higher mammals, the lateral, basal, and medial nuclei, which lie in a position justifying their names, are shifted in man with the lateral nucleus being most ventral and the medial nucleus most dorsal.

The earliest description of the components of the mammalian amygdaloid complex was made by Kolliker ('96). He described four nuclei in the basal part of the rabbit telencephalon which are now recognized as belonging to the amygdaloid complex, but gave only one the name nucleus amygdalae. A more detailed description of the amygdala in mammals was made by Volsch ('06, '11). In several species he identified seven nuclear groups within the amygdala, denoting them by letters. Nucleus "E" represented all which Volsch recognized of the larger central nucleus described by Johnston ('23), grouping the remaining part of the central nucleus with the putamen. Johnston ('23) (in the oppossum, bat, rabbit, and human fetus), Young ('34) (rabbit) and Humphrey ('36) (bat) all agreed in recognizing a lateral, basal, accessory basal, central, medial, cortical, and lateral olfactory tract nucleus within the amygdaloid complex. Koikegami ('63), in his exhaustive comparative study of the amygdala in several mammalian species, noted that Johnston's central nucleus becomes reduced in relative size in higher animals, for example, being large in the rodent and smaller in man. He felt the name to be inadequate as the nucleus does not lie in the central part of the amygdaloid complex in most mammals, but

rather in its dorsal part, and thus designated it the nucleus centralis dorsalis.

Johnston ('23) divided the nuclei into two distinct groups on the basis of origin and age: the primitive or little modified central, medial, cortical and nucleus of the lateral olfactory tract; and the new nuclei formed by infolding or migration of cells - the lateral and basal nuclei. He recognized the central nucleus as representing the deeper part of the lateral olfactory area of lower vertebrates, and along with the medial nucleus, gave rise to the largest part of the tract connecting the amygdala with the hypothalamus. Johnston's phylogenetic division of the amygdaloid nuclei into the corticomedial and basolateral groups has persisted into the present decade, but the results of recent anatomical studies are altering this concept (De Olmos et al., '85; Price et al., '87). For example, De Olmos et al. ('85) has suggested that on the basis of histochemistry and connectivity, the amygdala can be divided into an "olfactory amygdala", a "medial amygdaloid group", a "basolateral group", and a "central amygdaloid group".

Cytoarchitecture. The CeA in the rodent stands out clearly at most levels as a circular group of small cells separated from the adjacent putamen by a cell-poor zone (Hall, '72). It lies dorsally in the amygdala, bounded superiorly by the globus pallidus, and separated from it by the caudal extension of the basal nucleus of Meynert (De Olmos et al., '85). At its most rostral extent, the CeA blends with the anterior amygdaloid area and sublenticular substantia innominata (Gurdjian, '27; Brodal, '47; Krettek and Price, '78a; De Olmos et al., '85). The CeA is surrounded by fibers of the longitudinal association bundle laterally and ventrally, demarcating it from the lateral and basolateral amygdaloid nuclei, and by fibers of the stria terminalis

medially, separating it from the medial amygdaloid nucleus (Krettek and Price, '78a; De Olmos et al., '85). At caudal levels the CeA is separated from the anterior wall of the lateral ventricle (temporal horn) by a cell-poor zone and small islands of intercalated cells (De Olmos et al., '85).

Johnston ('23) noted some dense, deeply stained, wedge-shaped or triangular masses, and rounded or ovoid clumps of cells within the CeA embedded in the general neuropil. He observed that these appeared to divide the CeA into certain subdivisions, but otherwise attached no significance to them. Gurdjian ('27) referred to the CeA as a homogeneous mass, composed of cells smaller than those found in the ventral portion of the lateral amygdaloid nucleus, and surrounded by a rather distinct capsule, especially on its lateral aspect. Later investigators, in the rat and numerous other species, recognized a medial and a lateral division within the CeA, but differed as to their precise delineations (Fox, '40; Brodal, '47; Uchida, '50; Koikegami, '63; Krettek and Price, '78a).

The medial subdivision (CeM) (Fig. 1) in the rat is usually described as composed of larger, more tightly packed cells (Brodal, '47; Krettek and Price, '78a; Schwaber et al., '81; McDonald, '82; Cassell et al., '86). The CeM continues more rostrally than any other CeA subdivision, blending anteriorly and ventrally with the anterior amygdaloid area and substantia innominata (Cassell et al., '86). The lateral subdivision (CeL) (Fig. 1) consists of more loosely arranged, medium-sized cells that are partially encapsulated by small bundles of fibers (Krettek and Price, '78a; McDonald, '82; Cassell et al., '86). On the basis of Nissl-stained sections, both McDonald ('82) and Cassell et al. ('86) further subdivided the CeL into a CeL proper (designated by Schwaber et al ('81) as the "central group") and an additional sub-

division, the lateral capsular (CeLC) (Fig. 1). In coronal sections CeL appears as a round nuclear mass in the caudal two-thirds of the CeA, becoming progressively narrower rostrally to lie dorsal to CeM. Cells in the the CeL are ovoid or spherical in shape and are surrounded by a capsule of loosely arranged myelinated fibers, running into the ansa lenticularis and stria terminalis. Fibers of the lateral portion of the capsule are associated with diffusely arranged neurons containing small, ellipsoid nuclei which distinguish this area as clearly separate from adjacent subdivisions at mid-rostrocaudal levels. Both McDonald ('82) and Cassell et al. ('86) termed this subdivision the lateral capsular division (CeLC) (Fig. 1), though there was some disagreement as to its boundaries. Schwaber et al. ('81) described this subdivision as a crescent-shaped lateral rim of loosely arranged medium and large-sized cells.

Near the rostral pole of the CeA, a small area lateral to CeM, containing tightly packed ovoid neurons, was designated the intermediate subdivision of the CeA (CeI) by McDonald ('82). This zone was only recognized in the material of Cassell et al. ('86) following injections of horseradish peroxidase into the bed nucleus of the stria terminalis. The CeI of McDonald ('82) may form a component of the "central group" designated by Schwaber et al. ('81) (Wray and Hoffman, '83). Ventral to the subdivision CeL is an area described only as a transitional zone by McDonald ('82), but classified by Cassell et al. ('86) as the ventral division of the CeA (CeV) (Fig. 1). According to Cassell et al. ('86), this subdivision is present at all levels of the CeA except its most rostral extent and contains a heterogeneous population of ellipsoid cells.

Wray and Hoffman ('83) proposed parcellation of the CeA on the basis of neuropeptide content. They distinguished three different

zones: medial, central, and lateral capsular. For example, neurotensin cell bodies and fibers are densely concentrated within the lateral capsular zone, vasoactive intestinal polypeptide fibers form a dense plexus within the central zone, and sparse neurotensin, enkephalin and substance P fibers innervate the medial zone (Wray and Hoffman, '83). These zones were approximated with the cytoarchitectural divisions proposed by Schwaber et al. ('81) and McDonald ('82). Veening et al. ('84) and Cassell ('86) also examined the distribution of certain peptides within the CeA. In general, the results supported those of Wray and Hoffman, in that the distribution of individual populations of peptidergic neurons is complex and does not reflect a simple division of the CeA into medial and lateral zones.

The connections of the CeA with other brain regions show a topographical variation as well. These connections are examined in detail in later sections, but with regard to cytoarchitecture, Cassell et al. ('86) concluded there is a considerable degree of overlap that occurs in the distributions of various populations of projection neurons, i.e., again they do not reflect a simple division of the CeA into medial and lateral. In fact, most of the populations of projection-specific or peptide containing neurons identified in their study were not confined to a single cytoarchitectonic division. Comparative cytoarchitectonic studies employing Golgi-techniques and well-impregnated immunoreactive neurons suggest: (a) the cytoarchitectonic subdivisions of the CeA reflect differences in neuronal morphology (McDonald, '82); and (b) the morphology of peptide-containing neurons in the CeA may depend on which subdivision it is located in (Cassell et al., '84). Taken together, the results of these studies suggest that the morphology of neurons in the CeA is determined by their cytoarchitectonic location, irrespective of their peptidergic content or target location

(Cassell et al., '86).

Although cytoarchitectonic subdivisions in the CeA apparently do not reflect segregation of target-specific or neurochemically-specific neurons (or both), some evidence suggests that the subdivisions do receive specific afferent inputs. The projection from the ventromedial and lateral hypothalamus to the CeA terminate in CeLC (Saper et al., '76; Swanson, '76; Otterson, '80), while the termination of afferents from the nucleus of the solitary tract terminates mainly within CeM and CeV (Ricardo and Koh, '78; Zardetto-Smith and Gray, '87). The distribution of noradrenergic, dopaminergic and peptidergic terminals within the CeA also appear to correlate well with cytoarchitectonic subdivisions (Fallon et al., '78; Cassell et al., '82; Wray and Hoffman, '83; Gray et al., '84). Thus, even though CeA neurons may have similar neurotransmitter/peptide content or projection targets, their morphology and afferent input may differ on the basis of their cytoarchitectonic localization (Cassell et al., '86).

Neurogenesis. Bayer ('80) examined neurogenesis in the rat amygdala using progressively delayed comprehensive labeling (3-H-thymidine) radiography. All large and many small neurons originated in most nuclei, including the CeA, between E13 and E17. Neurogenesis within the CeA appeared to occur simultaneously with other amygdaloid nuclei (i.e., medial and basolateral), but independant of them. The CeA was organized in a longitudinal strip, with neurons generated in a strong anterior to posterior gradient. Within the CeA, there was an intranuclear gradient of medial to lateral, as neurogenesis in the medial parts of the CeA significantly preceded that occurring in more lateral parts. Also, the medial part of the CeA acted as an "early originating center", becoming surrounded by younger neurons both

anteromedially and laterally. Several older embryonic studies of amygdala development had traced its neuroepithelial source to the posterior basal telencephalon, with multiple centers serving as sources for cytogenetic zones in the amygdala (Holmgren, '25; Hewitt, '50; Humphrey, '68). The neurogenetic patterns demonstrated by Bayer ('80) supported this theory, i.e., the corticomedial group may originate from more medial neuroepithelium, while the basolateral complex may originate more laterally.

Connectivity.

The efferent and afferent connections of the CeA in several species have been studied and well-characterized in recent years with the advent of anterograde and retrograde anatomical tracing techniques (for recent reviews see De Olmos et al., '85; Price et al., '87). The CeA has extensive and reciprocal connections with cortical, diencephalic, mesencephalic, and brainstem autonomic nuclei.

Efferent Connections. The efferent connections (as derived from anatomical studies utilizing retrograde/anterograde tracing methods) of the CeA in several species are summarized in Table I. Cortical and intraamygdaloid efferents from the CeA appear to be minimal (De Olmos et al., '85). The CeA is unique among the amygdaloid nuclei, in that it projects caudal to the hypothalamus, sending fibers into the mesencephalon, pons, medulla, and spinal cord (Price et al., '87). The projections of the CeA in the rat, cat, and monkey appear to be similar (Price, '81).

Afferent Connections. The afferent connections (as derived from anatomical studies utilizing retrograde/anterograde tracing methods) of the CeA in several species are summarized in Table II. In the rat, the CeA appears to be the main recipient of cortical and intraamygdaloid

afferents to the central amygdaloid group (De Olmos et al., '85). A variety of hypothalamic nuclei project to the CeA, along with extensive thalamic afferents. In the rat, the CeA receives afferents from a number of brainstem areas, including the nucleus of the solitary tract. However, this particular pathway has not been demonstrated in the cat (Russchen, '82) or monkey (Beckstead, '80; Mehler, '80).

Immunocytochemistry. Studies in recent years have identified several different neuropeptidergic cell bodies and terminals concentrated within the CeA (for recent reviews, see Price et al., '87; Gray, '89). As referred to earlier, the distribution of peptides within the CeA is complex and does not reflect a simple division of the CeA into medial and lateral zones (Cassell et al., '86). Though the distribution of each peptide is somewhat different, there is a large concentration of several peptides (both perikarya and terminals) within the lateral and lateral capsular subdivisions of the CeA (Tables III and IV). However, it has been estimated that the neuropeptide-positive cell bodies identified to date comprise only 25% of the total neuronal cell population within the CeA; thus, the chemical content of the majority of CeA neurons, particularly those in CeM, remains unknown (Gray, '89). Corticotropin releasing factor (CRF), neurotensin, and somatostatin cells form the largest portion of peptide-containing cells in the CeA, with fewer enkephalin, substance P, galanin, and dynorphin cell bodies comprising the remainder (Gray, '89). In contrast to the limited number of peptide cell types, at least sixteen different neuropeptides (and several classical neurotransmitters) have been identified in nerve terminals and fibers within the CeA (Gray, '89). With the exception of neuropeptide Y, somatostatin, and proopiomelanocortin, the majority of peptidergic terminal labeling is present within

the lateral and lateral capsular subdivisions of the CeA (Table IV).

Table V lists the descending peptide pathways of the CeA identified to date. A large part of the known descending peptidergic output arises from CRF, somatostatin, and neurotensin cells, while substance P and galanin cells make a minor contribution (Moga and Gray, '85; Gray and Magnuson, '87a, b). Enkephalin cells do not contribute to the descending pathway to the brainstem (Moga and Gray, '85; Gray and Magnuson, '87b), but do project to the bed nucleus of the stria terminalis (Palkovits et al., '81). Though past studies indicated most of the efferent projections of the CeA originated in its medial portion (Hopkins and Holstege, '78; Schwaber et al., '82), it now appears the lateral aspects of the CeA also contribute, especially in terms of peptidergic output. For example, the peptidergic projections from the CeA to the PBN arises mostly from CeL (Moga and Gray, '85).

Table VI lists the ascending peptide and transmitter inputs to the CeA identified to date. This list does not include preliminary reports of peptidergic efferents from the parabrachial nucleus, nucleus of the solitary tract and ventrolateral medulla identified in experiments performed for this dissertation. Considering the many different types of peptide terminal immunoreactivity present within the CeA, relatively few studies have analyzed the possible source of these afferents, leaving the peptide content of ascending pathways, especially from the brainstem, largely unknown. Also, as mentioned earlier, the distribution of catecholaminergic and peptidergic terminals within the CeA appears to correlate well with cytoarchitectonic subdivisions, and the morphology and afferent input to CeA neurons may differ depending on their cytoarchitectonic localization (see "Cytoarchitecture" above).

Central Nucleus Function.

Phylogenetic Perspective: Differentiation of Mammalian Amygdaloid Function, From Olfactory to Visceral. A brief description of the vomeronasal organ is prerequisite to understanding the evolution of amygdaloid function. Among tetrapods, and in some fish, there is a ventral segment of the olfactory epithelium which more or less becomes separated from the nasal passageway. In some species, it becomes an independent olfactory organ called the vomeronasal (or Jacobson's) organ (Kent, '73). In amphibians the vomeronasal organ appears as a deep groove or blind sacs in the ventromedial floor of the nasal canal (Kent, '73). In lizards and snakes, the organs are tubular, lose their connection with the nasal canal, and open into the anterior roof of the oral cavity (Kent, '73). In most mammals (including man) the vomeronasal organs are vestigial, but in the cat and some rodents, are retained as tubular structures above the false palate, retaining an opening into the oral cavity via the incisive foramen (Switzer et al., '85). A separate division of the olfactory nerve, the vomeronasal nerve, arises from the epithelium of the vomeronasal organ and terminates within a differentiated portion of the olfactory bulb, the accessory olfactory formation (Switzer et al., '85). Efferents from the accessory olfactory formation travel through the dorsolateral olfactory tract to the "vomeronasal amygdala" (the medial and posteromedial cortical amygdala and posterior part of the medial bed nucleus of the stria terminalis), through the dorsolateral olfactory tract (Scalia and Winans, '75). Both the medial and posteromedial cortical nuclei, in turn, project to the CeA (Table II).

In amphibians, the opening of the vomeronasal organ into the oral cavity appears to be its first phylogenetic differentiation, i.e., expanding its function from olfaction to taste and possibly tactual and

other general forms of sensibility within the mouth. Herrick ('33) speculated that in the frog, the amygdala began to differentiate under influence of sensory input from the vomeronasal organ. From that point, further development of the system progressed in higher vertebrates through the inclusion of input from related sensory systems, possibly profoundly modifying the functional aspects of the complex as a whole. Herrick stated: "So great may be this deviation from the primative physiological pattern in some cases that the suppression of the vomeronasal organ, as in man, or even the entire olfactory system, as in the dolphin, does not destroy the integrity of the surviving components of the amygdaloid complex, which retains its individuality in modified form". Electrophysiological experiments have lent credence to this theory. For example, Azuma et al. ('84) demonstrated that taste-responsive neurons in the rat amygdala are also responsive to tactile or thermal stimulation of the tongue, or to tactile stimulation of other body regions.

Herrick was the first to recognize the function of the olfactory system to be two-fold: 1) visceral or interoceptive in relation to the selection and digestion of food, and 2) somatic or exteroceptive in relation to the adjustment of the organism to environmental conditions. Today, over fifty years later, Herrick's original premise is embodied in the recognition that a fundamental role of the amygdala may be the monitoring of environmental stimulation in order to detect those stimuli to which an autonomic response is appropriate (Price et al., '87). The phylogeny of the CeA is conserved in its inputs from the vomeronasal amygdala, as well as from almost every nucleus in the olfactory amygdala (Table II), but it has evolved functionally to play a major role in mediating this aspect of amygdaloid function through its multiple, reciprocal connections with other autonomic nuclei.

Visceral Functions of the CeA.

Ingestive Behavior. As might be expected from its phylogenetic history, the CeA receives input conveyed from the parabrachial taste neurons (Norgren, '74, '76; Yamamoto et al., '80; Block and Schwartzbaum, '83) and the cortical gustatory area (Norgren and Grill, '76); Yamamoto et al., '84). Studies in the rabbit and rat show neurons in the CeA respond to sapid stimuli as well as to nongustatory stimuli (Schwartzbaum and Morse, '78; Azuma et al., '84). Lesions of the amygdala including the CeA result in aphagia and adipsia (Kling, '66; Fondberg, '69; Box and Mogenson, '75), while lesions separating the CeA and cortical gustatory area result in impaired retention of taste aversion learning (Yamamoto et al., '84). Possibly, the CeA modulates hypothalamic satiety mechanisms (Box and Mogenson, '75; Kaada, '72). Taste stimuli are important in induction and modulation of ingestive behavior, and taste input to the CeA may be related to the motivational and hedonic aspects of feeding and drinking behavior (Pfaffman et al., '77).

Cardiovascular Regulation. A wide variety of autonomic and endocrine effects are elicited by amygdaloid stimulation (for review, see Gloor, '63; Kaada, '72). Since many of the same effects of amygdaloid stimulation could be also be obtained by stimulating the hypothalamus/preoptic area, it was thought the amygdala did not affect those perturbations directly, but rather, played a modulatory role in hypothalamic elicitation of them (Gloor, '72; Price et al., '87). However, the demonstration of efferent projections from the amygdala (predominately from the CeA in particular) to the lower brainstem to nuclei concerned with adjustments of autonomic or nociceptive responses provided an anatomical basis for direct influences of the amygdala in

autonomic control.

In the early forties, Masserman ('41) and Hess and Brugger ('43) reported that hypothalamic stimulation in the awake cat produced a coordinated behavior pattern ("the defense reaction") which began as an alerting response, progressed to include piloerection, hissing, and exposure of the claws, and culminating in attack or flight (LeDoux, '86). Later in the fifties, Kaada ('51) and MacLean and Delgado('53) were among the first to demonstrate in the cat and monkey that stimulations of the amygdala resulted in a behavioral pattern similar to that evoked by hypothalamic stimulation. Stimulation of the cortico-comedial amygdaloid group, or the CeA alone, in the awake animal, resulted in automatisms related to defense or attack: swallowing, vocal components of states such as attack, defense and escape, and stances and movements associated with pause, altering, and searching. In addition to the motor responses, a number of autonomic components occurred that are associated with the "defense response", such as increased respiratory rate, elevations of blood pressure accompanied by bradycardia, alteration of gastric motility, pupillary dilitation, micturition and piloerection (Kaada, '51; MacLean and Delgado, '53; Gloor, '60; Hilton & Zbrozyna, '63; Kaada, '72). A column of electrical stimulation sites that elicit the defense response, or its autonomic components, stretches from the basal amygdaloid nucleus, through the CeA and lateral hypothalamus and down into the brainstem, paralleling the trajectory of projections to the brainstem from both the CeA and hypothalamus (Price et al., '87).

In the anesthetized rat and monkey and in the awake or anesthetized rabbit, electrical stimulation of the CeA results in hypotension and decreased heart rate (Reis & Oliphant, '64; Mogenson & Calaresu, '73; Fredericks et al., '74; Faiers et al., '75; Kapp et al., '82;

Applegate et al., '83; Galeno and Brody, '83; Cox et al., '86; Gelsma et al., '87). In the awake cat or rat, stimulation of the CeA causes tachycardia and increased arterial pressure (Hilton & Zbrozyna, '63; Stock et al., '78; Galeno and Brody, '83; Schlor et al., '84; Gelsema, '87). Apparently, anesthesia masks the tachycardic and pressor response that normally occurs during CeA activation (Mogenson and Calaresu, '73; Galeno and Brody, '83; Gelsema et al., '87). Although defensive or aggressive behavior is not always exhibited during CeA stimulation in the conscious rat, an orienting or alerting reaction (the initial stage of the defense reaction in the cat) has been observed (Galeno and Brody, '83; Gelsema et al., '87). The behavioral responses accompanying the changes in heart rate and blood pressure observed during CeA stimulation in the conscious animal indicate the hemodynamic responses observed are truly part of the overall pattern occurring in the natural state (Mogenson and Calaresu, '73; Galeno and Brody, '83; Gelsema et al., '87). Thus, the CeA appears to be one area in the forebrain that is involved in integrating the somatic and autonomic responses during fear, anger, flight, orientation, and the defense reaction (Kaada, '72; Mogenson and Calaresu, '73; Galeno et al., '83; Gelsema et al., '87).

Role in Heart Rate Conditioning. In addition to its role in mediating the cardiovascular responses to unconditioned threating stimuli, the CeA contributes to the acquisition of conditioned responding to threatening or fear-arousing stimuli (Kapp et al., '81). The defensive behavior and accompanying autonomic changes elicited by electrical stimulation of the CeA resemble those evoked by an aversive conditioned stimulus (see above). LeDoux ('87) has pointed out that aversive classical conditioning is also described as defensive conditioning, reflecting the fact that the conditioned stimulus evokes a

response pattern characteristic of the organism's species typical reaction to threat. Lesions of the amygdaloid nuclei, particularly those involving the corticomedial nuclei, alter the performance of rats in several different aversive conditioning tasks (Kemble and Tapp,'68; Pelligrino, '68). A consistent pattern of change in the reaction to threatening stimuli is produced in the rat by corticomedial amygdaloid lesion, such that avoidance decrements are obtained for both active- and passive-avoidance responses (Blanchard and Blanchard, '72). Studies in the rat in which the lesions were confined to the CeA show there are marked deficits in the acquisition of conditioned responding in passive avoidance paradigms (McIntyre and Stein, '73; Grossman et al., '75), results consistent with those obtained with larger lesions (Blanchard and Blanchard, '72). Both Blanchard and Blanchard ('72) and Slotnick ('73) have proposed that the poor avoidance behavior of amygdala-lesioned animals is related to a deficit in the arousal of fear behavior. However, lesions of the CeA with ibotenic acid, which damages neurons but spares fibers-of-passage, results in a delay, but not a deficit, in the acquisition of passive avoidance, suggesting lesion of the neuronal cell bodies of the CeA is not responsible for impairment in this paradigm (Jellestad et al., '86; Riolobos et al., '87). However, CeA neuronal damage may have interfered with the arousal of fear, thus causing the delay in passive avoidance conditioning, i.e., a temporary decrease resulting from impaired processing of incoming external stimuli, delaying the formation of associations between neutral and noxious stimuli (Jellestad et al., '86).

To study the neural pathways mediating long-term associative learning, Cohen ('75) investigated the involvement of the pigeon archistriatum (homologue of the mammalian amygdala) by comparing visually conditioned heart rate changes (light-shock pairings) before

and after archistriatal lesion. Sizable performance deficits were found in groups sustaining lesions of the postero-medial region, i.e., the conditioned cardioacceleration response was diminished. In the rabbit, the bradycardic and depressor responses elicited by stimulation of the CeA are similar to those observed during the initial stages of Pavlovian fear conditioning (Powell and Kazis, '76). The rabbit, unlike the pigeon, exhibits primarily a vagal response to tone-shock presentations, i.e., a conditioned cardiac deceleration (Kapp et al., '81). Kapp et al. ('79) has shown that lesions of the CeA greatly attenuate the magnitude of this bradycardia, suggesting the CeA may play a direct role in the expression of cardiovascular and possibly other autonomic and somatic responses to conditioned stimuli during Pavlovian fear conditioning (Kapp et al., '81). Collectively, these results suggest a role for the amygdala, and the CeA in particular, in the establishment of conditioned, as well as unconditioned, cardiovascular responses (Kapp et al., '79; Kapp et al., '81; Schwaber et al., '86) and therefore, in emotion, associative learning, and memory formation (Amaral, '87; LeDoux, '87; Squire, '87).

Role of the CeA in Stress. As cited earlier, impairment in the acquisition of conditioned responding in avoidance studies was thought to be related to a deficit in the arousal of fear behavior (see above). Davis et al. ('84) has recently reviewed the evidence that the CeA and its many efferent targets form a central fear system. It is not surprising, then, that the CeA has been implicated in the response to stressful environmental conditions which involve a state of chronic fear or anxiety. Henke ('80a, '80b) demonstrated immobilization of rats produced gastric ulcers, but bilateral lesions involving the CeA attenuated their development. Restraint initiates changes in firing in

some units in the CeA that can be correlated with the different degrees of stomach pathology (Henke, '83, '88). Electrical stimulation of the area of these multiple units produces stomach ulcers (Henke, '85). The CeA may be a primary site for opiate-mediated attenuation of stress ulcerogenesis, as bilateral injections of beta-endorphin into the CeA inhibit stress ulcer formation in a dose-dependant manner (Ray et al., '87). Lesions of the CeA also decrease fasting levels of gastric acidity and attenuate the formation of mucosal erosion induced by bilateral hypothalamic lesion (Grijalva et al., '86).

Intensified environmental stimuli, resulting in a "prolonged defense reaction" in which sympathetic activity to the heart and peripheral circulation are elevated over a long period of time, is hypothesized to contribute to the development of hypertension (Folkow, '82a). Spontaneously hypertensive rats (SHR), a model for neurogenic human primary hypertension, exhibit centrally intensified defense reactions to alerting stimuli (Hallback and Folkow, '74). Stressful environments greatly aggravate hypertension in the SHR (Yamori et al., '69), and amygdala-lesioned rats respond less than controls to stressful, fear-inducing stimuli (Folkow et al., '82b). Bilateral lesions of the CeA in young SHR attenuate the development and delay the onset of hypertension (Folkow et al., '82b; Galeno et al., '82). However, the CeA is not the source of the exaggerated cardiovascular responsiveness SHR demonstrate in response to environmental alerting stimuli, but may only reinforce defense reactions to stressful situations when such stimuli are at hand (Folkow et al., '82b; Galeno and Brody, '83).

A variety of environmental stimuli that do not produce obvious pain, such as restraint and hypoglycemia, are accompanied by analgesia (Hayes et al., '78; Amir and Amit, '78; Bodnar et al., '79). The stress of prolonged isolation alters activity in CeA neurons and in-

creases the responsiveness to painful stimulation (Thoa et al., '76). Discrete lesions in both the CeA and lateral amygdala reduce shock-motivated avoidance behavior and fighting in rats (Melzak et al., '74). Melzack and Casey ('68) distinguished between the sensory-discriminative aspects of pain, transmitted via the spinothalamic system, and the motivational affective components of pain, associated with the thalamus and limbic system. Amygdalar lesions reduce the responsiveness to several non-painful but aversive stimuli, suggesting the CeA may be part of the "ancillary pain system" that mediates the presumed affective-motivational components of aversive experiences (Henke, '79, '82). Microinjection of morphine and neurotensin into the CeA produce increases in nociceptive threshold, thus possibly acting to alter the affective component of behavioral responses to noxious stimuli (Kalivas et al., '82). Aversive inputs may reach the CeA via the thalamus, neocortex, or directly from nociceptive fibers associated with the substantia nigra and locus coeruleus (Henke, '83). An important area in analgesia mechanisms, the periaquaductal gray, is reciprocally connected with the CeA (see Tables I and II). In addition, there is evidence that cardiovascular and pain pathways are linked, such that analgesia coupled with a pressor response, with subsequent inhibition of pain and/or associated motivation-affective changes, may aid in reducing the stress associated with aversive environmental stimulation (for review, see Randich and Maixner, '84). The CeA, which participates in both pathways, may be one such site of linkage, where pain and cardiovascular systems overlap (Moga and Gray, '85).

Besides mediating some of the autonomic components involved in stress, the CeA may participate in the concommitant neuroendocrine response. The amygdala is known to participate in the tonic secretion of adrenocorticotropic hormone (ACTH) under nonstressful conditions

(Zolovick, '72; Allen and Allen, '75), but its contribution to corticosteroid secretion in response to stress is controversial (Beaulieu et al., '86). In the monkey amygdalectomy blocks the increase in plasma cortisol in response to to stressful emotional stimuli (Kling, '66). Bilateral destruction of the CeA diminishes plasma ACTH levels in response to immobilization stress compared to intact or sham-lesion rats exposed to the same stress (Beaulieu, '86). Anterograde tracing studies show the medial CeA innervates the posterior parts of the medial and lateral parvocellular paraventricular nucleus, possibly terminating directly on corticotropin, vasopressin, and oxytocin immunoreactive cells (Gray et al., '89; Magnuson and Gray, '88). This suggests that the CeA can affect pituitary ACTH release through direct modulation of these paraventricular hormone releasing cells (Gray et al., '89). As the CeA contains a high concentration of glucocorticoid-concentrating cells and receptors, circulating glucocorticoids (known to influence mood, perception, and learning) may also influence amygdaloid modulation of stress (McEwen et al., '86).

Summary.

Though the existence of the CeA in mammals has been recognized since the late nineteenth century, most of our knowledge concerning its cytoarchitecture, connectivity, and neurochemistry is derived from studies conducted in the last twenty-five years. Advances in anatomical tracing techniques and staining methods have shown the CeA is an important forebrain component in central circuits of the autonomic nervous system. The functional implications suggested by anatomical studies of the CeA have led, in turn, to physiological and behavioral studies. The data accumulated in recent years has shaped the concept that the CeA is a key structure in the integration and mediation of

visceral responses involved in various adaptive or motivated behaviors.

TABLE I
CeA EFFERENTS

TELENCEPHALON

Perirhinal
Deacon et al. '83 (rat)

Caudate-putamen
Russchen & Price '84 (rat)

Basal forebrain/fundus striatum
Grove & Nauta '84 (rat)
Zaborszky et al. '84, '85 (rat)
Price & Amaral '81 (monkey)

Bed nucleus of the of the stria terminalis
Price & Amaral '81 (monkey)
Weller & Smith '82 (rat)
Cassell et al. '86 (rat)
Krettek & Price '78a (rat, cat)

INTRAAMYGDALOID

Anterior amygdaloid area
Krettek & Price '78a (rat, cat)

Substantia innominata
De Olmos '72 (rat)
Krettek & Price '78 (rat , cat)
Price & Amaral '81 (monkey)

Basomedial
Danielson et al. '89 (rat)

Medial
Danielson et al. '89 (rat)

Posterolateral cortical
Nitecka et al. '81 (rat)
Otterson '82 (rat)
Danielson et al. '89 (rat)

Basolateral
Danielson et al. '89 (rat)

Posteromedial cortical
De Olmos '72 (rat)
Danielson et al. '89 (rat)

DIENCEPHALON

HYPOTHALAMIC NUCLEI

Dorsomedial
Luiten & Room '80 (rat)
Berk & Finkelstein '81 (rat)

Lateral hypothalamic/
perifornical nucleus
Swanson '76 (rat)
Krettek & Price '78b (rat, cat)
Shiosaka et al. '80 (rat)
Berk & Finkelstein '81 (rat)
Veening et al. '82 (rat)
Danielson et al. '89 (rat)
Price & Amaral '81 (monkey)

Paraventricular
Berk & Finkelstein '81 (rat)
Silverman et al. '81 (rat)
Sawchenko & Swanson '83 (rat)
Gray et al. '89 (rat)

Lateral preoptic
Kita & Oomura '82b (rat)

Medial preoptic
Berk & Finkelstein '81 (rat)

Posterior
Hopkins & Holstege '78 (cat)

Ventromedial
De Olmos & Carrer '78 (rat)
Berk & Finkelstein '81 (rat)
Kita & Oomura '82a (rat)
Cassell et al. '86 (rat)

THALAMUS

Midline Nuclei

Herkenheim '79 (rat)
Hopkins & Holstege '78 (cat)
Price & Amaral '81 (monkey)
Aggelton & Mishin '84 (monkey)
Price et al. '87 (monkey)

MESENCEPHALON

Periaquaductal gray

Swanson '76 (rat)
Morrell et al. '81 (rat)
Beitz '82 (rat)
Swanson et al. '84 (rat)
Van der Kooy et al. '84 (rat)
Hopkins & Holstege '78 (cat)
Price & Amaral '81 (monkey)

Retrorubral field

Wallace et al. '89 (rat)

Substantia nigra/ventral tegmental area

Bunney & Aghajanian '76 (rat)
Krettek & Price '78b (rat, cat)
Cassell et al. '86 (rat)
Danielson et al. '89 (rat)
Wallace et al. '89 (rat)
Hopkins & Holstege '78 (cat)
Price & Amaral '81 (monkey)

Mesencephalic reticular formation

Hopkins & Holstege '78 (cat)

BRAINSTEM

PONS

Pedunculopontine

Jackson & Crossman '81 (rat)
Swanson et al. '84 (rat)
Hopkins & Holstege '78 (cat)

Subcoeruleus

Wallace et al. '89 (rat)
Hopkins & Holstege '78 (cat)
Price & Amaral '81 (monkey)

Raphe

Hopkins & Holstege '78 (cat)
Price & Amaral '81 (monkey)

Parabrachial

Fulwiler & Saper '84 (rat)
Van der Kooy et al '84 (rat)
Danielson et al. '89 (rat)
Hopkins & Holstege '78 (cat)
Price & Amaral '81 (monkey)

Locus coeruleus

Van der Kooy et al. '84 (rat)
Danielson et al. '89 (rat)
Wallace et al. '89 (rat)
Hopkins & Holstege '78 (cat)
Price and Amaral '81 (monkey)

MEDULLA

Nucleus of the solitary tract
Cassell et al. '86 (rat)
Danielson et al. '89 (rat)
Wallace et al. '89 (rat)
Hopkins and Holstege '78 (cat)
Onai et al. '87 (cat)
Schwaber et al. '82 (rabbit)
Price and Amaral '81 (monkey)

Nucleus ambiguus
Van der Kooy et al. '84 (rat)
Schwaber et al. '82 (rabbit)
Price & Amaral '81 (monkey)

Ventrolateral medulla
Danielson et al. '89 (rat)
Cassell and Gray, '89b (rat)
Wallace et al. '89 (rat)

Medullary reticular formation
Kawai et al. '82 (rat)

Dorsal motor nucleus of 10
Cassell et al. '86 (rat)
Danielson et al. '89 (rat)
Hopkins & Holstege '78 (cat)
Schwaber et al. '82 (rabbit)
Price & Amaral '87 (monkey)

SPINAL CORD

Cervical segments
Mizuno et al. '85

TABLE II
CeA AFFERENTS

TELENCEPHALON

CORTEX

Piriform
Veening '78 (rat)
Otterson '82 (rat)

Insular
Saper '82 (rat)
Otterson '82 (rat)
Russchen '82 (cat)
Turner & Zimmer '84 (rat)
Kapp et al. '85 (rabbit)

Infralimbic/prelimbic
Otterson '82 (rat)
Russchen & Lohman '79 (cat)
Powell '78 (monkey)
Baleydier & Mauguiere '80 (monkey)

Periamygdaloid
Otterson '82 (rat)
Aggleton et al. '80 (monkey)
Price & Amaral '81 (monkey)

Entorhinal
Veening '78 (rat)
Otterson '82 (rat)
Russchen '82 (cat)
Lusken & Price '83 (rat)

Tenia tecta
Otterson '82 (rat)
Cassell and Wright '86 (rat)

Perirhinal
Norgren & Grill '76 (rat)
Veening '78 (rat)
Otterson '82 (rat)
Russchen '82 (cat)
Turner & Zimmer '84 (rat)

CA1 hippocampus/subiculum
Otterson '82 (rat)
Veening '78 (rat)
Russhen '82 (cat)
Aggelton et al. '80 (monkey)
Witter & Groenewegen '86 (monkey)

Basal forebrain
Cechetto et al. '83 (cat)
Domesick '76 (rat)
Otterson '80 (rat)

INTRAAMYGDALOID

Bed nucleus of the stria terminalis
Conrad & Pfaff '76 (rat)
Swanson & Cowan '79 (rat)
Otterson '80 (rat)
Millhouse & De Olmos '83 (rat)
Saper '84 (rat)

Medial amygdala
Roberts et al. '82 (rat)
Cechetto et al. '83 (cat)
Aggelton '85 (monkey)
Price et al. '87 (monkey)

Basolateral amygdala
Otterson '82
Krettek & Price '78 (rat, cat)
Cechetto et al. '83 (cat)
Price & Amaral '81 (monkey)
Smith and Millhouse '85 (mouse)

Basomedial amygdala
Weller & Smith '82 (rat)
Otterson '82 (rat)

Posteromedial cortical amygdala
De Olmos et al. '85 (rat)

Anterior amygdaloid area
Otterson '80 (rat)

Posterolateral cortical amygdala
Luskin & Price '83 (rat)
Otterson '80 (rat)

Anterior cortical amygdala
Otterson '82 (rat)

Lateral amygdala (possibly intraamygdaloid portion of bed nucleus of the stria terminalis)
Krettek & Price '78 (rat, cat)
Otterson '82 (rat)
Cechetto et al. '83 (cat)

Substantia Innominata
Otterson '80 (rat)
Russchen '82 (cat)
Nagai '82 ( )

DIENCEPHALON

HYPOTHALAMIC NUCLEI

Lateral hypothalamic /perifornical
Renaud & Hopkins '77 (rat)
Veening '78 (rat)
Pretorious et al. '79 (rat)
Otterson '80 (rat, cat)
Amaral et al. '82 (monkey)
Russchen '82 (cat)
Cechetto et al. '83 (cat)

Dorsal
Otterson '80 (rat, cat)
Cechetto et al. '83 (cat)

Anterior
Cechetto et al. '83 (cat)

Paraventricular
Russchen '82 (cat)
Cechetto et al. '83 (cat)

Arcuate
Renaud & Hopkins '77 (rat)
Otterson '80 (rat, cat)
Russchen '82 (cat)

Posterior
Pretorius et al. '79 (rat)
Otterson '80 (rat, cat)
Cechetto et al. '83 (cat)

Ventromedial
Veening '78 (rat)
Saper et al. '76
Cechetto et al. '83 (cat)
Amaral et al. '82 (monkey)

THALAMUS

Parafasicular complex
Veening et al. '78 (rat)
Otterson & Ben-Ari '79 (rat, cat)
Aggelton '80 et al. (monkey)

Paraventricular
Cechetto et al. '83 (cat)
Otterson & Ben-Ari '79 (rat)
Aggelton '80 et al. (monkey)

Premammillary
Krieger et al. '79 (rat)
Otterson '82 (rat)

Medial geniculate
Otterson & Ben-Ari '79 (rat)
LeDoux et al. '84 (rat)

MESENCEPHALON

Central grey
Otterson '82 (rat)
Aggelton et al. '80 (monkey)

Ventral tegmental area
Otterson & Ben-Ari '78 (rat)
Amaral et al. '82 (monkey)

Substantia nigra
Otterson & Ben-Ari '78 (rat)
Aggelton et al. '80 (monkey)

Peripeduncular nucleus
Otterson & Ben-Ari '78 (rat)
Aggelton et al. '80 (monkey)

BRAINSTEM

Parabrachial nucleus
Norgren '76 (rat)
Otterson & Ben-Ari '78 (rat)
Veening '78 (rat)
Vooshart & Van der Kooy '81 (rat)
Saper & Loewy '80 (rat)
Cechetto et al. '83 (cat)

Dorsal raphe
Otterson & Ben-Ari '78 (rat)
Veening '78 (rat)

Nucleus of the solitary tract
Ricardo & Koh '78 (rat)
Zardetto-Smith & Gray '86a (rat)

Locus coeruleus
Cechetto et al. '83 (cat)

TABLE III
LOCALIZATION OF NEUROPEPTIDE PERIKARYA
WITHIN THE CeA

PEPTIDE	CeA SUBDIVISION	REFERENCE
Neurotensin	CeLC, CeL & some CeM	Cassell et al. '86 Gray & Magnuson '87a Wray & Hoffman '83
CRF	CeL & CeV, also dorsal CeM	Cassell et al. '86 Gray & Magnuson '87a
Somatostatin	CeL & CeLC, also lateral CeM	Cassell et al. '86 Gray & Magnuson '87a Wray & Hoffman '83
Enkephalin	CeL & CeLC	Cassell et al. '86 Gray & Magnuson '87a
Substance P	CeM & CeLC	Cassell et al. '86 Gray & Magnuson '87a Wray & Hoffman '83
Galanin	CeM	Gray & Magnuson '87b
Dynorphin	CeL & CeLC	Zardetto-Smith et al. '84

Table IV
DISTRIBUTION OF NEUROPEPTIDE/NEUROTRANSMITTER TERMINALS WITHIN THE CeA

PEPTIDE	CeA SUBDIVISION	REFERENCE
Angiotensin II	CeL & CeLC	Cassell et al. '82
Atriopeptin	CeM & CeV	Standaert et al. '86
Bombesin	Not specified	Panula et al. '82
Calcitonin-gene related peptide	CeL & CeLC some CeM	Schwaber et al. '88
Catecholamine	CeM, CeV, some CeL & CeLC	Fallon et al. '78
Cholecystokinin	Not specified	Loren et al. '79 Vanderhaeghen et al. '81
CRF	CeL	Veening et al. '84
Dynorphin	CeL & CeLC some CeV & CeM	Zardetto-Smith et al. '84
Enkephalin	CeL, CeLC, CeV some CeM	Gray et al. '84 Zardetto-Smith et al. '84
Galanin	CeM	Rokaeus et al. '84
Neurotensin	CeLC	Cassell et al. '82 Wray & Hoffman '83
Neuropeptide Y	CeM, few CeL	Gray et al. '86
Proopiomelano-cortin	CeM	Gray et al. '84
Serotonin	All divisions	Fallon '81
Somatostatin	All divisions	Cassell et al. '82 Wray & Hoffman '83
Substance P	CeL & CeLC	Cassell et al. '82 Wray & Hoffman '83
Thyrotropin-releasing factor	Not specified	Lechan et al. '83
Vasoactive intestinal polypeptide	CeL	Cassell et al. '82 Wray & Hoffman '83 Gray et al. '84

TABLE V
NEUROPEPTIDE CONTENT OF CeA EFFERENTS

PEPTIDE	SITE OF TERMINATION	REFERENCE
CRF	Parabrachial nucleus	Moga & Gray '85
	Dorsal vagal complex	Veening et al. '84
		Gray & Magnuson '87b
Enkephalin	Bed nucleus of the stria terminalis	Uhl et al. '78
Galanin	Central gray	Gray & Magnuson '87a
Neurotensin	Parabrachial nucleus	Moga & Gray '85
	Dorsal vagal complex	Veening et al. '84
		Gray & Magnuson '87b
Somatostatin	Medial preoptic-hypothalamic region	McDonald '87
	Reticular formation	Kawai et al. '82
	Parabrachial nucleus	Moga & Gray '85
	Dorsal vagal complex	Higgins & Schwaber '83
		Gray & Magnuson '87b
Substance P	Parabrachial nucleus	Milner & Pickel '86
	Dorsal vagal complex	Veening et al. '84
		Gray & Magnuson '84

TABLE VI
NEUROPEPTIDE/NEUROTRANSMITTER CONTENT OF CeA AFFERENTS

PEPTIDE	SITE OF ORIGIN	REFERENCE
Calcitonin gene-related peptide	Parabrachial nucleus	Shimada et al. '85 Schwaber et al. '88
Cholecystokinin	Substantia nigra/ventral tegmentum	Fallon et al. '83
Dopamine	Substantia nigra/ventral tegmentum	Fallon et al. '78
Dynorphin	Lateral hypothalmus Substantia nigra/ ventral tegmentum	Zardetto-Smith et al. '88 Code & Fallon '86
Neurotensin	Parabrachial nucleus Pons & medulla	Block et al. '89 Kawakami et al. '84
Norepinephrine	A5/A2 catecholaminergic groups	Fallon et al. '78
Proopiomelano-cortin	Arcuate nucleus	Gray et al. '84
Serotonin	B7, B6, B5, B8 serotonergic groups	Fallon '81
Substance P	Parabrachial nucleus	Block et al. '89
Vasoactive intes-tinal polypeptide	Central gray/raphe	Eiden et al. '85

Figure 1. Schematic illustration of cytoarchitectural subdivisions of the central nucleus of the amygdala (CeA) as per the nomenclature of Cassell et al. '86, at three different rostral-caudal levels (distance from bregma (mm) is given to the left of each line drawing). Abbreviations for central nucleus subdivisions: CeM = medial; CeL = lateral; CeV = ventral; CeLC = lateral capsular.

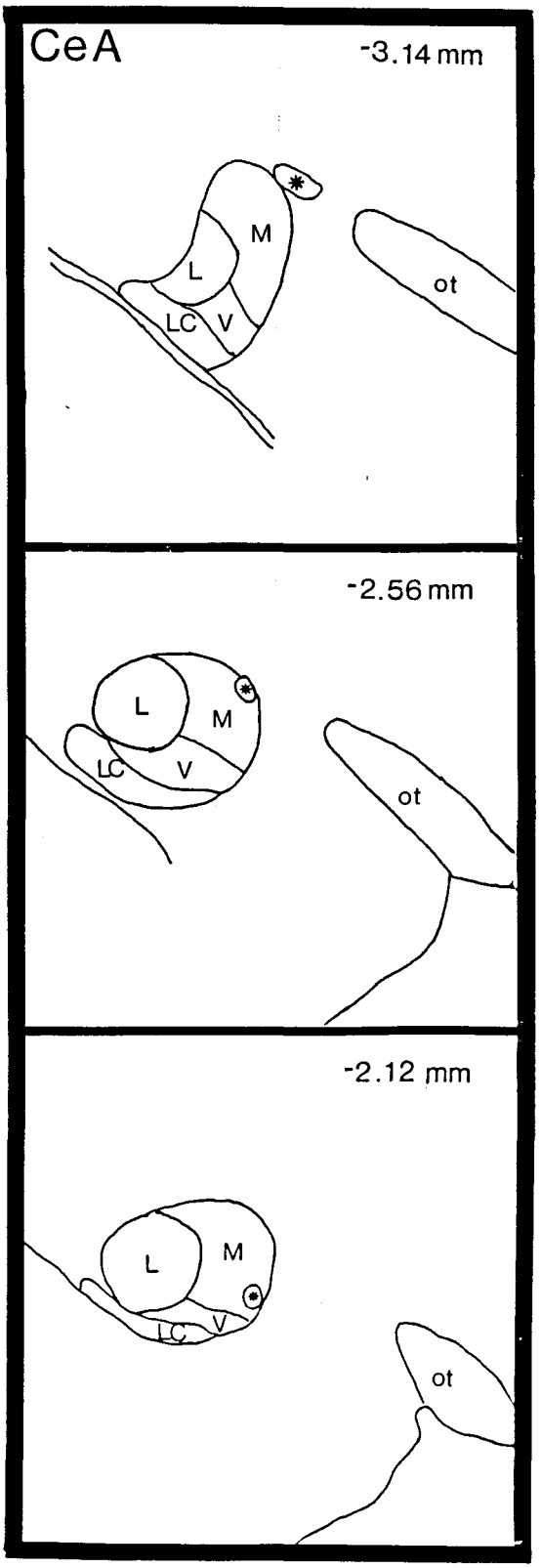
CeA
-3.14 mm
M
L
LC
V
ot
-2.56 mm
L
M
LC
V
ot
-2.12 mm
L
M
LC
V
ot

CHAPTER III

ORGANIZATION OF EFFERENTS FROM THE NUCLEUS OF THE SOLITARY TRACT TO THE AMYGDALA AND BED NUCLEUS OF THE STRIA TERMINALIS IN THE RAT: A PHA-L STUDY

INTRODUCTION

The central nucleus of the amygdala (CeA) is distinctive among the amygdaloid nuclei by virtue of its multiple connections with brainstem and forebrain nuclei directly involved in autonomic control (Mogenson and Calaresu, '73; Faiers et al., '75; Kapp et al., '82; Galeno and Brody, '83). Reciprocal connections with brainstem and forebrain nuclei that modulate sympathetic and parasympathetic outflow provide an anatomical basis for direct amygdaloid influences on autonomic-related nuclei. These nuclei collectively mediate the autonomic responses associated with various adaptive behaviors, e.g., fear, anger, flight, orientation, and the defense reaction (Hilton and Zbrozyna, '63; Kaada, '72).

Sensory feedback from the viscera is an integral feature of central nervous system regulation of the cardiovascular, respiratory, and gastrointestinal systems. The general visceral afferent fibers of the glossopharyngeal and vagus nerves terminate within the brainstem in the caudal portion of the nucleus of the solitary tract (NTS) (for reviews, see Paintal, '73; Kalia, '81; Altshuler at al., '89). These afferents convey primarily baroreceptor, chemoreceptor, and visceral

stretch receptor input to the central nervous system. The rostral part of the NTS is concerned primarily with gustatory function (Norgen and Leonard, '73).

Bailey and Bremer ('38) were the first to note that stimulation of the central stump of the vagus nerve in the cat increased electrical potentials in the frontal lobe, giving support to the notion that vagal afferent input could reach forebrain structures. Similarly, Dell and Olsen ('51) stimulated the central stump of the cervical vagus in the cat and recorded evoked potentials with short latencies in insular cortex, thalamus, and hypothalamus. Nearly thirty years later, Ricardo and Koh ('78) became the first investigators to demonstrate anatomically that the NTS projected directly to the amygdala using both anterograde (autoradiography) and retrograde (horseradish peroxidase, HRP) tract tracing methods. Their initial findings were later confirmed in other HRP studies in the rat (Pretorius et al., '79; Otterson, '81), although studies in the cat (Russchen, '82; Cechetto et al., '83) and monkey (Mehler '80) have failed to provide unequivocal evidence of a NTS-CeA pathway.

In autoradiographic experiments, Ricardo and Koh ('78) also noted a substantial amount of axonal label present in the lateral part of the subcommissural bed nucleus of the stria terminalis (BST) following injections into the NTS. Retrograde experiments, in which HRP was injected into this region of the BST, confirmed this projection. In these experiments the medial part of the NTS was the most heavily labeled. The BST, particularly its lateral subdivision, is similar to the CeA in some aspects of its cytoarchitecture (McDonald, '83) and chemoarchitecture (Woodham et al., '83; De Olmos et al., '85). Like the CeA, the lateral BST can be distinguished by its reciprocal connections with nuclei involved in central autonomic regulation

(Holstege et al., '85; Sofroniew, '83; Moga et al., '86).

The assumption of a functional role in autonomic regulation for the CeA and BST on the basis of their anatomic circuitry has been supported by physiologic studies. For example, stimulation of the CeA in various species causes changes in heart rate, blood pressure, blood flow distribution, and respiration (Mogenson and Calaresu, '73; Faiers et al., '75; Kapp et al., '82; Galeno and Brody, '83; Harper et al., '84; Brown et al., '86). Also, the CeA has been shown to be involved in learned cardiovascular responses (Kapp et al., '81; Zhang et al., '86). Chronic stimulation of the CeA produces gastric ulcers, while its destruction reduces the incidence and severity of stress-induced ulcers (Henke, '82; Ray et al., '87). In the rat stimulation of the aortic nerve causes an increase in 2-deoxyglucose uptake within the CeA (Ciriello et al., '83). The BST may participate in the baroreceptor reflex and possibly plays a role in fluid intake and electrolyte balance (Swanson and Sharpe, '73; Lind et al., '84).

The direct projection from the NTS to the CeA and BST in the rat represents one route by which visceral afferent information is conveyed from peripheral receptors to the forebrain. In this investigation, the NTS-CeA and NTS-BST ascending pathway was examined in further detail using the sensitive anterograde tracer Phaseolus vulgaris leucoagglutinin (PHA-L). This technique offers several advantages over previously used anatomical tracing techniques. It is not taken up by fibers-of-passage, injections can be extremely discrete, and axons and terminals are labeled in a Golgi-like manner (Gerfen and Sawchenko, '84). The present study confirms the topographical relationship between the neurons within the caudal NTS and their terminal fields within the CeA and BST implied in the Ricardo and Koh ('78) study, and extends their original observations concerning this ascending pathway.

In the course of these experiments, a direct projection from the NTS to the subfornical organ, a circumventricular organ involved in regulating fluid balance in response to angiotensin II and changes in blood pressure (Miselis, '81; Lind et al., '82; Lind et al., '84; Dellman, '85; Swanson and Lind, '86), was demonstrated for the first time. This finding is discussed separately in Chapter 7 of this dissertation.

METHODS

Long-Evans male rats (200-475 gm) were used in this study. Animals were anesthetized with sodium pentobarbital (55 mg/kg) and placed in a stereotaxic apparatus (Kopf). PHA-L (Vector Laboratories) was dissolved to a 2.5% solution of 0.1 M phosphate buffered saline (PBS) at pH 7.6 and placed in a glass micropipette (outer tip diameter 10-20 um) that was lowered into the brainstem. The NTS was accessed by way of a dorsal surgical approach through the atlanto-occipital membrane. Placement of the pipette tips was determined by stereotaxic coordinates (Paxinos and Watson, '86), using the obex as a reference point. Several different sets of coordinates were used to target various subregions of the NTS at different rostral-caudal locations of the NTS. In each animal a single unilateral iontophoretic application of PHA-L was placed within the dorsal medulla using a Midgard Electronics model CS3 constant current device (5-7 uA delivered in 7 s pulses every 14 s over a 30-45 min period).

Animals survived 10-21 days and then were administered a lethal dose of sodium pentobarbital. The animals were perfused according to the method described by Gerfen and Sawchenko ('84). Briefly, 100 ml of PBS (pH 7.6, 37 C) was perfused through the ascending aorta. This was followed by 250 ml of 4% paraformaldehyde and 0.05% gluteraldehyde in 0.167 M phosphate buffer (pH 6.5, 4 C), after which 250 ml of 4% paraformaldehyde and 0.05% gluteraldehyde in 0.167 M phosphate buffer (pH 8.5, 4 C) followed. The brains were removed and postfixed 20-60 min. Adjacent 20 um coronal sections of the brainstem and forebrain were cut using a vibratome (Lancer). Sections were washed first in phosphate buffered saline containing 0.25% Triton-X 100 (Mallinckrodt) (PBS-tx) for 30-60 min in order to remove excess fixative. Next, the tissue was

incubated for 30-45 min in 0.3% hydrogen peroxide, followed by a short PBS rinse. Sections were next incubated 24-36 h in either rabbit or goat antibodies to PHA-L (Dako) diluted 1:1000 in a solution of 1% normal goat, normal swine, or normal donkey serum and PBS-tx. After incubation with the primary antibody, sections were rinsed for 20 min in PBS-tx and placed in the appropriate immunogammaglobulin-conjugated biotin: either goat anti-rabbit (Bethesda Research Laboratories, diluted 1:300 in 0.25% PBS-tx), swine anti-goat (Tago, diluted 1:500 in 0.25% PBS-tx), or donkey anti-rabbit (diluted 1:5000 in 0.25% PBS-tx) (Bethesda Research Laboratories) for 45-60 min. The tissue was then rinsed briefly in PBS-tx (15 min) and the sections placed in a solution of streptavidin-bound horseradish peroxidase (Bethesda Research Laboratories) diluted (concentration depended on lot number of streptavidin-HRP received) in PBS-tx for 45-60 min. Following this incubation, the tissue was washed 15 min in 0.1M Tris (trizma base, Sigma Chemicals) buffer (pH 7.6) and reacted using 12.5 mg diaminobenzidine (DAB, Hach) as a substrate in 25 ml 0.1M Tris buffer (pH 7.6) to which 50 ul 0.3% H2O2 was added. The reaction was stopped by placing the sections in cold PBS. Sections were then mounted on acid-cleaned, gel-coated slides and cover-slipped with Permount (Fischer Scientific Chemicals) mounting media. Adjacent sections were counterstained with cresyl violet or left unstained. Slides were examined using an Olympus microscope with both dark and light field illumination. Axonal and cell body PHA-L immunoreactivity was plotted using a camera lucida attachment, and photographs taken using Polaroid coaterless land pack film 667, ASA 3000/35 DIN or Kodak Ektachrome color slide film, ASA 400 daylight.

To aid in cytoarchitectonically defining NTS terminal fields, in three cases in which the injection was centered within the NTS, two

sets of tissue from each animal were processed further for peptide immunoreactivity using a modification of the glucose-oxidase (GO) technique (Piekut, '87). This procedure labeled immunocytochemically identified cells with a blue to purple reaction product, in contrast to the brown reaction product of the PHA-L. Thus, PHA-L labeling (brown) was observed in relationship to immunostained terminal fields and/or cell bodies (purple-blue). The procedure began by rinsing the PHA-L DAB reacted sections in 0.25% PBS-tx, agitating for several hours at room temperature, on the day the DAB reaction was done. The tissue was then transferred to fresh 0.25% PBS-tx, and left in the refrigerator for 5-7 days. The sections were then pretreated with phenazine methosulfate (Sigma Chemical) to inhibit the DAB from reacting with the glucose-oxidase solutions. After several rinses in 0.25% PBS-tx, sections were incubated for 42-66 hr with anti-neurotensin (Dr. Marvin Brown, diluted 1:1000 in 0.1% PBS-tx and 1% normal donkey serum). Following incubation with the primary antibody, sections were rinsed in 0.25% PBS-tx for 30 min, then incubated for 60 min in biotinylated immunogammaglobulin (donkey anti-rabbit, Jackson Immunoresearch, dilution 1:5000 in 0.25% PBS-tx). Sections were then rinsed again in 0.25% PBS-tx for 15 min and incubated in egg white avidin-glucose oxidase (Jackson Immunoresearch, dilution 1:150) for 60 min.

The next step was to rinse the sections for 15 min with 0.05 M phosphate buffer, pH 8.3. Following this, the sections were placed in the GO solution. This solution was made by combining 1 ml of phenazine solution (6.7 mg of phenazine methosulfate (Sigma Chemical) in 10 ml of 0.05 M, pH 8.3 phosphate buffer) and 49 ml of nitro blue solution (165 mg B-deoxyglucose [Mannheim Chemicals], 16.5 mg nitro-p-blue tetrazolium [Research Organics Inc] in 49 ml 0.05M, pH 8.3 phosphate buffer). During the reaction, sections were kept in the dark, in a water

bath heated to approximately 40 C. The reaction was stopped by immersing the sections in cold PBS, and mounted on acid-cleaned, gel-coated slides immediately. Slides were coverslipped with Permount without defatting or immersion in xylene, and examined as outlined above.

RESULTS

Injections of PHA-L into the NTS were attempted in a total of 51 animals. Of these, 18 had discernible injection sites visible within the NTS or surrounding areas. In 12 of the 18 cases, the injection was primairly confined to the NTS, labeling a total of 10 or less neurons within the borders of the dorsal motor nucleus of the vagus (DMV) or nucleus gracilis. In 2 animals, the injection was centered in the NTS but also labeled several neurons within the DMV and hypoglossal nucleus. In 4 other cases, the injection was not centered within the NTS. In 2 of these 4 cases, the injection site was confined to either the hypoglossal or cuneate nucleus, and did not involve neurons in the NTS (NP 2, NP 21; Fig. 1). In these particular animals, PHA-L terminal or fiber labeling was not present within the CeA or BST. The remaining 2 cases had injection sites centered within the DMV or gracilis fasciculus, with minor spread to the NTS; in these 2 animals, only trace fibers were observed in the CeA and BST.

PHA-L labeled axons and terminals were present within the CeA and BST in all 14 cases in which the injection was centered in the NTS, although their topographic distribution appeared to vary with the rostro-caudal level of the NTS involved. For this reason, injection sites within the NTS were classified as a) caudal to the area postrema (n=4); b) at the level of the area postrema (n=6); or c) rostral to the area postrema, either ventricular (n=2) or subvestibular portions (n=2) of the NTS. The location of the injection centers within the NTS were determined through cytoarchitectural delineation of nuclear boundries (as previously defined by Kalia and Sullivan, '82 and Altshuler et al., '89) in Nissl-stained sections.

One representative case for each type of NTS injection is

illustrated in Figures 3, 4, 5, 6, and 7. The distribution of PHA-L label within the CeA and BST in these cases shown is representative of labeling in other cases produced by injections at that particular level of the NTS. In each figure, the injection site, and the resultant labeling produced in the CeA and BST in that case, are plotted. For the sake of clarity, only sections ipsilateral to the injection are shown. Labeling was, however, present bilaterally in all areas, though much sparser on the contralateral side. Within each figure, sections are arranged in a caudal-to-rostral fashion so that differences in the patterns of ascending NTS efferents can be easily compared. The nomenclature and cytoarchitectural differentiation of the BST and CeA (see Fig. 2 and List of Abbreviations for subnuclei classification) were made according to the descriptions of Moga et al. ('89) and Cassell et al. ('86), respectively.

Caudal injections. NP 5 is a case typifying axonal labeling in the CeA and BST resulting from a PHA-L injection into the caudal NTS (Fig. 3A). The majority of labeled cells at this injection site were located within the commissural nucleus of the NTS, just lateral to the central canal and dorsal to the DMV. A scattering of labeled neurons extended laterally just above the DMV, ending medial to the solitary tract. A few labeled cell bodies were present along the dorsal and lateral border of the DMV. Some labeled cells and fibers extended across the midline to the contralateral NTS, where 2-3 labeled cells were present.

At the most caudal level of the CeA (Fig. 3B-1), where the stria terminalis joins the optic tract, one or two varicose fibers with terminal boutons were present within the CeA, with several more varicose fibers present within the basolateral nucleus of the amygdala.

Sparse label was also observed within the intercalated amygdaloid nuclei. Fibers could be seen passing along and over the optic tract to enter the amygdala, within the ventral amygdalofugal pathway, while some fibers appeared in the medial forebrain bundle. At intermediate levels of the CeA, a few axons were present within the CeM and CeLC, with a somewhat heavier concentration of labeling within CeV (Fig. 8B). Some fibers appeared to exit the CeA at this level, dorsal to the stria terminalis and extending medially into the substantia innominata. These fibers became more numerous at the most rostral extent of the CeA (Fig. 3B-3), ascending through the sublenticular substantia innominata, and reaching the ventral BST, where a very dense plexus of fibers appeared (Fig. 8A). Generally, posterior (Fig. 3C-1) and medial divisions (Fig. 3C, 1-3) of the BST received few fibers, though the ventral medial (VM) and preoptic (PO) subnuclei were lightly innervated.

At the level where the anterior commissure crosses the midline, most axons and terminals were densely localized to the ventral lateral (VL) subnucleus (Fig. 3C-3). A few beaded fibers were present within the anterior lateral (AL), parastrial (PS), dorsal lateral (DL), and anterior medial (AM) subnuclei. At the most rostral limits of the BST, varicose fibers surrounded the dorsal, medial and ventral aspects of the anterior commissure.

Tables 1 and 2 indicate the relative density of labeling observed in various subnuclei of the CeA and BST for each representative case discussed. In NP 5, PHA-L labeling within the BST was heaviest in a ventral subnucleus, VL. Likewise, within the CeA, PHA-L label was most concentrated within CeV. Comparatively, BST-VL appeared to be more densely innervated than CeV (i.e., Fig. 3B-3 vs. Fig. 3C-3; Fig. 8A vs. 8B).

Fibers within the basolateral and intercalated amygdaloid

nuclei exhibited what appeared to be varicosities of the en passant type, with terminal varicosities observed less frequently. The injection in NP 5 (and all other caudal injections) labeled a number of other forebrain areas previously shown to receive innervation from the NTS (Table 3). With the exception of the parvocellular paraventricular hypothalamic nucleus (PVNp), the perifornical-lateral hypothalamic area (PeF-LH), and periventricular nucleus (Pe), labeling in these areas was sparse.

Injections at the level of the area postrema. The density and distribution of labeled fibers within the CeA and BST varied with the site of injection within the NTS at this level (Table 1). For this reason, labeling within the CeA in all three cases will be collectively discussed first. A similar collective discussion of labeling in the BST in the same three cases will then follow.

At the level of the area postrema, one injection (NP 41) into the NTS was centered at the lateral aspect of the solitary tract (Fig. 4A). Cells in the ventrolateral and interstitial subnuclei of the NTS were labeled, with spread of labeled cells dorsally into the cuneate nucleus. At caudal levels to intermediate levels of the CeA, only one or two fibers were present in CeM, while at more rostral levels, a few more varicose fibers were present (Fig. 4B, 1-3). Fibers or terminals were not observed in other amygdaloid nuclei.

Two injections at the level of the area postrema involved the dorsal and medial aspects of the solitary tract, labeling cells in the dorsolateral, intermediate, and central subnuclei of the NTS (NP 19, Fig. 5A). Some labeled cells were present within the solitary tract itself, ventral to the solitary tract, and at the lateral aspects of the DMV bordering the NTS. A few labeled neurons were also present

within the subnucleus gelatinosus of the NTS. At caudal aspects of the CeA, some fibers passed along and over the optic tract (within the ventral amygdalofugal pathway) to enter CeM. Several varicose fibers were present within CeM, with sparser labeling in CeV, CeL and CeLC (Fig. 5B-1, Fig. 9) At mid-level, several very fine, beaded fibers were seen in CeV and CeL (Fig. 5B-2). Labeled axons in CeLC appeared to continue into the intercalated and basomedial amygdaloid nuclei (Fig. 5B-3), while a few scattered fibers were present within the basolateral amygdaloid nucleus. At rostral extents of the CeA, several fibers extended from its dorsomedial aspect into the sublenticular substantia innominata (Fig. 5B-3).

Three injections at the level of the area postrema were centered in the area of the NTS dorsal to the DMV and ventral to the area postrema. The largest of the injections (NP 45) included neurons in the medial and commissural subnuclei (Fig. 6A). Labeled cells were not present in the area postrema, though fibers extended from the injection site into it. This particular injection, by far, produced the greatest amount of axonal and terminal labeling within the CeA of any injection in this study. The two other injections into this area also produced comparatively more labeling in the CeA than injections at other levels of the NTS. Although the topographic distribution of fibers and terminals in these two cases were the same as that seen in NP 45, their density and number was considerably less.

Figure 6B illustrates the distribution of PHA-L immunoreactivity present within the CeA in case NP 45. At the most caudal end of the CeA, numerous varicose fibers and terminal sprays were present in CeM, and CeV, with fewer fibers and terminal varicosities scattered through CeL and CeLC (Fig. 10A). In addition, varicose fibers were scattered through the medial, basomedial, and basolateral amygdaloid

nuclei (Fig. 6B, 1-3). Beaded axons and terminals were also observed in the cortical amygdaloid nuclei. Several fibers were seen coursing in the medial forebrain bundle and along the medial and dorsal edge of the optic tract.

At intermediate levels of the CeA, fibers were concentrated within the ventral CeM, CeV, and CeLC (Fig. 6B-2, Fig. 10B). Fibers appeared to surround the dorsal and dorsolateral edges of the CeL, but few fibers were present within the subdivision itself. Sparser labeling was observed within the basomedial, basolateral, lateral, medial, and cortical amygdaloid nuclei. In particular, a prominent plexus within the posterior lateral cortical nucleus was present (Fig. 6-B2, Fig. 11). At its more rostral levels, CeM, CeV, and the medial aspect of the CeLC remained heavily innervated, with scattered fibers in CeL (Fig. 10C). Varicose axons coursed dorsally and medially from the CeA into and through the sublenticular substantia innominata to reach the BST (Fig. 6B-3).

In NP 45, beaded fibers continued dorsomedially from the substantia innominata into the posterior lateral (PL) subnucleus of the BST (Fig. 6C-1), with fewer fibers present in the posterior intermediate (PI), posterior medial (PM), and posterodorsal (PD) subnuclei (Fig. 6C-1; Fig. 12A). Several fibers were scattered throughout BST-PO. In contrast, only a few fibers were labeled within posterior subnuclei in NP 19 (Fig. 6C-1). Also, 4-5 fibers were observed within the stria terminalis itself. Further rostrally, in both NP 19 and NP 45, axonal and terminal labeling became especially dense within BST-VL (Fig. 5C-2, 6C-2; Fig. 9A, 12B). BST-AL was lightly innervated in NP 19, and moderately in NP 45 (Fig. 5C-3; Fig. 6C-3; Table 2). BST-PS was also more heavily innervated in NP 45 than in NP 19. In NP 45, PHA-L immunoreactive fibers and terminals were also scattered through-

out BST-AM, -VM, and the supracapsular (SC) subnucleus. Also, the juxtacapsular (JXC) and dorsal lateral (DL) subnuclei appeared sparsely innervated, with fibers appearing to terminate in the vicinity of the fibrous capsule surrounding DL (Fig. 5C-2). Both the CeA and BST received substantial innervation from the NTS in NP 45; however, in NP 19, more fibers appeared to terminate within the BST, especially BST-VL, than in the CeA (Tables 1 and 2; compare Fig. 9A and 9B). Again, in both NP 45 and 19, ventral portions of the CeA and BST appeared to be the most heavily innervated, i.e., BST-VL and CeV. In NP 41 (lateral NTS injection), only very sparse labeling was present within the BST; however, it was confined to the same subnuclei as in NP 19 and NP 45, i.e., BST-AL and -VL (Fig. 4C, 1-4).

In all injections centered at this level in the NTS, PHA-L immunoreactivity was present in several diencephalic nuclei known to receive NTS efferents, through the density of innervation varied with the site of injection (Table 3). In NP 41, the heaviest label was present within PVNp and PeF-LH, with very sparse innervation of all other areas. These areas received a more substantial input in NP 19 and 45. Also in these cases, PeV received a moderate amount of innervation. Within the thalamus, more fibers were present within the paraventricular nucleus (PVT) in NP 19 than in either NP 41 or 45. Of the three types of injections, varicose fibers within the subfornical organ were noted only in cases such as NP 19, in which the injection involved the dorsal and dorsolateral NTS (see Chapter 7).

Injections at levels rostral to the area postrema. Injections of PHA-L into the NTS rostral to the area postrema, either its ventricular (n=2) or subvestibular (2) portions, produced similar patterns of labeling withn the CeA or BST, as demonstrated by the distribution of

PHA-L immunoreactivity seen in NP 34 (Fig. 7). The injection in this case was centered in the medial subnucleus of the NTS, at a level just rostral to the area postrema, where the nucleus borders the fourth ventricle (Fig 7A). A few neurons within the intermediate subnucleus and subnucleus gelatinosus were also labeled.

At caudal levels of the CeA, distinct varicose fibers were observed in CeV, extending up into CeM (Fig. 7B-1; Fig. 13C). Few fibers were present in CeLC and CeL. At intermediate levels, long axons extended through CeLC into CeV (Fig. 7B-2). A few varicose fibers were present in the basomedial and medial amygdaloid nuclei. Again, at intermediate to rostral levels of the CeA, fibers exited dorsomedially to the stria terminalis into the sublenticular substantia innominata (Fig. 13B). At rostral levels of the CeA, labeled axons were sparsely scattered in CeL, CeLC, and CeV. The dorsal aspect of CeM appeared moderately innervated. Several fibers were present within the basomedial amygdaloid nucleus (Fig. 7B-3). PHA-L immunoreactivity at caudal levels of the BST was confined primarily to BST-PL and -PO. Farther rostrally, only 1-3 fibers were present within BST-VL, -PS, and -AL (Fig. 7C, 3-4). The density of label within BST-PL, -VL, and -AL was extremely reduced in comparison to that seen in caudal and intermediate NTS injections, with the exception of NP 41 (Table 2). Ventral subnuclei, i.e. CeV and BST-VL appeared to again be the most heavily innervated areas in this these injections (Tables 1 and 2), but the CeA received a more substantial innervation than the BST (compare Fig. 13A and 13C). The basomedial amygdaloid nucleus appeared to contain the most labeled fibers of any of the other amygdaloid nuclei, though most varicosities were of the en passant, (rather than the terminal) type. In other forebrain areas, label within the supraoptic and dorsomedial nuclei, PVNp, PeF-LH, and Pe was especially prominent. The antero-

ventral preoptic and arcuate hypothalamic nuclei, and the PVT, received a more modest innervation.

DISCUSSION

Methodological Considerations. In comparison to pressure injections, iontophoretic delivery of PHA-L produces the smallest possible injection sites, with reasonable degrees of reproducibility, and little tissue damage (Luiten et al., '87). A major advantage of the PHA-L technique lies in the clarity of labeling of neurons at the site of injection, allowing the effective injection site to be defined quite precisely (Gerfen and Sawchenko, '84). As only neurons whose cell bodies or dendrites lie within the central core of the injection site take up the lectin, axonal and terminal labeling observed can be interpreted reliably as arising only from cell types labeled at the injection site (Gerfen and Sawchenko, '84). Therefore, in the context of the present study, differences in the density of labeled terminals and axons within the forebrain may be attributed to differences in the size of the effective injection, whereas differences in the topography of labeling are not. Labeling within the CeA and BST produced by discrete injections of PHA-L into the NTS may be interpreted as accurately representing the terminal fields of those particular NTS neurons labeled at the injection site.

Localization of BST- and CeA-Projecting Neurons Within the NTS. The present study demonstrates that the most extensive axonal and terminal labeling within the BST and CeA resulted from injections centered in the medial subnucleus of the NTS (mNTS) at the level of the area postrema, with the BST being the most heavily innervated forebrain structure. The mNTS in the rat is the site of termination of afferent fibers from subdiaphragmatic branches of the vagus nerve (Kalia and Sullivan, '82; Shapiro and Miselis, '85; Altshuler et al., '89). The

mNTS in both the cat (Kalia and Mesulam, '80; Davies and Kalia, '81) and rat (Ciriello et al., '83; Higgins et al., '84; Altshuler et al., '89) is also the site of termination for some cardiac sensory, baroreceptor, and chemoreceptor fibers, although subnuclei located dorsal to the solitary tract appear to be the main targets within the NTS for these particular afferents. The central subnucleus, which was involved to some extent in the injection in NP 45, is the site of termination of esophageal efferents (Alstshuler et al., '89). However, unlike the mNTS, which projects to the parabrachial nucleus and forebrain (including the CeA and BST), the central subnucleus sends a major efferent projection to the nucleus ambiguus (Altshuler et al., '89; Herbert et al., '89).

The commissural subnucleus of the NTS in the cat (Kalia and Mesulam, '80; Davies and Kalia, '81) and rat (Ciriello et al., '83; Higgins et al., '84; Altshuler et al., '89) has also been shown to receive a substantial number of afferents via the carotid sinus nerve and vagus. The ventral, ventrolateral and interstitial subnuclei receive mostly respiratory related input (Kalia and Mesulam, '80; Altshuler et al.'89). In this study, injections of PHA-L into the commissural subnucleus (NP 5) resulted in a moderate amount of label within the BST, and less label within the CeA, while only trace fiber labeling was observed in either nucleus following injections which included the ventral, ventrolateral, and interstitial subnuclei (NP 41).

The injections in this study did not encompass the most rostral and lateral extents of the NTS (the area in which most gustatory nerves terminate, Hamilton and Norgren, '84). The four injections classified as "rostral" were located at the caudal or middle of the "gustatory" NTS. The gustatory NTS begins at the level where it meets the fourth ventricle; proceeding rostrally, the lingual-tonsilar branch of the

glossopharyngeal nerve, conveying gustatory information, terminates in both the medial and lateral NTS (Hamilton and Norgren, '84). The lack of substantial PHA-L label in the BST from rostral, medial NTS injections in this study may reflect the beginning of the transition in the NTS from visceral to gustatory function. Alternatively, the majority of taste information may be relayed to the BST via the parabrachial nucleus (Norgren, '76), instead of directly through the NTS. Taste input to the CeA is also conveyed from the parabrachial nucleus (Norgren, '74, '76; Yamamoto et al., '80; Block and Schwartzbaum, '83) as well as the cortical gustatory area (Norgren and Grill, '76; Yamamoto et al., '84). Possibly, taste information relayed to the CeA from the rostral NTS complements that conveyed to the CeA indirectly, and may be significant in the motivational aspects of ingestive behavior, in which the CeA is thought to play a role (Pfaffman et al., '77). Further anatomical and physiologic experiments will be required to define clearly the extent of rostral NTS input to both the BST and CeA, and their significance in gustatory function and ingestive behavior.

Collectively, these results imply the BST is a major forebrain target of the caudal NTS, possibly more so than the CeA. Subnuclei of the NTS which receive input from cardiovascular and gastrointestinal afferents project to both the BST and CeA. In contrast, respiratory-related subnuclei appear to have virtually no input to the CeA or BST.

Organization of Efferents to the BST and CeA Within the NTS. The origin of NTS efferents to the CeA and BST differed in two aspects of its organization. First, there were differences in the density of labeling within the BST and CeA when different caudal-rostral levels of the NTS were injected, indicating the presence of a caudal-to-rostral organization. Secondly, NTS efferents to the BST and CeA originated

from the medial NTS, rather than the lateral NTS, indicating neurons projecting to the CeA and BST also are organized in a medial-to-lateral fashion.

Caudal-to-rostral organization. The density of labeling within the BST and CeA appeared to differ with the particular caudal-rostral level of the NTS injected. Possibly this was artifactual, resulting from the extent to which a particular subnucleus was labeled by the PHA-L injection at given level, i.e., topographic variations in reality represent efferents arising from different NTS subnuclei. Evidence from this study and others does not support this view. In the present study, NP 45 and NP 34 are examples of injections which primarily involved the medial subnucleus of the NTS at different caudal-rostral levels. In NP 45, where the injection was at the level of the area postrema, dense labeling within the ventral BST and CeA (Fig. 6B-2, 6C-3) was present. The injection at a more rostral level of the medial subnucleus (NP 34) produced sparse label within the ventral BST, but moderate innervation of the ventral CeA (Fig. 7C-3, 7B-2). Approximately the same number of neurons were labeled at the injection site in NP 45 than in NP 34 (143 vs. 128, raw counts, uncorrected for double-counting errors); thus, size of the injection alone is unlikely to account for the differences observed. For example, comparing the number of neurons labeled in NP 5 versus NP 34 that were labeled at the injection site (144 vs. 128, raw counts, uncorrected for double-counting errors), though the number of cells were nearly equal, labeling within the ventral BST (BST-VL, BST-VM) was judged in NP 5 to be qualitatively heavier (Table 2). And, in comparing NP 45 to NP 5, though the injections were of nearly equal size (144 vs. 143 labeled neurons, raw counts, uncorrected for double-counting errors), the labeling within the CeA was qualitatively much more substantial (Fig.

8B vs. Fig. 10B).

Evidence supporting differences in the caudal-to-rostral distribution of neurons within the NTS which project to the forebrain is also derived from studies in which retrograde tracers were injected into the CeA (Ricardo and Koh, '78; Zardetto-Smith and Gray, '86a; see Chapter 4, this dissertation). In these studies, retrogradely-labeled neurons were consistently present within the commissural portion of the NTS through its ventricular portion. However, retrogradely-labeled cells were rarely present within the NTS at levels rostral to the area postrema (see Fig. 3, Chapter 4).

Further evidence of caudal-rostral differences in organization may be derived from studies of the connectional relationships between the subdivisions of the NTS and various visceral organs in the cat and the rat. These studies demonstrated the central representation of thoracic and abdominal viscera did not conform to topography in the caudal-rostral plane; visceral afferent fibers terminated throughout the entire extent of the NTS, but within specific cytoarchitectonically-defined subnuclei (Kalia and Mesulam, '80; Altshuler et al., '89). This, however, does not preclude the possibility that afferent terminal distribution within a given subnucleus could vary with different caudal-rostral levels. For example, in the cat the area of densest labeling following injections of HRP into the extrathoracic trachea occurred within the ventrolateral subnucleus of the NTS at a level 1.5 mm rostral to the obex, though some label was present within the subnucleus at more caudal and rostral levels (Kalia and Mesulam, '80). And, following injections of HRP into the larynx, the area of densest labeling within NTS subnuclei was in the interstitial subnucleus at levels 1-3 mm rostral to the obex, with less label present at other levels of this subnucleus. Injections of HRP in the rat into the soft

palate demonstrated heavy anterograde labeling present in the interstitial subnucleus rostral to the obex, with lighter labeling present in more caudal portions of the subnucleus (Altshuler et al., '89). Kalia and Mesulam ('80) concluded from their study in the cat that the central representation of viscera is subtle, lying within the organization of nuclear subgroups within the NTS, a finding supported by studies in the rat showing a topographic termination of visceral afferents within the NTS (Shapiro and Miselis, '85; Altshuler et al., '89). However, since sensory afferents from a specific viscera may terminate at different rostro-caudal levels of a given subnucleus, this representation may be even more subtle, reflecting not only cytoarchitectural differences, but differences in the organization of processing of visceral afferent input. Functional subdivisions of the NTS, have in fact, been made based on rostro-caudal locations of secondary neurons receiving specific types of carotid sinus nerve input (Miura and Takayama, '86).

Termination of specific primary visceral afferent fibers within the brainstem do demonstrate rostral-caudal differences. The preferential sites of termination (confirmed by electron microscopy) of primary cardiac afferent nerves in the cat is in the middle-third of the NTS (Chiba and Doba, '75). Kalia ('81) describes the greatest intensity of anterogradely-labeled sensory terminals following exposure of the cut end of the carotid sinus and aortic nerves in the cat to be within the medial and dorsolateral subdivisions of the NTS at the level of the obex. Also, the rostro-caudal extent of the projection of the carotid sinus nerve is twice that of the aortic nerve (Kalia, '81). Afferents of the glossopharyngeal nerve in the rat terminate more heavily in the rostral 1.5 mm of the dorsomedial NTS, with a less dense innervation of the dorsal NTS more caudally (Altshuler et al., '89). Up-

per alimentary tract afferents terminate topographically within NTS subnuclei in a rostral-to-caudal fashion, such that rostral viscera are represented in rostral portions of NTS subnuclei, and caudal viscera in the more caudal portions of the NTS subnuclei (Altshuler et al., '89). Possibly, a caudal-rostral representation of sensory information within the NTS is conserved in its efferents to the BST and CeA.

Medial-to-lateral organization. NTS efferents to the BST and CeA differed in their medial versus lateral organization. Although this study included only one injection of PHA-L into the lateral NTS (at the level of the area postrema) the sparsity of label within the CeA in this case was in agreement with the results of studies employing the injection of retrograde tracers into the BST and CeA (Ricardo and Koh, '78; Zardetto-Smith and Gray, '86a; Chapter 4, this dissertation). In these studies, retrogradely-labeled neurons were consistently found within the medial NTS, beginning caudally at its commissural portion, and extending rostrally to the level where the NTS borders the fourth ventricle. The majority of BST- and CeA-projecting neurons were located at the level of the area postrema, and were especially numerous in the area corresponding to the medial subnucleus of the NTS. The results of the present study, demonstrating that the most prominent labeling of fibers and terminals within the BST and CeA was produced by PHA-L injections into this area correlate well with the results from retrograde studies. In addition, injections of wheat germ agglutinin HRP into the dorsomedial NTS in rats results in numerous anterogradely-labeled fibers within the BST ventral to the anterior commissure (Sofroniew, '83). Anatomical studies of descending efferents from the BST and CeA also lend support to this medial-lateral organization of connections. For example, connectional studies using HRP or fluorescent tracing techniques have demonstrated the main terminal zone of

the amygdalo-vagal pathway to be the medial NTS (Van der Kooy et al., '84; Schwaber et al., '82). Also, following injections of PHA-L into the BST (Zardetto-Smith et al., '89) or CeA (Danielson et al., '89) the majority of axonal labeling is found withn the medial NTS; few fibers and terminals are present within the lateral subnuclei. Interestingly, these studies have demonstrated the CeA to innervate rostral levels of the NTS more heavily than caudal levels (Hopkins and Holstege, '78; Danielson et al., '89).

Topographical Organization of NTS Efferent Input Within the BST and CeA. In general, NTS efferents innervated more rostral portions of the BST, primarily the anterior lateral (BST-AL) and ventral lateral (BST-VL) subnuclei. PHA-L injections centered within the caudal and medial intermediate NTS produced dense labeling, and more rostrally centered injections produced little or no labeling, within these subnuclei. The relative absence of PHA-L immunoreactive fibers and terminals throughout the BST in each of the four rostral injections was striking, especially in comparison to the dense label seen resulting from caudal and medial intermediate NTS injections. The posterior lateral (BST-PL) subnucleus, which replaces BST-AL at more caudal levels of the BST, received moderate innervation in medially placed injections at the intermediate level of the NTS (e.g., NP 45). Sparser innervation resulted when the injection was placed more laterally within the medial NTS at the same level (e.g., NP 19) or further rostrally (e.g., NP 34).

The parastrial (PS) subnucleus is a ventrally placed cellular group that has recently been included within the BST (Moga et al., '89). Parastrial neurons are cytoarchitecturally similar to those within BST-VL, and at rostral levels of the BST, are indistinguishable

from them (Moga et al., '89). At the most rostral extent of the BST, neurons of BST-VL are thought to be present but cannot be identified with certainty (Moga et al., unpublished observations). As a result, it is difficult to localize the termination of NTS efferents to either subdivision at these levels. At mid-BST levels, prominent innervation of BST-VL, compared to the light innervation of the BST-PS subnucleus, suggests the majority of NTS efferents at rostral levels of the BST are targeting cells in BST-VL. Innervation of BST-PS was most evident in NP 45, in which a moderate amount of fiber and terminal labeling was present (Fig. 10B).

The sublenticular substantia innominata forms a continuous structure with the BST anteromedially and with the CeA posterolaterally (Heimer et al., '85). Recent reviews (De Olmos et al., '85; Price et al., '87) have re-emphasized the original concept of Johnston ('23) that the BST and amygdala were once a single structure, but in mammals has become separated by the development of the internal capsule. Though not specifically addressed in their study, Ricardo and Koh ('78) demonstrated figuratively that injections of tritiated amino acids into the NTS labeled fibers scattered throughout the sublenticular substantia innominata, between the CeA and the ventral and lateral BST. This type of labeling has also been observed in studies of parabrachial efferents to the forebrain (Fulwiler and Saper, '84). The present study demonstrates similar results; in all cases, the sublenticular substantia innominata received sparse to moderate innervation from the NTS. Axonal PHA-L labeled fibers exhibited numerous en passant and some terminal varicosities. In other brain areas, PHA-L terminal boutons seen at the light level have been identified under electron microscopy as axon terminals containing synaptic vesicles and forming synaptic junctions (Wouterlood and Groenewegen, '85). In the context of the

present study, this suggests indirectly that NTS efferents are making synaptic contacts in their course throughout this gray matter.

On the basis of cytoarchitectural, immunocytochemical, and hodological studies, the dorsal portion of the lateral BST has been considered to be homologous to the lateral CeA and the ventral portion of the lateral BST homologous to the medial CeA (Gray and Magnuson, '87a). It is not clear whether this homology extends through the interconnecting substantia innominata, although it appears that CeM-related neurons are most characteristic of this area, rather than CeL type neurons (McDonald, '83). From this standpoint, it was not surprising to find NTS efferents terminating in both the medial CeA and ventral BST, as well as throughout the continuum of gray matter (the sublenticular substantia innominata) extending between them.

Some attempts have been made to correlate anatomical connections of cytoarchitectonically-defined subdivisions of the CeA with its embryological development. Bayer ('80) examined neurogenesis in the rat amygdala using progressively delayed comprehensive labeling (3-H-thymidine) autoradiography. In this study, the CeA was found to be organized in a longitudinal strip, with neurons generated in a strong anterior to posterior gradient. Also, neurogenesis in the medial CeA proceeded that in the lateral CeA, resulting in an intranuclear gradient of development occurring from medial to lateral. Bayer proposed that subdivisions of the CeA based on neurogenetic gradients (medial and lateral) matched subdivisions based on anatomical connections. Cassell et al. ('86) expanded this idea, suggesting subdivisions of the CeA based on cytoarchitecture might represent afferent integration from specific sources. Both authors cited the work of Ricardo and Koh ('78) as an example of restricted input to the medial CeA from the NTS. The present study demonstrates the afferent input to the CeA is more com-

plex. For instance, injections into the medial NTS (NP 45) produced a significant amount of label within the lateral aspects of the CeA, though not as extensive as that seen ventrally and medially (Fig. 10). Recently, Cassell and Gray ('89a) have suggested afferent input to the CeA may be related more to neuronal morphology rather than cytoarchitecture. For example, one type of neuron found within the CeM, CeV, and ventral BST has long dendrites with few spines; in addition, neurons of this type are scattered throughout the CeL and dorsal BST (McDonald, '82; '83). Also, neurons resembling this type extend through the substantia innominata. This may be one explanation for the particular pattern of NTS efferent innervation within the CeA, substantia innominata, and BST.

Anterior and posterior differences in both efferent and afferent connections of the CeA have also been linked to its neurogenesis (Bayer, '80). The present study does not support a differential rostro-caudal distribution of NTS efferents within the CeA. Also, the study by Hopkins ('75) suggests the descending input to the NTS does not originate from different rostro-caudal portions of the CeA, as both rostral and caudal portions of CeM contribute efferent innervation.

NTS Efferents to Other Amygdaloid Nuclei. Retrograde tracing studies in the rat by Otterson ('81) and Veening ('78) employing injections of HRP into various amygdaloid nuclei did not demonstrate efferents from the NTS to terminate in any amygdaloid nuclei other than the CeA. The results plotted by Ricardo and Koh ('78), showing the distribution of fibers within the forebrain following a large injection of tritiated amino acids into the medial NTS, indicated anterograde labeling was not entirely restricted to the CeA. In the present study, axonal and terminal labeling was observed in several amygdaloid nuclei,

most likely because of the greater sensitivity of the PHA-L method. The innervation of the posterior lateral cortical nucleus seen in NP 45, in particular, has not been previously described. However, most of the fibers exibited en passant swellings rather than terminal varicosities, though these probably do represent synaptic terminals (see above; Wouterlood and Groenwegen, '85). As electron microscopic analysis was not performed for this study, the possibility that these fibers were ascending to the CeA, in part, through these nuclei, and not specifically innervating them, cannot be ruled out.

In most injections, the intercalated, basolateral, and basomedial amygdaloid nuclei contained several labeled fibers and terminals, though this innervation was minor in comparison to that of the CeA. The medial, anterior and posterior cortical, and basomedial amygdaloid nuclei received innervation from the medial NTS subnucleus at either intermediate or rostral levels. Injections of PHA-L centered within the commissural, or dorsal and dorsolateral subnuclei, failed to label the basomedial nucleus with more than 1-2 fibers. These results indicate there may be a topographical projection of NTS efferents to other amygdaloid nuclei, as well as the BST and CeA, but again, further studies are needed to clarify this possibility.

Neurochemical Identity of NTS-BST and NTS-CeA Efferents. A variety of neuropeptides and classical transmitters have been identified in nerve terminals and fibers within the BST and CeA in recent years (for review, see Woodhams et al., '83; Price et al., '87; Gray, '89). Combined retrograde tracing-immunohistochemical studies have demonstrated that enkephalin, neurotensin, neuropeptide Y (NPY), and catecholamine-containing (mainly noradrenergic, A2) cells within the NTS project to the CeA (Zardetto-Smith and Gray, '86a, '88). Catechol-

amine- and enkephalin-positive neurons are mainly distributed within the medial NTS at the level of the area postrema (see Chapter 4, this dissertation), which is shown in the present study to provide substantial innervation to the CeA. Neurotensin- and NPY-immunoreactive cells are localized differently within the NTS in areas not providing a large input to the CeA (Chapter 4, this dissertation). It is, therefore, not surprising to find a larger proportion of CeA-projecting cells within the NTS are catecholamine- and enkephalin-immunoreactive, compared to the proportion of CeA-projecting neurons positive for NPY and neurotensin (Chapter 4, this dissertation). Neuropeptides and neurotransmitters have yet to be identified in NTS-BST efferents. However, the lateral BST also contains terminals immunoreactive to catecholamines (Swanson and Hartman, '76) and enkephalin (Fallon and Leslie, '86). In particular, BST-VL demonstrates the densest concentration of tyrosine hydroxylase immunoreactive terminals (Phelix et al., '86). It is probable that some catecholaminergic and enkephalinergic terminals within the BST are also derived from the intermediate medial NTS, especially in considering the similarity of the projection from this area to the CeM and the ventral portion of the lateral BST, and the homologies that exist between these two forebrain nuclei.

Functional Considerations. A fundamental role of the amygdala and lateral BST may be to monitor environmental conditions, detecting those stimuli to which an autonomic response is appropriate (Price et al., '87). Panksepp ('82) proposed that hard-wired neural circuits in the limbic-visceral brain (which includes the CeA and BST; see Cechetto, '87), facilitating diverse and adaptive behavioral and physiological responses to various environmental challenges, form the basis of emotion. In particular, the properties of the circuits that

mediate escape and flight (defensive) behaviors have not been well-defined (Panksepp, '80). Davis et al. ('84) has recently reviewed the evidence that the CeA and lateral BST (included herein as a related nucleus), and their connections, comprise a "central fear system".

Additional support for this hypothesis comes from studies directly implicating the CeA in pathophysiological responses, such as hypertension, to stressful environmental conditions which involve a chronic state of fear or anxiety (defined by Panksepp as a diminutive form of fear). Intensified environmental stimuli, resulting in a "prolonged defense reaction" in which sympathetic activity to the heart and peripheral circulation remain elevated over a long period of time, may contribute to the development of hypertension (Folkow, '82; Lawler et al., '85). In spontaneously hypertensive rats (SHR), a model for neurogenic human primary hypertension, a centrally intensified defense reactions to alerting stimuli is exhibited (Hallback and Folkow, '74). Stressful environments greatly aggravate hypertension in SHR, and amygdala-lesioned rats respond less than controls to stressful, fear-inducing stimuli (Folkow et al., '82). Bilateral lesions of the CeA in young SHR attenuate the development and delay the onset of hypertension (Folkow et al., '82; Galeno et al., '82). However, the CeA is not the main source of the exaggerated cardiovascular responsiveness SHR exhibit in response to environmental alerting stimuli, but may only reinforce intensified defense reactions to stressful situations when such stimuli are presented (Folkow et al., '82; Galeno and Brody, '83).

Altered baroreflex control of the heart and circulation has been demonstrated in both human and animal models of hypertension (for reviews, see Brown, '81; Thames, '84). The NTS is a critical integrative area for sensory input arising from various afferent pathways, and for the modulation of reflex autonomic activity (Schmitt and Laubie,

'80; Carey, '84). Conceivably, NTS input to the CeA and BST is affected in the hypertensive state. Evidence supporting this hypothesis is derived from one particular model of neurogenic hypertension in the rat. Selective aortic baroreceptor denervation alters metabolic activity within the CeA (as well as other forebrain structures implicated in body water balance and arterial pressure), suggesting these structures are involved in the hypertensive process after baroreceptor feedback is removed by nerve transection (Turton et al., '86). The role of the BST in hypertension has not been specifically investigated, but in view of its relationship to the CeA, and the heavy input to its ventral lateral portion from the dorsal/dorsolateral and medial baroreceptive portions of the NTS demonstrated in the present study, it seems likely the BST would be involved to some degree. Physiological studies lend some support to this speculation; electrical stimulation of the dorsal preoptic hypothalamus, including the ventral BST, results in a vasodepressor response (Hilton and Spyer, '71; Faiers et al., '76), while lesions of this area attenuate the baroreceptor reflex (Hilton and Spyer, '71). The integrity of the central noradrenergic system, to which the NTS-CeA pathway (and probably the NTS-BST pathway; see above) contributes, may be crucial for the prevention of renal hypertension (Petty and Reid, '77). Interestingly, in conscious, renal hypertensive dogs, abnormal control of heart rate is the result of changes in the control of vagal motor neurons (Thames et al., '81); the dorsal motor nucleus of the vagus is one brainstem target of both CeA and BST (lateral) output (Holstege et al., '85; Danielson et al., '89).

Another pathophysiological process related to stress in which the CeA has been implicated is gastric ulceration. Henke ('80a, '80b) demonstrated immobilization of rats produced gastric ulcers which were attenuated by bilateral lesions involving the CeA. Restraint initiates

changes in CeA neuronal unit firing that can be correlated with different degrees of gastric pathology (Henke, '83, '88). Also, stomach ulcers can be produced by electrical stimulation of these units (Henke, '85). Lesions of the CeA decrease fasting levels of gastric acidity and attenuate the formation of mucosal erosion induced by bilateral hypothalamic stimulation (Grijalva et al., '86). Electrical stimulation of the medial, lateral, and basal amygdalar nuclei also increase gastric acid secretion (Zawoiski, '67). Ablation of the BST increases gastric pathology induced by physical restraint (Henke, '84). The present study demonstated the medial subnucleus of the NTS, in which some gastric afferents terminate (Kalia, '81; Shapiro and Miselis, '85; Altshuler et al., '89), heavily innervated the CeA and BST, and provided some innervation to other amygdaloid nuclei as well. Based on the model of pyschosomatic disorders formulated by Schwartz ('77), Henke ('83) suggested that feedback information from gastric receptors is used to maintain homeostasis of the brain-gut regulatory system, and that the amygdala might be involved in autonomic and behavioral regulatory actions (such as fright or flight) when this system is under stress. Maintained interference with behavioral adaptations, such as restraint, might consequently impair the effectiveness of negative feedback to regulate this homeostasis, resulting in gastric pathology. The cortical, medial, and basolateral amygdaloid nuclei, in addition to the CeA, have each been implicated in mediating different aspects of ingestive behavior (Rolls and Rolls, '73; Rolls and Rolls, '73; Nachman and Ashe, '74; Fonberg, '81). The input from gastric stretch or acidic receptors (relayed through the NTS), conveying the state of gastric distention (and therefore satiety or hunger; for review, see Paintal, '73), may function in this regard.

Input from the NTS to the BST, CeA and the basal amygdaloid

nuclei may also participate in the role of the limbic system in drinking behavior. Swanson and Mogenson ('81) have reviewed the complex circuitry involved between cortical association areas and the amygdala which may mediate the drinking response. One important component of this circuitry is the input from peripheral sensory receptors (which may be involved in the initiation of thirst) relayed to the forebrain from the NTS and other subcortical structures.

In the present study, PHA-L labeled fibers were present in several of the amygdaloid nuclei. With the exception of the posterior lateral cortical amygdaloid nucleus, the projections were minor in comparison to the innervation of the CeA. As discussed previously, it is difficult without the benefit of electron microscopy to assume definitively that these labeled axons ended in synapses in these nuclei. Possibly, however, input from visceral receptors, relayed through the NTS, may be integrated with (for example) descending cortical output to other nuclei of the amygdaloid complex (see Price et al., '87 for review). As the CeA is the major recipient of intra-amygdaloid efferents (De Olmos et al., '85), these pathways may represent a convergence of an integrated amygdaloid-brainstem input into the CeA. Also, the NTS input to the nuclei of the "vomeronasal" or "olfactory" related amygdaloid nuclei (in particular, the posterior cortical) may be involved in the relay of nongustatory visceral stimuli from the orophayrngeal mucosa.

Recently, reciprocal connections between the CeA and NTS were demonstrated electrophysiologically by microstimulation of the NTS, which activated CeA neurons both orthodromically and antidromically (Rogers and Fryman, '88). Neurons concentrated in the ventrolateral portion of the CeA responded to orthodromic stimulation of the NTS, while CeA-NTS projecting neurons were located mostly dorsomedially.

The present anatomical study, however, demonstrates clearly that afferent input from the NTS is not limited to the ventrolateral CeA, but encompasses its medial subdivision as well. Previous studies of CeA efferents indicated its descending projection to the dorsal vagal complex (NTS and dorsal motor nucleus of the vagus) to originate in the medial subdivision (Hopkins and Holstege, '78; Schwaber et al., '82). However, combined retrograde/immunohistochemical tracing studies have demonstrated that lateral aspects of the CeA also contribute, especially in terms of peptidergic output (i.e., Moga and Gray, '85). Afferents from the NTS terminate in areas giving rise to CeA-NTS descending projections (which distribute within the medial NTS, where most NTS-CeA efferents orginate). Thus, the circuitry exists whereby visceral afferent input might directly influence amygdaloid output, that may, in turn, further modulate incoming sensory signals. In support of this framework, electrophysiological evidence has been provided in the rabbit for a convergence of inputs on a limited number of NTS neurons from both the aortic nerve and CeA (Cox et al., '86). In comparison, most NTS afferents to the BST terminated within its ventral portion, from which most hypothalamic efferents originate (Moga et al., '89). Thus, ascending NTS input to the ventral BST may be related more to modulation of hypothalamic function. The descending output to the NTS arises mainly from the posterior lateral subnucleus of the BST (Sofroniew, '83; Gray and Magnuson, '87a; Zardetto-Smith et al., '89) which in the present study, was moderately innervated.

Concluding Comments. The seminal work of Ricardo and Koh ('78) on NTS projections to the CeA and BST have been confirmed and expanded by the present study. A decade has passed since Ricardo and Koh ('78) speculated as to the functional significance of subcortical input to

the forebrain, but the mechanisms through which visceral feedback may influence the integration of autonomic responses with various behaviors are still largely unknown. This is especially true with regard to the BST, as few studies have addressed its role in central autonomic regulation. The results of the present study should provide a more defined anatomical framework for future studies of functional correlates to this pathway.

TABLE 1

Central Nucleus of the Amygdala

and Substantia Innominata

Relative Comparison of PHA-L Innervation

Produced by NTS Injections

	SUBDIVISION				
	CeM	CeV	CeL	CeLC	SI
Case #					
caudal NTS					
5	2	2	1	1	2
dorsal NTS - AP					
19	2	3	1	1	2
lateral NTS- AP					
41	1	1	0	0	1
medial NTS - AP					
45	3	4	2	3	3
rostral NTS					
34	3	3	1	1	2

Ratings:

0 = no fiber or terminal label

1 = trace fibers

2 = sparse innervation

3 = moderate innervation

4 = heavy innervation

TABLE 2

Bed Nucleus of the Stria Terminalis

Relative Comparison of PHA-L Innnervation

Produced by NTS Injections

	SUBNUCLEUS														
	AM	VM	PM	PI	SV	IM	AL	DL	VL	PL	SC	JXC	PO	PD	PS
Case #															
caudal NTS															
5	0	1	0	0	0	0	1	1	3	2	0	0	1	0	1
dorsal NTS - AP															
19	1	1	0	1	0	1	2	1	3	2	0	1	1	0	1
lateral NTS - AP															
41	0	1	0	0	0	0	1	0	1	1	0	0	0	0	0
medial NTS - AP															
45	1	2	1	2	1	1	3	1	4	3	1	1	2	2	2
rostral NTS															
34	1	1	1	1	1	1	2	1	2	1	1	1	2	1	1

Ratings:

0 = no fiber or terminal labeling

1 = trace fibers

2 = sparse innervation

3 = moderate innervation

4 = heavy innervation

TABLE 3

Hypothalamic and Thalamic Nuclei

Relative Comparison of PHA-L Innervation

Produced by NTS Injections

	NUCLEUS											
	MnPO	MPOA	AVPO	AMPO	SO	PVNp	PVNm	PeF	ARC	Pe	DM	PVT
Case #												
caudal NTS												
NP 5	1	2	1	1	1	2	1	2	1	2	1	1
dorsal NTS - AP												
NP 19	2	1	1	1	3	2	1	2	2	3	2	3
lateral NTS - AP												
NP 41	0	0	0	0	0	3	0	2	0	0	0	0
medial NTS - AP												
NP 45	3	2	3	2	2	3	2	3	2	3	2	2
rostral NTS - AP												
NP 34	1	2	3	2	3	3	2	3	3	3	3	3

Ratings:

0 = no fiber or terminal labeling

1 = trace fibers

2 = sparse innervation

3 = moderate innervation

4 = heavy innervation

Figure 1. Line drawing representing two control injections of PHA-L into the hypoglossal nucleus (NP 2) and gracile nucleus (NP 21). The asterik (*) in each drawing denotes the solitary tract. PHA-L labeled cell bodies are represented by filled circles; DAB-reaction product is represented as light stipple.

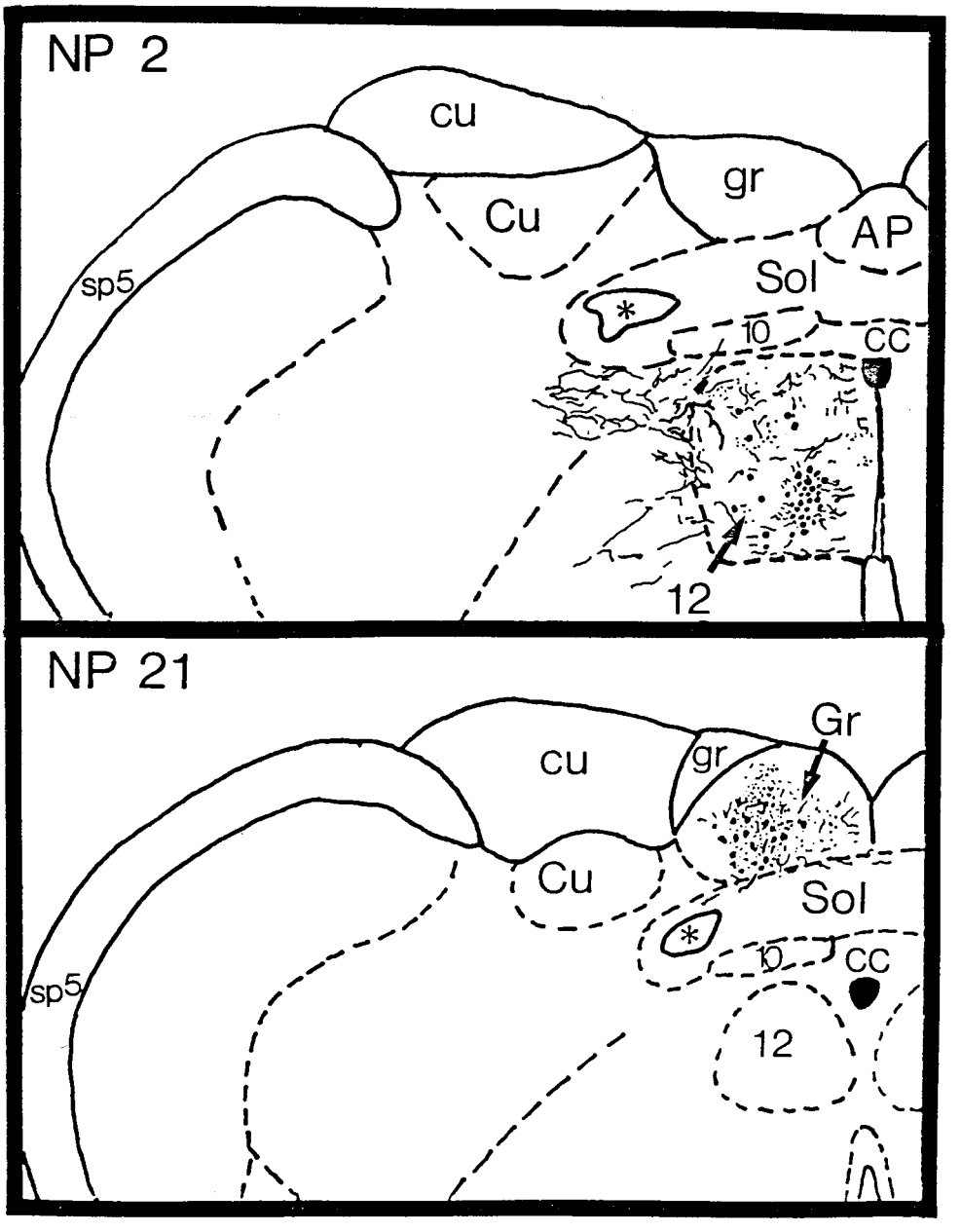
NP 2
cu
gr
Cu
AP
sp5
Sol
*
10
CC
5
12
NP 21
Gr
cu
gr
Cu
Sol
*
10
CC
sp5
12

Figure 2. Schematic representation of three levels through the CeA, and four levels through the BST, demonstrating cytoarchitectonic subdivisions as per the description of Cassell et al. ('86) and Moga et al. ('86), respectively. Coronal sections are arranged in a caudal-to-rostral fashion. Distance relative to bregma is indicated at each level. The stria terminalis is denoted in each figure by the asterik (*).

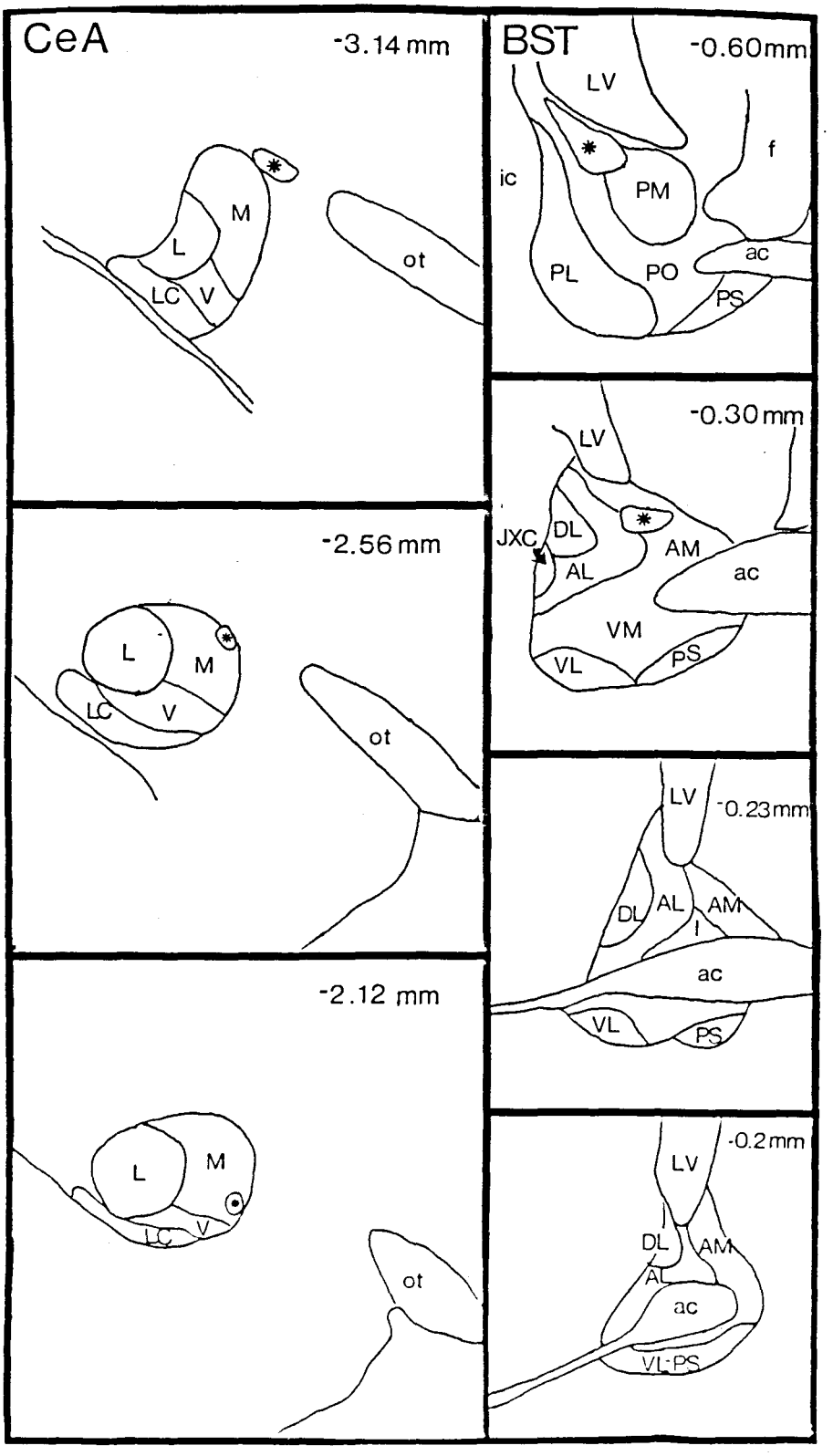
CeA
-3.14 mm
M
L
LC
V
ot
-2.56 mm
L
M
LC
V
ot
-2.12 mm
L
M
LC
V
ot
BST
-0.60mm
LV
ic
PM
f
PL
PO
ac
PS
-0.30mm
LV
JXC
DL
AM
AL
ac
VM
VL
PS
LV
-0.23mm
DL
AL
AM
ac
VL
PS
-0.2mm
LV
DL
AM
AL
ac
VL-PS

Figure 3. Line drawings of coronal sections through three levels of the CeA (B, 1-3; caudal to rostral) and four levels of the BST (C, 1-4; caudal to rostral) illustrating the distribution of PHA-L labeled axons in Case NP 5 following an injection into the caudal NTS (A). Neurons labeled with PHA-L at the injection site (A) are indicated by the filled circles. The asterik (*) in each drawing denotes the stria terminalis.

NP 5

A

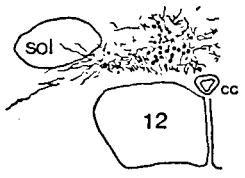
sol
cc
12

B

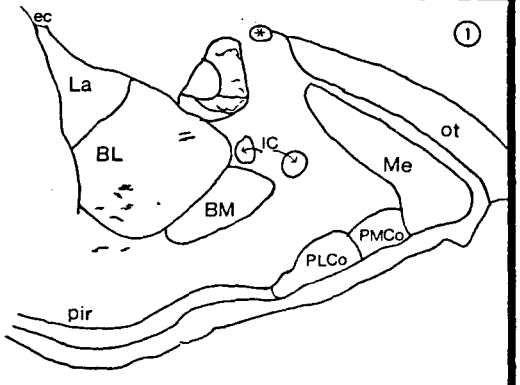
ec
La
BL
IC
BM
Me
ot
PMCo
PLCo
pir
①

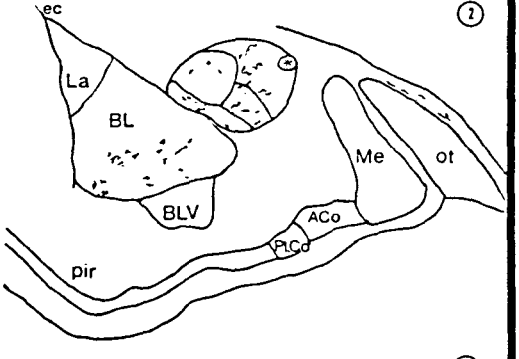
ec
La
BL
BLV
Me
ot
ACo
PLCo
pir
②

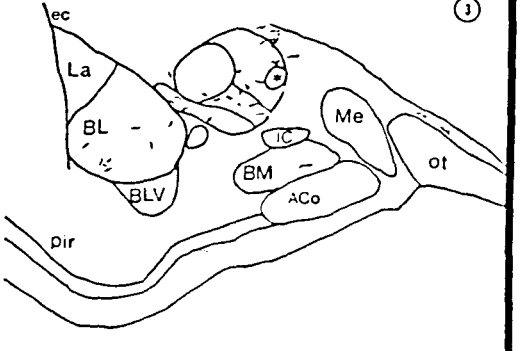
ec
La
BL
BLV
Me
IC
BM
ACo
ot
pir
③

C

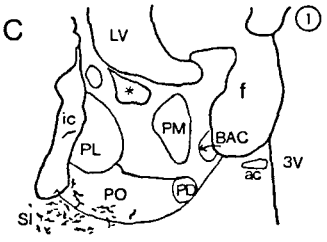
LV
①
f
ic
PM
PL
BAC
3V
ac
PO
PD
SI

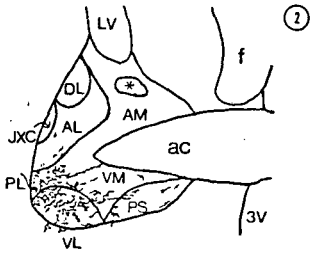
LV
②
f
DL
AM
JXC
AL
ac
PL
VM
PS
3V
VL

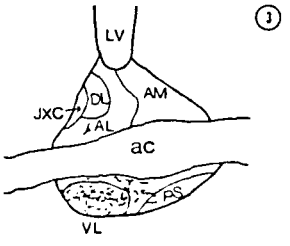
LV
③
JXC
DL
AM
AL
ac
PS
VL

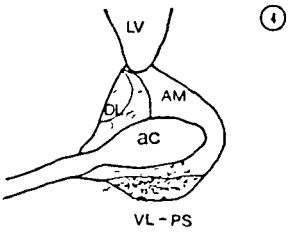
LV
④
DL
AM
ac
VL - PS

Figure 4. Line drawings of coronal sections through three levels of the CeA (B, 1-3; caudal to rostral) and four levels of the BST (C, 1-4; caudal to rostral) illustrating the distibution of PHA-L labeled axons in Case NP 41 following an injection into the lateral NTS at the level of the area postrema (A). Neurons labeled at the injection site (A) with PHA-L are indicated by the filled circles. The asterik (*) in each drawing denotes the stria terminalis.

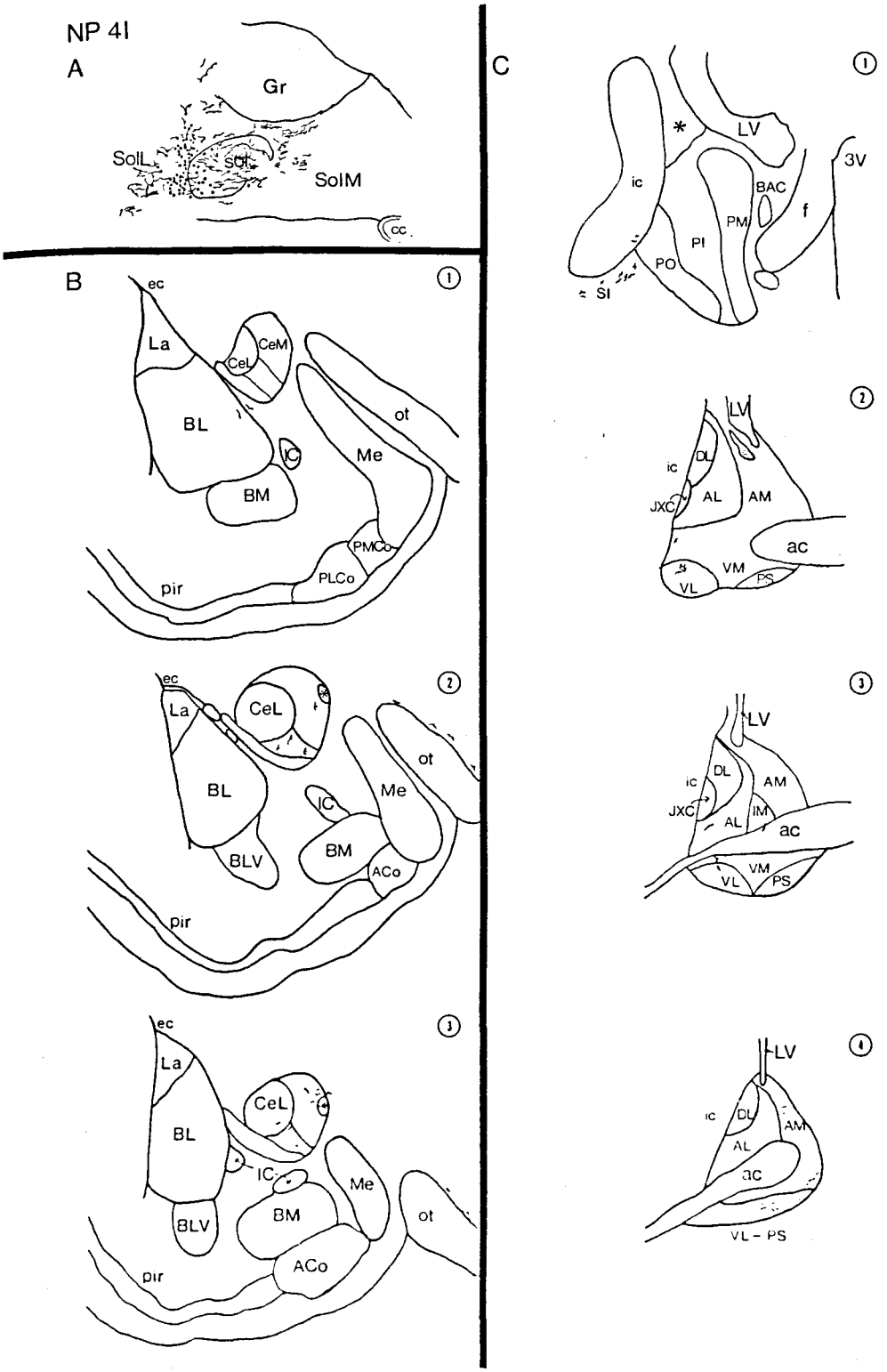
NP 41
A
Gr
SolL
SolC
SolM
cc
B
C
ec
La
CeM
CeL
BL
IC
Me
ot
BM
PMCo
PLCo
pir
BLV
ACo
LV
3V
BAC
f
PM
PI
PO
SI
ic
DL
JXC
AL
AM
ac
VM
VL
PS
IM

Figure 5. Line drawings of coronal sections through three levels of the CeA (B, 1-3; caudal to rostral) and four levels of the BST (C, 1-4); caudal to rostral) illustrating the distribution of PHA-L labeled axons in Case NP 19 following an injection into the dorsal NTS at the level of the area postrema (A). Neurons labeled at the injection site (A) with PHA-L are indicated by the filled circles. The asterik (*) in each figure denotes the stria terminalis.

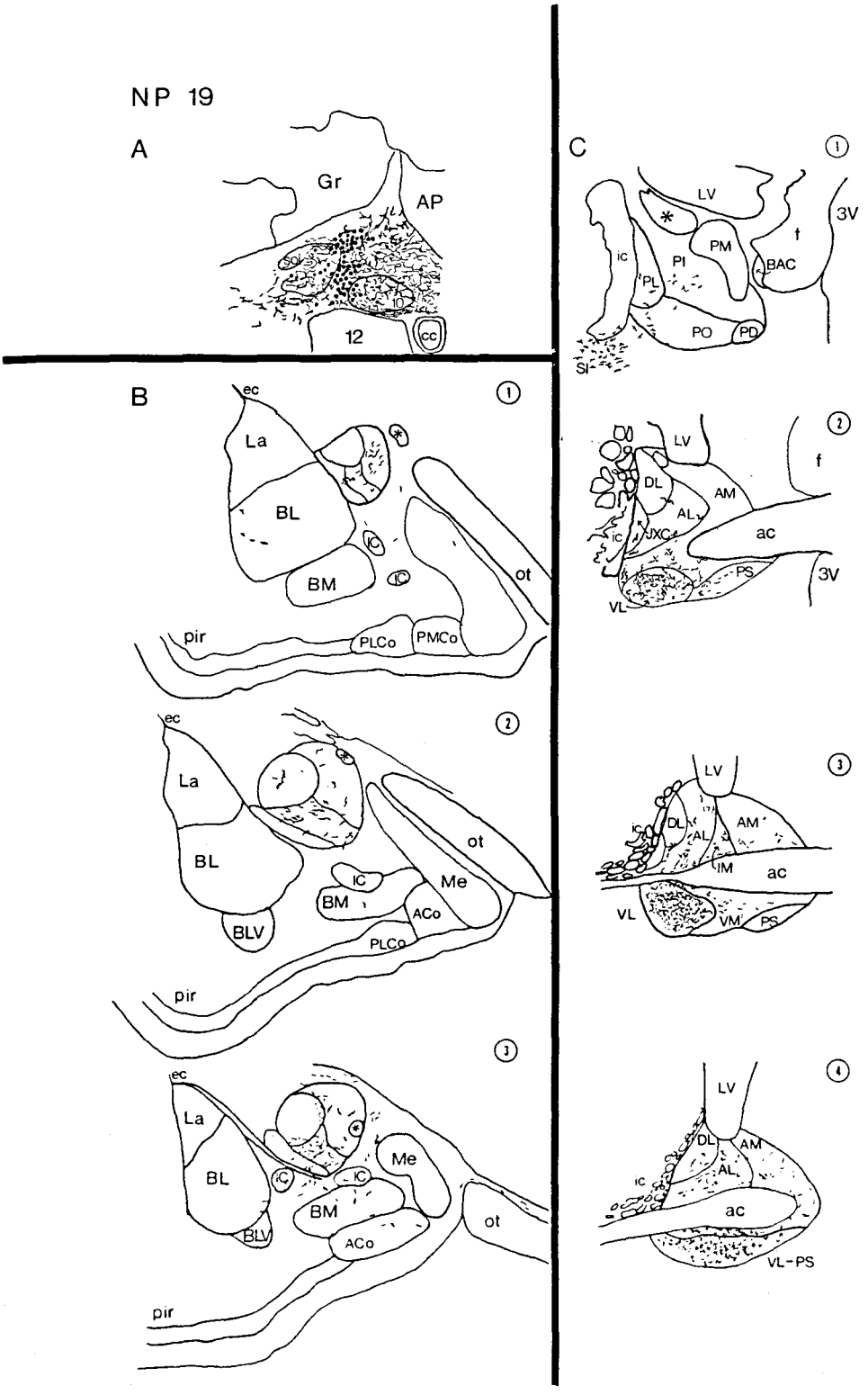
NP 19
A
Gr
AP
SOL
10
12
cc
B
ec
La
BL
BM
IC
ot
pir
PLCo
PMCo
Me
ACo
BLV
C
LV
3V
f
ic
PM
PI
BAC
PL
PO
PD
SI
AM
AL
DL
ac
PS
VL
IM
VM
VL-PS

Figure 6. Line drawings of coronal sections through three levels of the CeA (B, 1-3; caudal to rostral) and four levels of the BST (C, 1-4; caudal to rostral) illustrating the distribution of PHA-L labeled axons in case NP 45 following an injection into the medial NTS at the level of the area postrema (A). Neurons labeled at the injection site (A) with PHA-L are indicated by the filled circles. The asterik (*) in each drawing denotes the stria terminalis.

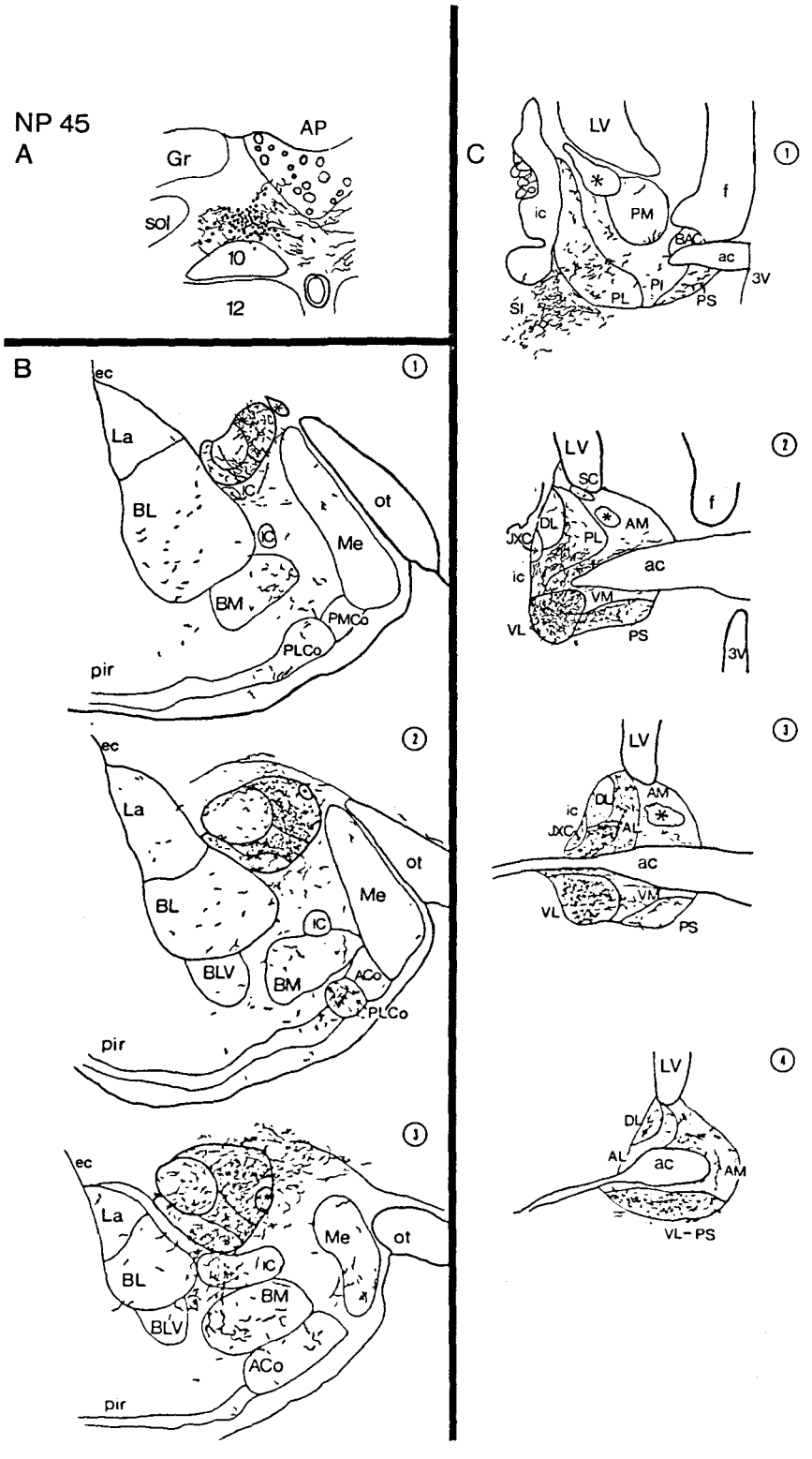
NP 45
A
Gr
AP
sol
10
12
B
ec
La
BL
ic
Me
ot
BM
PMCo
PLCo
pir
BLV
ACo
C
LV
f
PM
BA
ac
3V
PI
PL
PS
SI
SC
DL
AM
JXC
VM
VL
AL

Figure 7. Line drawings of coronal sections through three levels of the CeA (B, 1-3; caudal to rostral) and four levels of the BST (C, 1-4; caudal to rostral) illustrating the distribution of PHA-L labeled fibers in case NP 34 following an injection into the medial NTS rostral to the area postrema, where the nucleus borders the fourth ventricle (A). Neurons labeled at the injection site (A) are indicated by the filled circles. The asterik (*) in each drawing denotes the stria terminalis.

NP 34

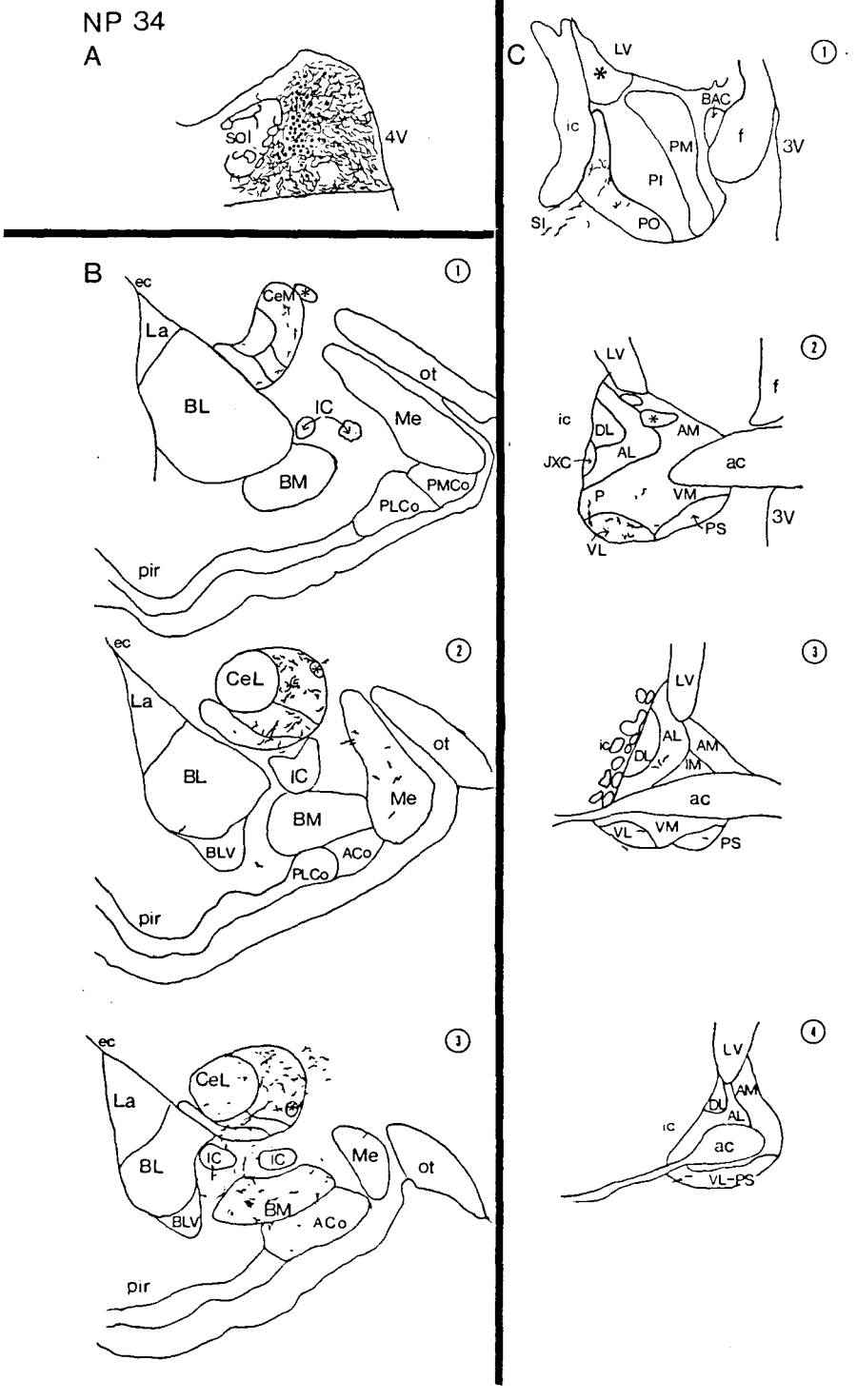
A
SOl
4V
B
ec
La
CeM
BL
IC
ot
Me
BM
PMCo
PLCo
pir
CeL
BLV
ACo
C
LV
BAC
ic
PM
f
3V
PI
SI
PO
JXC
DL
AL
AM
ac
P
VM
PS
VL
IM
VL-PS

Figure 8. (A) Dark-field low power photomicrograph of PHA-L immunoreactivity in the BST in Case NP 5 following an injection into the caudal NTS. (B) Dark-field low power photomicrograph of PHA-L labeled fibers within the CeA in the same case. PHA-L fibers and terminals appear gold. Note the density of innervation of BST-VL compared to CeV.

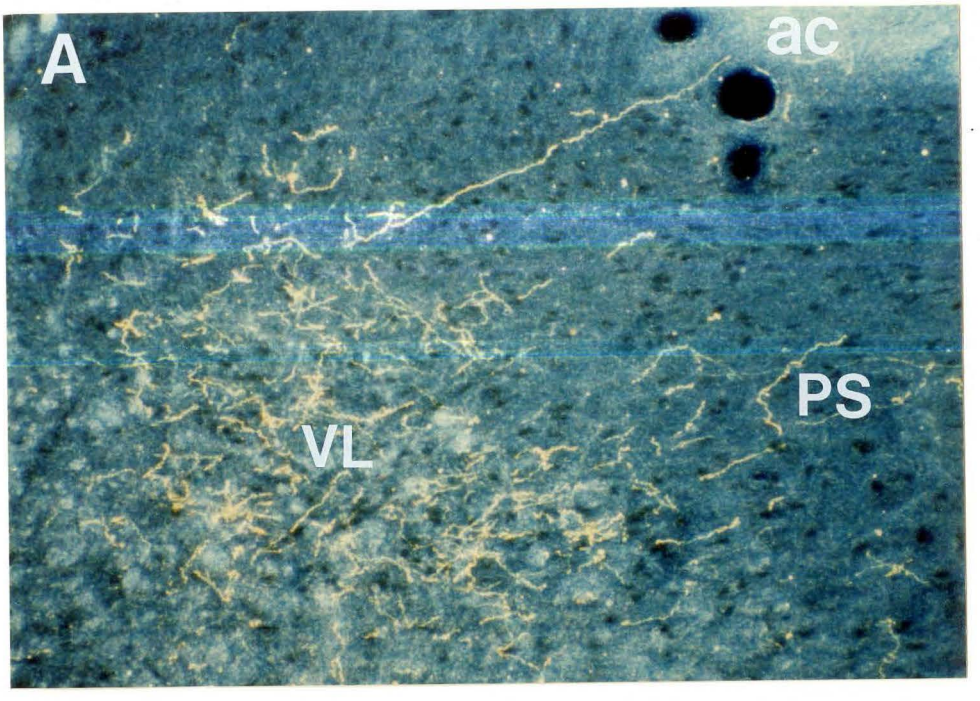
A
ac
PS
VL

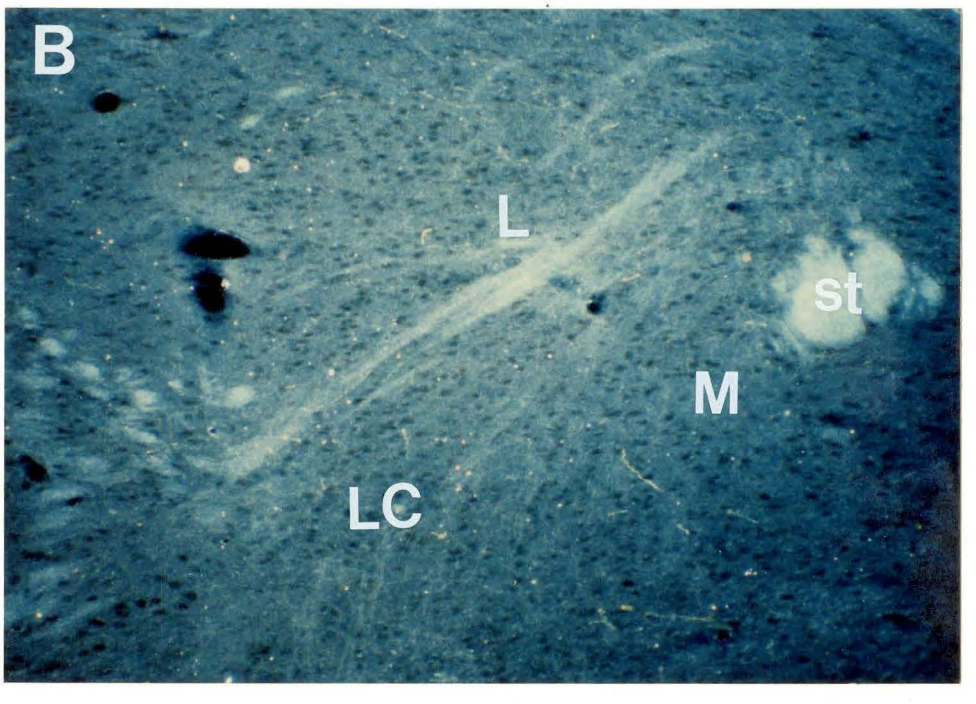
B
L
st
M
LC

Figure 9. (A) Dark-field low power photomicrograph of PHA-L immunoreactivity in the BST in case NP 19 following an injection into the dorsal NTS at the level of the area postrema. (B) Dark-field low power photomicrograph of PHA-L labeled fibers within the CeA in the same case. PHA-L labeled fibers and terminals appear gold. BST-VL is densely innervated compared to the CeA. In B, note the PHA-L fibers encircling the dorsal and ventral aspects of the lateral subdivision.

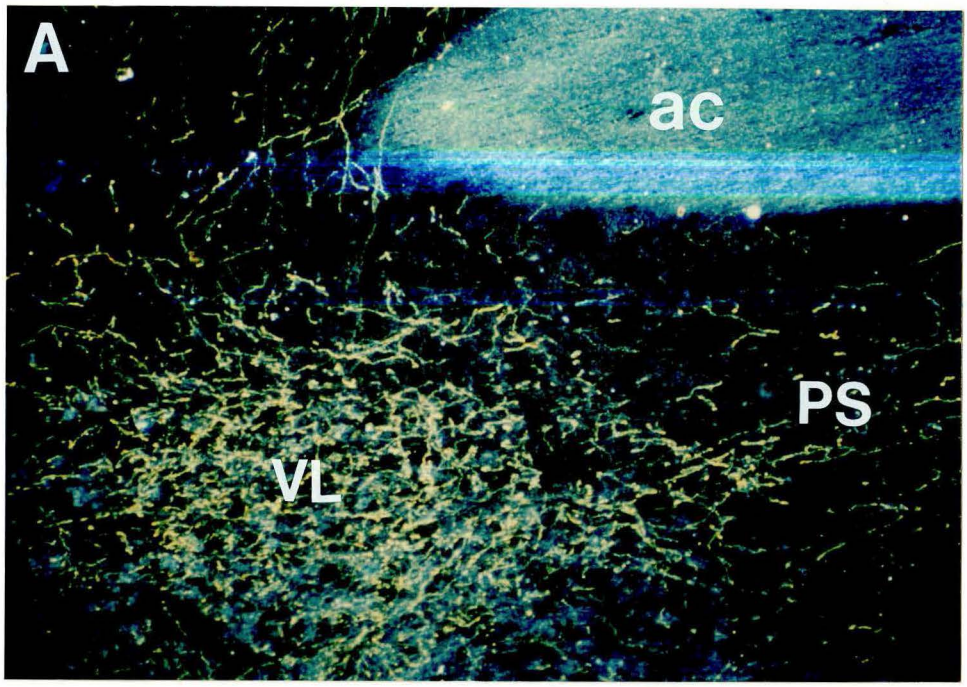
A
ac
PS
VL

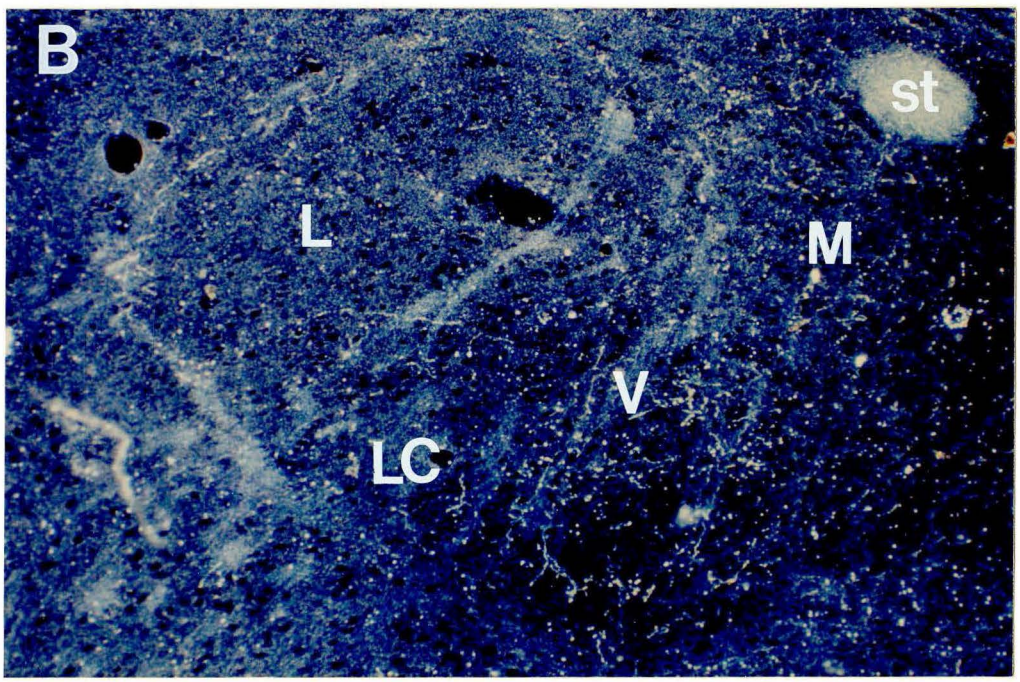
B
st
L
M
V
LC

Figure 10. Light-field photomicrographs of PHA-L labeling within three levels of the CeA in case NP 45. These sections have also been stained for neurotensin-immunoreactivity, which appears as purplish reaction product especially concentrated within the lateral capsular (LC) subdivision (white triangles). Magnification is indicated on each photo. (A) (Opposite page) Caudal CeA. (B). (Following Page) Intermediate CeA. (C). Rostral extent ofthe CeA where all four subdivisions are still present.

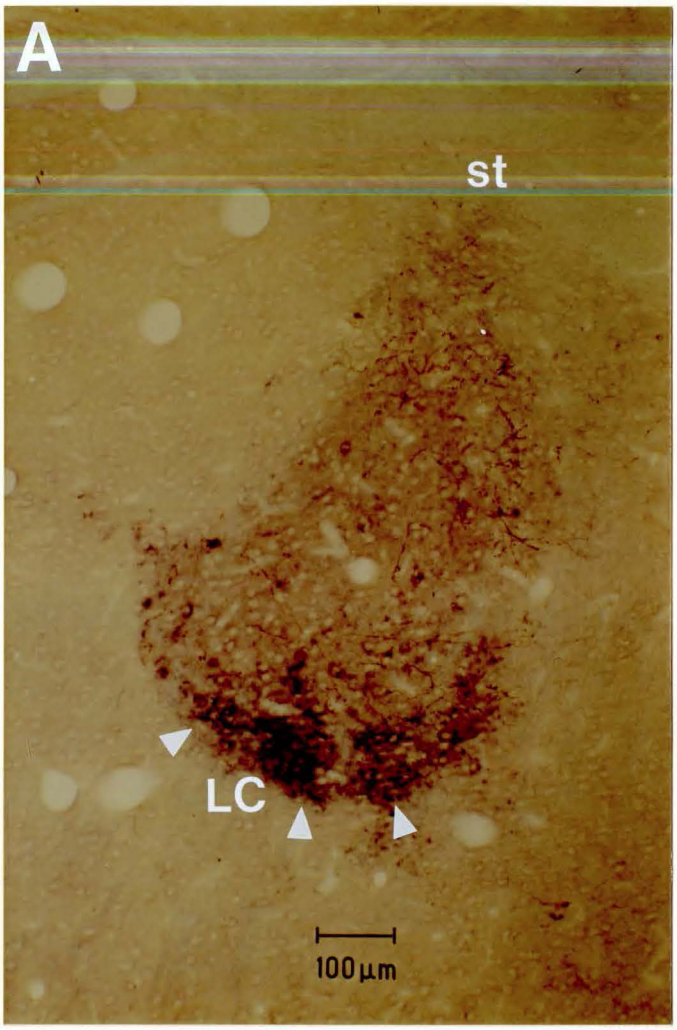
A
st
LC
100 µm

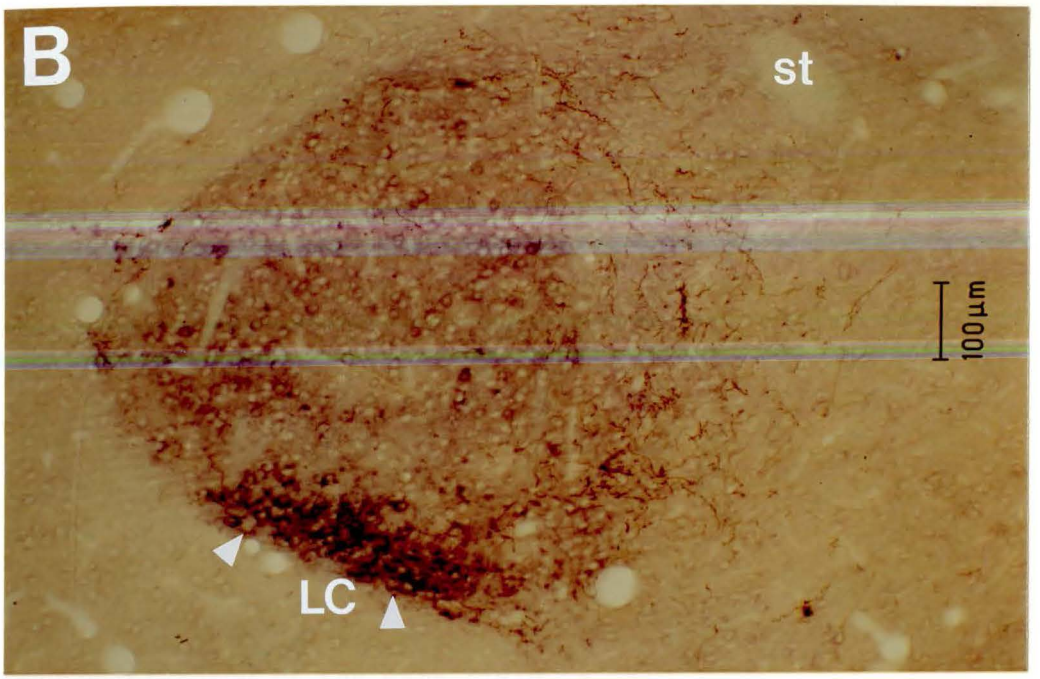
B
st
100µm
LC

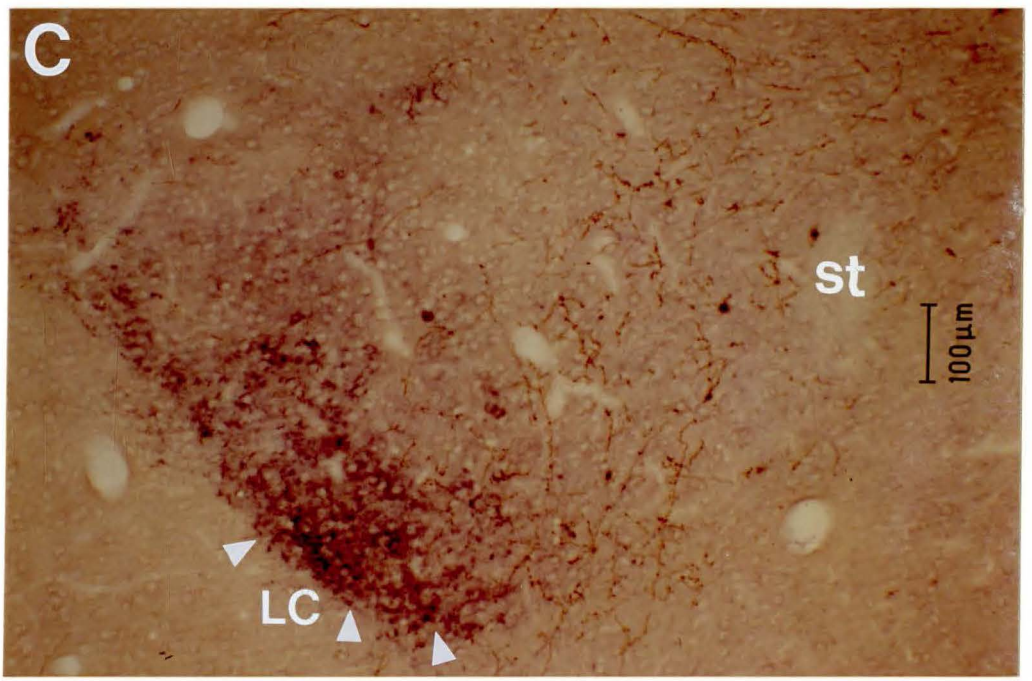
C
st
100µm
LC

Figure 11. (A) Light-field low power photomicrograph of PHA-L fibers and terminals within the posterior lateral cortical amygdaloid nucleus in Case NP 45. (B) High-power (magnification indicated to the right) photomicrograph of the same field as (A). White arrows mark PHA-L terminal swellings.

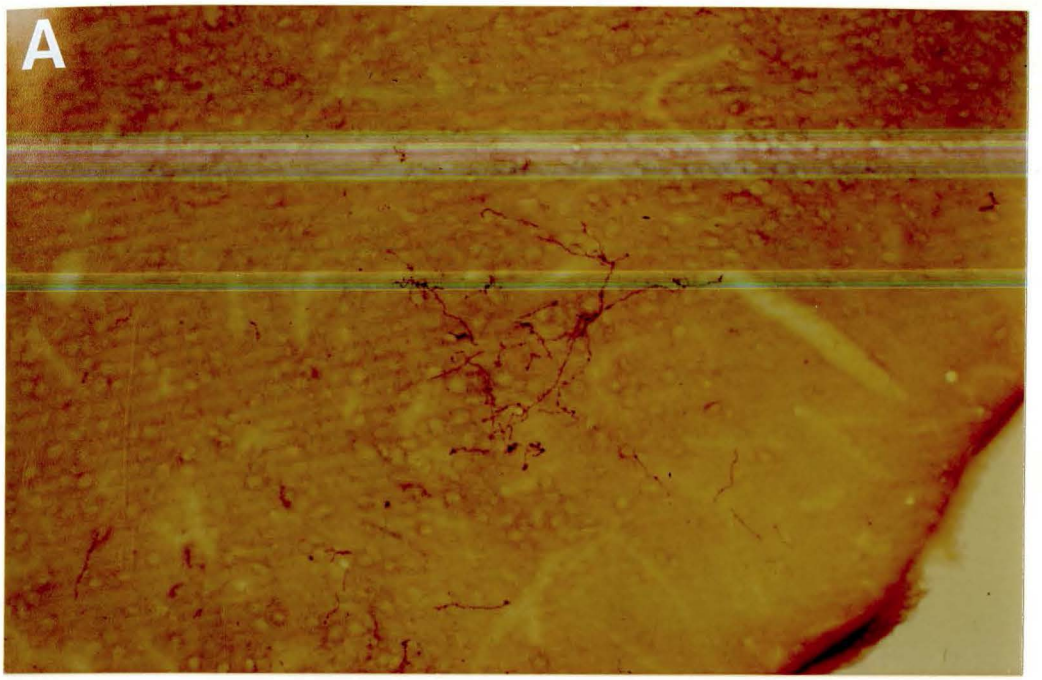
A

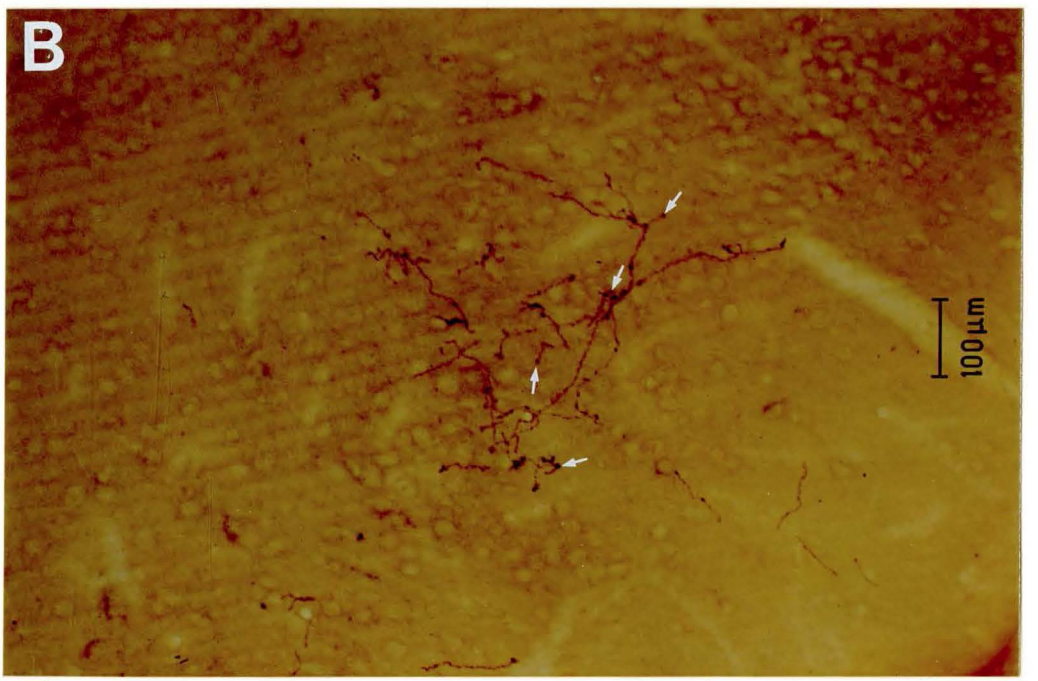
B
100µm

Figure 12. Light-field photomicrographs of PHA-L label within the caudal (A) and rostral (B) BST in Case NP 45. Magnification is indicated at the bottom of A, and to the right in B. Posterior subnuclei of the BST were not as heavily innervated as more rostral levels.

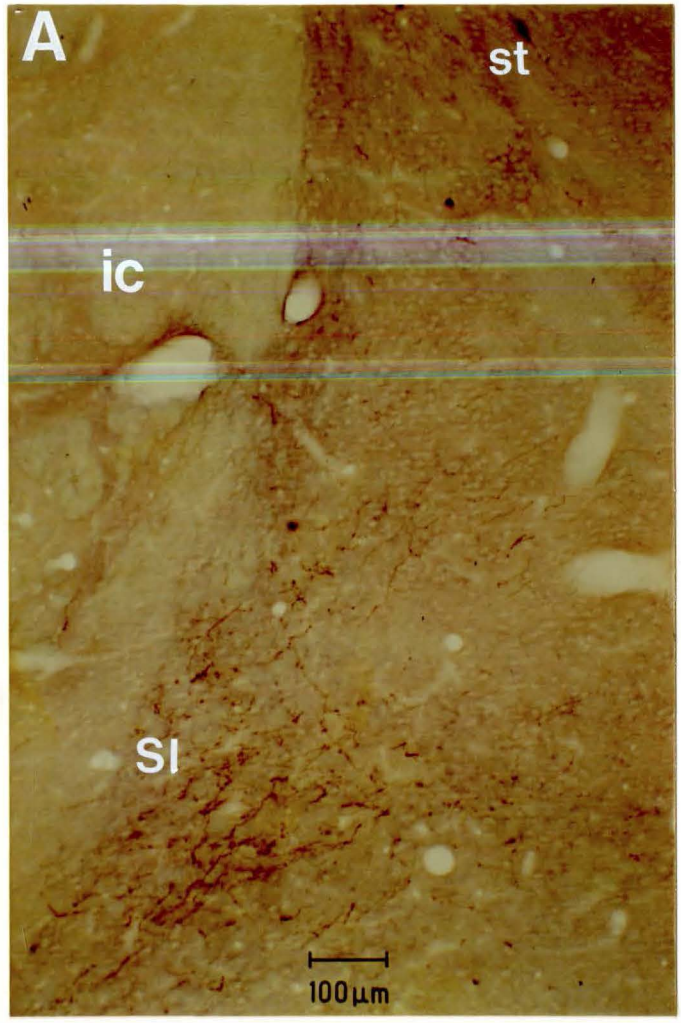
A
st
ic
SI
100µm

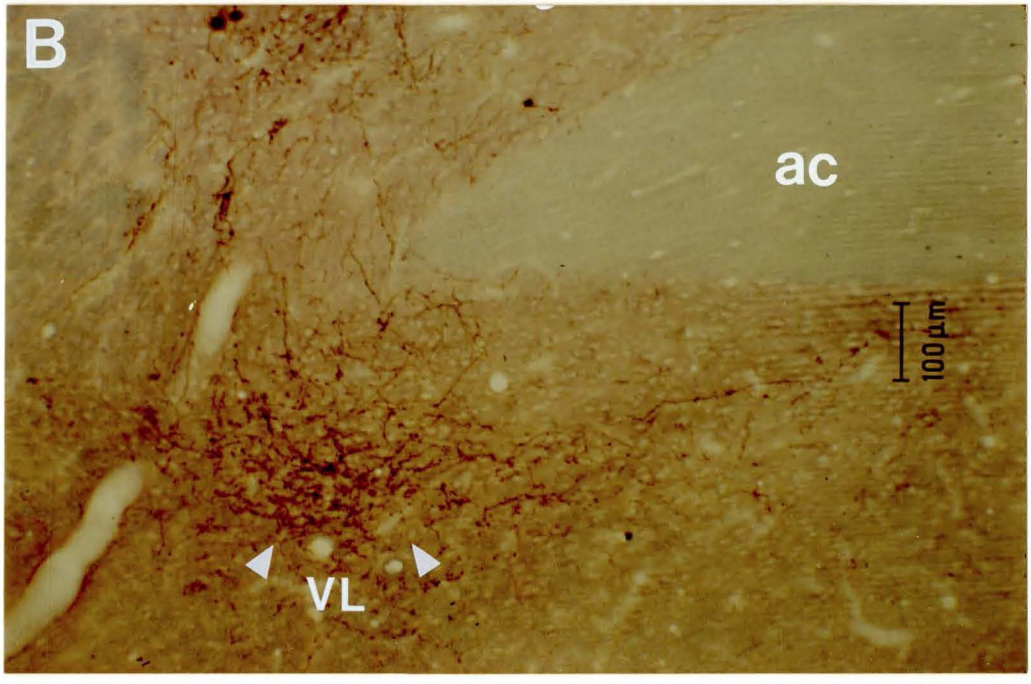
B
ac
100µm
VL

Figure 13. Dark-field low power photomicrographs of PHA-L immunoreactivity within the rostral BST (A) and CeA (B) in Case NP 34. The absence of label within the BST in comparison to NP 5, 19 or 45 (preceeding figures) is especially striking.

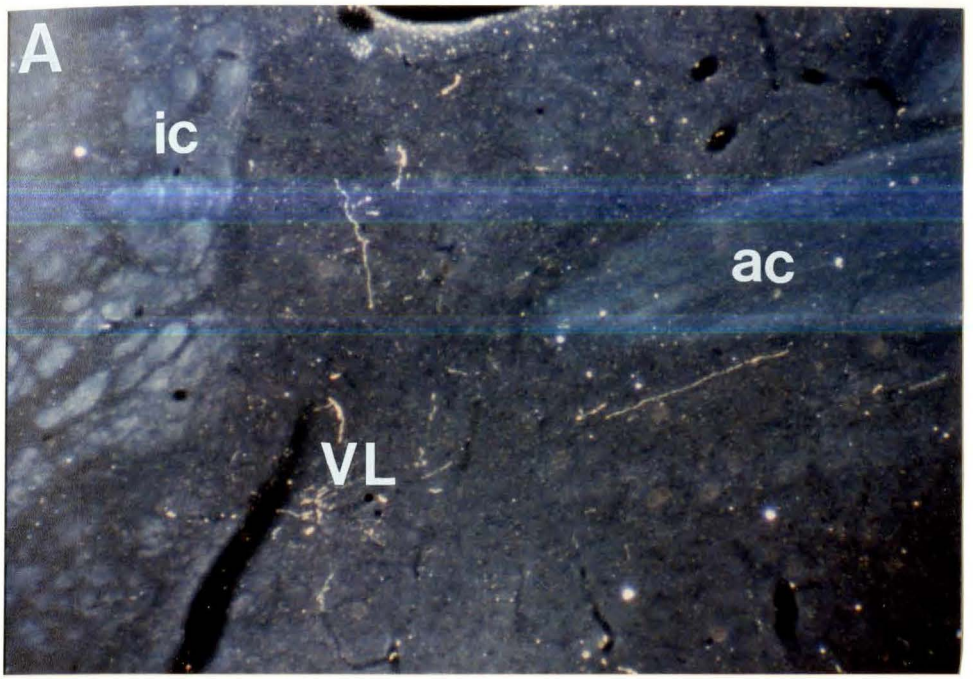
A
ic
ac
VL

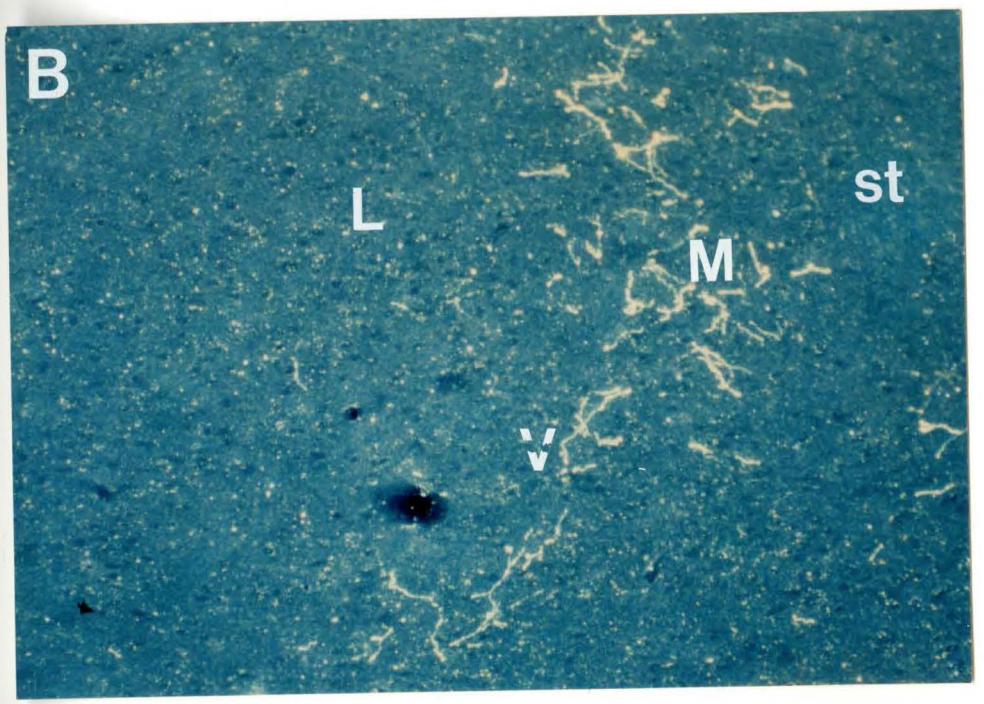
B
L
st
M
V

CHAPTER IV

ORGANIZATION OF PEPTIDERGIC AND CATECHOLAMINERGIC EFFERENTS FROM THE NUCLEUS OF THE SOLITARY TRACT TO THE AMYGDALA IN THE RAT: A COMBINED RETROGRADE TRACING-IMMUNOHISTOCHEMICAL STUDY

INTRODUCTION

Several physiological studies have focused on the role of the central nucleus of the amygdala (CeA) in cardiovascular and other visceral functions. Stimulation of the CeA in the awake cat or rat causes tachycardia and increased arterial pressure (Hilton and Zbrozyna, '63; Stock et al., '78; Galeno and Brody, '83; Schlor et al., '84; Gelsema et al., '87), a response similar to that evoked during the defense reaction, fear, anger, flight and arousal (Kaada, '51, '72; Hilton and Zbrozyna, '63). The CeA contributes to the acquisition of conditioned heart rate responses to threatening or fear-arousing stimuli (Kapp et al., '81). It also has been implicated in mediating visceral responses (such as ulcerogenesis and hypertension) to stressful environmental conditions involving a chronic state of fear or anxiety (Folkow et al., '82; Galeno et al., '82; Henke, '80a, b; '88).

The CeA receives a projection from the caudal part of the nucleus of the solitary tract (NTS), the site of first synapse for the majority of general visceral afferent fibers of the glossopharyngeal and vagus nerves carrying baroreceptor, chemoreceptor, and visceral stretch receptor input (for review, see Paintal, '73; Kalia, '81). Ricardo and

Koh ('78) were the first to show that labeled cells were found in the medial portion of the ipsilateral NTS after injecting horseradish peroxidase (HRP) into the rat CeA. These findings have been confirmed in the rat in other HRP studies (Pretorius et al., '79; Otterson, '81) but studies in the cat (Russchen, '82: Cechetto et al., '83) and monkey (Mehler et al., '80) have failed to provide unequivocal evidence of an NTS-CeA pathway. A recent study with the highly sensitive anterograde tracer, Phaseolus vulgaris leucoagglutinin (PHA-L), has demonstrated the projection to originate in the caudal, medial portion of the NTS and terminate topographically within the medial and ventral subdivisions of the CeA (Zardetto-Smith and Gray, '87; Chapter 3, this dissertation).

The catecholaminergic cells of the A2 noradrenergic and C2 adrenergic group are located primarily within the medial division of the NTS (Dahlstrom and Fuxe, '64; Kalia et al., '85a, b; Ruggerrio et al., '85). The function of these two groups in central cardiovascular control and the neuroanatomical pathways involved have been intensely studied in recent years (for review, see Richardson and Chiu, '83). Cell bodies in the NTS are also immunoreactive for a number of peptides suspected to act as neuromodulators or neurotransmitters in autonomic pathways, such as enkephalin (Hokfelt et al., '77; Sar et al., '78; Finley et al., '81; Khachaturian et al., '83; Williams and Dockray, '83; Fallon and Leslie, '86), neurotensin (Jennes et al., '82; Hokfelt et al., '84), and neuropeptide Y (Yamazoe et al., '85; Everitt et al., '84; Harfstrand et al., '87). Both neurotensin (NT) and neuropeptide Y (NPY) are extensively co-localized with catecholamine neurons of the A2 and C2 groups (Everitt et al., '84; Hokfelt et al., '84). Enkephalin (ENK) also co-exists within catecholamine neurons of the A2/C2 groups, but to a much lessor extent (Murakami et al., '89).

A variety of different peptide-containing terminals have been localized within the CeA, as well as the presence of noradrenergic terminals (Fallon et al., '78). Enkephalin, NT, and NPY terminals are especially dense within the CeA (Gray et al., '84; Cassell et al., '82; Wray and Hoffman, '83; Gray et al., '86). To date, the origin of these peptidergic terminals within the CeA remains unspecified. However, transection studies by Fallon et al. ('78) provided evidence that some noradrenergic terminals in the CeA were derived from the A2 group in the NTS (and probably the A1 group as well), the main source being the locus coeruleus (A5 group). The disappearance of NT-immunoreactivity in the CeA after surgical hemitransection of the ascending noradrenergic fiber system has been attributed to disruption of an ascending neuronal pathway from the brainstem (perhaps the NTS) that contained NT as well as norepinephrine (Kawakami et al., '84).

Identifying the chemical organization of peptide and neurotransmitter inputs from the NTS to the CeA may ultimately lead to a better understanding of how visceral feedback influences the integration of autonomic responses with various behaviors. In this study, the combined retrograde tracing/immunohistochemical method was used to test for the presence of ENK, NT, NPY, and catecholamine cells in the NTS which project to the CeA. Preliminary results from this study have been reported previously (Zardetto-Smith and Gray, '86a, '88).

METHODS

The subjects of this study were male Long-Evans rats, 150-325 gm (n=162). Each animal was anesthetized with sodium pentobarbital (Butler) (55 mg/kg). Unilateral injections of fast blue or Fluoro-Gold, or microintophoretic deposits of Fluoro-Gold were made into the CeA. Injections (50 nl) of 2% fast blue dye (D.R. Iling) in dH2O, or 5% Fluoro-Gold (Fluorochrome Inc.) in dH2O, were made with a 1.0 ul Hamilton syringe fitted with a glass micropipette with an outside diameter of 20-25 um. Each injection was made over a 15 min period, with the pipette tip being left in place a minimum of 15 additional minutes. Iontophoretic application of 2% Fluoro-Gold in Ringer's lactate (Baxter-Travenol was placed within the CeA using a glass micropipette (10-20 um outside diameter). Cathodal current was applied at 8 uA delivered in 7-s pulses every 14 s over a 45 min period, using a constant current device (Midgard Electronics Model CS3). These current parameters resulted in a discretely dense deposit of tracer within the CeA and consistently produced robust label within neurons of the NTS. Stereotaxic coordinates (interaural AP = 6.7 mm, ML = -4.5 mm, DV = -6.9 mm) for the CeA were derived from the Paxinos and Watson rat brain atlas (1986).

After 11-15 days rats were reanesthetized and 2.5 ul of colchicine (dissolved in saline, 20 ug/ml) injected into each of the lateral ventricles stereotaxically (interaural AP = 7 mm, ML = $\pm$ 1.3 mm, DV = -2.8 mm). Colchicine has been shown to block axonal transport, causing accumulation of peptides within the perikarya, thus enhancing their visualization using immunocytochemical techniques (Skirboll et al., '84). In addition, 2.5 ul of colchicine (also 20 ug/ml) was injected into the fourth ventricle using the stereotaxic

coordinates interaural AP = -3.8 mm, ML = 0, DV = -7.6 mm.

Twenty-four to forty-eight hours following colchicine administration, animals were administered a lethal dose of sodium pentobarbital. In earlier experiments animals were perfused through the ascending aorta with approximately 200 ml of 0.01M phosphate buffered saline (pH 7.6, 38 C) followed by a 0.167M phosphate buffered 3% paraformaldehyde (pH 7.6, 4 C). In later experiments the pH variation method of perfusion (Berod et al., '81) was utilized. Animals were perfused through the ascending aorta with approximately 200 ml of 0.01M phosphate buffered saline (pH 7.6, 38 C), followed by 250 ml of 0.167M phosphate buffered 4% paraformaldehyde, pH 6.5 (4 C), and then 250 ml of 0.167M phosphate buffered 4% paraformaldehyde, pH 8.5 (4 C). In each perfusion protocol, 100 ml of a 30% sucrose solution (sucrose in phosphate buffered saline, pH 7.6, 4 C) followed the fixative.

Brains were removed immediately and sliced into coronal blocks. Adjacent coronal sections were cut using a Lancer Series 1000 vibratome. Sections from the injection site (40 um) were mounted directly onto acid-cleaned, gel-coated slides in serial order as cut. Adjacent coronal sections of the brainstem (20-25 um) were collected into three vials of cold (4 C) PBS or 0.1% PBS-Triton X (PBS-tx). While cutting, one set of sections was serially mounted onto acid-cleaned, gel-coated slides and retained as a control for any fading of fluorescence that could occur during immunocytochemical processing (Skirboll et al., '84), and for cell counts to assess the magnitude of the NTS-CeA pathway.

Sections were incubated 24-72 hrs with antiserum to three of the following peptides or enzymes: met-enkephalin (ENK) (Immunonuclear Corp. or Penninsula Laboratories), neuropeptide Y (NPY) (Dr. Bibi Chronwall or Dr. Marvin Brown), neurotensin (NT) (Dr. Marvin Brown),

phenylethanolamine-N-methyltransferase (PNMT) (Pennisula Laboratories) or tyrosine hydroxylase (TH) (Dr. John Haycock). All antibodies were raised in rabbit with the exception of TH, which was raised in sheep. Anti-NPY, anti-NT, and anti-PNMT were used at a dilution of 1:1000; anti-ENK and anti-TH were used at a dilution of 1:500. Primary antibodies were diluted in a solution of 0.1% PBS-tx and 10% normal donkey serum (Jackson Laboratories). Antiserum specificity was controlled by pre-incubating 1 ml of each diluted antiserum with 10 ug of its homologous synthetic peptide. The tissue was then processed as described and examined for the presence of any immunohistochemical staining. Although immunohistochemical staining was blocked in these controls, cross-reactivity with as-yet-unidentified antigens cannot be excluded. The term "peptide-like" is, therefore, implicit in the following descriptions of neuropeptide immunoreactivity (neuropeptide-ir).

Following incubation with the primary antisera, sections were rinsed with PBS. In earlier experiments sections (except those incubated with TH) were incubated in rhodamine-conjugated goat anti-rabbit immunogammaglobulin (Cooper Biomedical, diluted 1:10 in PBS-tx) at 45 C for 10 min and then at room temperature for 60 min. Sections incubated with TH were incubated with fluorescein-conjugated anti-sheep immunogammaglobulin (Jackson ImmunoResearch) at room temperature for 60 min. Sections were then transferred to cold PBS and mounted on acid-cleaned, gel-coated slides. In later experiments, sections (except those to be incubated with TH antiserum) were incubated with the primary antisera, rinsed with PBS, and then incubated with biotinylated donkey anti-rabbit immunogammaglobulin (IncStar) for 1 hr at room temperature. Sections incubated with the primary antibody to TH were rinsed in PBS and then incubated with biotinylated donkey anti-sheep immunogammaglobulin (IncStar) at room temperature for 1 hr. After a 10 min rinse

in cold PBS, all sections were then incubated with streptavidin-Texas Red conjugate (IncStar) for 1 hr at room temperature.

The sections were then transferred to cold PBS, mounted on acid-cleaned, gel-coated slides, and covered with DePex (BDH Chemicals). The material was examined with an Olympus BH-2 or Olympus Vannox microscope equipped with a 100 W or 200 W mecury light source, respectively. Fast blue or Fluoro-Gold was visualized with an excitation wavelength centered at 330-360 nm (Olympic ultraviolet filter system) and Texas Red immunofluorescence was viewed using the 546 nm (green) filter system. Cells that contained both retrograde label and Texas Red immunofluorescence (i.e., "double-labeled") could be detected by switching between filter sytems. Sections were photographed with Polaroid coaterless land pack film 667, ASA 3000/36 DIN, and cell counts made using a 20x UV fluorite objective. The location of immunocytochemically-labeled, retrogradely-labeled, and double-labeled cell bodies were plotted using a drawing tube attached to the Olympus BH-2 microscope.

RESULTS

Injection Sites. A total of 162 animals received injections of either fast blue (N = 50) or Fluoro-Gold (N = 112) into the central nucleus or surrounding area. The study was initially begun using fast blue; during its course, a new retrograde tracer, Fluoro-Gold became available. The use of this tracer was adopted because of its greater sensitivity and resistance to fading during immunocytochemical processing and microscopic examination; additionally, it does not appear to label undamaged fibers-of-passage (Schmued and Fallon, '86; Pieribone and Aston-Jones, '88). In this study, a small percentage (<20 %) of the total number of experiments attempted (162) met the criteria of having the injection centered within the CeA, and having detectable retrograde and immunocytochemical label within the NTS. Most cases did not meet this criteria for a variety of reasons, underscoring the potential problems (see discussion below) encountered using the combined retrograde tracing/immunohistochemical technique.

Figure 1 schematically illustrates three representative fast blue injection sites, and four Fluoro-Gold injection sites, that produced characteristic retrograde-labeling within the NTS. These injections most often encompassed both the lateral and medial subdivisions of the CeA. Retrograde label within the NTS was also observed with injections involving only the lateral subdivision (Fig. 1, for example, CFC 18), though the number of cells was reduced in comparison to that seen when the injections included both subdivisions. Fast blue injections were fairly restricted in size, but Fluoro-Gold pressure injections tended to produce larger sites (Fig. 1, compare CFC 28 with CGC 8). Iontophoresis of Fluoro-Gold produced more discrete injection sites (Fig. 1, CGC 80). The sublenticular substantia innominata (SI) was included in

the spread of the injection in some cases (such as CGC 8), as evidenced by the "capping pattern" (surrounding the superior cerebellar peduncle) within the parabrachial nucleus of the pons (see Chapter 5), which is characteristic of injections of the CeA that involve the SI (Fulwiler and Saper, '84).

Retrograde and/or immunocytochemical staining was also examined in cases (N = 11) in which the injection was not centered within the CeA; a composite, schematic illustration of such representative injection sites is shown in Fig. 2. Few, if any, retrogradely-labeled cells were observed within neurons of the NTS in these cases, and if present, were never double-labeled. This is consistent with anterograde studies demonstrating that amygdaloid nuclei other than the CeA receive only minor innervation from the NTS (Zardetto-Smith and Gray, '87; Chapter 3, this dissertation).

Distribution of Retrogradely-Labeled Cells. A few retrogradely labeled cells were present within the most caudal levels of the NTS, in the commissural subnucleus (as defined by Kalia and Sullivan, '82). Most retrogradely-labeled cells were located ipsilateral to the injection within the medial NTS at the level of the area postrema (Fig. 3, 6, 8, 10, 12). Several CeA projecting-neurons were present in an area corresponding to the overlap between the A2/C2 catecholamine groups. Rostral to the level of the area postrema, where the NTS borders the fourth ventricle (periventricular NTS), fewer retrogradely-labeled cells were present within the medial NTS. At more rostral levels of the NTS (subvestibular NTS), only one or two retrogradely labeled cells were usually present. Also, at more rostral levels, 1-2 neurons were occasionally present near the midline, in an area corresponding to the C3 group of adrenergic cells described by Howe et al. ('80). Fast blue

or Fluoro-Gold labeled cells were rarely observed in the contralateral medial NTS, or in subnuclei lateral to the solitary tract (Fig. 3, 6, 8, 10, 12). Using Abercrombie's ('46) correction formula for double counting errors, it was estimated that 328 ± 45 (SEM, n= 7) retrogradely-labeled cells were present within the NTS following injections of tracer into the CeA.

Distribution of Immunocytochemically-Labeled Cells. The distributions of ENK-, NT-, NPY-, TH-, and PNMT-immunoreactivity were the same as that described in previous immunohistochemical studies of the NTS (Jennes et al., '82; Everitt et al., '84; Hokfelt et al., '84; Kalia et al., '85a, '85b; Ruggerio et al., '85; Yamazoe et al., '85; Fallon and Leslie, '86; Harfstrand et al., '87; Kawai et al., '88; Murakami et al., '89) and therefore, will be only briefly described. At the most caudal levels of the NTS, a dense population of neurons immunoreactive for TH was present within the commissural nucleus of the NTS, marking the caudal extent of the A2 catecholaminergic group (Fig. 10). As PNMT-ir cells are not present at this level (Kalia et al., '85a, b) (Fig. 12), these neurons were most likely noradrenergic in nature. One or two NT- and NPY-ir neurons were occasionally present (Fig. 6 and 8, respectively). Several ENK-ir neurons were usually observed at this level but were much fewer in number compared to the population of TH-ir cells (Fig. 3).

At the level of the area postrema, TH-, ENK- and NT-ir cells were present within the medial NTS, dorsal to the motor nucleus of the vagus (Fig. 10, 3, 6, respectively). Again, the TH-ir neurons comprised the densest population of immunocytochemically-labeled neurons at this level. ENK- and NT-ir cells were distributed more discretely within the NTS at this level (Fig. 3, 6). ENK-ir cells occupied a more ven-

tral position within the nucleus, lying medial to the solitary tract and lateral to the dorsal motor nucleus of the vagus. Several more ENK-ir neurons were distributed medially, just dorsal to the motor nucleus of the vagus, but ventral to the area postrema. NT-ir cells occupied a more dorsal portion of the medial NTS, lying dorsal to the solitary tract and in the dorsal strip region of the NTS. NT-ir neurons slightly overlapped the population of ENK-ir cells lying dorsal to the motor nucleus of the vagus, but unlike the ENK-ir cells, densely bordered and continued into the area postrema (Fig. 6). A few NPY- or PNMT-ir neurons appeared at this level, within the dorsal NTS, as well as immediately ventral to the area postrema (Fig. 8).

Rostral to the area postrema, where the NTS borders the fourth ventricle, ENK- and NT-ir cells were much less numerous, while NPY-, TH-, and PNMT-ir neurons formed prominent populations (Fig. 3, 6, 8, 10, 12). All immunoreactive cell types were restricted to the medial NTS, with the exception of ENK-ir cells, some of which were also located in the lateral NTS (Fig. 3). At more rostral (subvestibular) levels of the NTS, a few NT- or NPY-ir neurons were present in the medial NTS (Fig. 6, 9). PNMT-ir neurons clustered within the dorsomedial NTS, and medial border of the dorsal motor nucleus of the vagus (Fig. 12). TH-ir neurons were distributed in a pattern similar to that of the PNMT-ir cells, probably representing adrenergic neurons (Fig. 10). ENK-ir neurons were more scattered throughout the medial (and some lateral) NTS (Fig. 3).

Distribution of Retrogradely-Labeled Immunocytochemically-Labeled Cells. Double-labeled neurons were consistently found within the caudal, medial NTS. Retrogradely-labeled, immunocytochemically-labeled, and double-labeled cells for each peptide/catecholamine-synthesizing

enzyme wre counted in at least two cases (Table 1). These cell counts included labeled cells from both medial and lateral subdivisions of the NTS, and represent the raw (uncorrected for double-counting errors) cell counts.

Enkephalin (ENK-ir). Cells double-labeled for ENK-ir and retrograde tracer were present caudally, within the commissural NTS, and in the medial NTS at levels extending through its ventricular portion (Fig. 3). Double-labeled cells were most numerous within the ventral, medial NTS around the level of the area postrema, often located between the solitary tract and the dorsal motor nucleus of the vagus (Fig. 4, 5), in a region corresponding to the intermediate subnucleus of the NTS (Kalia and Sullivan, '82). Within the subvestibular portion of the rostral NTS, double-labeled cells were rarely observed, due to the fact that few CeA-projecting cells are located at these levels (Fig. 3). Cell counts indicated only a small percentage of the entire ENK-ir population of cells in the NTS project to the CeA (17%), but an average of 22% of the CeA-projecting cell population within the NTS were ENK-ir (Table 1).

Neurotensin (NT-ir). One or two cells double-labeled for NT-ir and retrograde tracer were occasionally present within the caudal, commissural NTS, but like retrogradely-labeled ENK-ir cells, were most numerous within the medial NTS at the level of the area postrema (Fig. 6, 7). However, NT-ir cells were most commonly observed more medially and dorsally than ENK-ir double-labeled cells, at the point of overlap between NT-ir cell and retrogradely-labeled cell populations (Fig. 6, 7). Approximately 12% of the NT-ir neurons within the NTS were retrogradely-labeled following injections into the CeA; an average of only 9% of the CeA-projecting NTS neurons contained NT-ir (Table 1).

Neuropeptide Y (NPY-ir). NPY-ir double labeled cells were

usually not observed at caudal levels of the NTS, as few NPY-ir cells were present within the commissural NTS. Retrogradely-labeled NPY-ir cells were concentrated within the medial NTS at the level where it is immediately adjacent to the fourth ventricle, just rostral to the area postrema (Fig. 8, 9). At this level, double-labeled cells were observed medially, and occasionally, ventromedially (Fig. 9). Farther rostrally, a single double-labeled NPY-ir cell was sometimes present at the dorsomedial border of the vestibular NTS. An average of 14% of retrogradely-labeled cells were NPY-ir, while only 10% of the total NPY-ir cell population projected to the CeA (Table 1).

Tyrosine Hydroxylase (TH-ir). Double-labeled TH-ir cells formed the largest population of retrogradely-labeled immunoreactive neurons in this study. Cell counts show that 60-74% of CeA- projecting cells were TH positive (Table 2). TH-ir double-labeled neurons were found at all levels of the NTS which contained retrogradely-labeled cells (Fig. 10), though most were concentrated at the level of the area postrema and just rostral to it (Fig. 10, 11).

Phenylethanolamine-N-methyltransferase (PNMT-ir). Retrogradely-labeled PNMT-ir cells were fewer in number compared to TH-ir double-labeled cells. At the level of the area postrema, PNMT-ir double-double-labeled cells were sometimes observed in the dorsal strip portion of the NTS (Fig. 12). Most double-labeled cells were located at a level just rostral to the area postrema, where the medial NTS borders the fourth ventricle (Fig. 13A, B). Single, retrogradely-PNMT-ir cells were occasionally present at the dorsomedial border of the subvestibular NTS (Fig. 13C, D), or near the midline within the C3 adrenergic group (Fig. 13E, F). Approximately 9% of retrogradely-labeled cells were also PNMT-ir, while 5% of the total PNMT-ir population projected to the CeA (Table 1).

DISCUSSION

Methodological Considerations. Unsuccessful experiments (nearly 50% of the total number of cases) most frequently resulted from improper placement of the injection, extensive spread of the tracer outside the CeA proper, or failure of the tracer to diffuse properly into the tissue at the injection site. The latter problem occurred more often in cases in which iontophoresis of Fluoro-Gold into the tissue was employed. Several of these cases were utilized as control cases to examine the distribution of retrogradely-labeled cells within the NTS resulting from injections in areas surrounding the CeA (Fig. 2).

Loss of the retrograde tracer, or poor immunohistochemistry, accounted for failure in approximately 19% of the total number of cases. A drawback of the particular modification of the retrograde tracer/immunohistochemical technique used in this study is that sections are subjected to histochemical processing involving a water phase, which can cause diffusion of the retrograde tracer from the tissue if it is not adequately fixed (see Skirboll et al., '84 for review). Conversely, if the tissue is too well fixed, overfixation of the antigen occurs, resulting in poor immunohistochemistry (Berod et al., '81; Sawchenko and Swanson, '81). The perfusion technique employed in this study usually resulted in the brainstem being well-fixed, probably due to the excellent blood supply it receives from the vertebral artery (which branches from the subclavian artery, directly off the aorta). For this reason, different types of fixatives (3% paraformaldehyde, pH variation method) were tried in an attempt to control the degree of fixation.

Poor immunohistochemical visualization may also result from

failure of the colchicine to cause accumulation of peptide in the cell body in sufficient amounts to be detectable by immunocytochemical methods (Sawchenko and Swanson, '81). Most often, this can be ascribed to failure of the colchicine to reach the neurons in adequate amounts to block microtuble transport. Apparently, colchicine administered into the lateral ventricles alone did not always reach the fourth ventricle, as indicated by the presence of excellent immunohistochemical terminal staining and poor perikaryaral staining. Thus, an additional dose of colchicine was administered into the fourth ventricle, beginning with cases late in the series of fast blue injections. The toxicity of the colchicine, and the problems associated with its administration, accounted for early sacrifice of 16% of the animals following colchicine administration and prior to perfusion.

Early experiments used a rhodamine-conjugated secondary antibody. However, problems with the consistency of its manufacture (causing less than optimal immunocytochemistry in some cases) led to the adoption of an avidin-biotin secondary antibody system using Texas Red as the fluorophore (Titus et al., '82). Texas Red produced bright staining, was more resistant to fading (compared to rhodamine), and was reliable provided it was used with fresh biotinylated immunogammaglobulin.

The percentage of retrogradely-labeled cells immunoreactive for ENK, NT, NPY, TH, or PNMT was relatively consistent, from 14-33%, 9-14%, 12-17%, 60-74%, and 0-17%, respectively. In contrast, the absolute total number of retrogradely-labeled and immunocytochemically-labeled cells varied considerably (Table 1). This confirms previous observations in studies employing the retrograde tracing-immunohistochemical technique that assessing the relative contribution of a neuronal population on a percentage basis, rather than in absolute numbers,

is a more reliable index of its participation in a given pathway (Sawchenko and Swanson, '81; Skirboll et al., '84; Moga and Gray, '85).

NTS Peptidergic Efferents to the CeA. The present results provide evidence that ENK, NT, and NPY cells within the NTS innervate the CeA. Within the NTS, CeA-projecting peptidergic cells have a topographic organization. Most retrogradely-labeled ENK- and NT-ir neurons were found within the medial NTS at the level of the area postrema, with double-labeled NT-ir cells positioned dorsal to double-labeled ENK-ir cells. Retrogradely-labeled NPY-ir cells were also found within the medial NTS, but at levels rostral to the area postrema. NTS peptidergic efferents to the CeA are virtually restricted to the caudal, medial portion of the NTS, as few retrogradely-labeled cells were observed at rostral levels of the NTS.

NTS Catecholaminergic Efferents to the CeA. The original observations of Fallon et al. ('78) have been confirmed and extended by the present study, which demonstrates in a direct manner that TH-ir cells in the NTS innervate the CeA. Noradrenergic neurons within the A2 group, rather than adrenergic neurons of the C2 group, provide the bulk of catecholaminergic NTS input to the CeA from the NTS, as is evidenced by the small percentage of PNMT-ir double-labeled cells observed in this study. At the level of the area postrema small TH-positive cells that are found dorsolateral to the solitary tract are adrenergic in nature (Hokfelt et al., '84). Also at this level (and extending caudally), a small group of TH-positive, dopamine beta-hydroxylase negative (dopaminergic) neurons are present in the ventral and medial aspects of the dorsal vagal complex (Everitt et al., '84). As few cells of either type were retrogradely-labled in this study,

most of the TH-ir double-labeled cells at this level of the NTS probably represented CeA-projecting noradrenergic neurons.

The type of catecholaminergic input to the CeA from the NTS differs from that arising from catecholamine groups within the ventrolateral medulla (VLM). Cell counts in retrograde-tracing immunoflourescence studies examining the transmitter organization of CeA-projecting cells within the VLM indicate that a high percentage (> 40%) of adrenergic cells (C1 group) within the VLM send efferents to the CeA (see Chapter 6, this dissertation). In contrast, the present study indicates that the ascending catecholamine input from the NTS to the CeA is primarily noradrenergic in nature.

Co-localization of Neuropeptides Within CeA-Projecting Catecholamine Neurons. The majority of norepinephrine neurons and some epinephrine neurons within the medial NTS, as well as all of the small epinephrine neurons located dorsal to the solitary tract (within the dorsal subnucleus and dorsal strip region), are NT-immunoreactive (Hokfelt et al., '84; Kawai et al., '88). In the present study, double-labeled NT-ir cells (and an occasional double-labeled PNMT-ir neuron) were localized to the medial NTS, suggesting that neurotensin may be co-localized within some CeA-projecting catecholamine neurons. ENK-ir is also present within some catecholaminergic cells of the medial NTS at the level of the area postrema, and at the level where the NTS borders the fourth ventricle (Murakami et al., '89). As double-labeled ENK-ir were localized to these areas within the present study, ENK-ir may also be co-localized within some CeA-projecting catecholaminergic neurons.

The majority of adrenergic cell bodies of the C2 group in the NTS have also been found to contain NPY-immunoreactivity; conversely, few

noradrenergic neurons within the A2 group are NPY-positive (Everitt et al., '84; Hokfelt et al., '84). Thus, some of the double-labeled PNMT-ir neurons observed in the NTS, particularly at the level where it borders the fourth ventricle, most likely also contained NPY-immunoreactivity. However, the average percentage of retrogradely-labeled NPY-ir neurons was much higher comared to the average percentage of retrogradely-labeled PNMT-ir neurons, indicating that some NPY-ir cells that projected to the CeA were non-adrenergic in nature (14% vs. 9%). Catecholamine neurons within the NTS can be divided into distinct subgroups based upon the co-existence of a specific peptide(Everitt et al., '84; Kawai et al., '88; Murakami et al., '89). Clearly, retrograde tracing/immunohistochemical combined with co-localization studies will be required to identify definitively the subgroups from which CeA efferents originate.

Relationship of NTS Efferents to the Distribution of CeA Immunoreactive Terminals. The lateral and lateral capsular subdivisions of the CeA contain a high density of ENK (Gray et al., '84) and NT (Cassell et al., '82) immunoreactive terminals, while the bulk of catecholamine (Fallon et al., '78) and NPY (Gray et al., '86) immunoreactive terminals are distributed within the medial subdivision. The ventral subdivision of the CeA also contains enkephalin (Zardetto-Smith et al., '84) and catecholamine (Fallon et al., '78) terminal immunoreactivity. Anterograde tracing studies have shown neurons of the medial NTS, especially those at the level of the area postrema, densely innervates the ventral and medial subdivisions of the CeA, with the lateral and lateral capsular subdivisions receiving comparatively fewer NTS efferents (Ricardo and Koh, '78; Zardetto-Smith and Gray, '87; Chapter 3, this dissertation). In the present study, most TH-, ENK-, and NT-

retrogradely-labeled cells were distributed within this area. It seems likely, therefore, that the medial NTS is one source of catecholamine and enkephalin terminals within the ventral subdivision of the CeA, and neurotensin and enkephalin terminals within the lateral/lateral capsular subdivisions.

The medial NTS is also a probable source of NPY-terminal immunoreactivity within the medial subdivision of the CeA. NPY-ir terminals innervate neurons within the medial CeA that project to the dorsal vagal complex, suggesting they may directly modulate dorsal vagal complex neuronal activity (Gray et al., '86). Noradrenergic-terminal immunoreactivity within the CeA is also derived from the A5 (locus coeruleus) (Fallon et al., '78) and A1 (ventrolateral medulla) (Zardetto-Smith and Gray, '88) groups. The bed nucleus of the stria terminalis is a major source of ENK to the CeA (Palkovits et al., '81; unpublished observations cited by Gray and Magnuson, '87a), while the parabrachial nucleus is an additional source of NT (Block et al., '89).

Comparison of Neurochemical Content of NTS-CeA Efferents to CeA-NTS Afferents. Past studies indicated most of the efferent projections of the CeA to the dorsal vagal complex (dorsal motor nucleus of the vagus and NTS, DVC) to originate from the medial CeA (Hopkins and Holstege, '78; Schwaber et al., '82). More recently, retrograde tracing studies have demonstrated the descending projection also arises from cells located in the lateral and ventral subnuclei (Thompson and Cassell, '89). A large part of the descending peptidergic pathway from the CeA to the NTS arises mostly from its lateral subdivision, though most immunoreactive cells for these peptides are located medially (for review, see Gray, '89). A large part of the peptidergic ouput from the CeA to the DVC that has been identified arises from corticotropin re-

leasing factor, somatostatin, and neurotensin cells, while substance P cells make a minor contribution (Higgins and Schwaber, '83; Gray and Magnuson, '87a). The failure to identify descending projections from the medial CeA may be explained by the finding that a significant proportion of neurons in this area project to the ventrolateral medulla, rather than the NTS (Thompson and Cassell, '89).

Enkephalin cells in the CeA do not participate in the descending pathway to the DVC (Gray and Magnuson, '87a). The results of the present study demonstrate that although there are afferent and efferent connections between the NTS and CeA, their peptidergic connections may not necessarily be reciprocated. Additionally, the ascending pathway is distinguished from the descending projection by the contribution from noradrenergic and adrenergic neurons (Fallon et al., '78; present study).

Functional Considerations. The CeA is thought to integrate the somatic and visceral responses during various adaptive behaviors, and plays a role in emotion and memory formation, as well as in mediating the autonomic and neuroendocrine responses to certain stressful environmental conditions (see Chapter 2, this dissertation, for review). Neurophysiological and behavioral studies have demonstrated a role for catecholamines, opioids (including ENK), NT, and NPY in many of these same functions.

Central Cardiovascular Regulation. A role for noradrenergic and adrenergic neurons in central autonomic regulation, particularly of the cardiovascular system, has been suggested by several lines of anatomical and physiological evidence (see Richardson and Chiu, '83 for review). The NTS, site of the A2 and C2 catecholaminergic groups, is known to be a critical integrative area for sensory input arising from

various afferent pathways, and for the modulation of reflex autonomic activity (Carey, '84). A2 noradrenergic neurons are though to modulate the transmission of baroreceptor reflexes at this level (Schmitt and Laubie, '82). Likewise, enkephalin affects the discharge pattern of NTS neurons, occurring in conjunction with changes in cardiopulmonary function, suggesting indirectly that this peptide also plays a transmitter or neuromodulatory role in baroreceptor and chemoreceptor reflexes (Denavit-Saubie et al., '78; Hassen et al., '82). The NTS is one site where opioids may interact with the catecholamines to modulate the control of blood pressure (Akil et al., '84); in fact, clonidine, an alpha-2 agonist, is thought to exert its hypotensive effect, in part, by stimulating release of endogenous opioids (Farsang et al., '80; Kunos et al., '81). NPY may also have cardiovascular effects when administered centrally; intracisternal administration of NPY in anesthetized rats causes hypotension with no concommitant change in heart rate (Fuxe et al., '83). Stimulation of the CeA in the awake cat or rat causes tachycardia and increased arterial pressure (Hilton and Zbrozyna, '63; Stock et al., '78; Galeno and Brody, '83; Schlor et al., '84; Gelsema et al., '87), and in the anesthetized rat or monkey, hypotension and decreased heart rate (Reis and Oliphant, '64; Mogenson and Calaresu, '73; Faiers et al., '75; Galeno and Brody, '83; Gelsema et al., '87). In the present study, double-labeled TH-ir and ENK-ir neurons were found in the medial NTS in regions identified in the rat as receiving baroreceptor input (Kalia and Sullivan, '82; Ciriello et al.; '83). Possibly, this noradrenergic/peptidergic input to the CeA is involved in the integration of baroreceptor feedback and behavioral adjustments.

Arousal and Sleep. Central noradrenergic systems (possibly in close interaction with dopaminergic systems) have been suggested to

mediate arousal from sleep states and during certain motivated behaviors (Panksepp, '80). An orienting or alerting reaction (the first stage of the defense reaction in the cat) in the conscious rat has been observed to accompany the changes in heart rate and blood pressure during CeA stimulation (Galeno and Brody, '83; Gelsema et al., '87). Conversely, NPY administration (intracisternal) produces sedation, an effect also produced by the alpha-2 agonist, clonidine (Fuxe et al., '83). The CeA is one forebrain structure which modulates reflex responses to pressure changes during sleep (Frysinger et al., '84), and neurons in the CeA alter discharge rates with sleep-waking states (Jacobs and McGinty, '71). The noradrenergic and NPY-innervation of the CeA arising from the NTS may be involved in mediating some of the amygdala-brainstem interactions that are strongly influenced by wakefulness-sleep states (Frysinger et al., '84).

Stress. Fear has been hypothesized to be the emotion which evolved to avert threats to the integrity of the body surface. The major behavioral responses resulting from fear (including flight and defense) serve to ward off potential or actual bodily harm (Panksepp, '82). Davis et al. ('84) has recently reviewed the evidence that the CeA, related nuclei, and their connections, comprise a "central fear system".

Several studies have implicated the CeA in pathophysiological responses such as hypertension, to stressful environmental conditions involving a chronic state of fear or anxiety (defined as a diminutive form of fear, Panksepp, '82). Intensified environmental stimuli, resulting in a "prolonged defense reaction" in which sympathetic activity to the heart and peripheral circulation remains elevated over a long period of time, may contribute to the development of hypertension (for review, see Folkow et al., '82; Lawler et al., '85). Cen-

trally intensified defense reactions to alerting stimuli are present in spontaneously hypertensive rats (SHR), a model for human neurogenic hypertension (Hallback and Folkow, '74). In addition, stressful environments aggravate hypertension in SHR and amygdala-lesioned rats respond less than controls to stressful, fear-inducing stimuli (Folkow et al., '82). Bilateral lesions of the CeA in young SHR attenuate the development and delay the onset of hypertension (Folkow et al., '82; Galeno et al., '82). In both animal and human hypertension, altered baroreflex control of the heart and circulation occurs (for review, see Brown, '81; Thames, '84) and there are marked alterations in central concentrations of catecholamines (Versteeg et al., '76; Wijnen, '78; Saavedra, '81) and peptides, including enkephalin (Nosaka and Wang, '72; Morris et al., '81; Mohring et al., '80; Feurstein et al., '83). Also, alpha-2 adrenoceptors in the CeA have been found to be important in the neural control of renal function in conscious SHR during exposure to environmental stress (Koepke et al., '87). Thus, the genesis and expression of hypertension may be explained, at least in part, by catecholamine- and peptide-mediated interactions between the CeA and NTS.

Another pathological process related to stress in which the CeA has been implicated is gastric ulceration (for reviews, see Henke, '82, '88). Immobilization of rats produces gastric ulcers which are attenuated by bilateral lesions involving the CeA (Henke, '80a, b), and may be due, in part, to impairment of negative feedback from gastric receptors to the amygdala (Henke, '83). The CeA may also be a primary site for opiate-mediated attenuation of stress ulcerogenesis (Ray et al., '87).

Ingestive Behavior. Input from the gastric stretch or acidic receptors relayed through the NTS, conveying the state of gastric

distention, and therefore, satiety or hunger (for review, see Panital, '73), may also play a role in the modulation of hypothalamic satiety mechanisms (Box and Mogenson, '75; Kaada, '72). Norepinephrine, opioids, and NPY have been implicated as central modulators of appetite and feeding behavior, each increasing food intake (for reviews, see Morley et al., '83; Gray and Morley, '86). The opioids may exert their effects through activation of a noradrenergic mechanisim (Morley et al., '83), and the CeA may be one site within the satiety circuit where this interaction occurs.

Analgesia. A variety of stressful environmental stimuli that do not produce obvious pain, such as restraint and hypoglycemia, are accompanied by analgesia (Hayes et al., '78; Amir and Amit, '78; Bodnar et al., '79). Amygdalar lesions reduce the responsiveness to several non-painful, but aversive stimuli, suggesting the CeA may be part of the "ancillary pain system" that mediates the presumed motivational-affective components of aversive experiences (Henke, '82). Micro-injection of NT into the CeA produces an increase in nociceptive threshold, thus possibly acting to alter the affective component of behavioral resonses to noxious stimuli (Kalivas et al., '82). In addition, there is evidence that the cardiovascular and pain pathways are linked (for review, see Randich and Maixner, '84). Activation of the baroreceptor reflex in the rat induces analgesia, while enkephali-nergic compounds exert various cardiovascular changes (depending on the route of administration). Clonidine also produces antinociceptive, as well as hypotensive responses, following either central or oral ad-ministration (for review, see Randich and Maixner, '84). The NTS, cited earlier as one site where opioids may interact in cardiovascular control, has also been implicated in subserving the analgesia induced by opioids and clonidine (Randich and Maxiner, '84). Analgesia,

coupled with a pressor response, and subsequent inhibition of pain and/or associated motivation-affective changes, may aid in reducing the stress associated with adverse environmental stimulation (Randich and Maixner, '84). As the CeA participates in both pathways, it may be one such site of linkage between pain and cardiovascular pathways (Moga and Gray, '85).

In the rabbit, stimulation of the CeA causes a bradycardiac and depressor response, similar to that observed during the initial stages of Pavlovian fear-conditioning. Lesions of the CeA greatly attenuate the magnitude of this bradycardia (Kapp et al., '79), suggesting the CeA may play a direct role in the expression of cardiovascular and possibly other somatic and autonomic responses to conditioned stimuli during Pavlovian conditioning (Kapp et al., '81). Noradrenergic activity (affecting beta receptors) within the CeA contributes to this acquisition of the conditioned heart rate responding (Gallagher et al., '80). Randich and Maixner ('84) point out that the pressor response to psychogenic/pyschosocial stresses and its concommitant analgesia (which may serve as a form of psychophysiological relief), may be accompanied by engagement of conditioning mechanisims. Thus, in the future, the organisim would instrumentally evoke elevations in blood pressure (i.e., Pavlovian conditioned increase in arterial pressure) in anticipation of environmental stress, which over a period of time might contribute to the development of hypertension (Randich and Maixner, '84). This view implied that elevations in blood pressure are reinforcing (Randich and Maixner, '84), an interesting statement in light of the fact that both norepinephrine and opioids (for reviews, see Riley et al., '80; Panksepp, '80) are reported to facilitate brain reward sytems. It has been theorized that the behavioral activation during self-stimulation mobilizes a general stress mechanisim, causing

increased noradrenergic activity (Panksepp, '80). During self-stimulation of the medial forebrain bundle (by which some noradrenergic innervation reaches the forebrain, including noradrenergic input to the CeA), labeled norepinephrine is released from both the hypothalmus and amygdala (Stein and Wise, '69). Also, noradrenergic system of the amygdala has been implicated in some aspects of aversive information processing in intially threatening environments (Ellis et al., '84). Together, these observations again suggest a possible involvement of the noradrenergic and enkephalinergic pathways from the NTS to the CeA, though further studies are clearly needed in order to define their functional correlates more precisely.

Clinical Implications. Finally, the function of the amygdala, in general, is to interpret the significance of environmental stimuli and to bias the organisim towards the appropriate response (Gloor, '75; Price et al., '87). Dysfunction of structures in the temporal lobe associated with the limbic system is thought to be one possible cause of schizophrenia, because of the schizophrenic-like nature of the symptoms associated with temporal lobe epilepsy (unusual cognitive experiences, psychosis, stereotyped oral and motor behavior, and emotional changes) (Roberts et al., '83).

One aspect of schizphrenia is misperception, in part related to inappropriate emotional responses to normal environmental events (Gloor, '75). Data accumulated in recent years has demonstrated that schizophrenia can no longer be regarded as a functional psychosis, but an organic one, with the primary disturbance being an abnormality of transmitter function in the temporal lobe (Tyrer and MacKay, '86). In particular, biochemical studies have revealed specific abnormalities in the temporal lobe, including the amygdala, in schizophrenic patients. Amygdalar concentrations of met-enkephlin, substance P, and vasoactive

intestinal polypeptide are abnormally elevated, while in type II schizophrenic patients, cholecystokinin is decreased (Zech et al., '86; Roberts et al., '83; Ferrier, '83; Tyrer and MacKay, '86). Pharmacologic treatment of schizophrenia with an endorphin derivative and cholecystokinin have already been attempted (Van Praag and Vrhoeven, '81; Bloom et al., '83). Also, many of these peptides have intimate anatomical and physiological relationships with dopamine, the neurotransmitter that most often has been implicated in schizophrenia (for review, see Seeman, '85). In schizophrenia the CeA may be a future target area for pharmacologic therapy directed toward restoring or altering the chemical balance of neuropeptides and neurotransmitters that mediate the appropriate expression of emotional behaviors.

Concluding Comments. The central nucleus of the amygdala receives a prominant catecholaminergic innervation from the NTS that probably is largely noradrenergic in nature. Enkephalin and NPY cells, and to a minor extent NT cells, provide peptidergic input to the CeA. Each of these peptides may be co-localized (to varying extents) within catecholamine-projecting CeA neurons. The catecholaminergic and enkephalinergic contribution to the ascending pathway from the NTS to the CeA distinguishes it neurochemically from the reciprocal descending pathway. The specific mechanisms by which peptidergic and catecholaminergic neurons participate in the autonomic reponses associated with emotion, stress, and learning is not known. However, afferent visceroceptive input from these types of neurons within the NTS, relayed to the CeA, may be important in the etiology of a number of pathophysiological conditions including hypertension, gastric ulcers, and schizophrenia.

Table 1. Injection sites for all cases except CGC 3 and CGC 76 are illustrated in Figure 1. Numbers represent raw counts, uncorrected for double-counting errors.

ABBREVIATIONS:

RG	number of retrogradely-labeled cells
IR	number of immunoreactive cells
DL	number of double-labeled cells
DL/RG	ratio giving percent of retrogradely-labeled cells immunoreactive for given antigen
DL/IR	ratio giving percent of immunoreactive-cell population projecting to CeA

TABLE 1

Antigen	Case	# Sections	#RG Cells	#IR Cells	#DL Cells	DL/RG %	DL/IR %
ENK	CFC 18	14	72	126	10	14	8
	28	13	100	165	20	20	14
	CGC 3	15	86	187	17	20	9
	8	13	129	195	42	33	21
NPY	CGC 74	21	41	103	7	17	7
	76	24	73	92	9	12	10
	80	24	95	91	12	13	13
NT	CGC 3	9	63	91	9	14	10
	102	27	151	194	14	9	7
TH	CGC 80	25	85	402	63	74	16
	102	33	104	470	62	60	13
PNMT	CGC 74	17	50	21	0	0	0
	102	33	92	274	8	9	3
	112	31	121	161	21	17	13

Figure 1. Line drawings of coronal sections through four different levels of the CeA, and representative injection sites for both fast blue (CFC 18, 25, 28, 33) and Fluoro-Gold (CGC 8, 80, 102) injections into the CeA. Center of the injection is indicated by black shading; spread of the tracer is indicated by shaded area.

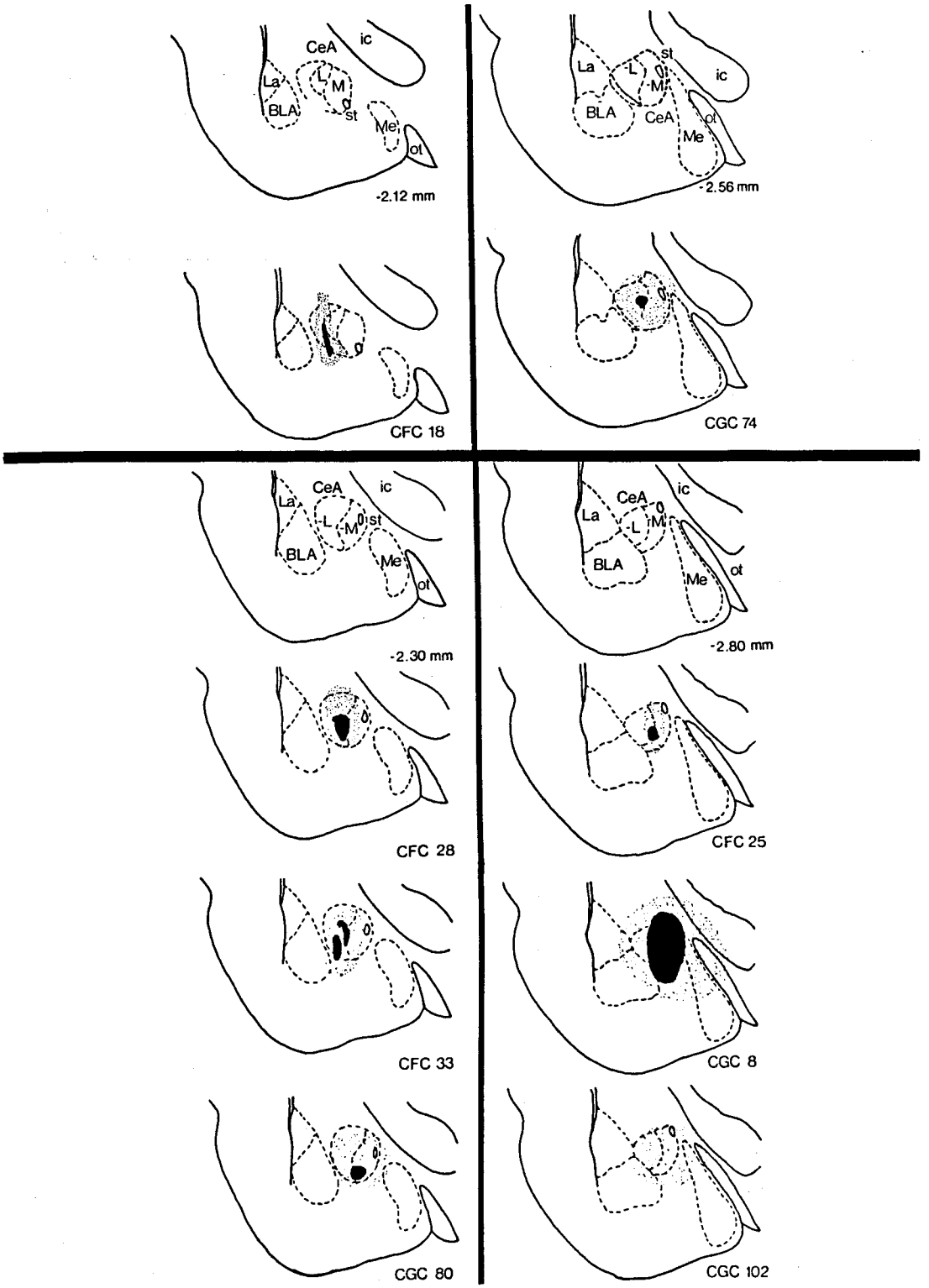
CeA
ic
La
L
M
BLA
st
Me
ot
-2.12 mm
La
st
L
M
ic
BLA
CeA
ot
Me
-2.56 mm
CFC 18
CGC 74
CeA
ic
La
L
M
st
BLA
Me
ot
-2.30 mm
CeA
ic
La
L
M
BLA
Me
ot
-2.80 mm
CFC 28
CFC 25
CFC 33
CGC 8
CGC 80
CGC 102

Figure 2. Line drawing of coronal section through the rat amygdaloid complex representing injection sites of retrograde tracer around the area of the CeA which did not produce retrograde labeling within the NTS.

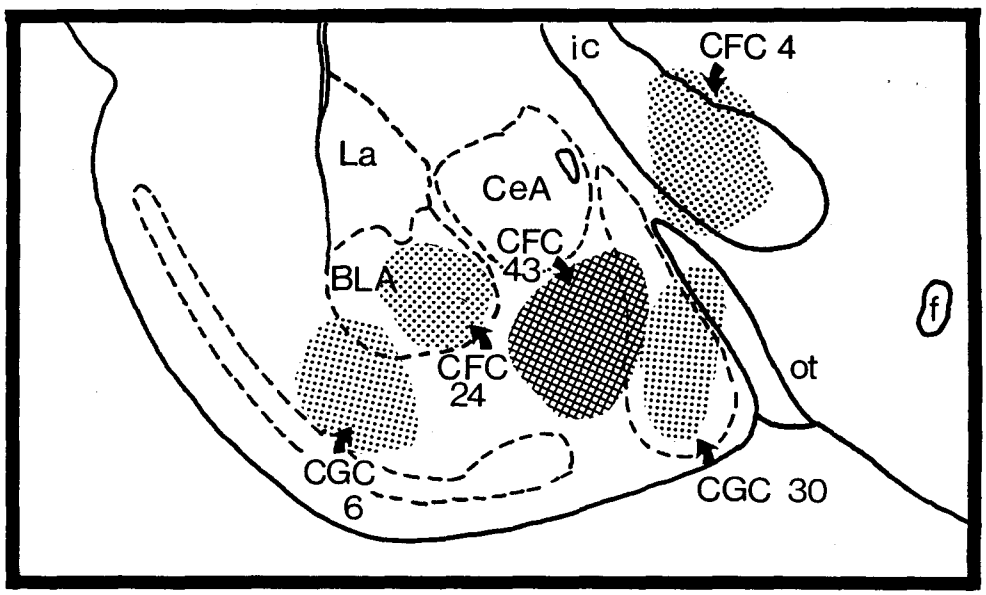
ic
CFC 4
La
CeA
CFC
43
BLA
f
ot
CFC
24
CGC
6
CGC 30

Figure 3. Line drawings of four coronal sections through the NTS illustrating the distributions of retrograde tracer (open circles), enkephalin (ENK)-immunoreactive (filled circles), and double-labeled cells (stars) found within the NTS following injections into the CeA.

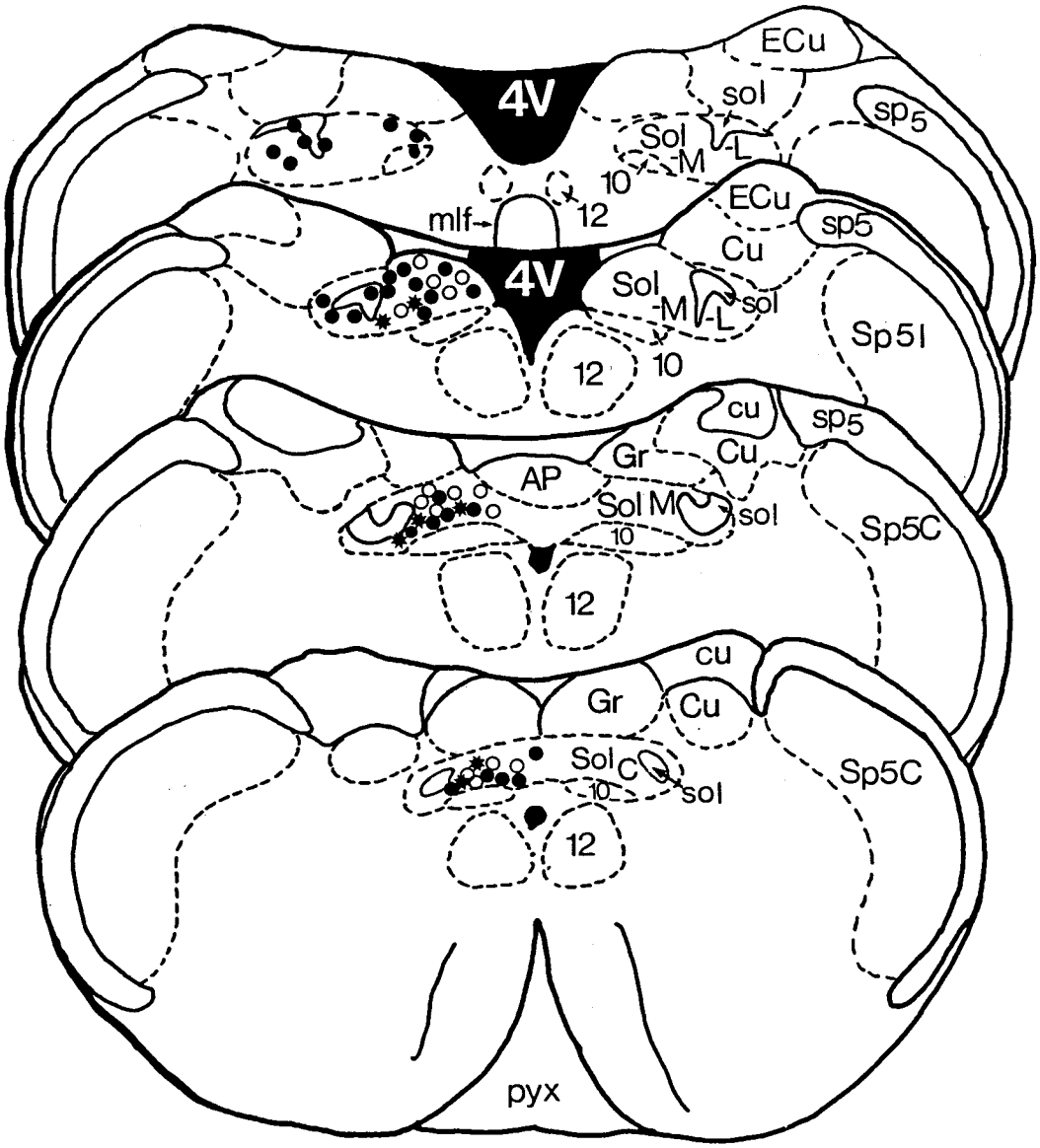
ECu
4V
sol
sp5
Sol
M
L
10
12
mlf
ECu
sp5
Cu
4V
Sol
M
L
sol
Sp5I
12
10
cu
sp5
Gr
Cu
AP
Sol M
sol
Sp5C
10
12
cu
Gr
Cu
Sol C
Sp5C
sol
10
12
pyx

ENK

Figure 4. Fluorescent photomicrographs of coronal sections through the NTS illustrating cells projecting to the CeA (A, C, E) and cells immunoreactive to ENK (B, D, F). Panels C and D are high power photomicrographs of panels A and B, respectively. Double-labeled cells are indicated by the white arrows. Magnifications: A and B, 390X; C and D, 625X; E and F, 525X.

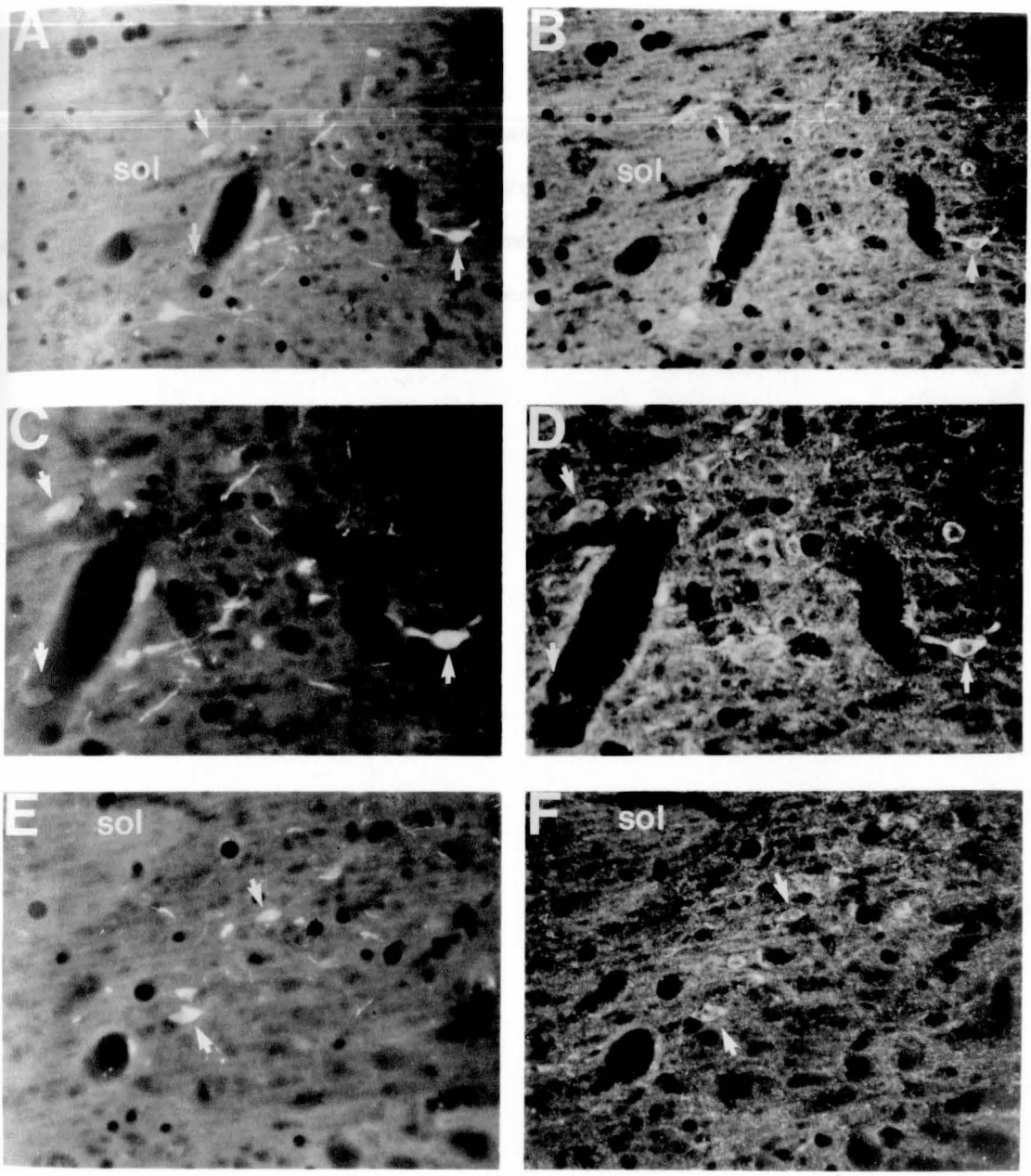
A
sol
B
sol
C
D
E
sol
F
sol

Figure 5. Low-power (188X, A and B) and high-power (375X, C and D) fluorescent photomicrographs of CeA-projecting cells (A and C) and ENK-immunoreactive cells (B and D) within the NTS. Double-labeled cells are indicated by arrows.

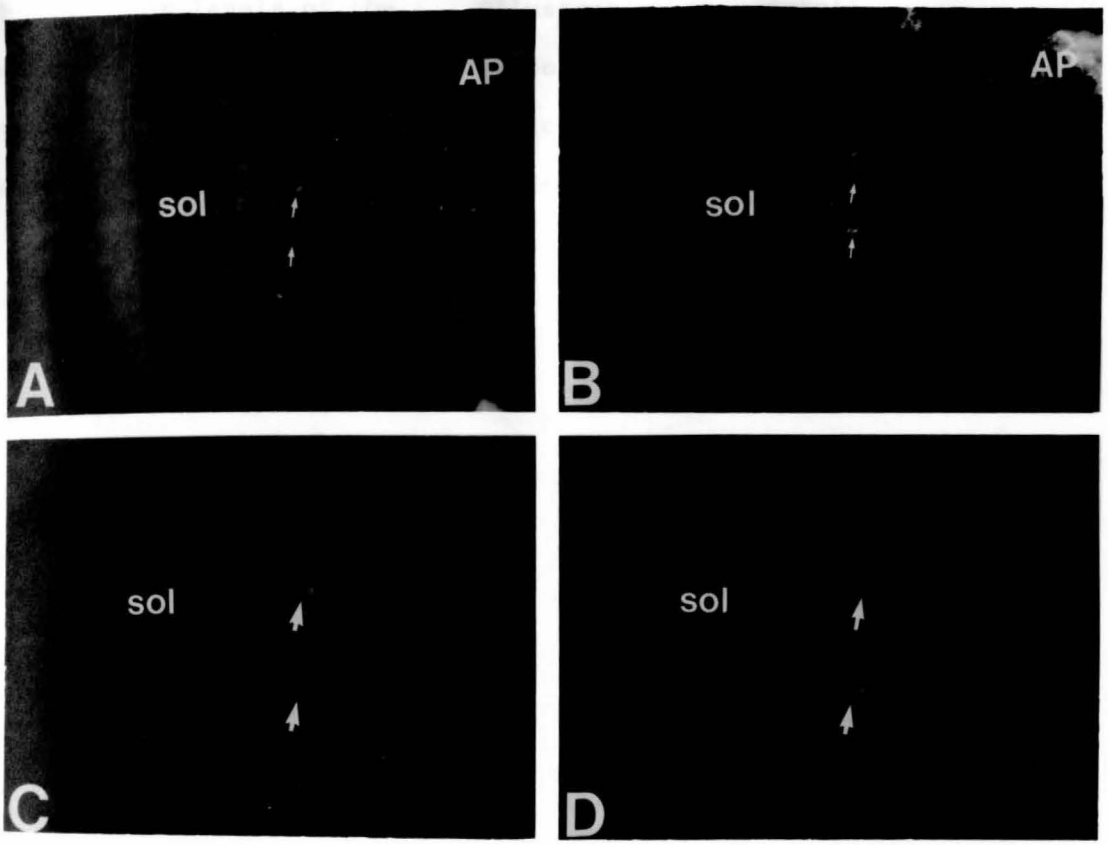
AP
sol
A
AP
sol
B
sol
C
sol
D

Figure 6. Line drawings of coronal sections through four levels of the NTS illustrating the distributions of retrogradely-labeled (open circles), neurotensin (NT)-immunoreactive (filled circles) and double-labeled cells (stars) following injections into the CeA.

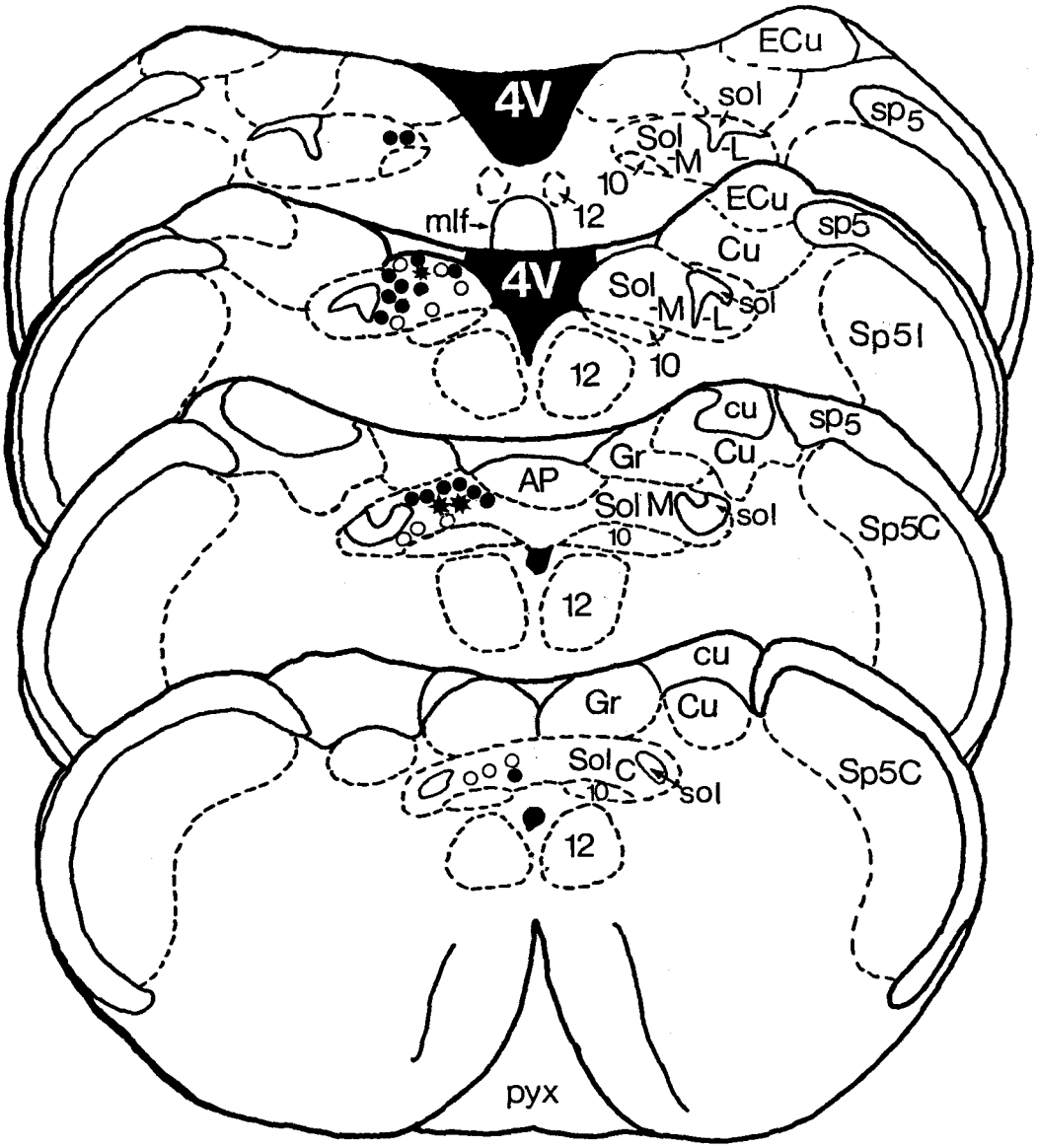
ECu
4V
sol
sp5
Sol
M
L
10
12
mlf
ECu
sp5
Cu
4V
Sol
M
L
sol
Sp5I
12
10
cu
sp5
Gr
Cu
AP
Sol M
sol
Sp5C
10
12
cu
Gr
Cu
Sol C
Sp5C
10
sol
12
pyx

NT

Figure 7. Fluorescent photomicrographs (A and D) of retrogradely-labeled cells in the NTS following injections of retrograde tracer into the CeA. On the right (B and D) are photomicrographs of the same area demonstrating neurotensin (NT)-immunoreactive cells. Double-labeled cells are indicated by white arrows. Magnification: A and B, 160X; C and D, 320X.

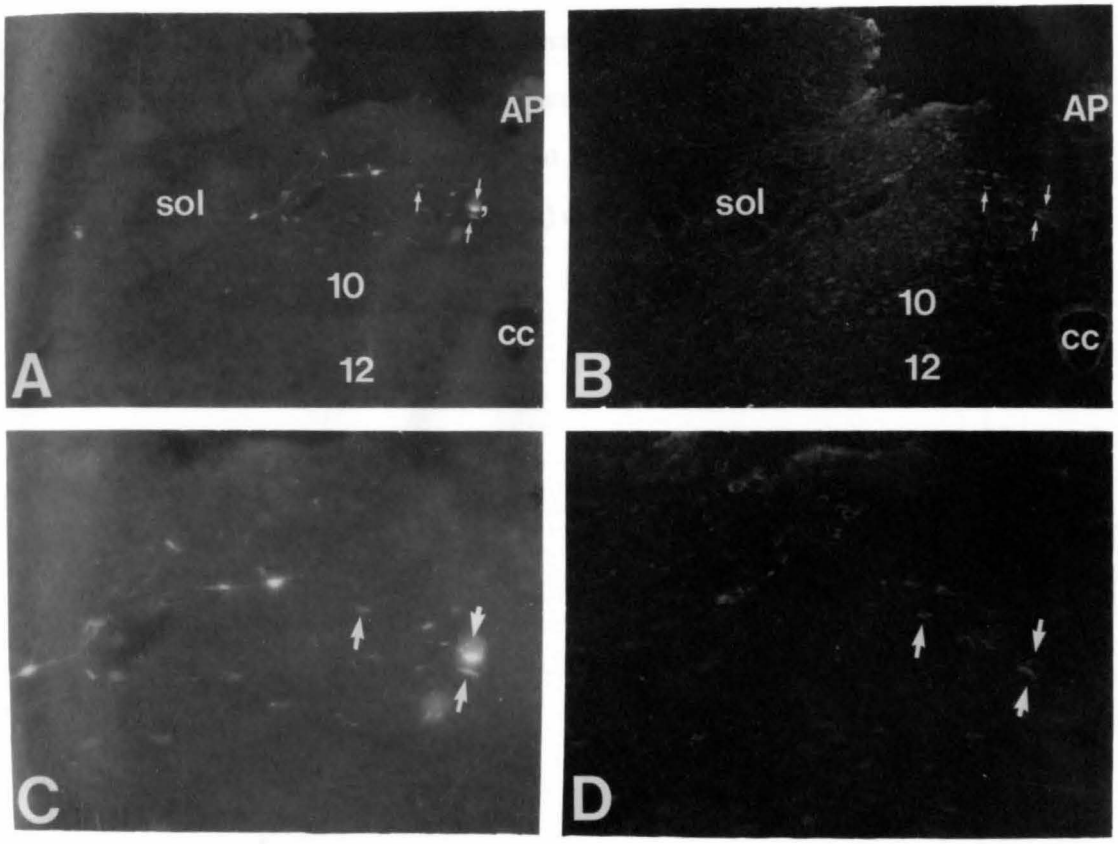
AP
sol
10
cc
12
A
AP
sol
10
cc
12
B
C
D

Figure 8. Line drawing of four coronal sections through the NTS illustrating the distributions of retrogradely-labeled (open circles), neuropeptide Y (NPY)-immunoreactive (filled circles), and double-labeled (stars) cells found within the NTS after injections into the CeA.

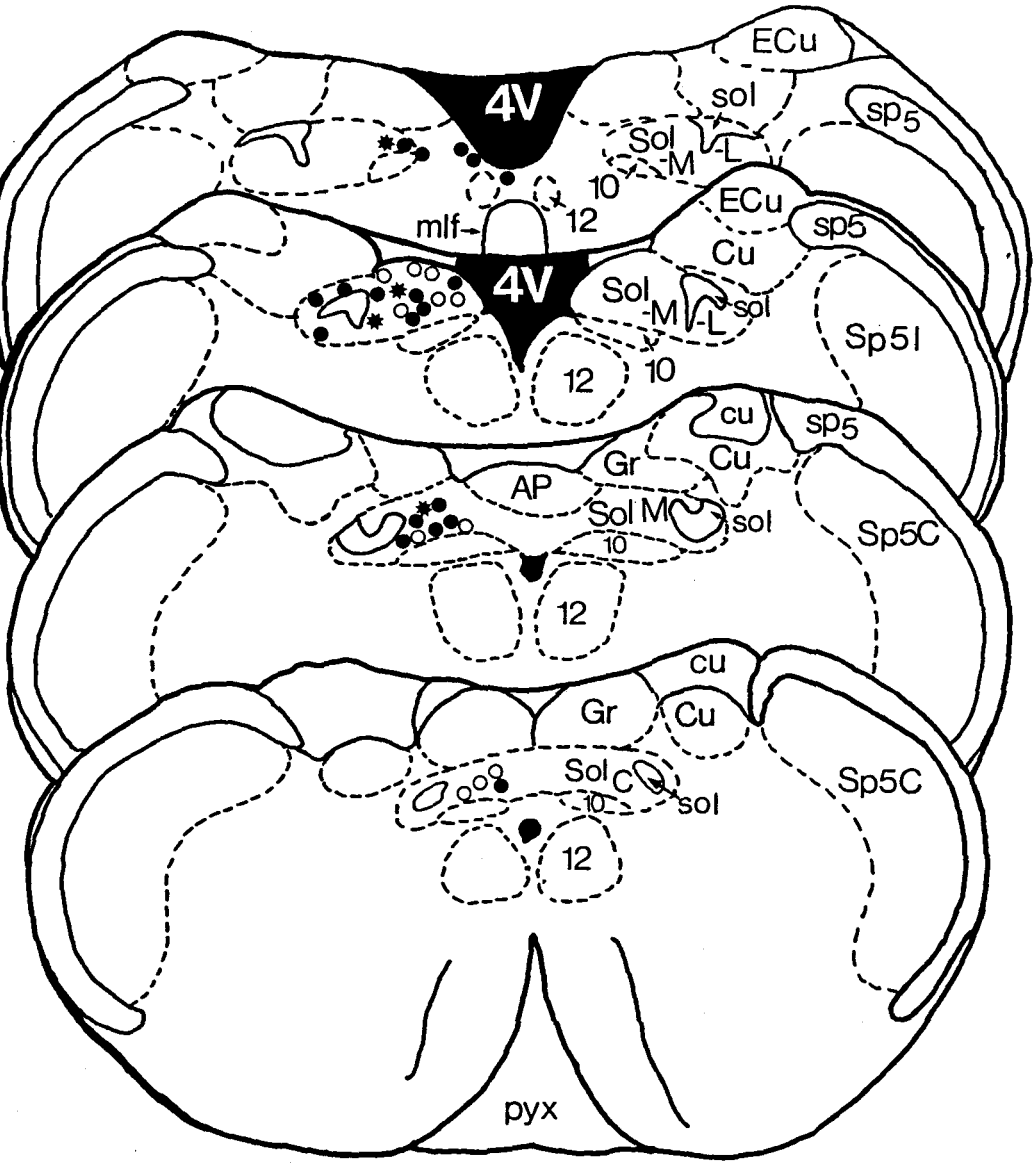
ECu
4V
sol
sp5
Sol
M
L
10
ECu
mlf
12
sp5
Cu
4V
Sol
M
L
sol
Sp5I
12
10
cu
sp5
Gr
Cu
AP
Sol M
sol
Sp5C
10
12
cu
Gr
Cu
Sol C
sol
Sp5C
10
12
pyx

NPY

Figure 9. Photomicrographs (A and C) of retrogradely-labeled neurons within the NTS following injections of Fluoro-Gold into the CeA. On the right (B and D) are photomicrographs of the same area demonstrating NPY-immunoreactive cells. Cells containing both Fluoro-Gold and NPY-immunofluorescence (double-labeled) are indicated by arrows. Magnification: A and B, 280X; C and D, 560X.

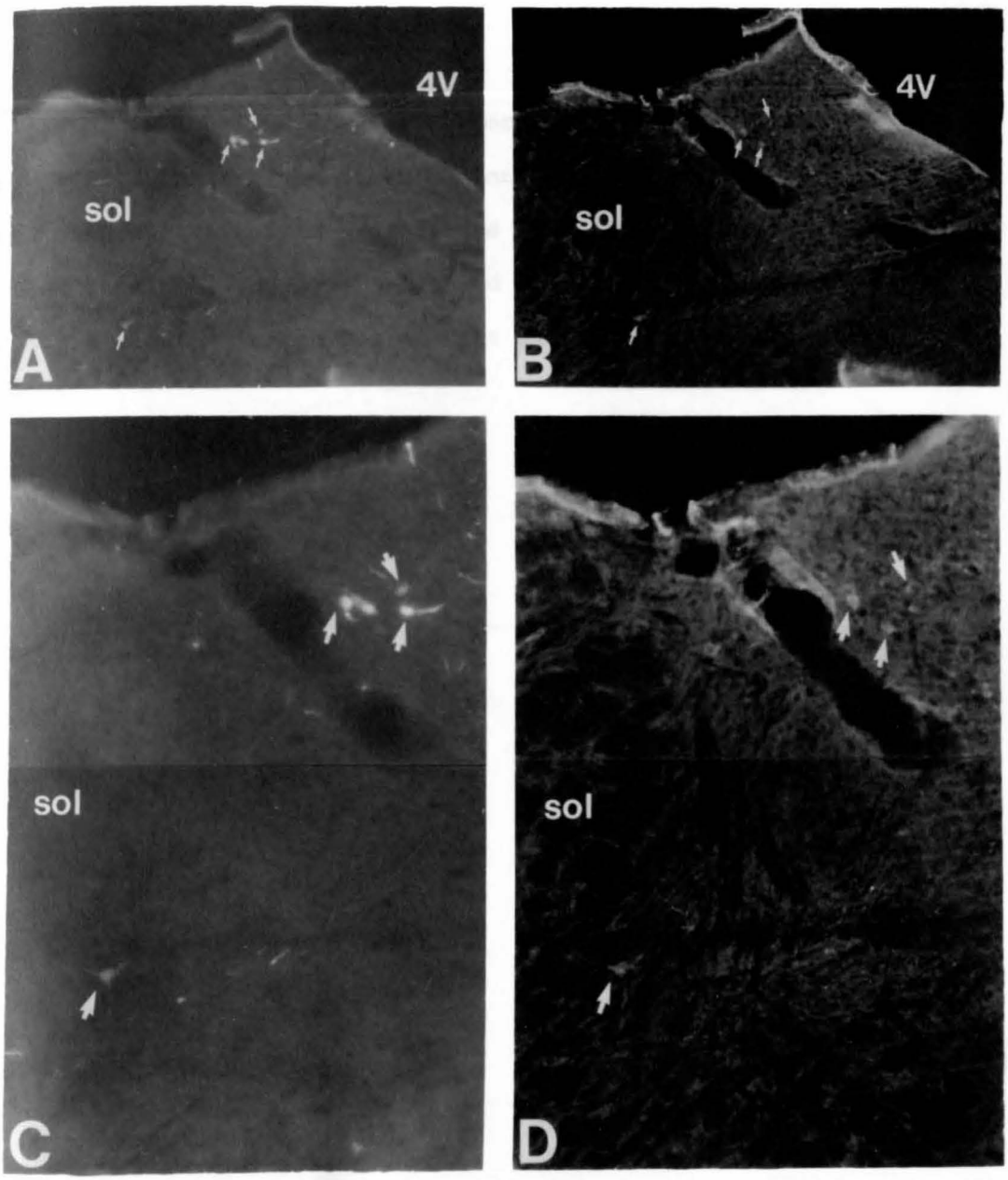
4V
sol
A
4V
sol
B
sol
C
sol
D

Figure 10. Line drawing of coronal sections through the NTS illustrating the distributions of retrograde tracer (open circles), tyrosine hydroxylase (TH)-immunoreactive (filled circles), and double-labeled (stars) neurons within the NTS following injections of fast blue or Fluoro-Gold into the CeA.

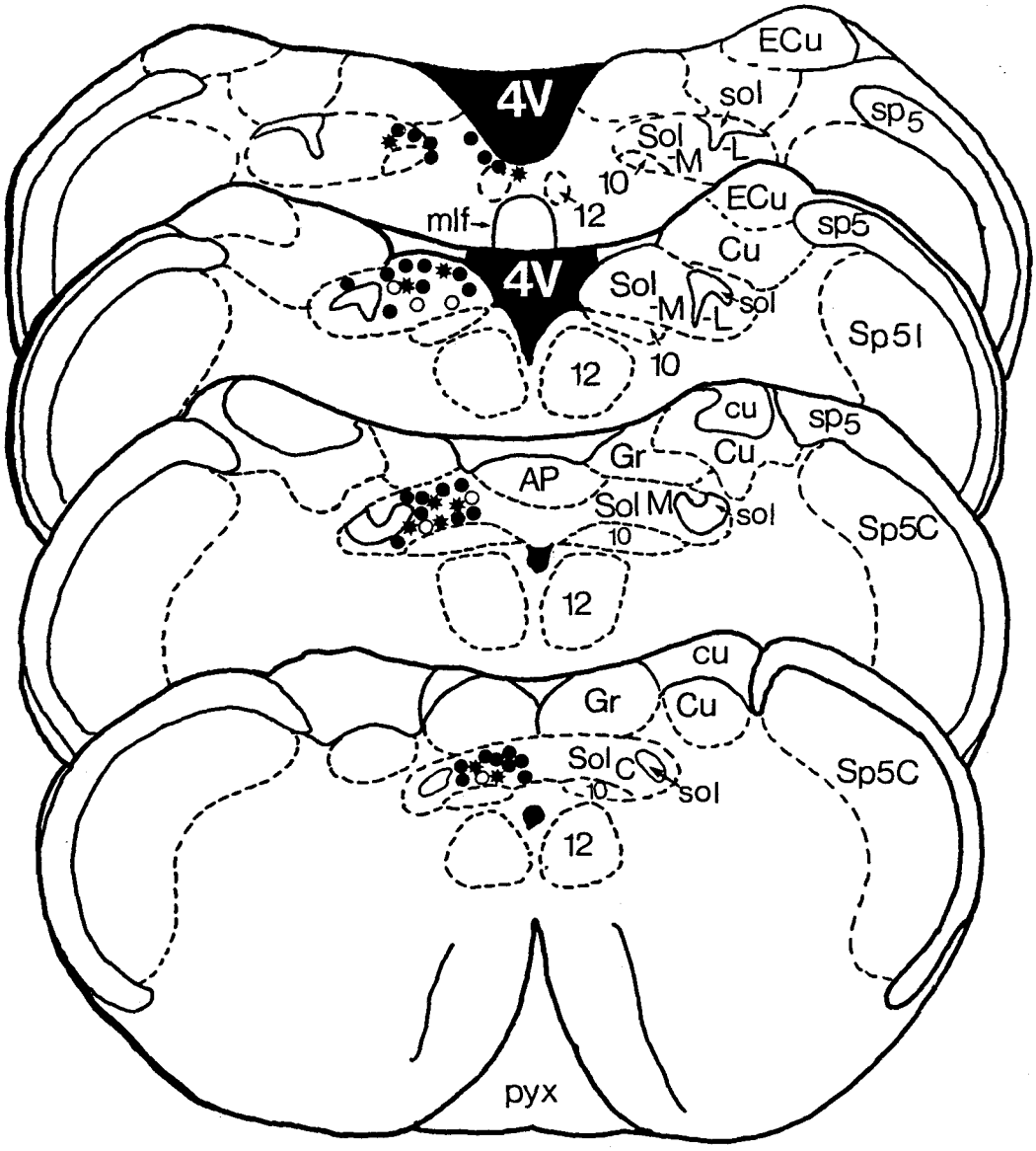
ECu
4V
sol
sp5
Sol
M
L
10
12
mlf
ECu
sp5
Cu
4V
Sol
M
L
sol
Sp5I
12
10
cu
sp5
Gr
Cu
AP
Sol M
sol
Sp5C
10
12
cu
Gr
Cu
Sol C
Sp5C
10
sol
12
pyx

TH

Figure 11. Fluorescent photomicrographs of a coronal section through the NTS at the level of the area postrema illustrating the distribution of (A) cells projecting to the CeA and (B) cells immunoreactive to TH. Five-double labeled cells (indicated by white arrows) are present within the medial NTS. Magnification: 900X.


A

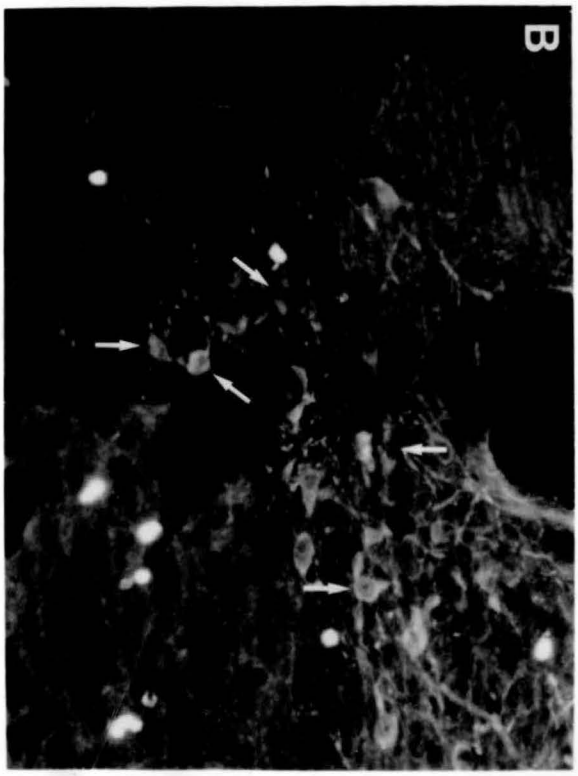
B

Figure 12. Line drawing of four coronal sections through the NTS illustrating the distribution of retrogradely-labeled (open circles), PNMT-immunoreactive (filled circles) and double-labeled (stars) cells found within the NTS after fast blue or Fluoro-gold injections into the CeA.

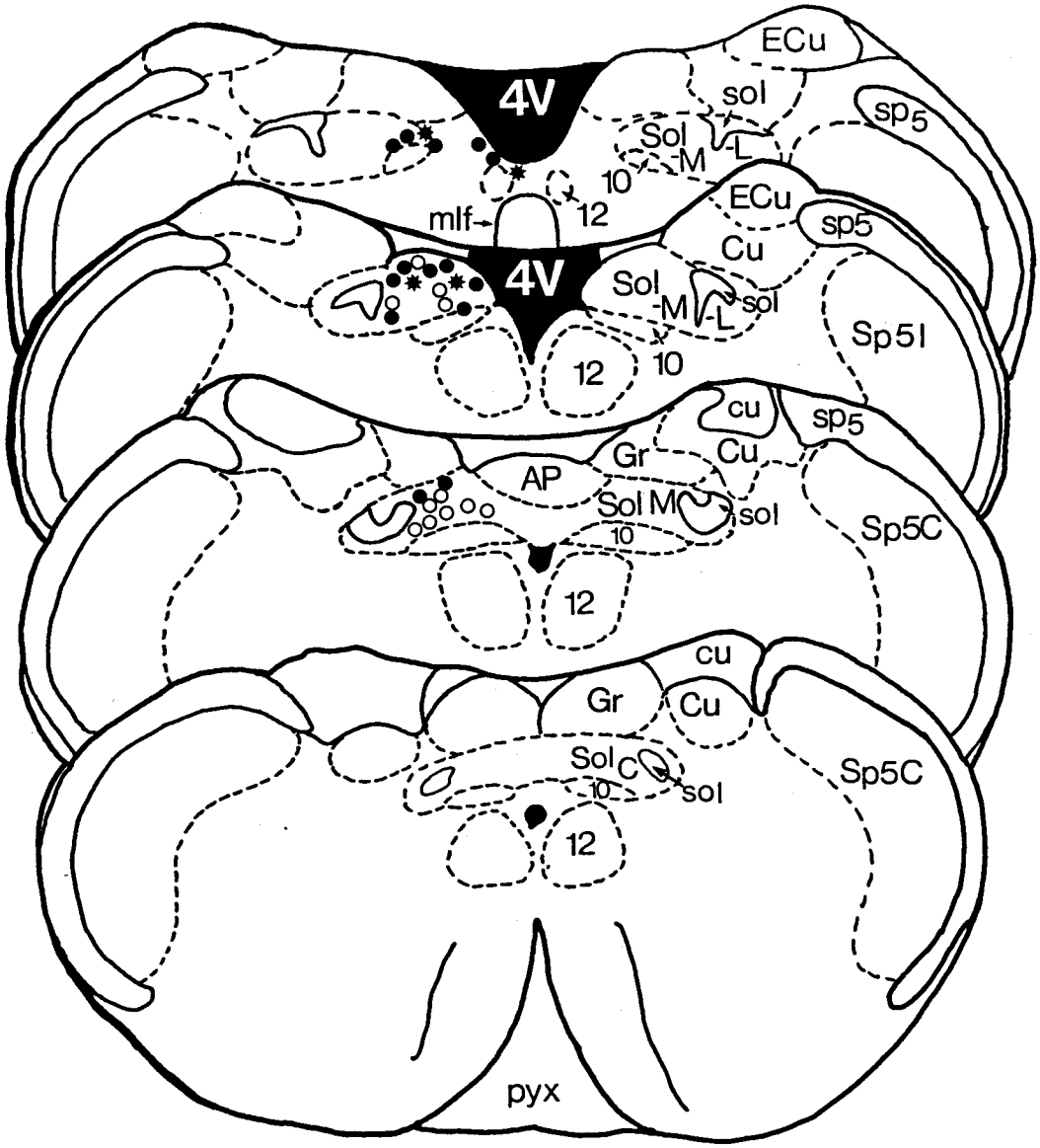
ECu
4V
sol
sp5
Sol
M
L
10
12
mlf
ECu
sp5
Cu
4V
Sol
M
L
sol
Sp5I
12
10
cu
sp5
Gr
Cu
AP
Sol M
sol
Sp5C
10
12
cu
Gr
Cu
Sol C
sol
Sp5C
10
12
pyx

PNMT

Figure 13. Fluorescent photomicrographs of coronal sections through the rostral NTS illustrating cells projecting to the CeA (A and C) and the same cells immunoreactive to PNMT (B and D). Panels E and F show a CeA-projecting cell that is also immunoreactive to PNMT located within the C3 midline group of adrenergic cells. Magnification: A and B, 325X; C and D, 650X; E and F, 450X.

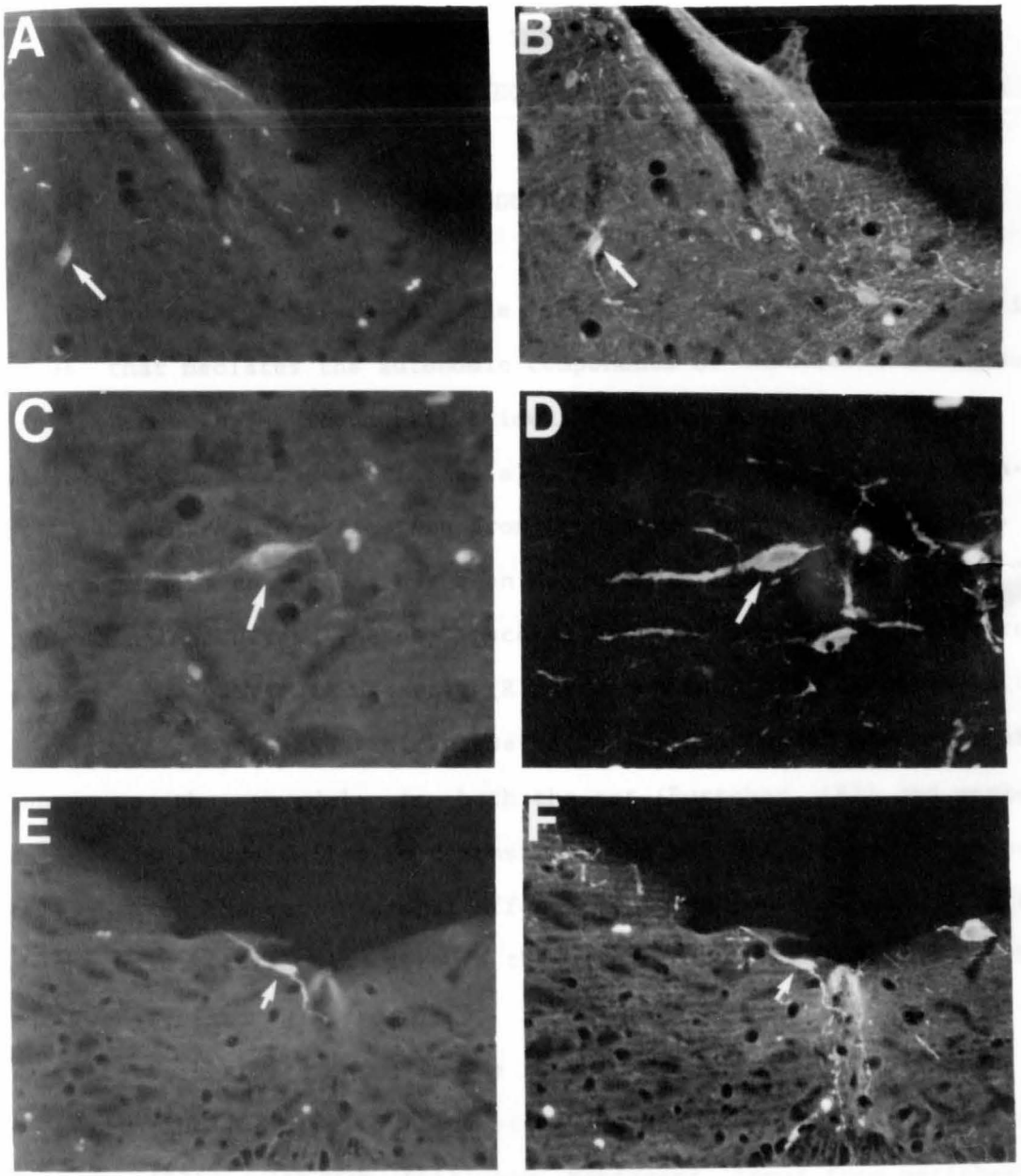
A
B
C
D
E
F

CHAPTER V

ORGANIZATION OF PEPTIDERGIC EFFERENTS FROM THE PARABRACHIAL NUCLEUS TO THE AMYGDALA IN THE RAT: A COMBINED RETROGRADE TRACING-IMMUNOHISTOCHEMICAL STUDY

INTRODUCTION

The central nucleus of the amygdala (CeA) is a telencephalic nucleus that mediates the autonomic components of behavioral responses to stress-inducing environmental stimuli (such as attack/defense behaviors) (for review, see Price et al., '87, Chapter 2, this dissertation). A topographic projection from the caudal nucleus of the solitary tract (NTS) to the CeA has been demonstrated in the rat, providing an anatomical substrate whereby visceral afferent feedback could be relayed to the amygdala directly (Ricardo and Koh, '78; Zardetto-Smith and Gray, '87; Chapter 3, this dissertation). Studies of brainstem efferents to the amygdala in both the cat (Russchen, '82) and monkey (Mehler, '80) have failed to demonstrate the NTS-CeA pathway in either species. In the cat, visceral afferent information may be relayed to the amygdala indirectly through the parabrachial nucleus (PB) of the pons (Cechetto and Calaresu, '85). Stimulation of the CeA antidromically activates single units in the PB that also respond to orthodromic activation of the carotid sinus and aortic nerves (Cechetto and Calaresu, '83), although this may represent input from peripheral chemoreceptors rather than baroreceptors (Cechetto and Calaresu, '85).

Cytoarchitectonically-defined subdivisions within the PB, speci-

fically, the external lateral, ventral lateral, central lateral, and medial subnuclei, project to the CeA (Fulwiler and Saper, '84). Immunohistochemical studies have demonstrated the presence of a number of peptides within the PB. These include calcitonin gene-related peptide (CGRP)(Kawai et al., '85; Shimada et al., '85; Skofitsch and Jacobowitz, '85; Schwaber et al., '88), neurotensin (NT) (Milner et al., '84; Block and Hoffman, '87), substance P (SP) (Milner et al., '84; Block and Hoffman, '87), enkephalin (ENK) (Milner et al., '84; Block and Hoffman, '87), somatostatin (SS) (Block and Hoffman, '87), corticotropin releasing factor (CRF) (Olschowka et al., '82; Cummings et al., '83) and bombesin (BOM) (Panula et al., '82). The pattern of distribution of immunoreactive terminals and cell bodies for several of these (and other) peptides has led to the proposal that the PB can be subdivided on the basis of neurochemical content (Block and Hoffman, '87), as well as cytoarchitectural characteristics and connectional specificity (Fulwiler and Saper, '84).

Recent studies have shown that some peptidergic neurons within the PB provide innervation to the CeA. Rosenfield et al. ('83) suggested CGRP innervation of the forebrain, including the CeA, to originate in the PB and peripeduncular nucleus and ascend via the median forebrain bundle. Destruction of the ventral portion of the PB results in a marked decrease in CGRP-immunoreactivity within the CeA (Shimada et al., '85) indicating CGRP-containing neurons in the PB to be a major source of CGRP terminals to the amygdala. Zardetto-Smith and Gray ('86b), employing retrograde tracing-immunohistochemical techniques, were the first to demonstrate directly that CGRP terminals within the CeA arise from the PB. Similarly, Schwaber et al. ('87) using similar methods, confirmed that CGRP cells located mainly within

the external lateral subnucleus provide an efferent projection to the CeA. Neurotensin and SP cells within the PB also innervate the CeA (Block et al., '89).

The PB is extensively connected with other nuclei involved in autonomic control and has been implicated in a variety of visceral and behavioral functions, including cardiopulmonary (Mitchell and Berger, '81; Mraovitch et al., '82; Galeno and Brody, '83; Harper et al., '84) and fluid (Ohman and Johnson, '86) regulation, nociception (Hammond and Proudfit, '80; Girardot et al., '87), sleep (Sieck and Harper, '80), gustation (Norgren and Pfaffman, '75) and feeding (Micco, '74; Schwartzbaum, '83). The CeA is thought to play a role in many of these same functions (for review, see Price et al., '87; Chapter 2, this dissertation), possibly mediating some responses (particularly cardiovascular and respiratory) through the descending pathway to the PB (Moga and Gray, '85). Intracerebroventricular administration of CGRP, CRF, BOM, ENK, NT, SP, and SS also exert a variety of autonomic effects (changes in heart rate, blood pressure, plasma catecholamine concentrations, and sympathetic nerve activity). These physiological effects, and the anatomical localization of these peptides within neurons associated with autonomic preganglionic neurons, has led to the speculation that they may act as neurotransmitters or neuromodulators in the regulation of central autonomic function (Brown and Fischer, '85; Brown and Fischer, '86; Brown and Gray, '88).

Identification of the chemical transmitters involved in the PB-CeA pathway is fundamental to understanding the relationship and interactions between these two nuclei in the integration of visceral efferent feedback with adaptive behaviors. In this study, the combined retrograde tracing and immunohistochemical technique was used to test for the presence of BOM, CGRP, CRF, NT, ENK, SP, and SS neurons within

the PB which project to the CeA. Preliminary findings of this investigation were previously reported (Zardetto-Smith and Gray, '86b).

METHODS

Coronal blocks of parabrachial tissue were obtained from 19 animals in which the injection was centered within the CeA from the series of retrograde tracer injections used in the previous study of the neurochemical organization of NTS efferents. Additionally, coronal blocks of tissue were also obtained from 8 animals in which the injection was not centered within the CeA to serve as controls. The methodology for fast blue or Fluoro-Gold injections, as well as for colchicine administration and perfusion procedures, was previously described (see Chapter 4).

After perfusion, brains were immediately removed and sliced into coronal blocks. Adjacent coronal sections were cut using a Lancer Series 1000 vibratome. Sections from the injection site (40 um) were mounted directly onto acid-cleaned, gel coated slides in serial order as cut. Adjacent coronal sections of the pons (20-25 um) were collected into three vials of cold (4 C) PBS or 0.1% PBS-Triton X. While cutting, one set of sections was serially mounted onto acid-cleaned, gel-coated slides and retained as a control for any fading of fluorescence that could occur during immunocytochemical processing (Skirboll et al., '84), and for cell counts to assess the magnitude of the PB-CeA pathway.

Sections were incubated 24-72 hrs with antiserum to three of the following peptides or enzymes: calcitonin gene-related peptide (CGRP, Dr. Wiley Vale) corticotropin releasing factor (CRF, Dr. T.L. O'Donohue) met-enkephalin (ENK, Immunonuclear Corp. or Penninsula Laboratories), neurotensin (NT, Dr. Marvin Brown), substance P (Sub P, Dr. Marvin Brown), somatostatin (SS, Immunonuclear Corp), and bombesin

(BOM, Immunonuclear Corp.). All antibodies were raised in goat against rabbit. Anti-CGRP and anti-CRF were used at a dilution of 1:1000; anti-BOM, anti-ENK, anti-SS, anti-Sub P, and anti-NT were used at a dilution of 1:500. Initially, primary antibodies were diluted in a solution of 0.1% PBS-tx and 10% normal goat serum (Cappel); in later experiments, a solution of 0.1% PBS-tx and 10% normal donkey serum (Jackson Laboratories) was used. Antiseum specificity was controlled by pre-incubating 1 ml of each diluted antiserum with 10 ug of its homologous synthetic peptides. The tissue was then processed as described, and examined for the presence of any immunohistochemical staining. Although immunohistochemical staining was blocked in these controls, cross-reactivity with as-yet-undefined antigens cannot be excluded. The term "peptide-like" is therefore implicit in the following descriptions of neuropeptide immunoreactivity (neuropeptide-ir).

Following incubation with the primary antisera, sections were rinsed with PBS. In earlier experiments, sections were incubated in rhodamine-conjugated goat anti-rabbit immunogammaglobulin (Cooper Biomedical, diluted 1:10 in PBS-tx) at 45 C for 10 min and then at room temperature for 60 min. Sections were then transferred to cold PBS and mounted on acid-cleaned, gel-coated slides. In later experiments, following incubation with the primary antisera sections were incubated with biotinylated donkey anti-rabbit immunogammaglobulin (IncStar) for 1 hr. at room temperature. After a 10 min rinse in cold PBS, all sections were then incubated with streptavidin-Texas Red conjugate (IncStar) for 1 hr at room temperature.

The sections were then transferred to cold PBS, mounted on acid-cleaned, gel-coated slides, and covered with DePex (BDH Chemicals). The material was examined with an Olympus BH-2 or Olympus Vannox AH-2 microscope equipped with a 100 W or 200 W mercury light source, respec-

tively. Fast blue or Fluoro-Gold was visualized with an excitation wavelength centered at 330-360 nm (Olympic ultraviolet filter system) and rhodamine or Texas Red immunofluorescence was viewed using the 546 nm (green) filter system. Cells that contained both retrograde label and rhodamine or Texas Red immunofluorescence (i.e., "double-labeled") could be detected by switching between filter sytems. Sections were photographed with Polaroid coaterless land pack film 667, ASA 3000/36 DIN. The location of immunocytochemically-labeled, retrogradely-labeled, and double-labeled cell bodies were plotted using a drawing tube attached to the Olympus BH-2 microscope, and cell counts made with a 40x fluorite objective. In some cases, after plotting and counting, slides were soaked in xylene to remove the coverslip and Nissl-stained with cresyl violet to determine the subnuclear location of the labeled cells.

RESULTS

Injection Sites. Both retrograde tracer and immunohistochemical staining were present in 10 of the 19 cases in which the injection/deposit of retrograde tracer was centered within the CeA. In each of these successful cases, the retrograde tracer used was Fluoro-Gold (FG); thus, the following descriptions concerning retrogradely-labeled cells pertains only to FG-labeling.

Retrogradely-labeled neurons were present in the PB following injections or iontophoretic deposits of Fluoro-Gold centered within the CeA. Three such representative injection sites are schematically illustrated in Fig. 1. In CGC 8, a large pressure injection of Fluoro-Gold was centered within the medial CeA, with spread of the tracer into the substantia innominata (SI), caudate-putamen, and basolateral and medial amygdaloid nuclei (Fig. 1, top). Iontophoretic delivery of Fluoro-Gold in CGC 80 resulted in a more discrete injection, centered within the medial CeA, with some spread to the medial amygdaloid nucleus (Fig. 1, middle). A longer delivery time was used in the iontophoretic deposit of Fluoro-Gold in CGC 102, resulting in a larger injection centered in the medial and ventral CeA, impinging on the caudal extent of the substantia innominata, the caudate-putamen, the basolateral and medial amygdaloid nuclei (Fig. 1, bottom). Control injections placed in the caudate-putamen, and basolateral, basomedial, and medial amygdaloid nuclei failed to retrogradely-label neurons within the PB, in agreement with a recent study (Block et al., '89).

Distribution of Retrogradely-Labeled Cells. Figure 2 illustrates four representative levels of the PB, and its cytoarchitectural subdivisions (Fulwiler and Saper, '84). Figure 2 also depicts the

ipsilateral distribution of Fluoro-Gold (FG) labeled cells for CGC 80 and 8, respectively. The pattern of labeling present in CGC 80 is representative of cases in which the injection was limited to the CeA and did not include the SI. At rostral levels of the PB, a few retrogradely-labeled neurons were present in the central lateral and ventral lateral subnuclei, with one or two FG-labeled neurons present in the medial PB. The greatest density of retrograde-label was present within the external lateral subnucleus in the caudal PB. At this level, scattered FG-labeled neurons were also present within the ventral lateral and medial subnuclei. Most caudally, retrogradely-labeled neurons were concentrated within the ventral lateral and medial subnuclei, in the dorsal and ventral recesses of the superior cerebellar peduncle, designated by Fulwiler and Saper ('84) as the "waist" of the PB. Numerous retrogradely-filled axons extended across the peduncle, between the two areas, and some retrogradely-labeled neurons were interspersed between fiber bundles of the peduncle itself.

The distribution of retrogradely-labeled cells in CGC 8, the large pressure injection which included both the CeA and the SI, the pattern of retrograde label was was similar to that seen in CGC 80, with the exception that the lateral portion of the medial PB, as well as the external lateral subnucleus, was heavily labeled at caudal levels. This has been described by Fulwiler and Saper ('84) as the "capping pattern" characteristic of injections involving the SI. A few FG-labeled cells were also noted at caudal levels within the Kolliker-Fuse nucleus.

Using Abercrombie's correction formula for double-counting errors, ('46) it was estimated that the PB contained 3892 $\pm$ 692 (SEM) retrogradely-labeled neurons (N=3).

Distribution of Immunocytochemically-Labeled Cells. The distributions of CGRP, CRF, ENK, NT, SS, and Sub P within the rat PB have previously been described (Cummings et al., '83; Milner et al., '84; Block and Hoffman, '87; Schwaber et al., '88; Yamono et al., '88; Block et al., '89) and therefore, will only be briefly summarized.

Neurotensin and CGRP are localized to the external lateral subnucleus at intermediate levels of the PB. A few scattered CGRP-immunoreactive (-ir) neurons were present within the Kolliker-Fuse nucleus, the ventral and central lateral subnuclei, and the medial subnucleus (Fig. 3B, C). In one case (CGC 111) several NT-ir cell bodies were present and concentrated within the external lateral subnucleus at mid-PB levels (Fig. 5B, C). In four other cases very few NT-ir neurons were detected in that area. This agrees with a previous study (Milner et al, '84) that cell bodies containing NT in the parabrachial region are rarely found. At caudal levels of the PB, scattered CGRP- and NT-ir neurons were present within the medial subnucleus and the "waist" area (Fig. 3D and 5D, respectively).

Enkephalin-ir (Fig. 7A-D) and SS-ir cell bodies were observed in the dorsal, central, and ventral lateral subnuclei at rostral levels of the PB. Some immunoreactive perikarya of both types of peptides were observed to surround the dorsomedial aspect of the superior cerebellar peduncle (Fig. 7B, 9C). Enkephalin-ir neurons were also most numerous at intermediate to caudal levels of the PB, within the ventral lateral and medial subnuclei (Fig. 7C,D). A few ENK-ir cells were noted in the external lateral subnucleus, with a cell or two present within the Kolliker-Fuse nucleus.

Substance P cells have been described as present within the rostral, lateral PB and within CGRP-containing cells of the external lateral nucleus (Block and Hoffman, '87; Yamono et al., '88; Block et al.,

'89). In the present study, only one or two SP cells were observed within the lateral PB, again in agreement with a previous observation that SP perikarya within the PB are rare (Milner at al, '84).

In agreement with the more general observation of a compact cluster of CRF neurons within the medial aspect of the lateral PB (Olschowka et al., '82; Cummings et al., '83), CRF-ir neurons were observed to be concentrated within the dorsal lateral subnucleus (Fig. 9-2). Additionally, some CRF-ir neurons were noted to be present in the external lateral subnucleus at caudal levels of the PB (Fig. 9-2, 4; 10A).

Lastly, BOM-ir cell bodies have been reported to be observed in the dorsal PB (Panula et al., '82) but in the present study, only BOM-immunoreactive terminals were observed. Terminals immunoreactive for BOM were found in the caudal PB, distributed within the external, central, and ventral lateral subnuclei (Fig. 10C).

Distribution of Retrogradely-Labeled Immunocytochemically-Labeled Cells. Double-labeled neurons were consistently found at intermediate levels of the PB, and were localized primarily to lateral subnuclei. Retrogradely-labeled, immunocytochemically-labeled, and double-labeled cells were counted (Table 1, raw or uncorrected count) to assess the relative contribution of each neuropeptide to the PB-CeA pathway. Cell counts included both the medial and lateral PB, and the Kolliker-Fuse nucleus.

CGRP (CGRP-ir). Neurons that were retrogradely-labeled and CGRP-ir were numerous and concentrated in the caudal half of the PB within the external lateral subnucleus (Fig. 3B, C). In cases where the FG deposit site included the SI, several retrogradely-labeled cells that formed part of the "cap" at the ventral aspect of the superior

cerebellar peduncle were also CGRP-positive (Fig. 4). Approximately 17% of the total number of CGRP-ir cells within the PB were retrogradely-labeled, but only about 5% of the retrogradely-labeled population were CGRP-ir (Table 1).

Neurotensin (NT-ir). Neurons exhibiting NT-ir and FG-labeling were found at mid-caudal levels of the PB within the external lateral subnucleus (Fig. 5C). One or two double-labeled cells were also observed in the external lateral subnucleus. Figure 6 shows an example of NT-ir cells in the PB which were also retrogradely-labeled with FG. As mentioned earlier, only one or two NT-ir cells were usually observed in the PB, with the exception of case CGC 111. In this instance, cell counts show approximately 19% of the NT-ir cells were also retrogradely-labled. Double-labeled NT-ir cells comprised only 1% of the total number of retrogradely-labeled cells in the PB (Table 1).

Enkephalin (ENK-ir). The majority of cells labeled for both ENK-ir and FG were found at intermediate levels of the PB, located within the ventral lateral subnucleus (Fig. 7B, C). An example of ENK-ir neurons labeled with FG is presented in Figure 8. Twelve to seventeen percent of the ENK-ir cells were retrogradely-labeled, but double-labeled ENK-ir neurons comprised less than 2-4% of the total number of retrogradely-labeled cells (Table 1).

Somatostatin (SS-ir). Cells labeled with SS-ir and FG were not observed in the PB following injections of the tracer into the CeA (or CeA and SI). At more rostral levels of the PB, where the bulk of SS-ir neurons were located, few retrogradely-labeled cells were present within the central lateral subnucleus, and virtually none were present in the dorsal or ventral lateral subnuclei, in agreement with the observations of Fulwiler and Saper ('84). Retrogradely-labeled cells were present in the caudal ventral lateral subnucleus (part of the "waist"

area), where SS cells are not present (Fig. 10B).

Corticotropin Releasing Factor (CRF-ir). Cells double-labeled for CRF-ir and FG were also not observed in the PB following injections of the tracer into the CeA (or CeA and SI). Corticotropin releasing factor-ir cells were observed adjacent to FG-labeled cells in the external lateral subnucleus (Fig. 9, 10A) but not in the cluster located in the dorsal lateral subnucleus (Fig. 9-2, 10A), since retrogradely-labeled cells were not present there.

DISCUSSION

PB Peptidergic Efferents to the CeA. In the present study, the combined retrograde tracing immunocytochemical technique was used to identify the presence of CGRP-ir, ENK-ir, and NT-ir in PB efferents to the CeA. Retrogradely-labeled CGRP-ir and NT-ir neurons were located mainly within the external lateral subnucleus, while double-labeled ENK-ir neurons were located primairly in the ventral lateral subnucleus. Corticotropin releasing factor-ir and SS-ir neurons were distributed primarily throughout subnuclei of the PB that do not have the CeA as their major terminal field, i.e., the dorsal lateral and rostral portions of the central and ventral lateral subnuclei. These results demonstrate that peptides in the PB exhibit characteristic distributions which are related to their connectional specificity.

It is likely that some of the double-labeled immunoreactive cells identified in this study projected to the SI. Fulwiler and Saper ('84) noted that retrograde labeling within the PB after injecting the SI was similar to that seen after CeA nucleus injections with the exception of the "capping pattern" at the base of the superior cerebellar peduncle. Some of the CGRP-ir retrogradely-labeled neurons seen in this study, particularly in the "capped" area, most likely were projecting to the SI, though to what degree cannot be assessed accurately from the data in this study. Of the four cases in which the number of CGRP-ir double-labeled neurons were assessed by cell counts, two cases (CGC 7, 8) had injections centered in the CeA, but which also involved a large extent of the SI. The number of retrogradely-labeled cells within the PB in these two cases was similar (Table 1). In CGC 102, in which the injection was centered in the CeA and included some of the caudal SI, the "capping" of the superior cerebellar peduncle was not as evident as

in CGC 7 or 8, and the number of retrogradely-labeled cells was reduced (Table 1). The number of retrogradely-labeled cells in this case was, however, slightly larger than the number of FG-labeled cells counted in CGC 80, in which the injection did not involve the SI (Table 1). The percentage of retrogradely-labeled CGRP-ir cells in both CGC 80 and 102, compared to CGC 7 and 8, was reduced by approximately 30% (Table 1). This agrees with the observations of Schwaber et al. ('88) that when the sublenticular SI was included in the injection of retrograde tracer into the CeA, a larger number of cells within the Kolliker-Fuse nucleus and medial nucleus were double-labeled. The possibilty that some ENK-ir and NT-ir double-labeled cells within the external lateral nucleus also projected to the SI cannot be excluded, as the SI contains fibers and terminals immunoreactive for both peptides (Finley et al., '81; Jennes et al., '82; Grove et al., '88). The sublenticular SI forms a continuous structure with the bed nucleus of the stria terminalis anteromedially and the CeA posterolaterally (Heimer et al., '85). In light of the continuity between the the CeA and SI and the similarity in their input from subcortical structures, it would not be surprising to find identical peptidergic inputs to these nuclei. Further studies are needed to clarify the contribution to SI efferents originating from various peptide cells in the PB.

The failure to find SP-ir and BOM-ir cells within the PB was puzzling. Block et al. ('89) described retrogradely-labeled SP cells in the external lateral subnucleus at mid-rostral and middle levels of the PB, which is consistent with the description of SP-ir co-localized in GGRP-ir neurons in that area (Yamono et al., '87). Large SP-ir cells were observed in the area of the central gray, while only SP-terminal immunoreactivity was observed in the PB. The same was true of BOM-ir staining; often, large cells within the pedunculopontine nucleus

were labeled, but only terminal immunoreactivity was visible within the PB. One explanation for these patterns of immunoreactivity would be the failure of the colchicine to reach the laterally located PB neurons. This was unlkely, however, as CGRP-ir or ENK-ir cell bodies were often present within the PB in sections from the same case. Another explanation, previously proposed by Milner et al. ('84) in regards to SP-ir staining (and likely in some of the cases observed in the present study), is that the dense terminal immunoreactivity in the external lateral subnucleus obscures the visibility of the few cell bodies present. Also, difficulty in establishing good perikaryal staining for these two peptides may simply have resulted from problems with the sensitivity of the particular type of antibody/fixative employed (Sawchenko and Swanson, '81).

Lastly, the number of retrogradely-labeled immunoreactive neurons identified in this study accounted for less than 5% of the total retrogradely-labeled population, though this is likely to be a conservative estimate. The small percentage of double-labeled cells is a consequence of the large number of retrogradely-labeled cells within the PB observed in each case (ranging from 750 to 1800) compared to the small number of double-labeled neurons for each peptide (<100). Thus, the neurochemical content of the majority of CeA-projecting neurons still remains unknown.

Relationship of PB Efferents to the Distribution of CeA Immunoreactive Terminals. The lateral and lateral capsular subdivisions of the CeA contain a high density of CGRP (Schwaber et al., '88), ENK (Gray et al., '84; Zardetto-Smith et al., '84), and NT (Cassell et al., '82) immunoreactive terminals. The specific terminal distributions of PB efferents within specific subdivisions of the CeA has not been

examined. It seems likely, however, that the lateral PB, where most of the double-labeled peptide cells were observed in the present study, is one source of ENK, NT, and CGRP-ir terminals within the lateral/lateral capsular subdivisions.

Comparison of Neuropeptidergic Content of PB-CeA Efferents to CeA-PB Afferents. Evidence exists that the descending projections from the CeA to the PB may be topographically organized. Past studies have indicated most of the efferent projections of the CeA to the PB to arise from its medial subdivision (Hopkins and Holstege, '78; Schwaber et al., '82), mainly innervating the dorsomedial and medial subnuclei (Moga and Gray, '85). Efferents arising from the lateral CeA may terminate in discrete areas within the lateral PB, namely, the central, ventral, and external lateral subnuclei (Moga and Gray, '85). Thus, the same PB subnuclei that give rise to the ascending input to the CeA also serve as the major terminal fields of descending efferents to the PB from the CeA. The peptidergic output to the PB from the CeA that has been identified to date arises from CRF-ir, SS-ir and NT-ir cells located within its lateral subdivision (Moga and Gray, '85).

Enkephalin cells in the CeA do not participate in the descending pathway to the PB (Moga and Gray, '85) or to the dorsal vagal complex (Gray and Magnuson, '87a). The present study demonstrates that ENK cells in the PB do contribute to the ascending pathway to the CeA. Also, the present study demonstrates that CRF and SS cells within the PB do not participate in the ascending pathway to the CeA, though both types of peptidergic cells within the CeA contribute to the descending pathway. These results indicate that although there are afferent and efferent connections between the CeA and PB, their peptidergic connections may not necessarily be reciprocated.

Functional Considerations. The CeA has been implicated in the cardiovascular and autonomic changes associated with defense or fear responses (for review, see Chapter 2, this dissertation). Among the amygdalar nuclei, the CeA is distinguished by its multiple, reciprocal connections with other brain nuclei that are important in the regulation of autonomic function (for recent reviews, see Price et al., '87; Gray, '89). Several cardiovascular, respiratory, and gastric responses typically observed during stress-related behaviors are elicited upon electrical stimulation of the CeA in the rat and the cat (Henke, '82; Galeno and Brody, '83; Frysinger et al., '84). In the awake cat or rat, the cardiovascular response consists of tachycardia and increased arterial pressure, a response similar to that resulting from stimulation of the PB in the cat (Mraovitch, '82). An increase in arterial pressure and heart rate, as well as an increase in plasma catecholamines, is found after microinjection of calcitonin gene-related peptide microinjected into the CeA (Brown and Gray, '88). Collectively, these studies suggest a role for the CGRP pathway from the PB to the CeA in mediating these responses.

A variety of stressful environmental stimuli that do not produce obvious pain, such as restraint and hypoglycemia, are accompanied by analgesia (Hayes et al., '78; Amir and Amit, '78; Bodnar et al., '79). A functional role in the "ancillary" pain system that mediates the presumed motivational-affective components of aversive experiences has been suggested for the CeA (Henke, '83). Microinjection of neurotensin into the CeA produces an increase in nociceptive threshold, thus possibly acting to alter the affective component of behavioral responses to noxious stimuli (Kalivas et al., '82). In addition, there is evidence that the cardiovascular and pain pathways are linked (for

review, see Randich and Maixner, '84). Activation of the baroreceptor reflex induces analgesia in the rat, while enkephalinergic compounds exert various cardiovascular changes (depending on the route of administration). Analgesia, coupled with a pressor response, and subsequent inhibition of pain and/or associated motivation-affective changes, may aid in reducing the stress associated with adverse environmental stimulation (Randich and Maixner, '84). The PB (in the cat) has been shown to be an important site of relay for some baroreceptor information to the forebrain, including the CeA (Cechetto and Calresu, '85). The functional significance of the presence of ENK and NT within the PB-CeA pathway is not known, but speculatively, it may be related to feedback involved in this aspect of the response to environmental stress.

Concluding Comments. The CeA receives peptidergic innervation from the PB, though the neurochemical content of the majority of retrogradely-labeled cells remains largely unknown. Peptides in the PB exhibit characteristic distributions which are related to their connectional specificity. The contribution of CGRP and ENK cells, and the non-participation of CRF and SS cells, to the ascending pathway from the PB to the CeA distinguishes it from the reciprocal descending pathway. Although the functional significance of these peptidergic pathways remains unclear, they may be important in providing feedback during stress-mediated responses.

Table 1. Injection sites for cases CGC 8, 80 and 102 are illustrated in Fig. 1. Numbers represent raw counts, uncorrected for double-counting errors.

ABBREVIATIONS:

RG	retrogradely-labeled cells
IR	immunoreactive cells
DL	double-labeled cells
DL/RG	ratio yielding percent of retrogradely-labeled cells immunoreactive for given antigen
DL/IR	ratio yielding percent of immunoreactive cell population projecting to the CeA

TABLE 1

Antigen	Case	# Sections	#RG Cells	#IR Cells	#DL Cells	DL/RG %	DL/IR %
CGRP	CGC 7	11	1610	427	108	7	20
	8	16	1828	501	94	5	20
	80	10	751	270	31	4	12
	102	10	882	308	46	5	15
ENK	CGC 4	11	1607	298	36	2	12
	80	10	806	199	34	4	17
NT	CGC 111	12	1344	70	13	1	19

Figure 1. Schematic representation of three injections of Fluoro-Gold into the CeA that produced retrograde labeling within the PB. See text for discussion.

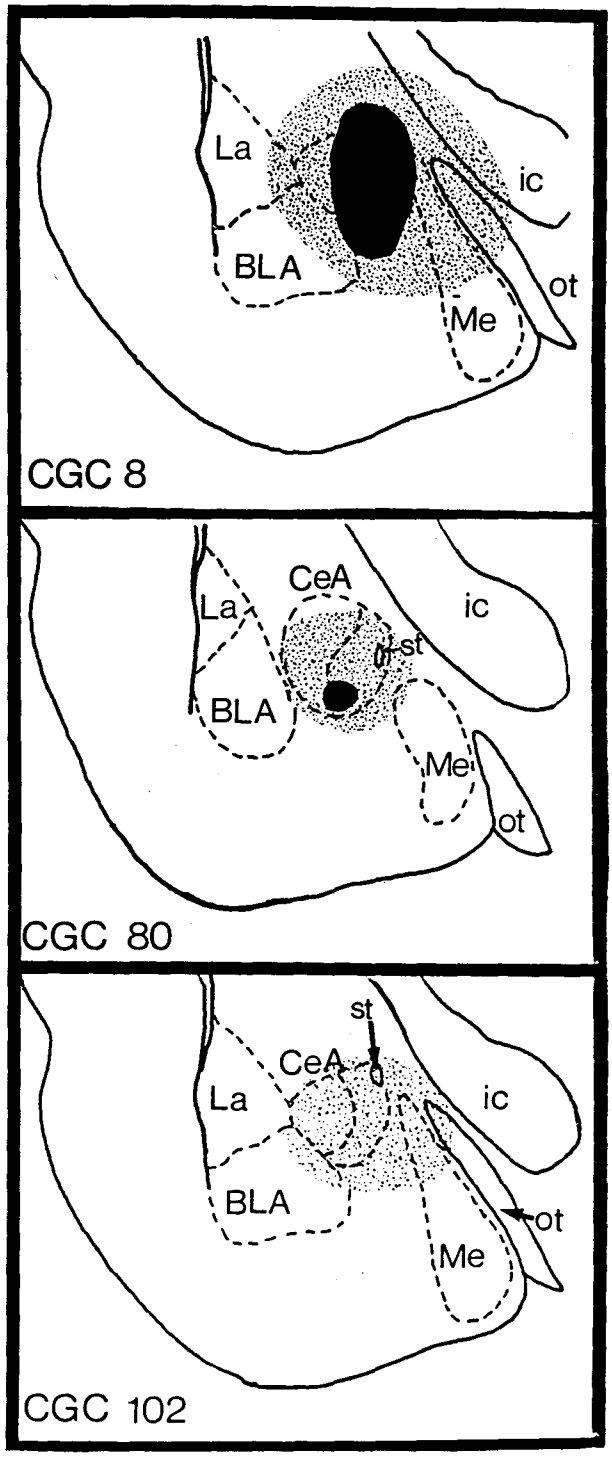
La
ic
BLA
ot
Me
CGC 8
CeA
La
ic
st
BLA
Me
ot
CGC 80
st
CeA
La
ic
BLA
ot
Me
CGC 102

Figure 2. (A) Line drawings representing four levels through the PB and its relevant cytoarcitectonic subdivisions. (B) Camera lucida drawings of four representative levels through the PB demonstrating the pattern of retrograde level following injections confined to the CeA. (C). Similar camera lucida drawings of the pattern of retrograde label present in CGC 8, in which the injection included both the CeA and the SI.

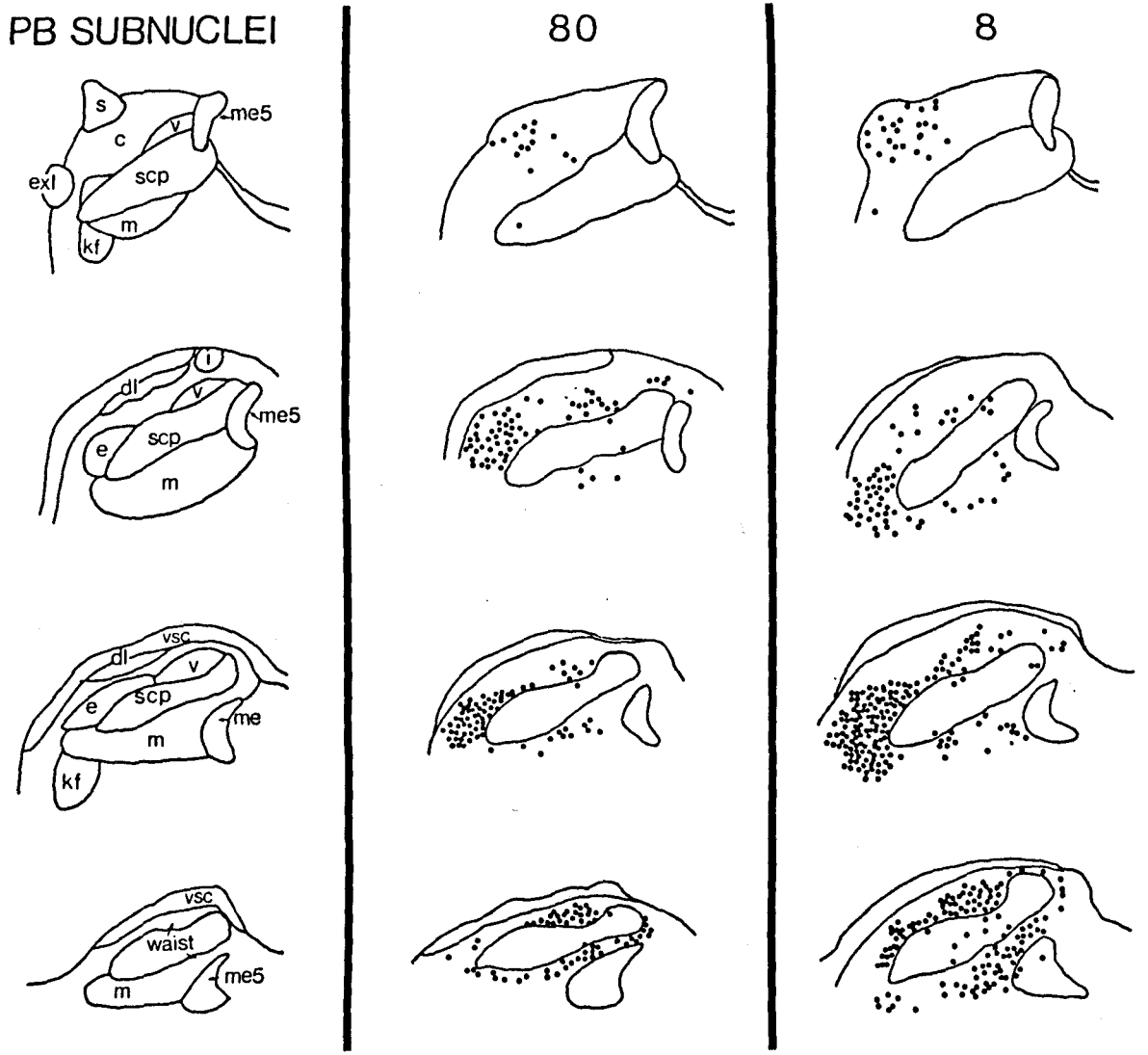
PB SUBNUCLEI
80
8
s
c
v
me5
exl
scp
m
kf
l
dl
v
me5
e
scp
m
vsc
dl
v
e
scp
me
m
kf
vsc
waist
m
me5

Figure 3. Line drawings of coronal sections through four levels of the PB (A-D, rostral to caudal) illustrating the distributions of Fluoro-Gold (open circles), calcitonin gene-related peptide (CGRP)-ir neurons (filled circles), and double-labeled cells (stars) after Fluoro-Gold injections into the CeA.

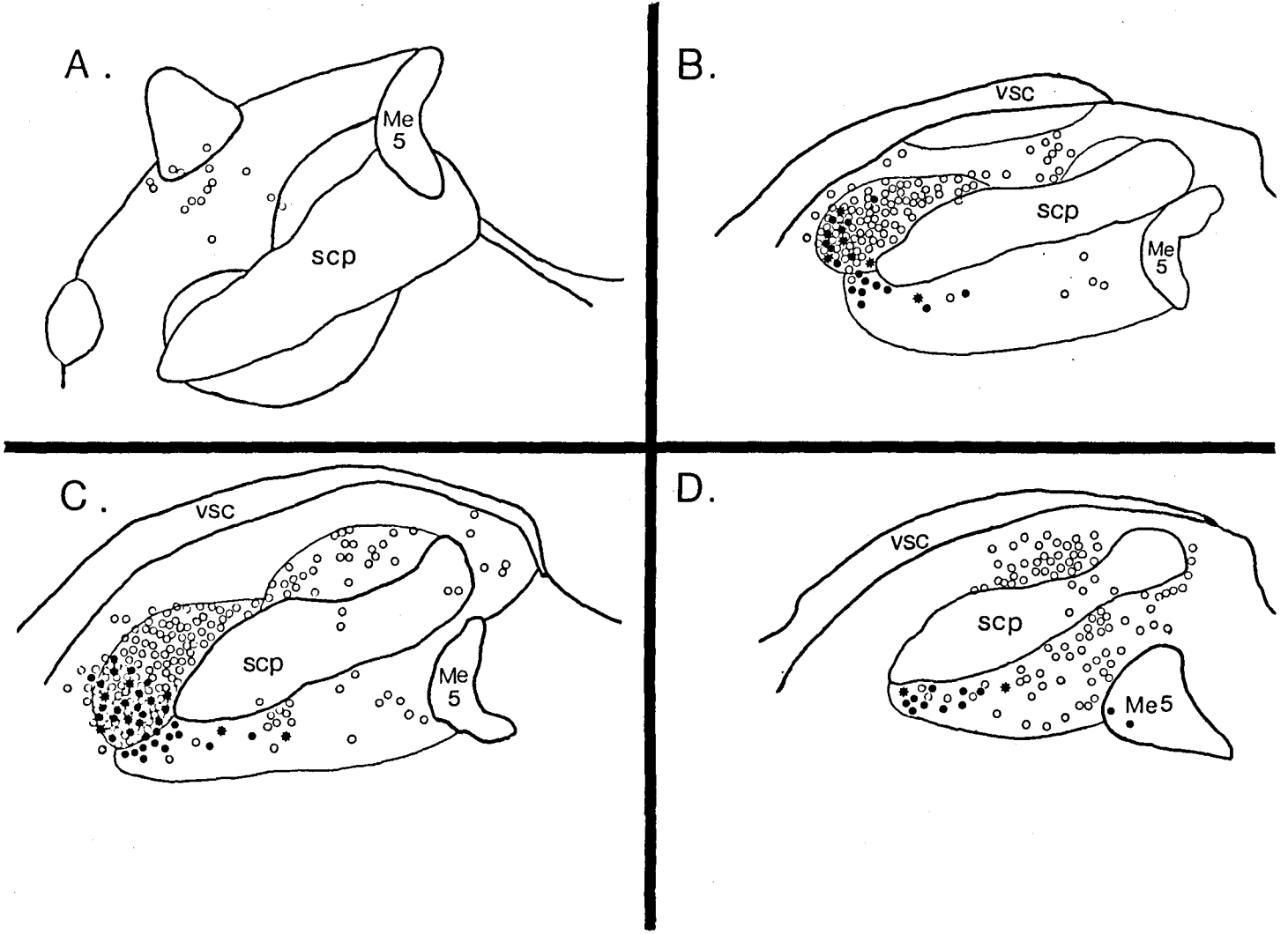
A.
Me
5
scp
B.
vsc
scp
Me
5
C.
vsc
scp
Me
5
D.
vsc
scp
Me5

Figure 4. Fluorescent photomicrograph of a coronal section through the PB illustrating (A) cells projecting to the PB, and (B) cells immunoreactive to calcitonin gene-related peptide (CGRP). Double-labeled cells are indicated by white arrows. Magnification: 450X.

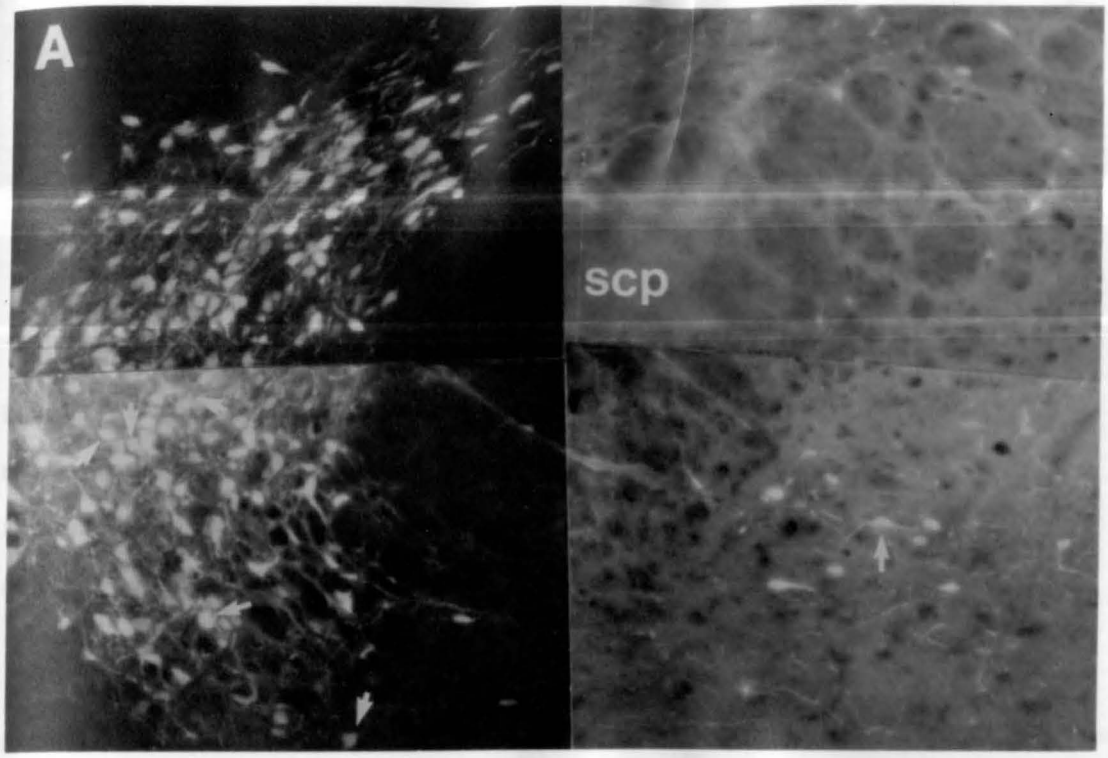
A
scp

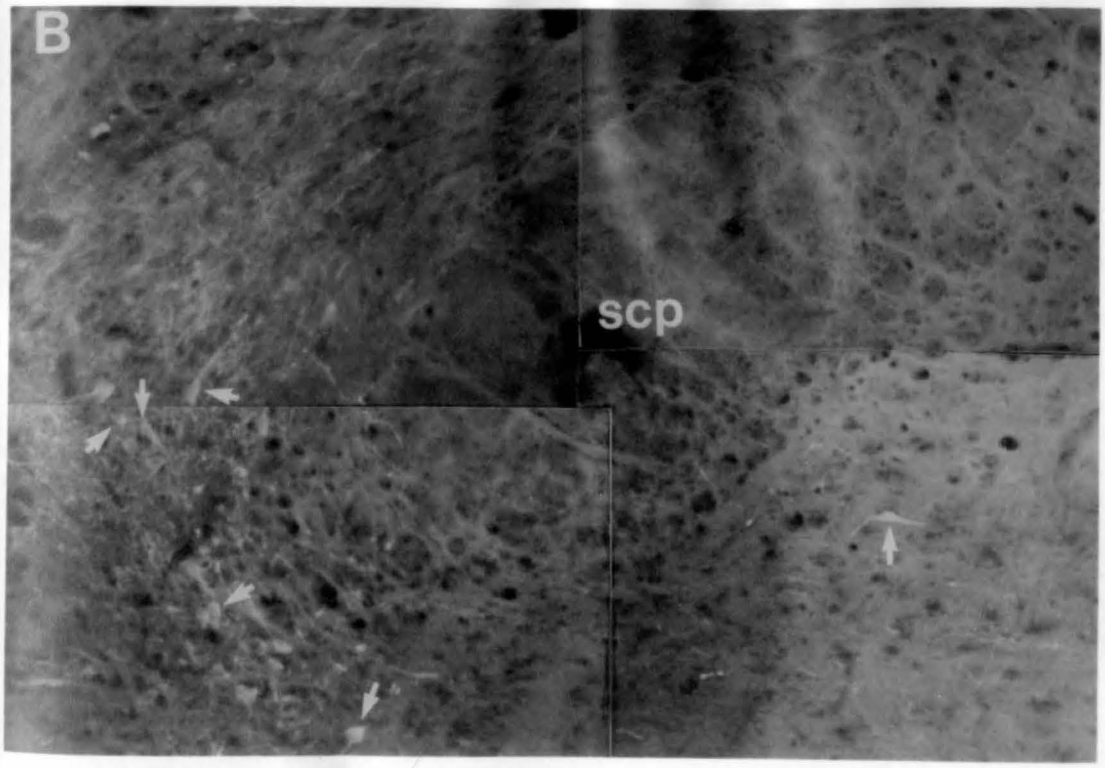
B
scp

Figure 5. Line drawings of coronal sections through four levels of the PB (A-D, rostral to caudal) illustrating the distributions of Fluoro-Gold (open circles), neurotensin (NT)-immunoreactive (closed circles) and double-labeled (stars) cells after Fluoro-Gold injections into the CeA.

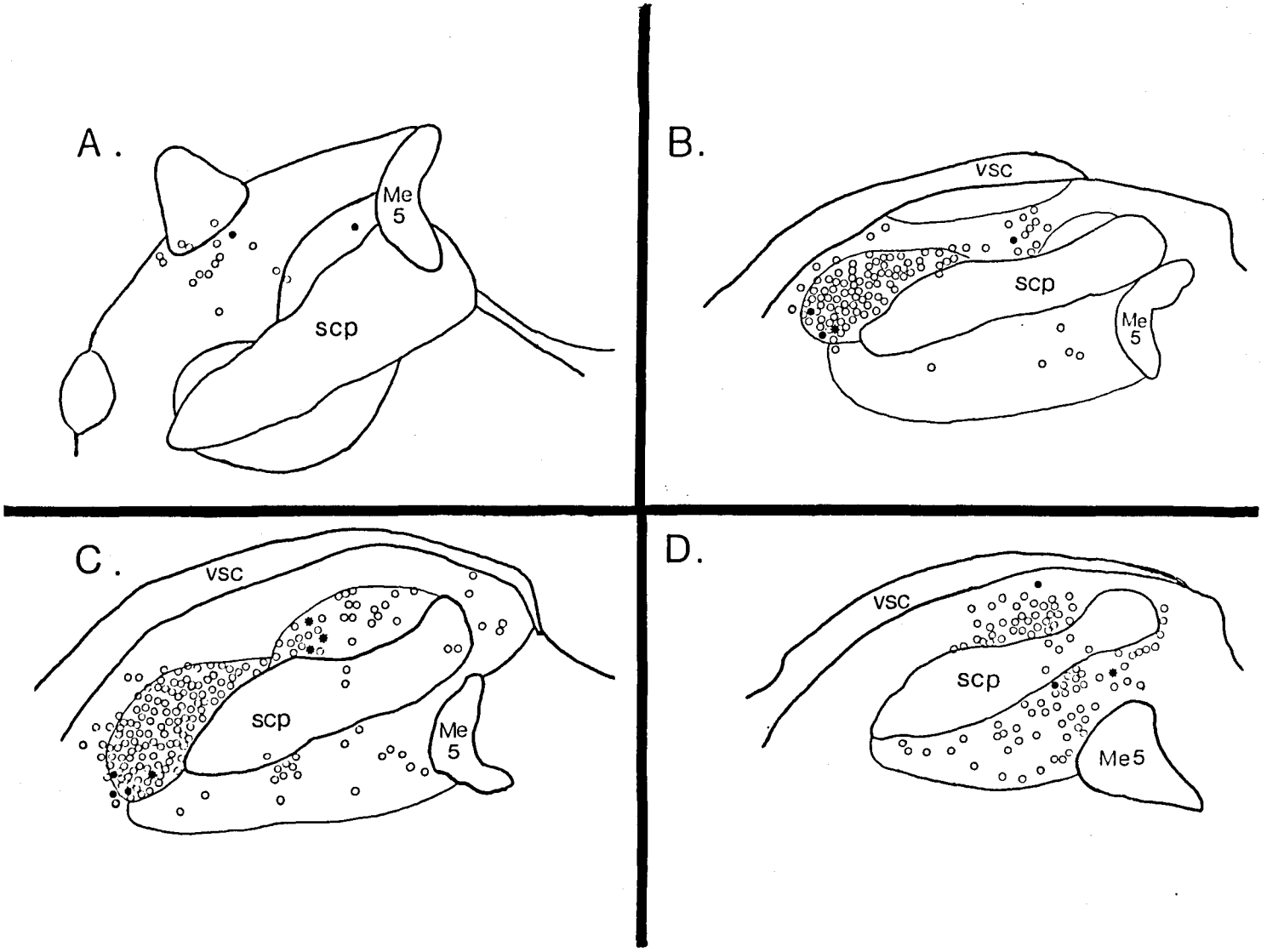
A.
Me
5
scp
B.
vsc
scp
Me
5
C.
vsc
scp
Me
5
D.
vsc
scp
Me5

Figure 6. Fluorescent photomicrographs of a coronal section through the PB illustrating (A) cells projecting to the CeA and (B) cells immunoreactive to neurotensin (NT). Double-labeled cells are indicated by white arrows. Magnifications: A and B, 400X; C and D, 600X.

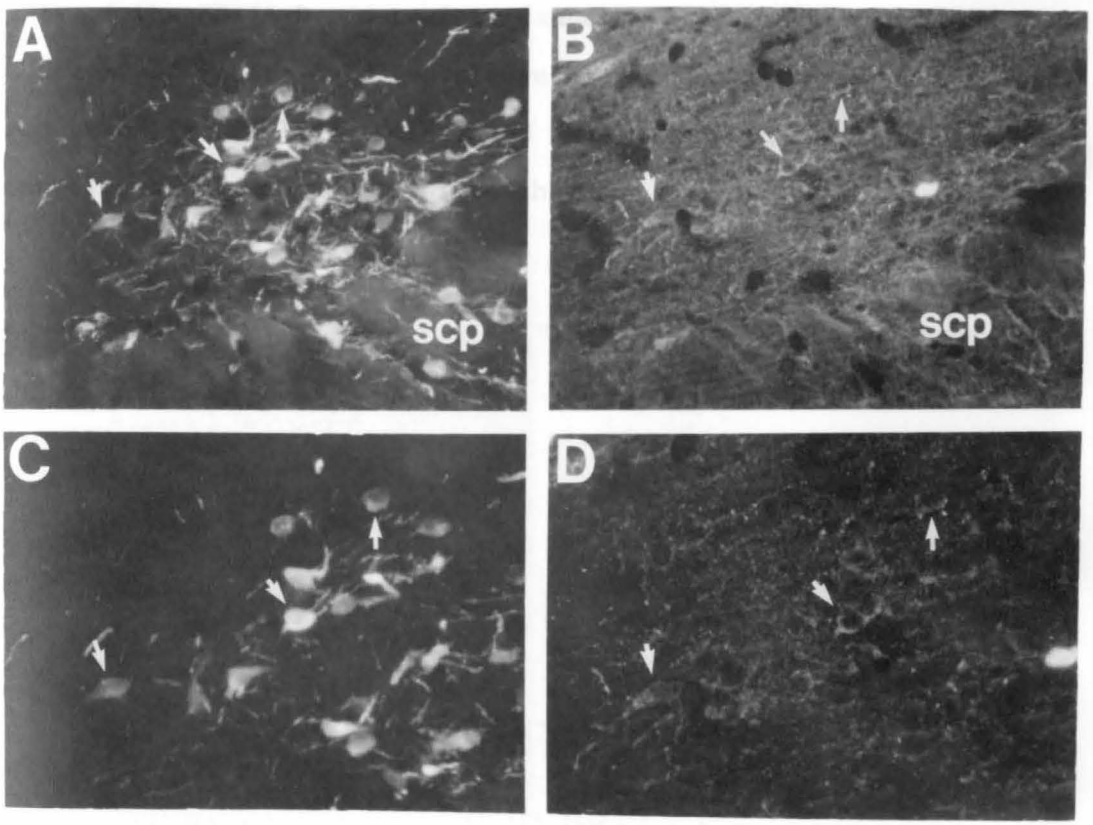
A
scp
B
scp
C
D

Figure 7. Line drawings of coronal sections through four levels of the PB (A-D, rostral to caudal) illustrating the distributions of Fluoro-Gold (open circles), enkephalin (ENK)-immunoreactive (filled circles) and double-labeled (stars) cells after Fluoro-Gold injections into the CeA.

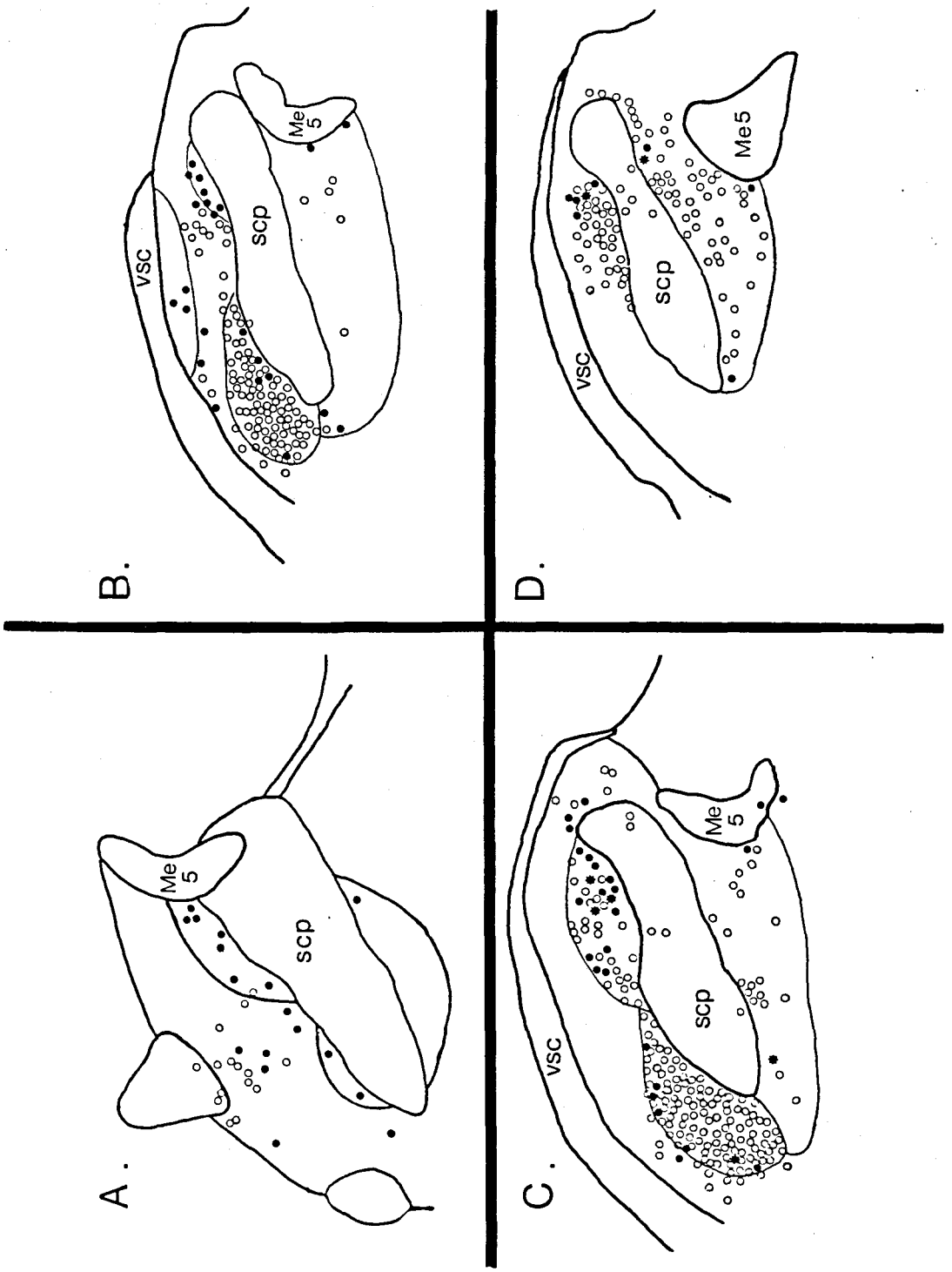
A.
Me 5
scp
B.
vsc
scp
Me 5
C.
vsc
scp
Me 5
D.
vsc
scp
Me5

Figure 8. Fluorescent photomicrographs of a coronal section through the PB illustrating (A) cells projecting to the CeA and (B) cells immunoreactive to ENK. Double-labeled cells are indicated by white arrows. Magnifications: A and B, 180X; C and D, 360X.

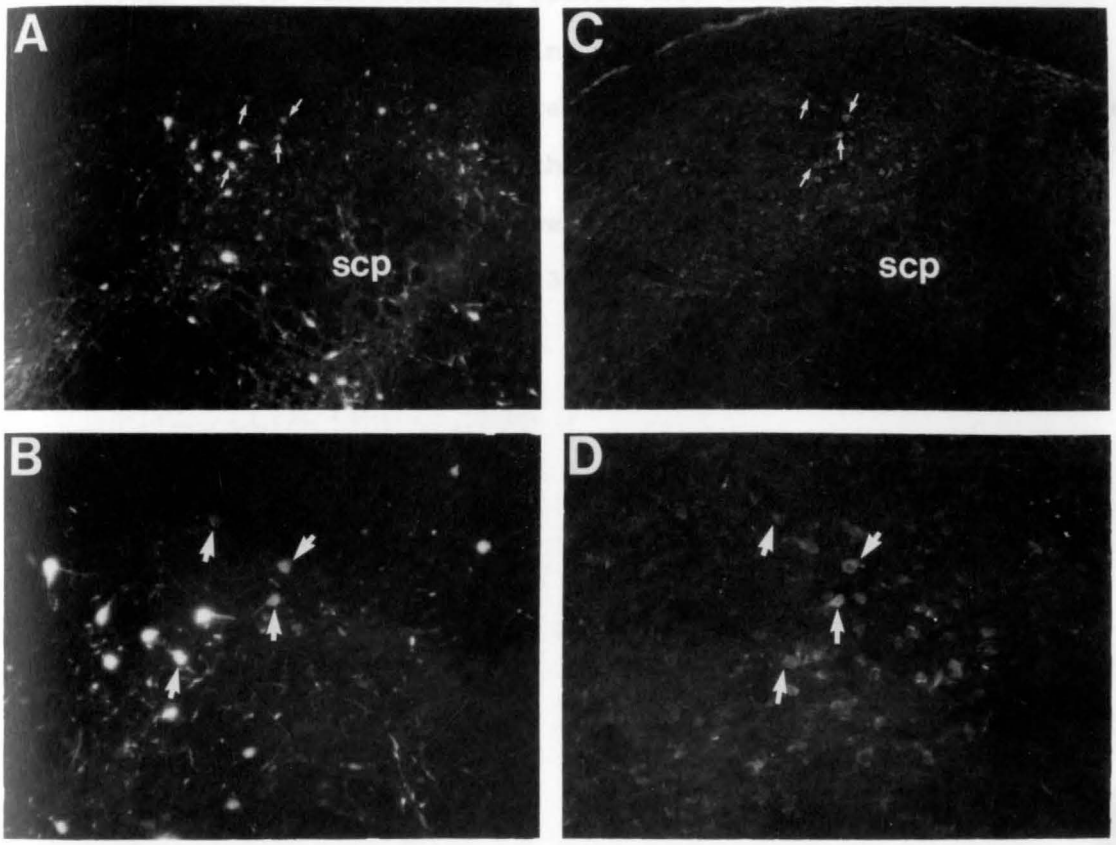
A
scp
C
scp
B
D

Figure 9. Fluorescent photomicrographs of a coronal section through the PB demonstrating Fluoro-Gold labeled cells (1 and 3) and corticotropin releasing factor (CRF)-immunoreactive cells (2 and 4). White arrows (panels 2 and 4) mark the location of a few CRF-ir cells in the same area as FG-labeled cells, but double-labeled neurons were not observed. Magnifications: A and B, 190X: C and D, 380X.

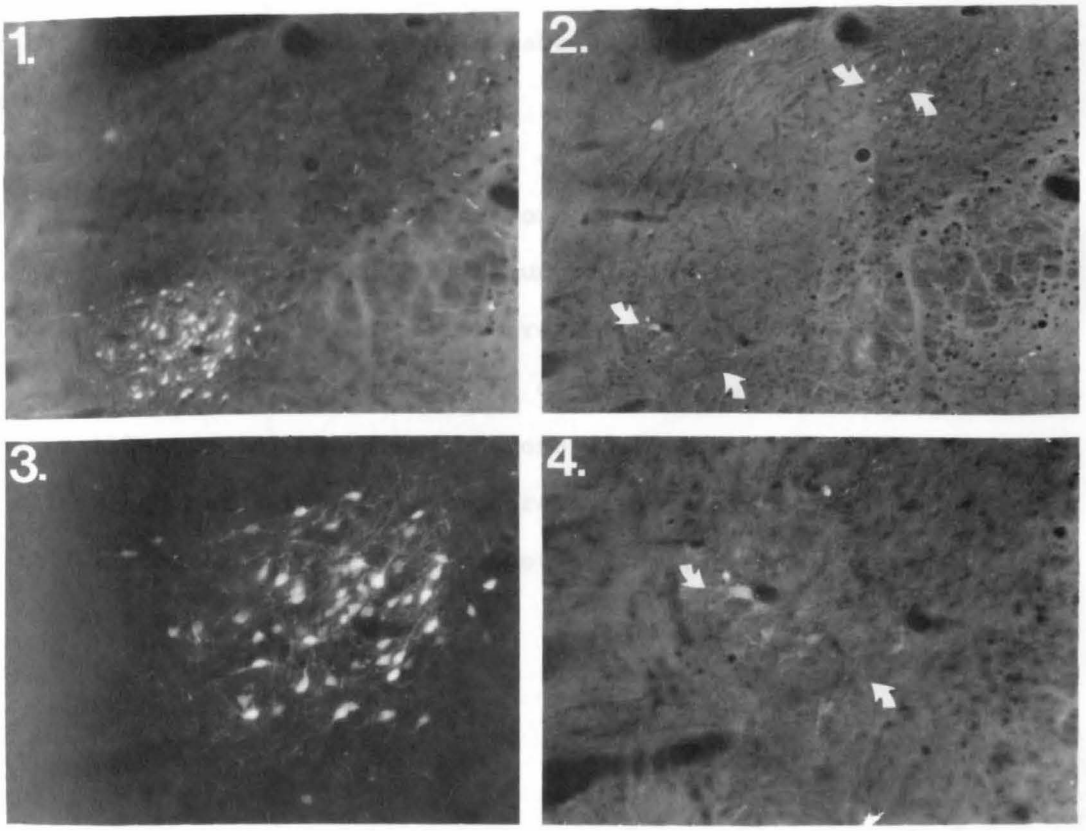
1.
2.
3.
4.

Figure 10. (A) Line drawing of a coronal section through the PB illustrating the distributions of Fluoro-Gold (open circles) and CRF-immuoreactive neurons after Fluoro-Gold injections into the CeA. Double-labeled neurons were not observed.

(B) Line drawing of a coronal section through the PB illustrating the distributions of Fluoro-Gold (open circles) and somatostatin (SS)-immunoreactive neurons (filled circles). Double-labeled cells were not observed.

(C) Line drawing of a coronal section through the PB illustrating the distributions of Fluoro-Gold (open circles) and bombesin (BOM) immunoreactive terminals (stipple). As BOM-immunoreactive cells were not present, double-labeled cells were not observed.

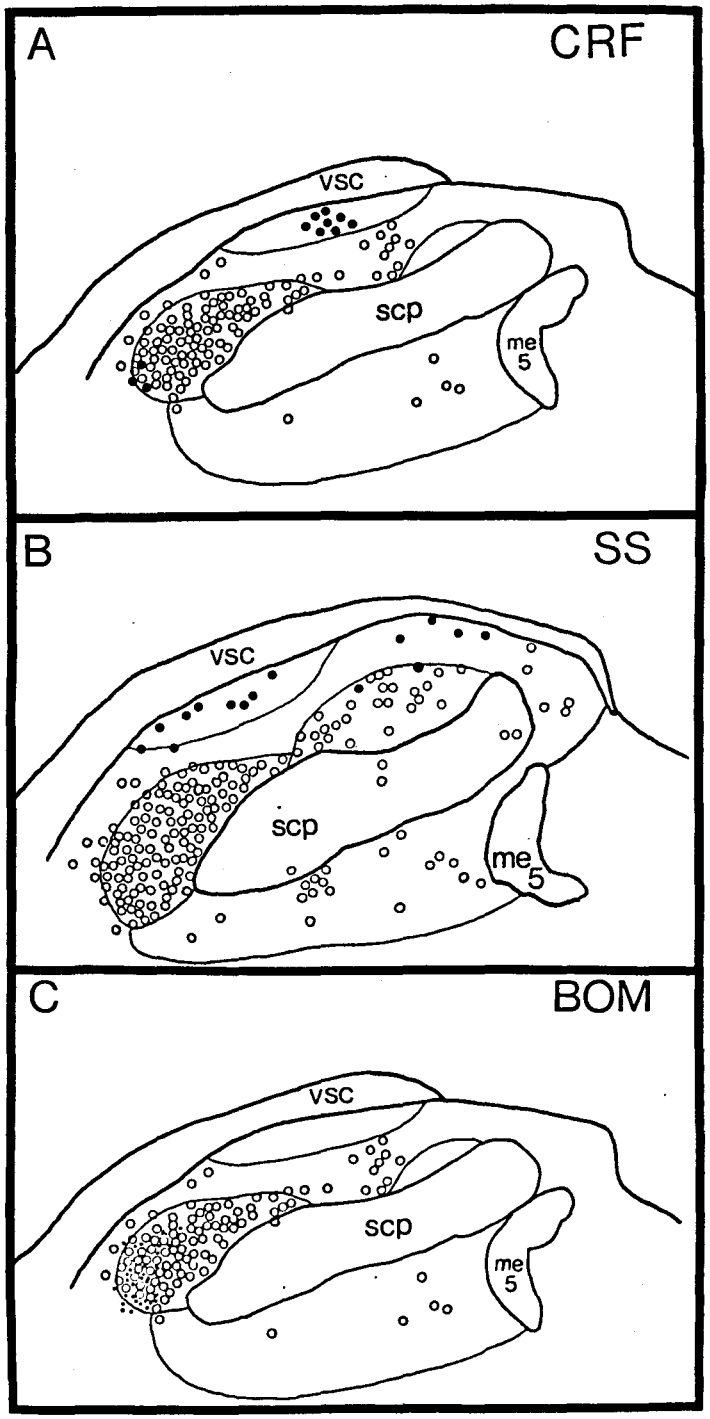
A
CRF
vsc
scp
me
5
B
SS
vsc
scp
me
5
C
BOM
vsc
scp
me
5

CHAPTER VI

CATECHOLAMINE AND NPY EFFERENTS FROM THE VENTROLATERAL MEDULLA TO THE AMYGDALA IN THE RAT: A COMBINED RETROGRADE TRACING-IMMUNOHISTOCHEMICAL STUDY

INTRODUCTION

The ventrolateral medulla (VLM) has been the focus in recent years of numerous anatomical, physiological, and immunohistochemical studies. Within the VLM, two groups of catecholamine-containing neurons have been identified. The A1 noradrenergic group (containing neurons positive for the enzyme tyrosine hydroxylase, TH) is located in the caudal VLM, at the dorsolateral pole of the lateral reticular nucleus (LRt) (Dahlstrom and Fuxe, '64; Kalia et al., '85a). The vast majority of neurons within the C1 adrenergic group (neurons positive for TH and the enzyme phenylethanolamine-N-methyltransferase, PNMT) are located rostral to the obex and occupy a wide area of the ventral medullary tegmentum, lying outside the major nuclear groups in that region (Kalia et al., '85b; Tucker et al., '87). Neuropeptide Y (NPY), a member of the pancreatic polypeptide family, has been shown to be co-localized within the catecholaminergic neurons of both groups (Everitt et al., '84). Although the functional role of this particular co-existence is unclear, a role in the regulation of vasomotor tone and vasopressin release for A1 and C1 neurons has been established (for review, see Ciriello et al., '86).

Several forebrain areas, in particular the supraoptic, paraventricular, and median preoptic nuclei, receive efferents from neurons in the VLM (Sawchenko and Swanson, '82; Tucker et al., '87; Cunningham and Sawchenko, '88). Another forebrain structure implicated in autonomic regulation, the central nucleus of the amygdala (CeA), also has been reported to receive a projection from the VLM. Otterson ('81) in the rat noted labeled cells in the contralateral VLM following a large injection of the retrograde tracer horseradish peroxidase (HRP) centered within the CeA, but also including the basolateral and basomedial amygdaloid nuclei. Although the position of these HRP-reactive cells within the VLM was described without reference to the catecholamine groups, the plot of their position places them within the area of the rostral VLM in an area corresponding to the C1 group (see his Fig. 3-M). In that same plot one HRP-reactive neuron is present within the contralateral caudal VLM (see his Fig. 3-O). In cases where the HRP injection was confined to the CeA, only one labeled cell is indicated to be present within the contralateral rostral VLM; HRP-reactive cells were not noted within the caudal VLM. In the same study injections into the basolateral, basomedial, lateral and cortical amygdaloid nuclei did not result in labeled cells in either the caudal or rostral VLM.

Within the amygdala two morphologically different types of noradrenergic fiber types have been described, one arising from the locus coerulus and one from other brainstem noradrenergic groups other than the locus coerulus (Fallon et al., '78). Fibers originating from the latter group are distributed within medial, ventral and lateral capsular subdivisions of the CeA; the medial and dorsolateral part of the basolateral amygdaloid nucleus receive a similar innervation (Fallon et al., '78). Other amygdaloid nuclei (e.g., the medial, lateral, intercalated, cortical, and lateral) contain some noradrenergic fibers of

the locus coerulus type (Fallon et al., '78). Lesioning the ventral tegmental area (transecting the ventral tegmental catecholamine bundle), sparing the dorsal bundle which arises exclusively in the locus coeruleus, resulted in a decrease of noradrenaline in the amygdala, giving supporting evidence that an efferent projection to the amygdala does arise from caudally located noradrenergic neurons (Fallon et al., '78). At least one such source is part of the the nucleus of the solitary tract (NTS) that corresponds to the A2 noradrenergic cell group. Combined retrograde tracer-immunohistochemical studies have shown directly that a large percentage of CeA-projecting cells within the medial NTS are tyrosine hydroxylase-positive (Zardetto-Smith and Gray, '88; Chapter 4, this dissertation).

NPY-immunoreactive terminals have been localized within the CeA to the same area containing noradrenergic terminals, i.e., primarily within the medial subdivision (Gray et al., '86). NPY-immunoreactive cell bodies in the medial NTS, just rostral to the area postrema, also contribute efferents to the CeA (Zardetto-Smith and Gray, '86a; Chapter 4, this dissertation). Some PNMT-positive neurons within the rostral NTS (part of the C2 adrenergic group) also project to the CeA, although the presence and distribution of adrenergic terminals within the amygdala has not been described (Zardetto-Smith and Gray, '88; Chapter 4, this dissertation).

In the course of studying the peptide/transmitter inputs to the CeA from the NTS and PB, we noted retrogradely-labeled neurons consistently localized within areas of the caudal and rostral VLM that corresponded to the A1 and C1 catecholamine groups. The presence of CeA-projecting neurons in the VLM, the confirmation that catecholamine and NPY efferents to the CeA originated from the NTS, and the co-localization of NPY within A1 and C1 neurons, was evidence suggesting that

catecholamine and/or NPY neurons within the VLM also provide an input to the CeA. This possibilty was examined in the present study, combining injections of the sensitive retrograde tracer Fluoro-Gold into the CeA with immunohistochemical methods. Preliminary findings of this investigation were previously reported (Zardetto-Smith and Gray, '88).

METHODS

Male Long-Evans rats (150-300 gm) were anesthetized using sodium pentobarbital (Butler, 55 mg/kg). Unilateral iontophoretic deposits of 2% Fluoro-Gold (Fluorochrome Inc.) in Ringer's lactate (Baxter-Travenol) was placed in the CeA using a glass micropipette (10-20 um outside diameter). Cathodal current was applied at 8 uA delivered in 7s pulses every 14 s over a 45 min period, using a constant current device (Midgard Electronics model CS3). Stereotaxic coordinates for the CeA were derived from the Paxinos and Watson rat brain atlas (1986).

After 11-15 days rats were reanesthetized and 2.5 ul of colchicine (dissolved in saline, 20 ug/ml) injected into each lateral ventricle, as well as the fourth ventricle. Twenty-four to forty-eight hours later, animals were administered a lethal dose of sodium pentobarbital and perfused through the ascending aorta utilizing the modified two-step pH variation method (Berod et al., '81) described in Chapter 4.

Brains were removed immediately and blocked. Adjacent coronal sections were cut using a Lancer Series 1000 vibratome. Sections from the injection site (40 um) were mounted directly onto acid-cleaned, gel coated slides in serial order as cut. Adjacent coronal sections of the brainstem (20 um) were collected into three vials of cold (4 C) PBS or 0.1% PBS-Triton X. A fourth series of sections was mounted as cut as a control for any fading of fluorescence that occur during immunocytochemical processing (Skirboll et al., '84).

Sections were incubated 24-72 hrs with antiserum to one of the following peptides or catecholamine synthesizing enzymes: goat anti-rabbit neuropeptide Y (NPY) (Dr. Bibi Chronwall or Dr. Marvin Brown); goat anti-sheep tyrosine hydroxylase (TH) (Dr. John Haycock); or goat

anti-rabbit phenylethanolamine-N-methyltransferase (PNMT) (Pennisula Laboratories). Anti-NPY and anti-PNMT were used at a dilution of 1:1000, while anti-TH was used at a dilution of 1:500. Primary antibodies were diluted in a solution of 0.1% PBS-Tx and 10% normal donkey serum. Antiserum specificity was controlled by pre-incubating 1 ml of each diluted antiserum with 10 ug of its homologous synthetic peptides. The tissue was then processed as described and examined for the presence of any immunohistochemical staining. Although immunohistochemical staining was blocked in these controls, cross-reactivity with as-yet-unidentified antigens cannot be excluded. The term "peptide-like" is, therefore, implicit in the following descriptions of neuropeptide immunoreactivity (neuropeptide-ir).

Following incubation with the primary antibody, sections were rinsed in PBS and incubated with biotinylated donkey anti-rabbit (NPY or PNMT) or donkey anti-sheep (TH) immunogammaglobulin (IncStar) for 1 hr. at room temperature. After a brief rinse in PBS, sections were then incubated with streptavidin-Texas red conjugate (IncStar) for 1 hr. at room temperature. Sections were transferred to cold PBS, mounted and analyzed as previously described in Chapter 4.

In five additional rats, the sensitive anterograde tracer Phaselous vulgaris leucoagglutinin (PHA-L) was injected into the VLM in an attempt to tentatively confirm the retrograde label seen in the VLM after Fluoro-Gold injections into the CeA. The protocol for these experiments was as described in Chapter 3. Briefly, each animal was anesthetized with sodium pentobarbital (55 mg/kg) and placed in a stereotaxic apparatus. The VLM was accessed by way of a dorsal surgical approach through the atlanto-occipital membrane. In each animal a single unilateral iontophoretic application of PHA-L (dissolved to a 2.5% solution, 0.1 M PBS) was placed within the VLM using a glass

micropipette (10-20 um outside diameter). Placement of the pipette tips was guided by obtaining co-ordinates from the Paxinos and Watson rat brain atlas ('86) using the obex as a reference point. Cathodal current was applied 8 uA delivered in 7-s pulses every 14 s over a 45 min period) using a constant current device (Midgard Electronics model CS3). After 14 d the animals were sacrificed and perfused, and the tissue processed as described previously (see Chapter 3). Adjacent sections were counterstained with cresyl violet or left unstained and examined for PHA-L immunoreactivity using both light- and dark-field microscopy.

RESULTS

Distribution of Retrogradely-Labeled Cells. Fluoro-Gold (FG) labeled cells were consistently noted in the VLM following iontophoretic deposits in which the pipette tip was centered within the CeA (Fig. 1). Retrogradely-labeled neurons were not observed in cases in which the deposit was centered within the medial, lateral and basolateral amygdaloid nuclei. Cell counts of the total number of FG-labeled cells in the VLM were made in six cases in which the injection was centered within the CeA. Using Abercrombie's correction factor ('46) for double-counting errors, it was estimated that an average of 89 $\pm$ 18 cells within the ipsilateral VLM were retrogradely labeled.

Caudal to the obex, several labeled cells were found within the VLM at the dorsolateral pole of the lateral reticular nucleus (LRt) ipsilateral to the side of the injection (Fig. 2, 4, 6). Contralaterally, labeled cells were present in the same area, dorsolateral to the LRt but were fewer in number compared to the ipsilateral side. Occasionally, a FG-labeled neuron was present ipsilaterally within the medullary reticular formation, in the zone lateral and ventral to the nucleus of the solitary tract. Further rostrally, at the level of the obex, retrogradely labeled cells clustered in a group (3-4 cells per section) dorsal to the LRt. Single retrogradely-labeled cells were sometimes observed scattered near the ventral surface of the medulla, medial to the LRt and lateral to the inferior olive. Again, labeled cells were present both ipsilateral and contralateral to the side of the injection, though fewer in number contralaterally. At the level of the area postrema, FG-labeled cells remain clustered dorsolateral to the ipsi- and contralateral LRt and numbered 3-4 cells per section each side .

Rostral to the level of the area postrema, where the nucleus of the solitary tract borders directly on the fourth ventricle, the number of labeled cells within the VLM decreases substantially, with only 1-2 cells present per section (Fig. 2, 4, 6). Usually, single cells were present both ipsilaterally and contralaterally, scattered throughout the ventral medullary tegmentum. Farther rostrally, this pattern of distribution continued. Most often, the few FG-labeled cells present were positioned near the ventral surface of the medulla and near the ventral or dorsolateral border of the lateral paragigantocellular nucleus (LPGi). Occasionally, a labeled cell was seen extending medially into an area directly dorsal to the pyramid. Retrogradely-labeled cells were infrequently observed in the VLM from the level of the subvestibular NTS to the most rostral extents of the VLM proper (level of the facial nucleus).

Distribution of Immunocytochemically-Labeled Cells. The distribution of TH-, NPY-, and PNMT-ir cells within the VLM in the present study was the similar to that described in recent immunocytochemical studies of the medulla (Everitt et al., '84; Kalia et al., '85a, b; Harfstrand et al., '87), and therefore, is only brBefly summarized. Caudal to the obex, TH-positive cells found in the VLM clustered dorsolateral to the LRt in an area corresponding to the A1 noradrenergic cell group (Fig. 2). Near the level of the obex and area postrema, some TH-ir neurons extended obliquely in the medullary reticular formation between the A1 group and the A2 noradrenergic group in the dorsal medulla. TH-ir cells remained positioned dorsolateral to the LRt until the level just rostral to the area postrema, where they became scattered ventral to the LPGi, and extending medially over the pyramids, in an area corresponding to the C2 adrenergic group (Fig. 2). Continuing

rostrally, TH-ir cells were distributed within the VLM in a pattern similar to that of PNMT-ir cells (described below).

At caudal extents of the medulla, PNMT-ir cells were not present (Fig. 4). Just caudal to the area postrema, a few PNMT-ir cells appeared within the VLM, dorsal to the LRt, in approximately the same position described for the TH-ir cells previously, and marking the beginning of the C1 catecholaminergic cell group. At the level of the area postrema and continuing rostrally, several PNMT-ir cells were present near the ventral surface of the medulla, and ventral and lateral to the LPGi; some surrounded the dorsolateral aspect of the nucleus, while a few cells were scattered through the nucleus itself (Fig. 4). Again, a few scattered cells extended through the medullary reticular formation between the VLM and the dorsal medulla. NPY-ir cells were present in the VLM beginning just caudal to the obex, in a cluster dorsal to the LRt similar to that of the TH-ir cells (Fig. 6). Some cell labeling was present ventral to the LRt. Rostrally, NPY-ir cells were distributed in the VLM a pattern resembling that described for PNMT-positive cells (Fig. 4, 6).

Distribution of Retrogradely-Labeled Immunocytochemically-Labeled Cells. Retrogradely-labeled neurons immunoreactive for both TH and NPY were consistently found within aspects of the caudal VLM, while double-labeled PNMT cells were present most often at levels rostral to the area postrema (Fig. 4, 5; Fig. 3). Immunoreactive and double-labeled neurons from different cases were counted (Table 1) to assess the relative contribution of the catecholamine- and NPY-containing cells to the VLM-CeA pathway. These cell counts included both the caudal and rostral VLM.

Tyrosine hydroxylase (TH-ir). Double-labeled cells were

present at the caudalmost extents (near the spino-medullary junction) of the A1 group in the VLM, a level where the C1 group is not yet present (Tucker et al., '87). Most retrogradely labeled neurons present at this level were TH-positive. Also, most double-labeled cells were distributed within the cluster of TH-ir cells dorsal to the LRt, although a few were also distributed close to the ventral surface of the medulla (Fig. 2). Rostral to the level of the area postrema, as there were fewer retrogradely-labeled cells present, the number of double-labeled TH-ir neurons label decreased. Fig. 3 is an example of three retrogradely labeled cells within the caudal VLM that were also TH-positive. The percentage of CeA-projecting cells that were TH-ir varied from 74-94% (average 84%); however, these double-labeled cells comprised a minor proportion of the total TH-ir cell population (an average of 11%) (Table 1).

Phenylethanolamine-N-methyl transferase (PNMT-ir). Some Fluoro-Gold labeled cells within the VLM at the level of the area postrema were also PNMT-positive. Most double-labeled PNMT-ir neurons were present at this level, and the level just rostral to the area postrema (Fig 4). At more rostral extents of the C1 group, some singly double-labeled neurons were present within the large scattering of PNMT-ir neurons in this area. Approximately 42% of the CeA-projecting neurons in the VLM were PNMT-positive, but only 5% of the total C2 adrenergic group participates in the pathway (Table 1). Fig. 5 shows examples of PNMT-ir double-labeled cells within the VLM.

Neuropeptide Y (NPY-ir). Occasionally, double-labeled NPY-ir neurons were seen in the VLM at the level of the obex, but were most common in the VLM rostral to the level of the area postrema (Fig.6). As discussed earlier, few retrogradely-labeled neurons were found in the rostral VLM; thus, few CeA-projecting NPY-ir cells were present at

the level of the subvestibular NTS, but when present, almost always were double-labeled. Approximately 41% of the CeA-projecting cells were also NPY-ir (range 26-53%), comprising an average of 15% of the total NPY-ir cell population in the VLM (Table 1).

Distribution of Anterograde Labeling. In one case out of five attempted, the PHA-L injection was successfully centered in the VLM at a level just rostral to the area postrema (Fig.8). PHA-L immunoreactive fibers and terminals were most numerous at intermediate to rostral levels of the CeA and localized primarily within the medial and ventral subdivisions (Fig. 9). A few fibers were observed within the medial and basolateral amygdaloid nucleus. Several fibers were present in the substantia inominata and the preoptic subnucleus of the bed nucleus of the stria terminalis. At more rostral levels of the bed nucleus, a few varicose fibers were present in the parastrial subnucleus. At its most rostral extent, little or no label was present within the bed nucleus, though the medial preoptic area appeared to be heavily innervated.

DISCUSSION

The results of the present study demonstrate the CeA is a forebrain target of neurons within the VLM. This is not surprising in light of the known multiple and reciprocal connections the CeA has with several other brainstem autonomic nuclei, including the nucleus of the solitary tract, the locus coeruleus, and parabrachial nucleus (Fulwiler and Saper, '84; Van der Kooy et al., '84; Cassell et al., '86; Danielson et al., '89; Wallace et al., '89). A substantial portion of the VLM projection to the CeA appears to arise from adrenergic cells of the C1 group, since an average of nearly 40% of the retrogradely-labeled cells were also PNMT-ir (Table 1). Like the projection of VLM catecholaminergic neurons to the PVN (Tucker et al., '87), the adrenergic projection to the CeA originates from the middle and rostral levels of the VLM; projections from the caudal VLM are predominately noradrenergic in nature. Interestingly, the VLM has been shown to receive a reciprocal, descending projection from the medial subdivision of the CeA which terminates preferentially on PNMT-immunoreactive neurons in the rostral part of the C1 group (Cassell and Gray, '89).

The high percentage of double-labeled NPY-ir cells (averaging 38%) suggests some degree of co-localization of NPY within CeA-projecting catecholaminergic neurons (Table 1). For example, in CGC 80, cell counts showed that 74% of the CeA-projecting cells were double-labeled for TH-ir. In the same case, cell counts indicated that 50% of the CeA-projecting neurons were also double-labeled for NPY-ir. As their combined total exceeds 100% in this case, NPY-ir must have been co-localized within some CeA-projecting TH-ir neurons.

The ascending projections from the VLM to other forebrain nuclei involved in autonomic and neuroendocrine regulation, particularly the

supraoptic (SO) and paraventricular (PVN) hypothalamic nuclei, have been extensively studied both anatomically and electrophysiologically (for recent review, see Ciriello et al., '86). Neurons in the A1 noradrenergic group in the rat VLM innervate the magnocellular, rather than the parvocellular, divisions of the paraventricular and supraoptic nuclei (Cunningham and Sawchenko, '88). In the cat, VLM neurons that terminate in the magnocellular divisions of the PVN and SO respond to electrical stimulation of the carotid sinus and aortic depressor nerves (Caverson and Ciriello, '84; Ciriello and Caverson, '84), demonstrating ascending pathways from the VLM to the forebrain may be involved in transmitting visceral afferent information (Sawchenko and Swanson, '82). In comparison, the A2 group within the NTS densely innervates the parvocellular division of the PVN, and it has been suggested that A2 noradrenergic neurons influence the hypothalamic-pituitary-adrenal axis (Cunningham and Sawchenko, '88).

The CeA also receives a differential catecholaminergic input from the NTS and VLM. In contrast to the high percentage of PNMT-positive neurons within the VLM that project to the CeA, catecholaminergic neurons within the NTS projecting to the CeA arise primarily from the noradrenergic A2 group (Zardetto-Smith and Gray, '88; Chapter 4, this dissertation). Due to the lack of experimental evidence, the functional significance of a differential noradrenergic vs. adrenergic innervation of the CeA may only be discussed in a speculative manner at this time. On a general scale, it has been proposed that differences in between the two neurotransmitters represent evolutionary modifications, with epinephrine still mediating functions it subserved in the periphery (vasomotor tone and energy metabolism), and norepinephrine mediating the elaboration of cortical arousal and attention (Panksepp, '82). In keeping with this hypothesis, the ascending noradrenergic

input to the CeA from the NTS may influence behavior-related functions, including alerting, sleep, conditioning, feeding, and stress (see Chapter 4 for discussion), while adrenergic input from the VLM to the CeA may be associated more specifically with cardiopulmonary function, i.e., relaying information related to the tonic maintenance of vasomotor tone (Ross et al., '83), baroreflex vasodepressor responses (Granata et al., '85), or central chemoreceptor activity (for review, see Ciriello et al., '86).

The CeA influences a wide range of autonomic and somatic functions through its descending projections to the brainstem (for review, see Gray '89). This is reciprocated by several parallel, multisynaptic pathways, both catecholaminergic and non-catecholaminergic (for review, see Price et al., '87; Chapter 2, this dissertation). Further physiological studies investigating the types of visceral information relayed to the CeA from the VLM will be needed in order to clarify the role of this pathway in the integration of autonomic responses within the forebrain.

Concluding Comments. In addition to receiving efferents from other brainstem autonomic-related nuclei (e.g., the nucleus of the solitary tract and the parabrachial nucleus) the CeA receives an efferent projection from neurons in the ventrolateral medulla. This ascending efferent pathway arises, in large part, from adrenergic cells of the C1 group. In contrast, the majority of the ascending catecholamine input from the nucleus of the solitary tract to the CeA is noradrenergic in nature (see Chapter 4, this dissertation). Some degree of co-localization of NPY within CeA-projecting VLM catecholaminergic neurons is suggested by the high percentage of double-labeled NPY-ir cells found in this study. The functional significance of a differen-

tial noradrenergic vs. adrenergic innervation of the CeA is not clear. Possibly, the noradrenergic input from the NTS to the CeA is related to general visceral feedback involved in a number of behavior-related functions, while adrenergic input from the VLM to the CeA may be more specific, i.e., cardiopulmonary only.

Table 1. Injection sites for cases CGC 74, 80, and 102 are illustrated in Figure 1. Numbers represent raw counts, uncorrected for double-counting errors.

Abbreviations:

RG	retrogradely-labeled cells
IR	immunoreactive cells
DL	double-labeled cells
DL/RG	ratio giving percent of retrogradely-labeled cells immunoreactive for given antigen
DL/IR	ratio giving percent of immunoreactive cell population projecting to CeA

TABLE 1

Antigen	Case	# Sections	#RG Cells	#IR Cells	#DL cells	DL/RG %	DL/IR %
TH	80	30	43	360	32	74	9
	91	35	59	401	49	83	12
	102	26	51	435	48	94	11
PNMT	74	17	11	83	4	36	5
	102	35	35	222	18	51	8
	112	27	112	220	44	39	2
NPY	74	27	19	151	5	26	3
	76	33	76	156	40	53	26
	80	29	44	194	22	50	11
	91	24	38	74	13	34	18

Figure 1. Line drawings of representative Fluoro-Gold injection sites in the CeA. Black area indicates center of injection, and shading indicates the spread of the fluorescent tracer.

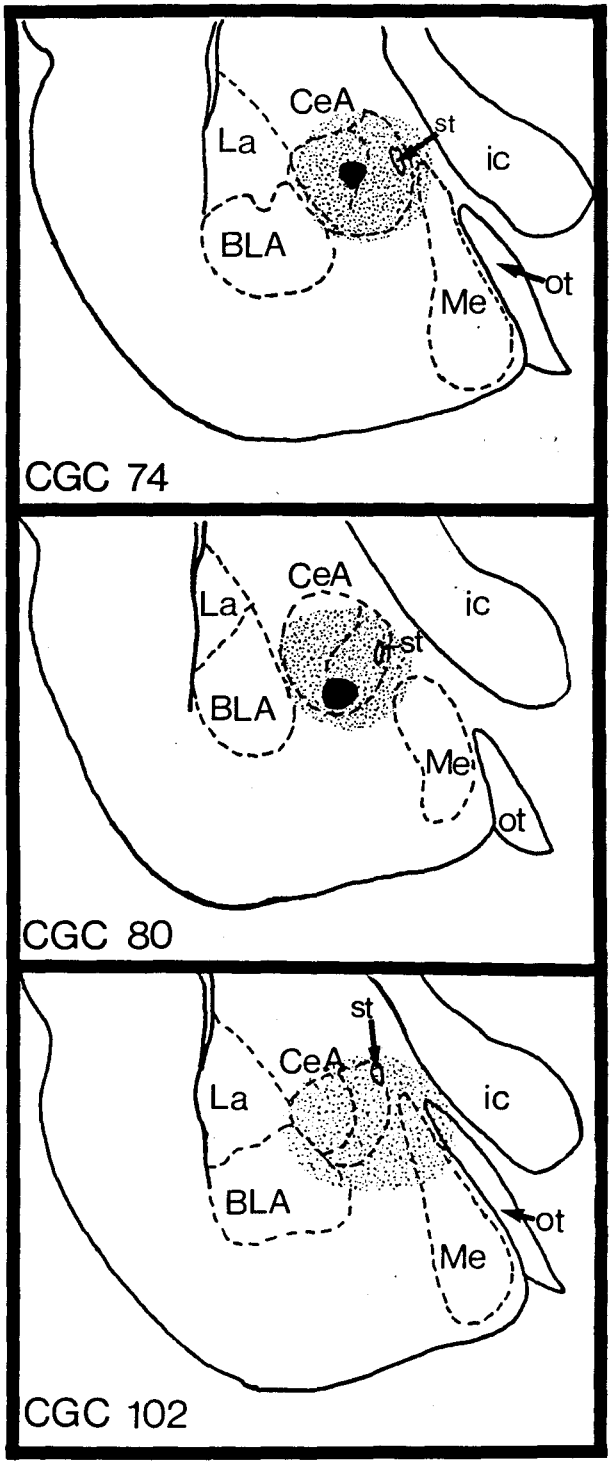
CeA
La
st
ic
BLA
ot
Me
CGC 74
CeA
La
ic
st
BLA
Me
ot
CGC 80
st
CeA
La
ic
BLA
ot
Me
CGC 102

Figure 2. Line drawings of four coronal sections through the ventrolateral medulla illustrating the distributions of retrogradely-labeled cells (open circles), tyrosine hydroxylase (TH)-immunoreactive (filled circles) and double-labeled (stars) cells found within the VLM after retrograde tracer injections into the CeA. Distance from bregma (mm) is noted to the left of each section.

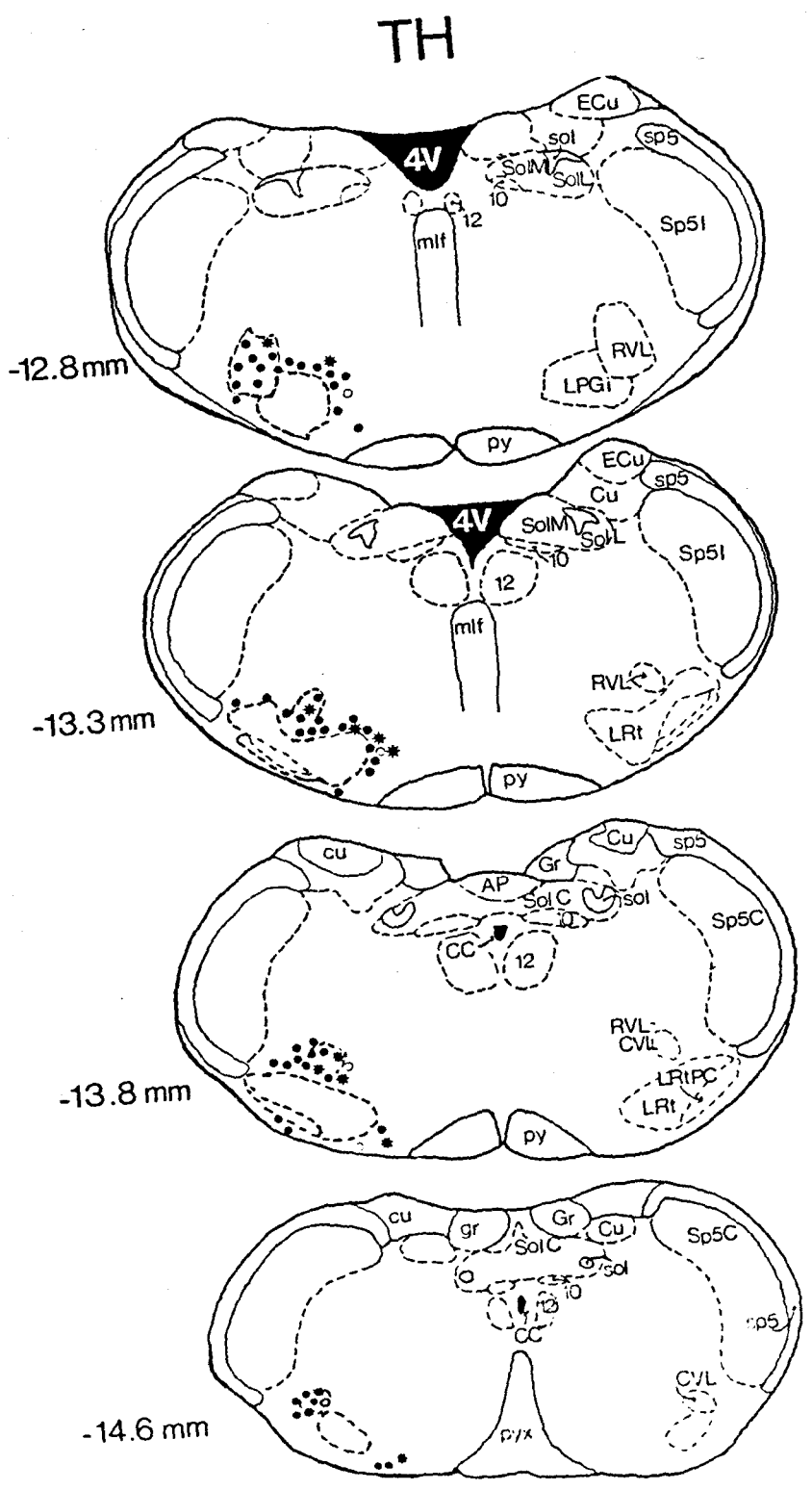
TH
ECu
sol
sp5
4V
SolM
SolL
10
12
Sp5I
mlf
RVL
LPGi
-12.8mm
py
ECu
Cu
sp5
4V
SolM
SolL
10
Sp5I
12
mlf
RVL
LRt
-13.3mm
py
cu
Cu
sp5
Gr
AP
Sol C
sol
Sp5C
CC
12
RVL
CVL
LRtPC
LRt
-13.8 mm
py
cu
gr
Gr
Cu
Sp5C
Sol C
sol
10
12
CC
sp5
CVL
-14.6 mm
py/x

Figure 3. Low-power (340X) fluorescent photomicrographs of coronal sections through the caudal ventrolateral medulla illustrating the distribution of neurons projecting to the CeA (A) and (C) and neurons immunoreactive to TH (B) and (D). White arrows indicate Fluoro-Gold labeled cells that are also TH-immunoreactive.

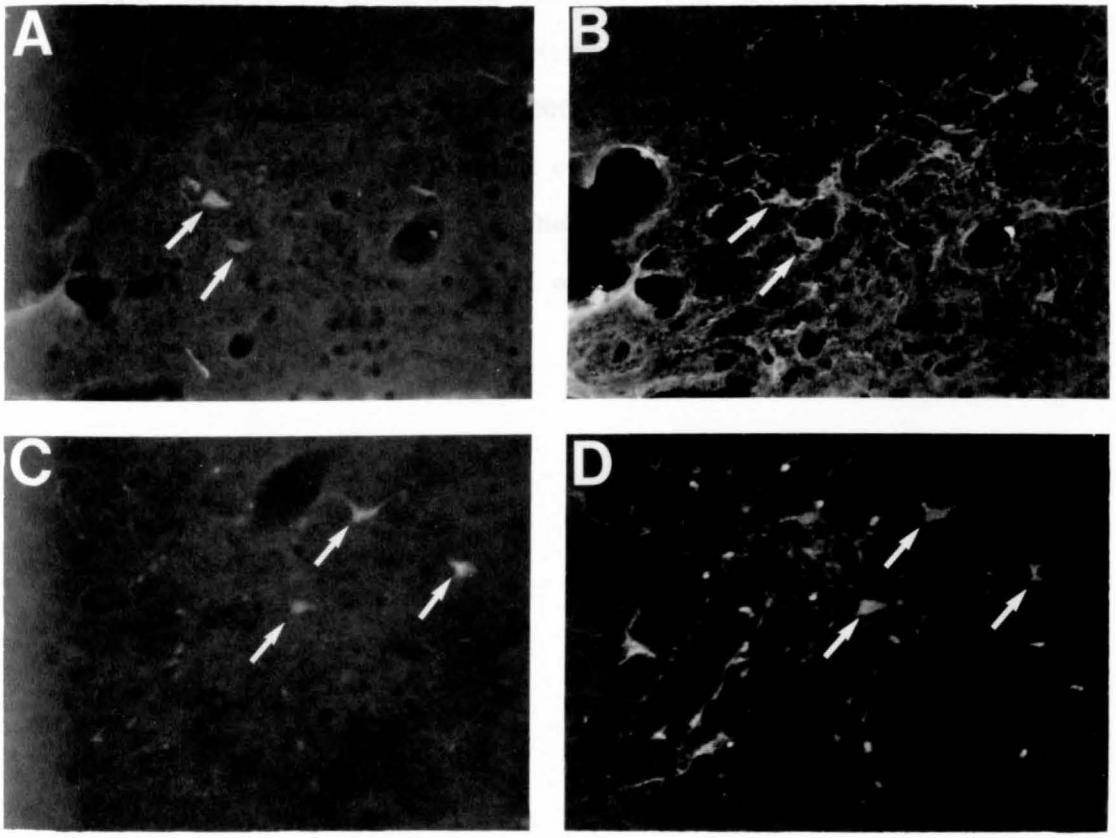
A
B
C
D

Figure 4. Line drawing of four coronal sections through the ventrolateral medulla illustrating the distributions of retrogradely-labeled (open circles), phenylethanolamine-N-methyltransferase (PNMT) immunoreactive (filled circles) and double-labeled cells (stars) after retrograde tracer injections into the CeA. Distance from bregma (mm) is noted to the left of each section.

PNMT

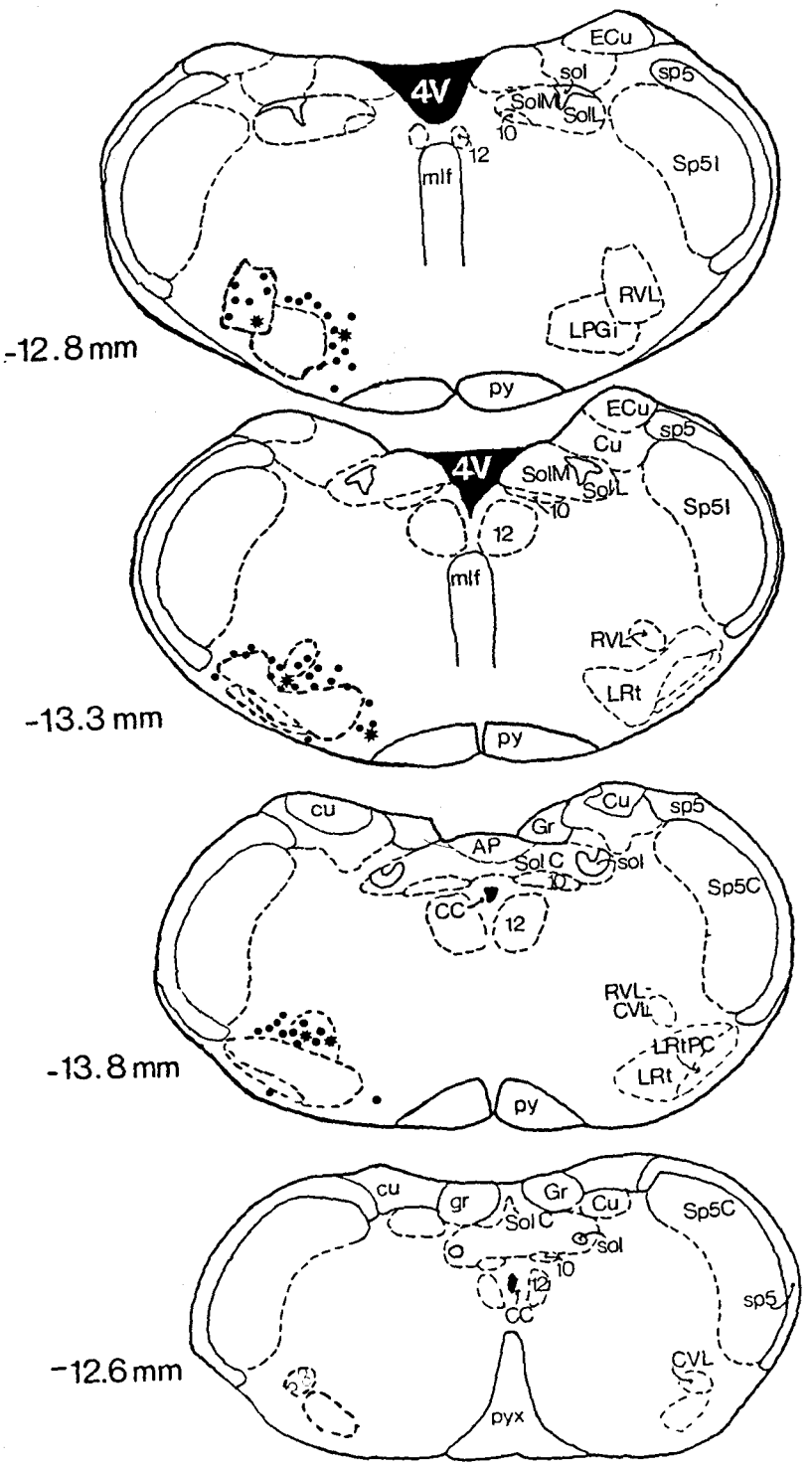
ECu
sol
sp5
4V
SolM
SolL
10
12
mlf
Sp5I
RVL
LPGi
-12.8 mm
py
ECu
sp5
Cu
4V
SolM
SolL
10
Sp5I
12
mlf
RVL
LRt
-13.3 mm
py
cu
Cu
sp5
Gr
AP
Sol C
sol
Sp5C
CC
12
RVL
CVL
LRtPC
LRt
-13.8 mm
py
cu
gr
Gr
Cu
Sp5C
Sol C
sol
10
12
CC
sp5
CVL
-12.6 mm
pyx

Figure 5. High-power (800X) fluorescent photomicrographs of coronal sections through the rostral ventrolateral medulla showing cells projecting to the CeA (A and C) that are also immunoreactive to PNMT (B and D). At rostral levels, retrogradely-labeled cells are fewer in number than at caudal levels, but when present, are almost always immunoreactive to PNMT.

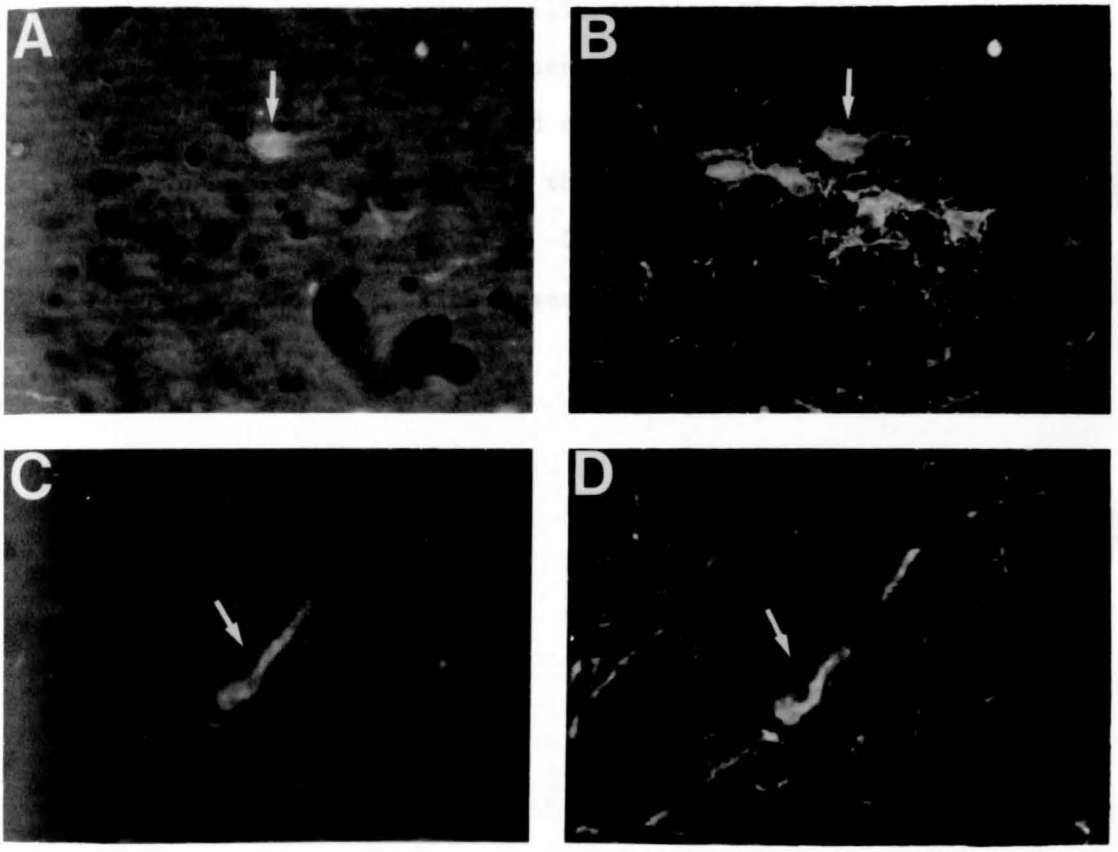
A
B
C
D

Figure 6. Line drawings of four coronal sections through the ventrolateral medulla illustrating the distributions of retrogradely-labeled (open circles), neuropeptide Y (NPY)-immunoreactive (filled circles), and double-labeled (stars) cells found within the VLM after injections of retrograde tracer into the CeA. Distance from bregma (mm) is noted to the left of each section.

NPY

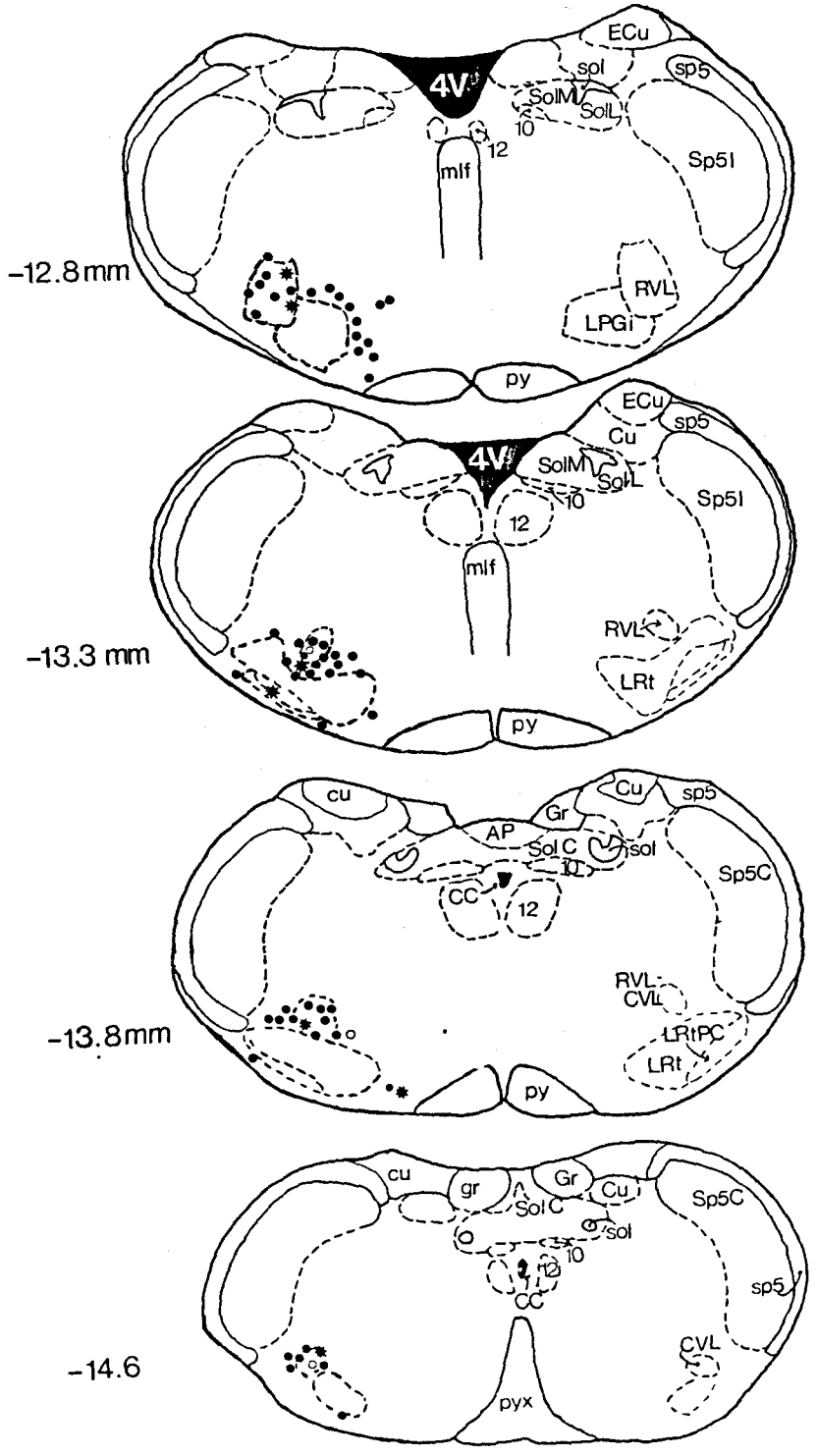
-12.8mm
4V
ECu
sol
sp5
SolM
SolL
10
12
mlf
Sp5I
RVL
LPGi
py
-13.3 mm
4V
ECu
sp5
Cu
SolM
SolL
10
12
mlf
Sp5I
RVL
LRt
py
-13.8mm
cu
Cu
sp5
Gr
AP
Sol C
sol
10
CC
12
Sp5C
RVL-
CVL
LRtPC
LRt
py
-14.6
cu
gr
Gr
Cu
Sol C
sol
10
12
CC
Sp5C
sp5
CVL
pyx

Figure 7. Low-power (160X, A and B) and high-power (240X, C and D) fluorescent photomicrographs of a coronal section through the ventrolateral medulla illustrating (A and C) cells projecting to the CeA, and (B) cells immunoreactive to NPY. Two double-labeled cells are indicated by white arrows.

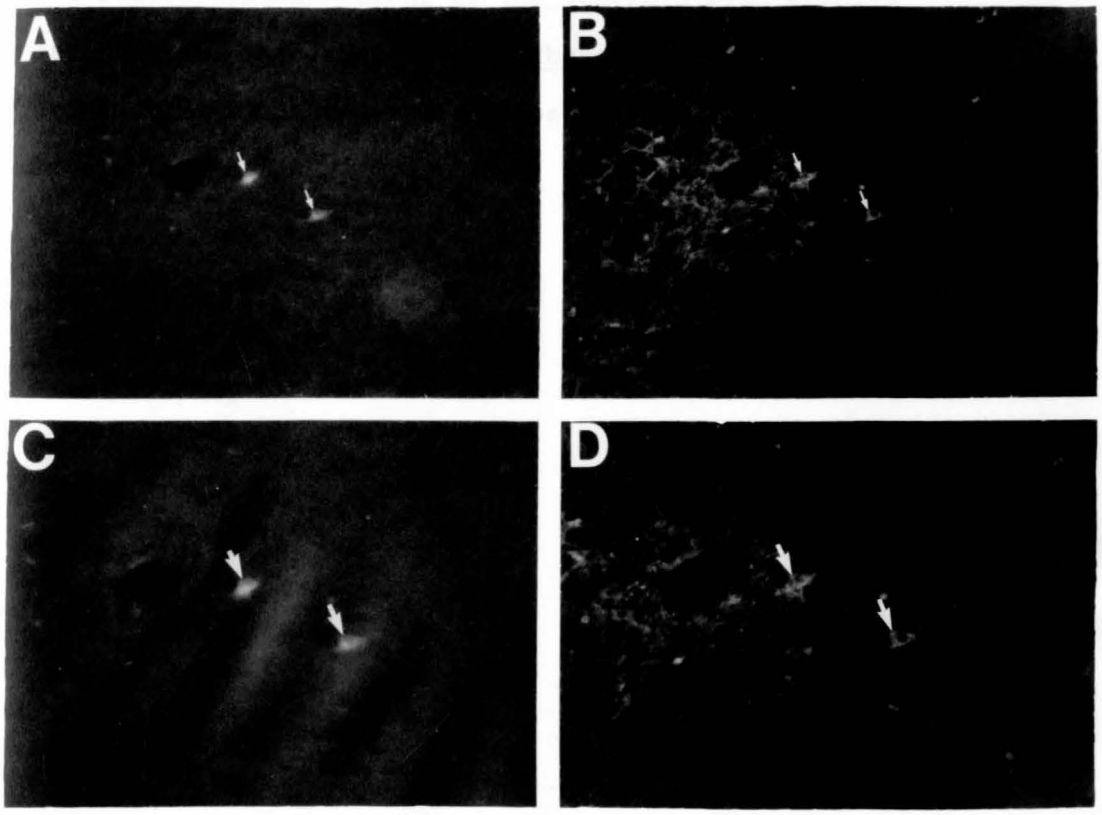
A
B
C
D

Figure 8. Line drawing of a coronal section through the mid-rostral-caudal extent of the ventrolateral medulla illustrating the injection site of Phaseolus vulgaris leucoagglutinin (PHA-L) that produced labeling of fibers and terminals within the CeA.

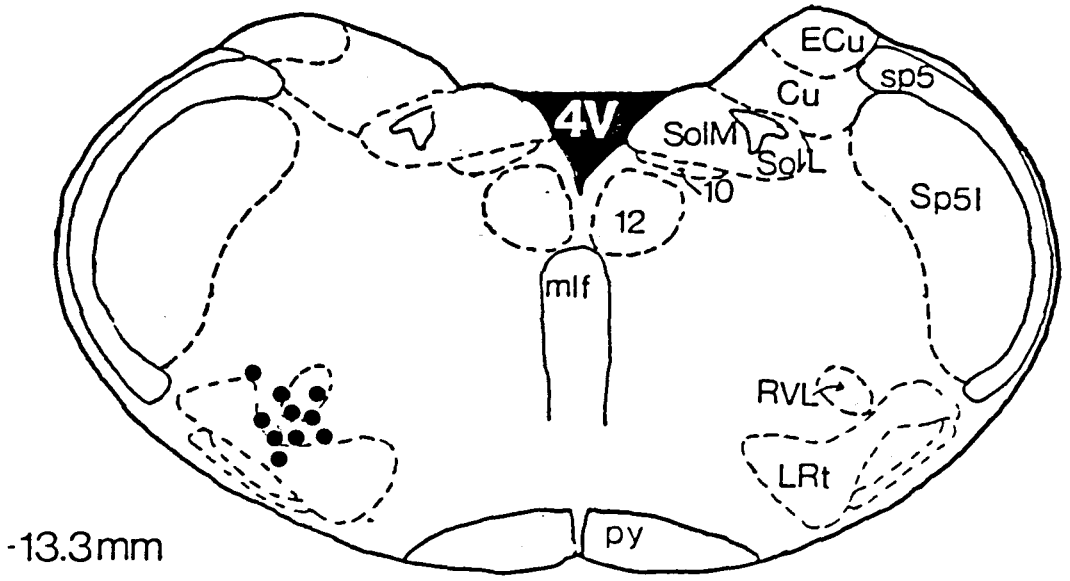
ECu
sp5
Cu
4V
SolM
SolL
10
12
Sp5I
mlf
RVL
LRt
py
-13.3mm

Figure 9. Schematic drawing of a coronal section through the CeA illustrating the distribution of labeled PHA-L fibers and terminals within the CeA after an injection of the anterograde tracer into the area of the VLM shown in the preceeding figure. The stria terminalis is denoted by an asterik (*). Distance from bregma (mm) is noted in the left corner of the figure.

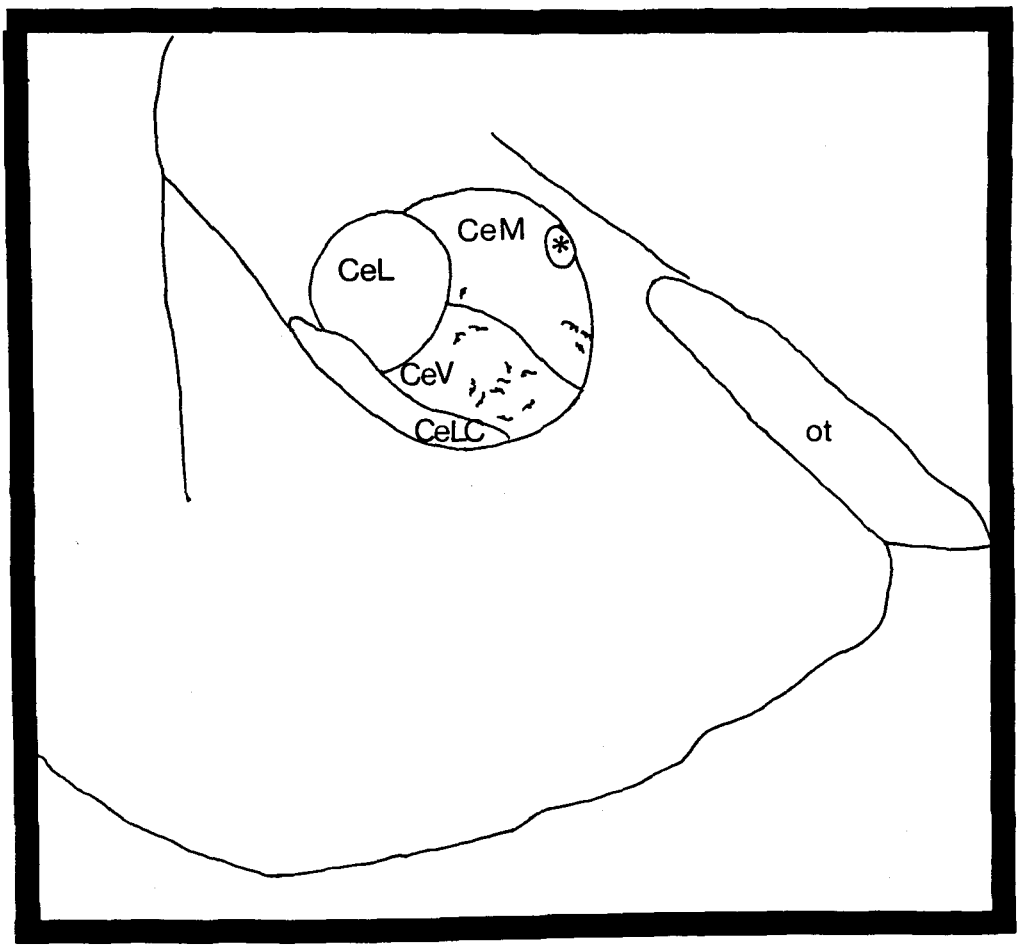
CeM
CeL
CeV
CeLC
ot

CHAPTER VII

A DIRECT NEURAL PROJECTION FROM THE NUCLEUS OF THE SOLITARY TRACT TO THE SUBFORNICAL ORGAN IN THE RAT

INTRODUCTION

The subfornical organ (SFO) of the rat is a circumventricular organ implicated in regulating fluid balance in response to increased circulating levels of angiotensin II and changes in blood pressure (Miselis, '81; Lind et al., '82; Lind et al., '84; Dellman, '85; Swanson and Lind, '86). Neuroanatomical tract tracing studies have demonstrated that the SFO has multiple efferent connections with regions of the basal forebrain that also are involved in the central regulation of fluid balance and blood pressure: the median preoptic, paraventricular and supraoptic hypothalamic nuclei (Hernesniemi et al., '72; Lind et al., '82; Miselis, '81). A recent study using discrete injections of the anterograde tracer Phaseolus vulgaris leucoagglutinin (PHA-L) demonstrated that SFO innervates widespread, but specific regions of the forebrain (Swanson and Lind, '86). These include sub-regions of the prefrontal cortex, septal area, substantia innominata, median and medial preoptic areas, zona incerta and the lateral hypothalamic area. Many of these regions in turn project back to the SFO (Lind et al., '82). These zones are thought to be involved in thirst-motivated behaviors as initiated by the SFO in response to circulating angiotensin II in blood (Swanson and Lind, '86).

Knowledge of the involvement of the SFO in body water balance and cardiovascular regulation through its efferent neural projections has greatly expanded in recent years. However, little is known about the function of the input to the SFO, although feedback from peripheral cardiovascular receptors would seem an integral part of its function. There are several possible multisynaptic pathways by which the SFO may receive feedback from baroreceptors and low-volume receptors that terminate within the nucleus of the solitary tract (NTS) (for review, see Kalia, '81). This could be accomplished by NTS projections to either the medial (Ricardo and Koh, '78) or median (Saper and Levisohn, '83) preoptic nuclei, each of which in turn projects directly to the SFO (Hernesniemi et al., '72; Lind et al., '82), and/or through NTS projections to the parabrachial nucleus, relayed through the median preoptic nucleus (Fulwiler and Saper, '84; Saper and Levisohn, '83). The present investigation demonstrates a direct projection from the NTS to the SFO using the PHA-L anterograde tracing method.

METHODS

Five male Long-Evans rats were the subjects of this study. Each animal was anesthetized with sodium pentobarbital (45 mg/kg) and placed in a stereotaxic apparatus (Kopf). The NTS was accessed by way of a dorsal surgical approach through the atlanto-occipital membrane. In each animal a single unilateral iontophoretic application of PHA-L was placed within the dorsal medulla using a glass micropipette (10-15 um outside diameter). Placement of the pipette tips were guided by obtaining coordinates from the Paxinos and Watson rat brain atlas ('86) using the obex as a reference point. Cathodal current was applied (5 uA delivered in 7-s pulses every 14 s over a 30-min period) using a constant current device (Midgard Electronics Model CS3). After a survival period of 14 days, the animals were administered a lethal dose of sodium pentobarbital. They were then perfused through the ascending aorta according to the method described by Gerfen and Sawchenko ('84). Adjacent 20-um coronal sections of the brainstem and forebrain were cut using a vibratome (Lancer). Sections were incubated with a 1:1000 dilution of PHA-L antibody (Dako) for 24 h. The tissue was then processed using the avidin-biotin immunoperoxidase method according to the procedures described by Gerfen and Sawchenko ('84). Tissue processed with the PHA-L antibody from a non-injected animal failed to produce any specific staining. Sections were mounted onto chrome-alum-coated slides. Adjacent alternate sections were counterstained with cresyl violet or left unstained. Individual sections were examined for the presence of PHA-L immunoreactivity using both light- and dark-field microscopy.

RESULTS

In 2 of the 5 cases studied, discrete deposits of PHA-L were confined entirely within the caudal NTS. PHA-L immunoreactive perikarya were observed within subregions of the NTS (i.e. medial, ventral and dorsolateral subnuclei) that receive cardiovascular afferents in the cat (Kalia, '81). In two other animals the injection sites included not only the NTS, but slightly involved the dorsolateral edge of the dorsal motor nucleus of the vagus (see Fig. 1). In these 4 cases, PHA-L immunoreactive perikarya were not observed within the nucleus gracilis, hypoglossal nucleus, area postrema, or adjacent medullary reticular formation. In the forebrain of all 4 of these animals, PHA-L immunoreactive fibers appeared to enter the SFO by descending vertically through the SFO from the subependymal regions ventral to the fornix (Fig. 2A, C). Varicose PHA-L immunoreactive axonal fibers were observed in the subependymal region and the central core of the SFO (Fig. 2). PHA-L immunoreactive fibers were also found throughout all forebrain regions previously demonstrated to receive direct projections from the NTS (Ricardo and Koh, '78; Saper and Levisohn, '83). These regions included the paraventricular, dorsomedial, median preoptic, medial preoptic, and lateral hypothalamic nuclei as well as the lateral part of the bed nucleus of the stria terminalis and central amygdaloid nucleus. In one additional case in which the PHA-L deposit was limited to the hypoglossal nucleus, immunoreactive fibers were not observed within the SFO or in any other regions of the forebrain.

DISCUSSION

To our knowledge, the present study is the first to demonstrate direct efferent connections from the NTS to the SFO. In electron microscopy studies, dense core vesicles which may be catecholaminergic have been identified in synaptic contact with neuronal perikarya in the subependymal as well as the central region of the SFO (Dellman, '85). Therefore, it is tempting to speculate that catecholamine-containing neurons within the NTS could directly innervate the SFO. Further studies are necessary to identify the possible neurotransmitter(s) within the neurons that participate in the NTS-SFO pathway. Nevertheless, the NTS projection to the SFO may play an important role in the control of blood pressure and fluid balance by providing visceral afferent feedback to the SFO.

This direct neural projection from the NTS to the SFO has recently been confirmed electrophysiologically in the rat (Tanaka and Seto, '88). In this study, more than two-thirds of the neurons projecting to the SFO in the region of the NTS are were found to be responsive to baroreceptor activation, thus providing functional evidence that NTS-SFO projecting neurons may indeed be transmitting peripheral baroreceptor information.

Figure 1. Light-field photomicrograph illustrating the center of a Phaseolus vulgaris leucoagglutinin (PHA-L) injection site within the medial nucleus of the solitary tract (see arrow) in a rat. ts, solitary tract; cc, central canal, AP, area postrema; magnification =

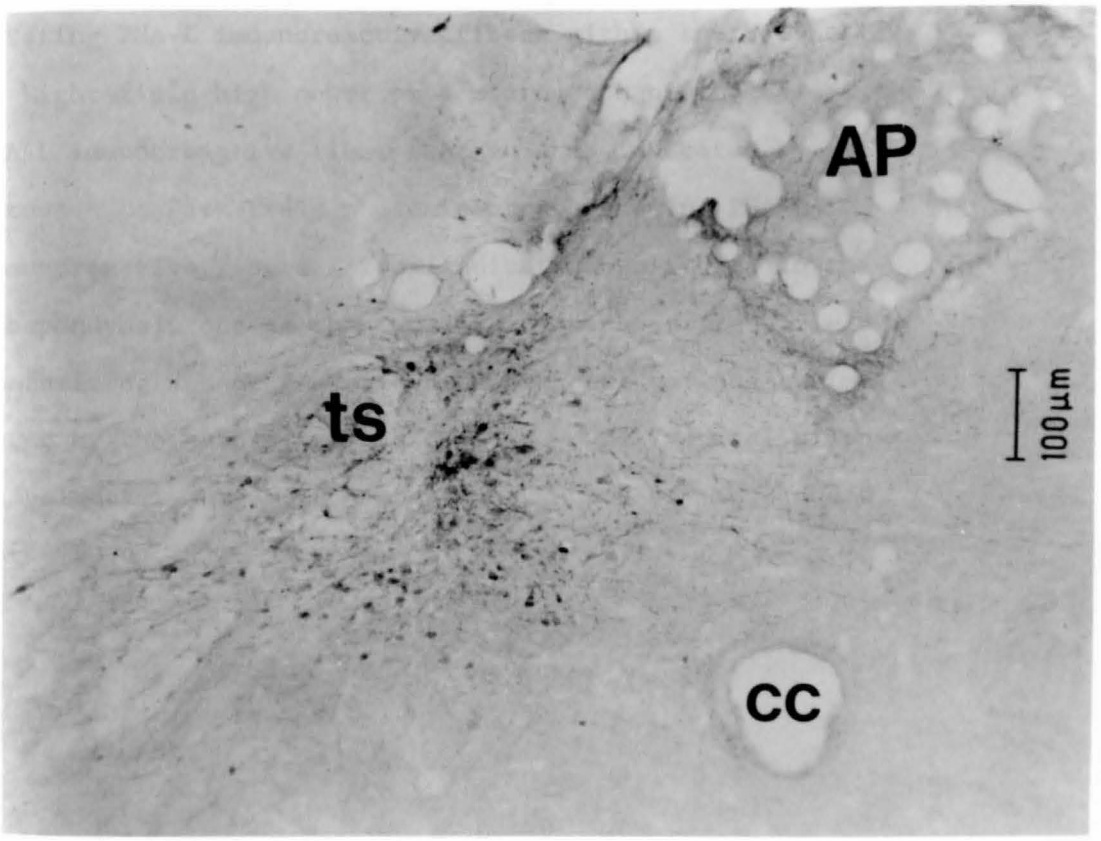
AP
ts
100µm
cc

Figure 2. A: Dark-field photomicrograph demonstrating PHA-L immunoreactive fibers within the SFO. B: Light-field high power photomicrograph of the same PHA-L immunoreactive fiber seen in A as indicated by the arrows. C: Dark-field photomicrograph showing PHA-L immunoreactive fibers (arrow indicates one fiber) in the subependymal zone of the SFO. D. High-power light-field photomicrograph of the same beaded axonal varicosity indicated by the arrows in both C and D. vhc, ventral hippocampal commissure. In A and C, bar = 100 um; in B and D, bar = 10 um.

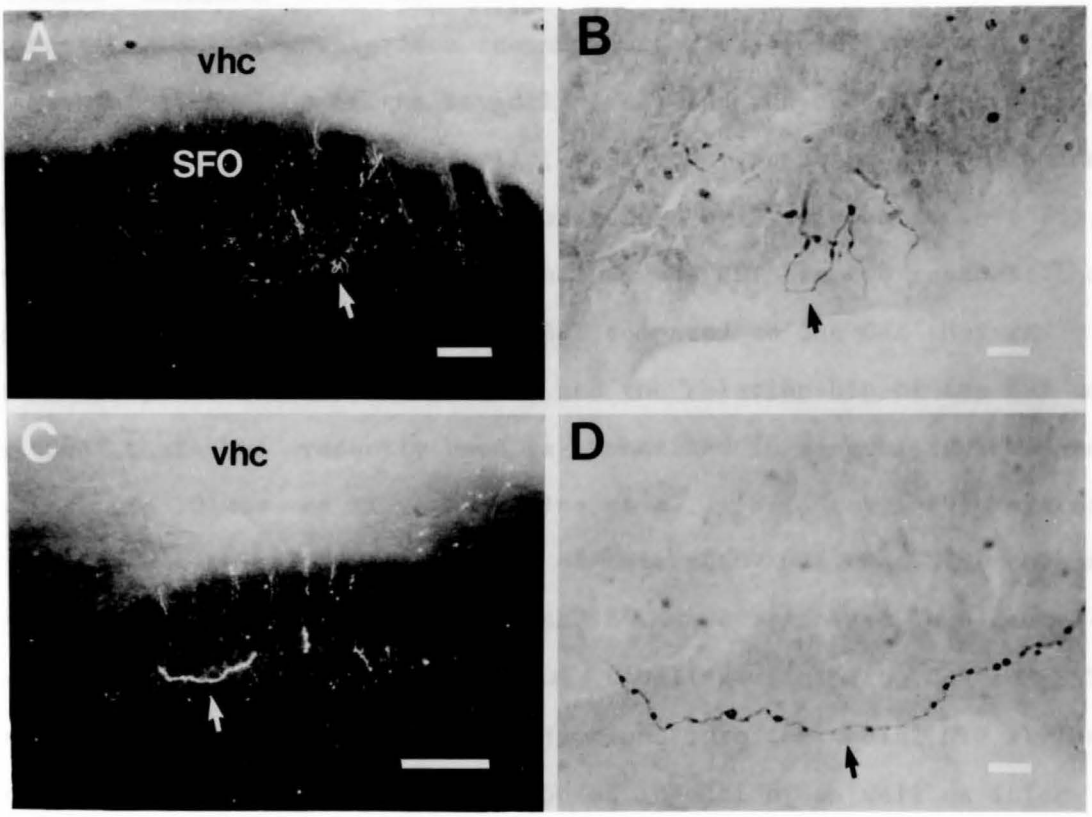
A
vhc
SFO
B
C
vhc
D

CHAPTER VIII

GENERAL DISCUSSION

Anatomical Organization of Brainstem Efferents to the CeA. The first study of this dissertation employed the anterograde tracer Phaseolus vulgaris leucoagglutinin (PHA-L) to examine in detail the termination of efferents from the nucleus of the solitary tract (NTS) to the central nucleus of the amygdala (CeA) and the bed nucleus of the stria terminalis (BST). Originally, this study proposed to re-examine only the NTS-CeA pathway first demonstrated by Ricardo and Koh ('78), but later it was expanded to include the BST for two reasons: the strikingly heavy innervation of the BST compared to the CeA that resulted from certain NTS injections, and the relationship of the BST to the CeA that has recently been re-emphasized in several reviews and studies (De Olmos et al., '85; Price et al., '87; Gray, '89; Moga et al., '89). A principal finding of this study was that NTS neurons giving rise to efferents to the CeA and BST were organized in a caudal-rostral, and medial-lateral fashion. Labeling within the CeA and BST was most dense following PHA-L injections into the medial NTS at the level of the area postrema. This type of injection, as well as injections of PHA-L into the commissural NTS, produced qualitatively more labeled fibers and terminals within the BST than the CeA. Rostral NTS injections, however, produced little labeling within the BST as compared to the CeA. The medially-located NTS subnuclei innervated the CeA and BST far more substantially than the ventral and laterally located-NTS subnuclei. The medial subnucleus of the NTS appeared to

innervate the CeA and BST more densely than the dorsal and dorsolateral NTS subnuclei. Also, NTS efferents terminated within the CeA and BST in a topographical pattern. The anterior lateral and ventral lateral subnuclei of the BST, and the medial and ventral subdivisions of the CeA, were the most heavily innervated. From a functional standpoint, these results implied:

a) both the BST and CeA may receive gastrointestinal and cardiovascular information conveyed through the medial NTS; the lateral NTS, which receives respiratory-related afferent information, has little input;

b) a rostro-caudal representation of sensory information within the NTS may be conserved in its efferents to the CeA and BST;

c) NTS efferents terminate within the CeA in areas shown anatomically (CeM) and electrophysiologically (CeV) to contribute to the reciprocal descending pathway to the NTS, thus providing an anatomical substrate whereby the CeA may directly modulate incoming sensory information;

d) NTS efferents terminate within the BST in its ventral portion, from which most hypothalamic efferents originate; thus, NTS input to the BST may be functionally related to modulation of hypothalamic function.

A study of the organization of efferents to the CeA from the parabrachial (PB) nucleus was not included in the present series of studies because of the previous definitive work of Fulwiler and Saper ('84). It would be of interest, in light of the present findings, (although admittingly difficult) to re-examine the termination of PB efferents within specific subdivisions of the CeA (and BST) and compare the topography (if any) with that of NTS efferents.

An anterograde study of the organization of efferents to the CeA

from the ventrolateral medulla (VLM) was not within the scope of the original dissertation proposal and, therefore, not comprehensively examined in the present series of experiments. The attempted PHA-L injections into the VLM were primarily aimed at confirming the results of the retrograde tracer injections into the CeA. However, the results of the one successful PHA-L injection within the VLM suggested a similar topography of termination within the CeA as NTS efferents, but clearly, more experiments of this nature will be required to definitively confirm this.

Neurochemical Organization of Brainstem Efferents to the CeA. Using the combined retrograde tracing-immunohistochemical technique, the neurochemical organization of the NTS-CeA, VLM-CeA, and PB-CeA pathways were examined (see summary diagram, Fig. 1). The CeA received a prominent catecholaminergic innervation from the medial NTS, which most likely was noradrenergic in nature. In contrast, the ascending efferent pathway from the VLM to the CeA originated in large part, from adenergic neurons (C1 catecholamine group). A high percentage of neuropeptide Y (NPY) CeA-projecting neurons were also found within the VLM, suggesting NPY to be co-localized within CeA-projecting catecholamine neurons. Within the NTS, NPY-immunoreactive neurons, as well as enkephalin (ENK)- and neurotensin (NT)-immunoreactive neurons, projected to the CeA. Similarly, ENK- and NT-immunoreactive neurons within the PB also innervated the CeA. In addition, calcitonin gene-related peptide (CGRP)-immunoreactive neurons within the PB were retrogradely-labeled. Somatostatin- and corticotropin releasing factor (CRF)-immunoreactive neurons were found to be distributed within subnuclei which did not have the CeA as a terminal field, and therefore, did not give rise to CeA efferents. As substance P- and bom-

besin-immunoreactive neurons were not demonstrated within the PB, a definitive conclusion as to their participation in the PB-CeA pathway could not be determined. Lastly, as most retrogradely-labeled cells within the PB were not immunoreactive for the peptides examined in this study, the neurochemical identity of the majority of CeA-projecting PB neurons remains to be determined.

Using Abercrombie's ('46) correction factor for double-counting errors, these studies estimated that there were 346 $\pm$ 45 retrogradely-labeled neurons within the ipsilateral NTS, 3892 $\pm$ 692 retrogradely-labeled cells within the ipsilateral PB, and 89 $\pm$ 18 retrogradely-labeled neurons within the ipsilateral VLM. Based on these numbers, it would appear that in the rat the efferent projection from the PB to the CeA is the major efferent pathway from the brainstem to the amygdala. As the NTS and VLM both project to the PB, which in turn projects to the CeA, the PB may act as the primary integrator of medullary and pontine afferent information that is relayed to the CeA. Also, although all three efferent pathways appear to be predominantly ipsilateral in nature, contralateral projections in each pathway were observed. Not surprisingly, the largest contribution to the contralateral brainstem efferent pathway to the amygdala also originated from the PB.

In addition, the results of these studies also demonstrated that ascending pathways from the NTS, VLM, and PB have unique neurochemical compositions which distinguish them from the reciprocal descending pathways from the CeA, as well as from each other (see Fig. 1). For example, ENK-immunoreactive cells in the CeA do not particpate in the descending pathway to the PB or NTS, but enkephalinergic neurons in the NTS and PB do project to the CeA. In contrast, CRF-immunoreactive cells within the CeA make a major contribution to the descending PB

pathway, but CRF-immunoreactivity is not contained in the ascending pathway to the CeA. The ascending pathways to the CeA are further uniquely characterized by the noradrenergic contribution from the NTS, the adrenergic contribution from the VLM, and the contribution of CGRP-immunoreactive neurons within the PB.

Role of visceral feedback in amygdaloid function. Like other limbic structures, the amygdala is involved in interpreting ongoing environmental conditions, and responds by inducing motivated behaviors that are linked to past experiences (memory). Alterations in ongoing behaviors involve changes in both somatic and visceral activity. Peripheral receptors convey the changing status of the viscera to the central nervous system via general visceral afferents. This sensory feedback is an integral feature of autonomic regulation (Cechetto, '87).

On a conscious level, sensory feedback to the amygdala may help define the seriousness of a threat, be it a physical threat, or, as it more commonly presents in humans, an emotional or mental stress. On an unconscious level, visceral feedback contributes to the formation of an emotional or "affective" significance to the threatening stimulus, i.e., a memory of the event, integrated with its visceral correlates ("how did it feel?") is formed.

Maintenance of the "milieu interieur" or the internal cellular environment (Bernard, 1878) is the primary aim of homeostatic mechanisms. The amygdala is one component of the hypothalamic-limbic system which participates in the regulation of homeostasis by receiving feedback directly from visceral receptors and by effecting changes within the internal environment via the autonomic nervous system, endocrine system, and the neural motivational system (Kupfermann, '81). In

contrast, thalamic and cortical mechanisims can be utilized to effect changes in the external environment, that is, a conscious motor activity. The role the CeA may play in the neuroendocrine and autonomic regulation of homeostasis, or the control of homeostasis by behavioral mechanisims, is still largely a matter of speculation. Presumably, neuronal transmission through the action of a neurotransmitter, perhaps in concert with a neuromodulator, mediate the mechanisims through which this is accomplished.

Directions for Future Experiments. The innervation of the BST by the NTS and PB would be an intriguing area to explore anatomically, neurochemically, and physiologically in the future. Further anterograde tracing studies are needed to confirm definitively the paucity of innervation by the rostral NTS. It would be interesting to study the peptidergic and catecholaminergic innervation of the BST by the NTS, VLM and PB, and compare it to the innervation received by the CeA from these same areas. As few studies have specifically focused on the role of the BST in autonomic function, physiological and behavioral studies of the BST similar to those already performed for the CeA would provide an interesting base of comparison for BST and CeA function.

Impairments in feedback circuits have been hypothesized to occur in several pathopysiological conditions such as hypertension, gastric ulcers, and schizophrenia (see Chapter 3 for discussion). Additionally, studies have implicated the CeA and some of the catecholamines/peptides examined in the present study in many of the same processes. The extent to which feedback to the CeA influences the development or maintenance of such states, and the specific neurochemicals that may be involved, is another direction for future research.

Past investigators have attempted to define and explain the

elusive concept of "emotion" by specific neural circuitries (Papez, '37; Panskepp, '84; Smith and De Vito, '84). In this context, the central nucleus may integrate autonomic sensory feedback (an emotionally significant correlate) with cognitive events, thus adding an emotional "color" onto already processed sensory information (Sarter and Markowitsch, '85). Perhaps in this regard, studies of the central nucleus will come to have its most relevance in man, as there are obvious, socially compelling reasons for understanding the basis of human aggression, fear, anxiety, loneliness, and most of all, hate and love.

Figure 1. Summary diagram of ascending and descending neuropeptide/neurotransmitter pathways between the CeA and the nucleus of the solitary tract, the ventrolateral medulla, and the parabrachial nucleus. For the sake of clarity, only ipsilateral pathways are indicated; contralateral ascending and descending pathways are present but minor in comparison to the ipsilateral component. Data on ascending pathways is derived from Chapters 4, 5 and 6 in this dissertation; data on ascending pathways is derived from Gray, '89. See text for further discussion.

CENTRAL NUCLEUS NEUROPEPTIDE/NEUROTRANSMITTER CONNECTIONS

DESCENDING PATHWAYS

CeA → NTS	CRF
	NT
	SS
	SUB P
CeA → PB	CRF
	NT
	SUB P
	SS
	GAL

ASCENDING PATHWAYS

NTS → CeA	ENK
	NT
	NPY
	TH
	PNMT
PB → CeA	CGRP
	ENK
	NT
VLM → CeA	TH
	PNMT
	NPY

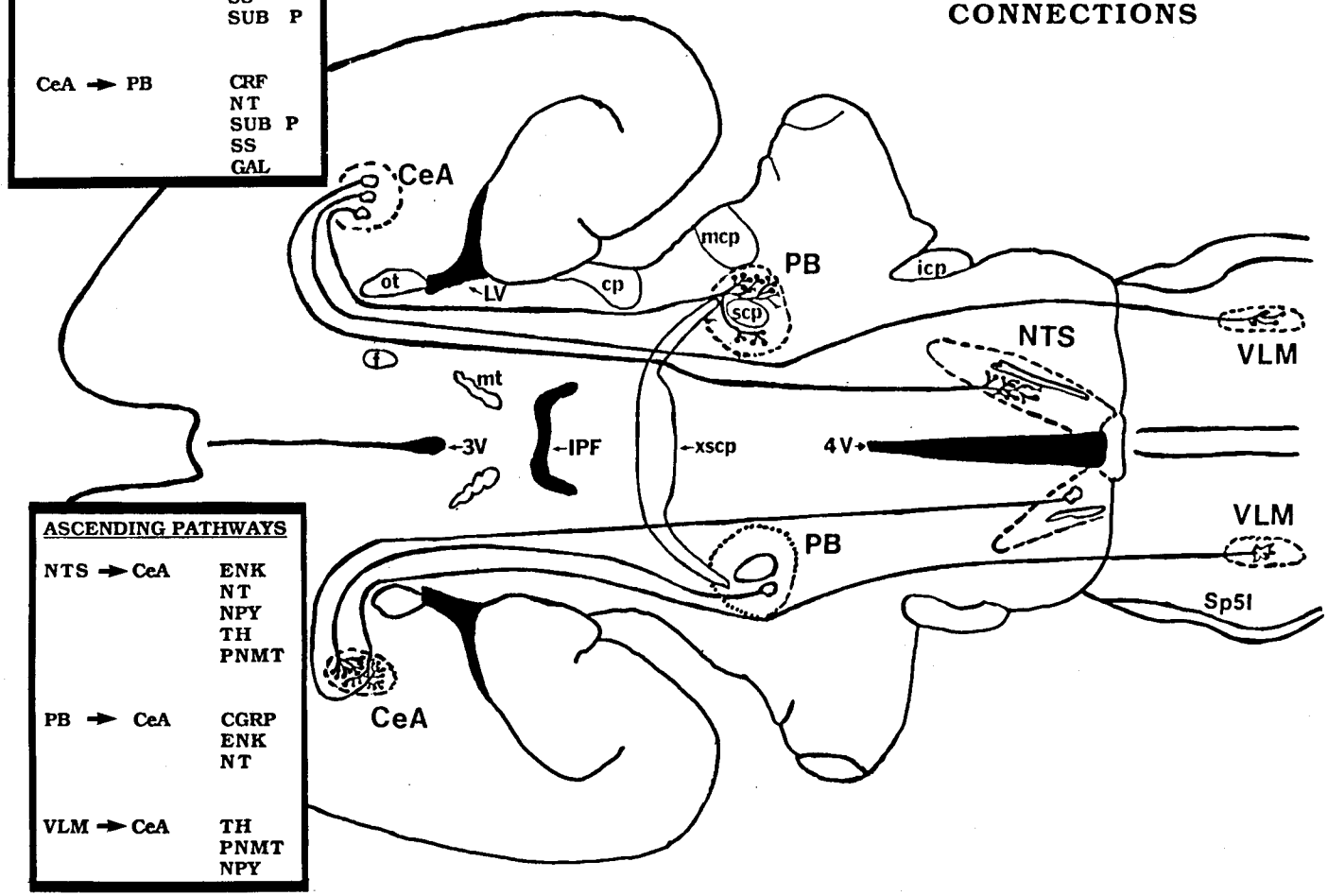

LITERATURE CITED

Abercrombie, M. (1946) Estimation of nuclear population from microtome sections. Anat Rec 94: 239-247.

Abrahams, V.C., S.M. Hilton, and A. Zbrozyna (1960) Active muscle vasodilatation produced by stimulation of the brain stem: Its significance in the defence reaction. J Physiol (Lond) 154: 491-513.

Aggleton, J.P. (1985) A description of intra-amygdaloid connections in old world monkeys. Exp Brain Res 57: 390-399.

Aggleton, J.P., M.J. Burton, and R.E. Passingham (1980) Cortical and subcortical afferents to the amygdala of the rhesus monkey (Macaca mulatta). Brain Res 190: 347-368.

Aggleton, J.P., and M. Mishkin (1984) Projections of the amygdala to the thalamus in the cynomolgus monkey. J Comp Neurol 222: 56-68.

Akil, H., S.J. Watson, E. Young, M.E. Lewis, H. Khachaturian, and J.M. Walker (1984) Endogenous opioids: biology and function. Ann Rev Neurosci 7: 223-255.

Allen, J.P., and C.F. Allen (1975) Amygdalar participation in tonic ACTH secretion in the rat. Neuroendocrinology 19: 115-125.

Altman, J., and S.A. Bayer (1980) Development of the brain stem in the rat. 1. Thymidine-radiographic study of the time of origin of neurons of the lower medulla. J Comp Neurol 194: 1-35.

Altshuler, S.M., X. Bao, D. Bieger, D.A. Hopkins, and R.R. Miselis (1989) Viscerotopic representation of the upper alimentary tract in the rat: sensory ganglia and nuclei of the solitary and spinal trigeminal tracts. J Comp Neurol 283: 248-268.

Amaral, D.G. (1987) Memory: anatomical organization of candidate brain regions. In V.B. Mountcastle, F. Plum, and S.R. Geiger (eds): Handbook of Physiology. Section 1: The Nervous System. Bethesda: American Physiological Society, pp. 211-294.

Amaral, D.G., R.B. Veazey, and W.M. Cowan (1982) Some observations on hypothalamic-amygdaloid connections in the monkey. Brain Res 252: 13-27.

Amir, S., and Z. Amit (1980) The role of endorphins in stress: Evidence and speculations. Neurosci Biobehav 4: 77-86.

Applegate, C.D., B.S. Kapp, M.D. Underwood, and C.L. McNall (1983) Autonomic and somatomotor effect of amygdala central nucleus stimulation in awake rabbits. Physiol Behav 31: 353-360.

Armstrong, D.M., V.M. Pickel, T.H. Joh, D.J. Reis, and R.J. Miller (1981) Immunocytochemical localization of catecholamine synthesizing enzymes and neuropeptides in area postrema and medial nucleus tractus solitarius of rat brain. J Comp Neurol 196: 505-517.

Azuma, S., T. Yamamoto, and Y. Kawamura (1984) Gustatory responses of amygdaloid neurons in rats. Exp Brain Res 56: 12-22.

Azuma, S., T. Yamanato, and Y. Kawamura (1984) Studies on gustatory responses of amygdaloid neurons in rats. Exp Brain Res 56: 12-22.

Bailey, P., and F. Bremer (1938) A sensory cortical representation of the vagus nerve. J Neurophysiol 1: 405-412.

Bayer, S.A. (1980) Quantitative 3-thymidine radiographic analyses of neurogenesis in the rat amygdala. J Comp Neurol 194: 845-875.

Beaulieu, S., T. DiPaolo, and N. Barden (1986) Control of ACTH secretion by the central nucleus of the amygdala: implication of the serotonergic system and its relevance to the glucocorticoid delayed

negative feedback mechanism. Neuroendocrinology 44: 247-254.

Beitz, A.J. (1982) The organization of afferent projections to the midbrain periaqueductal gray of the rat. Neuroscience 7: 133-159.

Benarroch, E.E., A.R. Granata, D.A. Ruggiero, D.H. Park, and D.J. Reis (1986) Neurons of C1 area mediate cardiovascular responses initiated from ventral medullary surface. Am J Physiol (Regulatory Integrative Comp Physiol) 250: R932-R945.

Berk, M.L., and J.A. Finkelstein (1981) Afferent projections to the preoptic area and hyothalamic regions in the rat brain. Neurosci 6: 1601-1624.

Bernard, C. (1878) Lecons sur les phenomenes de la vie communs aux animaux et aux vegetaux. Paris: Bailliere.

Berod, A., B.K. Hartman, and J.F. Pujol (1981) Importance of fixation in immunohistochemistry: use of formaldehyde at variable pH for the localization of tyrosine hydroxylase. J Histochem Cytochem 29: 844-850.

Blanchard, D.C., and R.J. Blanchard (1972) Innate and conditioned reactions to threat in rats with amygdaloid lesions. J Comp Physiol Psychol 81: 281-290.

Block, C.H., G. Hoffman, and B.S. Kapp (1989) Peptide-containing pathways from the parabrachial complex to the central nucleus of the amygdala. Peptides 10: in press.

Block, C.H., and G.E. Hoffman (1987) Neuropeptide and monoamine components of the parabrachial pontine complex. Peptides 8: 267-283.

Block, C.H., and J.S. Schwartzbaum (1983) Ascending efferent projections of the gustatory parabrachial nucleus in the rat. Brain Res 259: 1-9.

Bloom, D.M., N.P.V. Nair, and G. Schwartz (1983) CCK-8 in the treatment of chronic schizophrenia. Psychopharmacol Bull 19: 361-364.

Bodner, R.J., M. Glusman, M. Brutus, A. Spaggia, and D.D. Kelly (1979) Analgesia induced by cold-water stress: attenuation by hypophysectomy. Physiol Behav 23: 53-62.

Box, B.M., and G.J. Mogenson (1975) Alterations in ingestive behaviors after bilateral lesions of the amygdala in the rat. Physiol Behav 15: 679-688.

Brodal, A. (1947) The amygdaloid nucleus in the rat. J Comp Neurol 87: 1-16.

Brown, A.M. (1981) What the baroreceptors tell the brain in hypertension. In J.P. Buckley and C.M. Ferrario (eds): Central Nervous System Mechanisms in Hypertension. New York: Raven Press, pp. 1-7.

Brown, M., and L. Fischer (1986) Regulation of the autonomic nervous sytem by peptides. In A. Negro-Vilar and P.M. Conn (eds): Peptide Hormones: Effects and Mechanisims of Action. Boca Raton: CRC Press, pp. 343-367.

Brown, M.R., and L.A. Fischer (1985) Corticotropin-releasing factor: effects on the autonomic nervous system and visceral systems. Fed Proc 44: 243-248.

Brown, M.R., and T.S. Gray (1988) Peptide injections into the amygdala of conscious rats: effects on blood pressure, heart rate and plasma catecholamines. Regul Peptides 21: 95-106.

Brown, M.R., T.S. Gray, and L.A. Fischer (1986) Corticotropin-releasing factor receptor antagonist: effects on the autonomic nervous system and cardiovascular function. Regul Peptides 16: 321-329.

Bunney, B.S., and G.K. Aghajanian (1976) The precise localization of nigral afferents in the rat as detrmined by a retrograde tracing technique. Brain Res 192: 423-435.

Calaresu, F.R., J. Ciriello, M.M. Caverson, D.F. Cechetto, and T.L. Krukoff (1984) Functional neuroanatomy of central pathways controlling the circulation. In G.P. Guthrie and T.A. Kotchen (eds): Hypertension and the Brain. Mt. Kisco: Futura Pub. Co., pp. 3-21.

Carey, R.M. (1984) Experimental neurogenic hypertension. In G.P. Guthrie and T.A. Kotchen (eds): Hypertension and the Brain. Mt. Kisco: Futura Pub. Co., pp. 281-303.

Cassell, M.D., and T.S. Gray (1989a) Morphology of peptide-immunoreactive neurons in the rat central nucleus of the amygdala. J Comp Neurol : In Press.

Cassell, M.D., and T.S. Gray (1989b) The amygdala directly innervates adrenergic (C1) neurons in the ventrolateral medulla in the rat. Neurosci Lett 97: 163-168.

Cassell, M.D., T.S. Gray, and J.K. Kiss (1986) Neuronal architecture in the rat central nucleus of the amygdala: a cytological, hodological, and immunocytochemical study. J Comp Neurol 246: 478-499.

Cassell, M.D., N.J. Mankovich, T.S. Gray, and T.H. Williams (1982) Computer-assisted image analysis of the distribution of peptidergic terminals in the central nucleus of the amygdala: a preliminary study. Peptides 3: 283-290.

Cassell, M.D., and D.J. Wright (1986) Topography of projections from the medial prefrontal cortex to the amygdala in the rat. Brain Res Bull 17: 321-333.

Caverson, M.M., and J. Ciriello (1984) Electrophysiological identification of neurons in ventrolateral medulla sending collateral axons to paraventricular and supraoptic nuclei in the cat. Brain Res 305: 375-379.

Cechetto, D.F. (1987) Central representation of visceral function. Fed Proc 46: 17-23.

Cechetto, D.F., and F.R. Calaresu (1985) Central pathways relaying cardiovascular afferent information to amygdala. Am J Physiol (Reglatory Integrative Comp Physiol) 248: R38-R45.

Cechetto, D.F., J. Ciriello, and F.R. Calaresu (1983) Afferent connections to cardiovascular sites in the amygdala: a horseradish peroxidase study in the cat. J Auton Nerv Syst 8: 97-110.

Chalmers, J.P. (1975) Brain amines and models of experimental hypertension. Circ Res 36: 469-480.

Chiba, T., and N. Doba (1975) The synaptic structure of catecholaminergic axon varicosities in the dorso-medial portion of the nucleus tractus soliarius of the cat: possible roles in the regulation of cardiovascular reflexes. Brain Res 84: 31-46.

Chronwall, B.M., D.A. DiMaggio, V.J. Massari, V.M. Pickel, D.A. Ruggiero, and T.L. O'Donohue (1985) The anatomy of neuropeptide Y-containing neurons in rat brain. Neuroscience 15: 1159-1181.

Ciriello, J., and M.M. Caverson (1984) Ventrolateral medullary neurons relay cardiovascular inputs to the paraventricular nucleus. Am J Physiol (Regulatory Integrative Comp Physiol) 246: R968-R978.

Ciriello, J., M.M. Caverson, and C. Polosa (1986) Function of the ventrolateral medulla in the control of the circulation. Brain Res Rev 11: 359-391.

Ciriello, J., C.V. Rohlicek, and C. Polosa (1983) Aortic baroreceptor reflex pathway: a functional mapping using [3-H]2-deoxyglucose autoradiography in the rat. J Auton Nerv Syst 8: 111-128.

Code, R.A., and J.H. Fallon (1986) Some projections of dynorphin-immunoreactive neurons in the rat central nervous system. Neuropeptides 8: 165-172.

Cohen, D.H. (1975) Involvement of the avian amygdalar homologue (archistriatum posterior and mediale) in defensively conditioned heart rate change. J Comp Neurol 160: 13-36.

Conrad, L.C.A., and D.W. Pfaff (1977) Efferents from the medial basal forebrain and hypothalamus in the rat. J Comp Neurol 169: 185-220.

Cox, G.E., D. Jorden, P. Moruzzi, J.S. Schwaber, K.M. Spyer, and S.A. Turner (1986) Amygdaloid influences on the brain-stem neurones in the rabbit. J Physiol 381: 135-148.

Cox, G.E., D. Jorden, F.R. Paton, K.M. Spyer, and L.M. Wood (1987) Cardiovascular and phrenic nerve responses to stimulation of the amygdala central nucleus in the anaesthetized rabbit. J Physiol 389: 541-556.

Cummings, S., R. Elde, J. Ellis, and A. Lindvall (1983) Corticotropin-releasing factor immunoreactivity is widely distributed within the central nervous system of the rat: an immunohistochemical study. J Neurosci 3: 1355-1368.

Cunningham, E.T., and P.E. Sawchenko (1988) Anatomical specificity of noradrenergic imputs to the paraventricular and supraoptic nuclei of the rat hypothalamus. J Comp Neurol 274: 60-76.

Dahlstrom, A., and K. Fuxe (1964) Evidence for the existence of monoamine-containing neurons in the central nervous system I. Demonstration of monoamines in the cell bodies of brain stem neurons. Acta Physiol Scand 62: S.262 1-55.

Dampney, R.A.L., A.K. Goodchild, L.G. Robertson, and W. Montgomery (1982) Role of ventrolateral medulla in vasomotor regulation: a correlative anatomical and physiological study. Brain Res 249: 223-235.

Danielsen, E.H., D.J. Magnuson, and T.S. Gray (1989) The central amygdaloid nucleus innervation of the dorsal vagal complex in the rat: a Phaseolus vulgaris leucoagglutinin lectin anterograde tracing study. J Comp Neurol : In press.

Davies, R.O., and M. Kalia (1981) Carotid sinus nerve projections to the brain stem in the cat. Brain Res Bull 6: 531-541.

Davis, M., J.M. Hitchcock, and J.B. Rosen (1984) Anxiety and the amygdala: Pharmacological and anatomical analysis of the fear-potentiated startle paradigm. In G.H. Bower (ed): The Psychology of Learning Motivation: Advances in Research and Theory. Orlando: Academic Press, pp. 1-67.

De Jong, W., P. Zandberg, and B. Bohus (1975) Central inhibitory noradrenergic cardiovascular control. Prog Brain Res 42: 285- 298.

Deacon, T.W., H. Eichenbaum, P. Rosenberg, and K.W. Eckmann (1983) Afferent connections of the perirhinal cortex in the rat. J Comp Neurol 220: 68-190.

Dell, P., and R. Olson (1981) Projections thalamiques, corticales et cerbelleuses ses afferences viscerales vagales. C R Soc Biol (Paris) 145: 1084-1088.

Dellman, H.-.D. (1985) Fine structural organization of the subfornical organ. A concise review. Brain Res Bull 15: 71-78.

Denavit-Saubie, M., J. Champagnat, and W. Zieglgansberger (1978) Effects of opiates and methionine-enkephalin on pontine and bulbar respiratory neurones of the cat. Brain Res 155: 55-67.

DeOlmos, J., G.F. Alheid, and C.A. Beltramino (1985) Amygdala. In G. Paxinos (ed): The Rat Nervous System: Forebrain and Midbrain. Orlando: Academic Press, pp. 223-334.

DeOlmos, J.S. (1972a) The amygdaloid projection field in the rat as studied with the cupric-silver method. In B.F. Eleftheriou (ed): The Neurobiology of the Amygdala. New York: Plenum Press, pp. 145-204.

DeOlmos, J.S. (1972b) The amygdaloid projection field in the rat as studied with the cupric-silver method. In B.F. Eleftheriou (ed): The Neurobiology of the Amygdala. New York: Plenum Press, pp. 145-204.

DeOlmos, J.S., and H. Carrer (1978) A horseradish peroxidase study of the afferent connections of the medial basal hypothalamus in the rat. Anat Rec 190: 380.

Dietl, H. (1985) Temporal relationship between noradrenaline release in the central amygdala and plasma noradrenaline secretions in rats and tree shrews. Neurosci Lett 55: 41-46.

Doba, N., and D.J. Reis (1973) Acute fulminating neurogenic hypertension produced by brainstem lesions in the rat. Circ Res 23: 584-593.

Domesick, V.B. (1976) Projections of the nucleus of the diagonal band of Broca in rat. Anat Rec 184: 391-392.

Eiden, L.E., T. Hokfelt, M.J. Brownstein, and M. Palkovits (1985) Vasoactive intestinal polypeptide afferents to the bed nucleus of the stria terminalis in the rat: an immunohistochemical and biochemical

study. Neuroscience 15: 999-1013.

Ellis, M.E. (1984) Manipulation of the amygdala noradrenergic system impairs extinction of passive avoidance. Brain Res 324: 129-133.

Everitt, B.J., T. Hokfelt, L. Terenius, K. Tatemoto, V. Mutt, and M. Goldstein (1984) Differential co-existence of neuropeptide Y (NPY)-like immunoreactivity with catecholamines in the central nervous system of the rat. Neuroscience 11: 443-462.

Faiers, A.A., F.R. Calaresu, and G.J. Mogenson (1975) Pathway mediating hypotension elicited by stimulation of the amygdala in the rat. Am J Physiol (Regulatory Integrative Comp Physiol) 228: R1358-R1366.

Faiers, A.A., F.R. Calaresu, and G.J. Mogenson (1976) Factors affecting cardiovascular responses to stimulation of the hypothalamus in the rat. Exp Neurol 51: 188-206.

Fallon, J. (1981) Histochemical characterization of dopaminergic, noradrenergic, and serotonergic projections to the amygdala. In Y. Ben-Ari (ed): The Amygdaloid Complex. Amsterdam: Elsevier/North Holland, pp. 175-183.

Fallon, J.H., R. Hicks, and S.E. Loughlin (1983) The origin of cholecystokinin terminals in the basal forebrain of the rat: evidence from immunofluorescence and retrograde tracing. Neurosci Lett 37: 29-35.

Fallon, J.H., D.A. Koziell, and R.Y. Moore (1978) Catecholamine innervation of the basal forebrain. II. Amygdala, suprarhinal cortex and entorhinal cortex. J Comp Neurol 180: 509-532.

Fallon, J.H., and F.M. Leslie (1986) Distribution of dynorphin and enkephalin peptides in the rat brain. J Comp Neurol 249: 293-336.

Farsang, C., M.D. Ramirez-Gonzalez, L. Mucci, and G. Kunos (1980) Possible role of an endogenous opiate in the cardiovascular effects of central alpha adrenoreceptor stimulation in spontaneously hypertensive rats. J Pharmocol Exp Ther 214: 203-208.

Ferrier, I.N., G.W. Roberts, T.J. Crow, E.C. Johnstone, D.G.C. Owens, Y. C. Lee, D. O'Shaughnessy, and T.E. Adrian (1983) Reduced cholecystokinin-like and somatostatin-like immunoreactivity in limbic lobe is associated with negative symptoms in schizophrenia. Life Sci 33: 475-482.

Feuerstein, G., C.J. Molineaux, J.G. Rosenberger, A.I. Faden, and B.M. Cox (1983) Dynorphins and leu-enkephalin in brain nuclei and pituitary of WKY and SHR rats. Peptides 4: 225-229.

Finley, J.C., J.L. Maderdrut, L.J. Roger, and P. Petrusz (1981) The immunocytochemical localization of somatostatin-containing neurons of the rat central nervous system. Neuroscience 6: 2173-2192.

Folkow, B. (1982) Physiological aspects of primary hypertension. Physiol Rev 62: 347-504.

Folkow, B., J. Hallback-Nordlander, J. Martner, and C. Nordberg (1982) Influence of amygdala lesions on cardiovascular responses to alerting stimuli, on behavior and on blood pressure development in spontaneous hypertensive rats. Acta Physiol Scand 116: 133-139.

Fonberg, E. (1981) Specific versus unspecific functions of the amygdala. In Y. Ben-Ari (ed): The Amygdaloid Complex. Amsterdam: Elsevier/North Holland Biomedical, pp. 281-291.

Fox, C.A. (1940) Certain basal telencephalic centers in the cat. J Comp Neurol 72: 1-62.

Frysinger, R.C., J.D. Marks, R.B. Trelease, V.L. Schechtman, and R.M. Harper (1984) Sleep states attenuate the pressor response to central amygdala stimulation. Exp Neurol 83: 604-617.

Fuji, K., E. Senba, Y. Ueda, and M. Tohyama (1983) Vasoactive intestinal polypeptide (VIP)-containing neurons in the spinal cord of the rat and their projections. Neurosci Lett 37: 51-55.

Fulwiler, C.F., and C.B. Saper (1984) Subnuclear organization of the efferent connections of the parabrachial nucleus in the rat. Brain Res Rev 7: 229-259.

Fuxe, K., L.F. Agnati, A. Harfstrand, I. Zini, K. Tatemoto, E.M. Pich, T. Hokfelt, and L. Terenius (1983) Central administration of neuropeptide Y induces hypotension bradypnea and EEG synchronization in the rat. Acta Physiol Scand 118: 189-192.

Galeno, T.M., and M.J. Brody (1983) Hemodynamic responses to amygdaloid stimulation in spontaneously hypertensive rats. Am J Physiol (Regulatory Integrative Comp Physiol) 245: R281-R286.

Galeno, T.M., G.W. Van Hoesen, W. Maixner, A.K. Johnson, and M.J. Brody (1982) Contribution of the amygdala to the development of spontaneous hypertension. Brain Res 246: 1-6.

Galeno, T.M., G.W. VanHosen, and M.J. Brody (1984) Central amygdaloid nucleus lesion attenuates exaggerated hemodynamic responses to noise stress in the spontaneously hypertensive rat. Brain Res 291: 249-259.

Gallagher, M., B.S. Kapp, R.C. Frysinger, and P.R. Rapp (1980) B-adrenergic manipulation in amygdala central n. alters rabbit heart rate conditioning. Pharmac Biochem Behav 12: 419-426.

Gelsema, A.J., D.J. McKitrick, and F.R. Calaresu (1987) Cardiovascular responses to chemical and electrical stimulation of amygdala in rats. Am J Physiol (Regulatory Integrative Comp Physiol) 253: R712-R718.

Gerfen, C.R., and P.E. Sawchenko (1984) An anterograde neuroanatomical tracing method that shows the detailed morphology of neurons, their axons and terminals: immunohistochemical localization of an axonally transported plant lectin, Phaseolus vulgaris leucoagglutinin (PHA-L). Brain Res 290: 219-238.

Gloor, P. (1972) Inputs and outputs of the amygdala: what the amygdala is trying to tell the rest of the brain. In B.F. Eleftheriou (ed): The Neurobiology of the Amygdala. New York: Plenum Press, pp. 189-209.

Gloor, P. (1975) Electrophysiological studies of the amygdala (stimulation and recording): their possible contributions to the understanding of neural mechanisms of aggression. In W.S. Fields and W.H. Sweet (eds): Neural Basis of Violence and Aggression. St. Louis: Warren H. Green Inc, pp. 5-38.

Granata, A.R., D.A. Ruggiero, D.H. Park, T.H. Joh, and D.J. Reis (1983) Lesions of epinephrine neurons in the rostral ventrolateral medulla abolish the vasodepressor components of baroreflex and cardiopulmonary reflex. Hypertension 5: V80- V84.

Granata, A.R., D.A. Ruggiero, D.H. Park, T.H. Joh, and D.J. Reis (1985) Brain stem area with C1 epinephrine neurons mediates baroreflex vasodepressor responses. Amer J of Physiol 248: H547-H567.

Gray, T.S. (1989) Autonomic neuropeptide connections of the amygdala. In Y. Tache, J.E. Morley, and M.R. Brown (eds): Neuropeptides and Stress. New York: Springer-Verlag, pp. 92-106.

Gray, T.S., M.E. Carney, and D.J. Magnuson (1989) Direct projections from the central amygdalaoid nucleus to the hypothalamic paraventricular nucleus: possible role in stress induced adrenocorticotropin release. Neuroendocrinology : In Press.

Gray, T.S., M.D. Cassell, and Z. Kiss (1984) Distribution of pro-opiomelanocortin-derived peptides and enkephalins in the rat central nucleus of the amygdala. Brain Res 306: 354-358.

Gray, T.S., M.D. Cassell, T.H. Williams, G. Nilaver, and E. Zimmerman (1984) The distribution and ultrastructure of VIP-immunoreactivity in the central nucleus of the rat amygdala. Neuroscience 11: 399-408.

Gray, T.S., and D.J. Magnuson (1987a) Neuropeptide neuronal efferents from the the bed nucleus of the stria terminalis and central amygdaloid nucleus to the dorsal vagal complex in the rat. J Comp Neurol 262: 365-374.

Gray, T.S., and D.J. Magnuson (1987b) Galanin-like immunoreactivity within amygdaloid and hypothalamic neurons that project to the midbrain central gray in rat. Neurosci Let 83: 264-268.

Gray, T.S., and J.E. Morley (1986) Neuropeptide Y: Anatomical distribution and possible function in mammalian nervous system. Life Sci 38: 389-401.

Gray, T.S., T.L. O'Donohue, and D.J. Magnuson (1986) Neuropeptide Y innervation of amygdaloid and hypothalamic neurons that project to the dorsal vagal complex in the rat. Peptides 7: 341-349.

Grijalva, C.V., Y. Tache, M.W. Gunion, J.H. Walsh, and P. Gieselman (1986) Amygdaloid lesions attenuate neurogenic gastric mucosal erosions do not alter gastric secretory changes induced by intracisternal bombesin. Brain Res Bull 5: 55-61.

Grossman, S.P., L. Grossman, and L. Walsh (1975) Functional organization of the rat amygdala with respect to avoidance behavior. J Comp Physiol Psychol 88: 829-850.

Grove, E.A. (1988) Neural associations of the substantia innominata in the rat: afferent connections. J Comp Neurol 277: 315-346.

Grove, E.A., and W.J.H. Nauta (1984) Light microscopic evidence for striatal and amygdaloid input to cholinergic cell group CH4 in the rat. Soc Neurosci Abstr 10: 7.

Gurdjian, E.S. (1928) The corpus striatum of the rat. J Comp Neurol 45: 249-281.

Hall, E. (1972) Some aspects on the structural organization of the amygdala. In B.F. Elefteriou (ed): The Neurobiology of the Amygdala. New York: Plenum Press, pp. 95-120.

Hallback, M., and B. Folkow (1974) Cardiovascular responses to acute mental "stress" in spontaneously hypertensive rats. Acta Physiol Scand 90: 684-698.

Hamilton, R.B., H. Ellenberger, D. Liskowsky, and N. Schneiderman (1981) Parabrachial area as mediator of bradycardia in rabbits. J Auton Nerv Syst 4: 261-281.

Hamilton, R.B., and R. Norgren (1984) Central projections of gustatory nerves in the rat. J Comp Neurol 222: 560-577.

Hammond, D.L., and H.K. Proudfit (1980) Effects of locus coeruleus lesions on morphine-induced antinociception. Brain Res 188: 79-91.

Harfstrand, A., K. Fuxe, L. Terenius, and M. Kalia (1987) Neuropeptide Y-immunoreactive perikarya and nerve terminals in the rat medulla oblongata: Relationship to cytoarchitecture and catecholaminergic cell groups. J Comp Neurol 260: 20-35.

Harper, R.M., R.C. Frysinger, R.B. Trelease, and J.D. Marks (1984) State-dependant alteration of respiratory cycle timing by stimulation of the central nucleus of the amygdala. Brain Res 306: 1-8.

Hassen, A.H., G. Feuerstein, A. Pfeiffer, and A.J. Faden (1982) Delta versus mu receptors: cardiovascular and respiratory effects of opiate agonists microinjected into nucleus tractus solitarius of cats. Regul Peptides 4: 299-310.

Hayes, R.L., G.J. Bennet, P.G. Newlon, and D.J. Mayer (1978) Behavioral and physiological studies of non-narcotic analgesia in the rat elicited by certain environmental stimuli. Brain Res 155: 69-90.

Heimer, L., G.F. Alheid, and L. Zaborszky (1985) Basal ganglia. In G. Paxinos (ed): The Rat Nervous System: Forebrain and Midbrain. Orlando: Academic Press, pp. 37-86.

Henke, P.G. (1980a) The centromedial amygdala and gastric pathology in rats. Physiol Behav 25: 107-112.

Henke, P.G. (1980b) Facilitation and inhibition of gastric pathology after lesions in the amygdala of rats. Physiol Behav 25: 575-579.

Henke, P.G. (1982) The telencephalic limbic system and experimental gastric pathology: a review. Neurosci Behav Rev 6: 381-390.

Henke, P.G. (1984) The bed nucleus of the stria terminalis and immobilization-stress: unit actictivity, escape behavior, and gastric pathology in rats. Behav Brain Res 11: 35-45.

Henke, P.G. (1985) The amygdala and forced immobilization of rats. Behav Brain Res 16: 19-24.

Henke, P.J. (1983) Unit-activity in the central amygdalar nucleus of rats in response to immobilization-stress. Brain Res Bull 10: 833-837.

Henke, P.J. (1988) Recent studies of the central nucleus of the amygdala and stress ulcers. Neurosci Biobehav Rev 12: 143-150.

Herbert, H., M.M. Moga, and C.B. Saper (1989) Connections of the parabrachial nucleus with the nucleus of the solitary tract and the medullary reticular formation in the rat. J Comp Neurol : Submitted.

Herkenham, M. (1978) The connections of the nucleus reuniens thalami: evidence for a direct thalamo-hippocampal pathway in the rat. J Comp Neurol 177: 589-610.

Hernesniemi, J., E. Kawana, E. Bruppacher, and C. Sandri (1972) Afferent connections of the subfornical organ and of the supraoptic crest. Acta Anat (Basel) 82: 321-336.

Herrick, C.J. (1921) The connections of the vomeronasal nerve, accessory olfactory bulb and amygdala in amphibia. J Comp Neurol 33: 213-279.

Herrick, C.J. (1922) Functional factors in the morphology of the forebrain of fishes. Libro en Honor de D. Santiago Ramon Y Cajal 1: 143-204.

Herrick, C.J. (1933) The morphology of the forebrain in amphibia and reptilia. J Comp Neurol 20: 413-546.

Hewitt, W. (1958) The development of the human caudate and amygdala. J Anat 92: 377-382.

Higgins, G.A., G.E. Hoffman, S. Wray, and J.S. Schwaber (1984) Distribution of neurotensin-immunoreactivity within baroreceptive portions of the nucleus of the tractus solitarius and the dorsal vagal nucleus of the rat. J Comp Neurol 226: 155-164.

Higgins, G.A., and J.S. Schwaber (1983) Somatostatinergic projections from the central nucleus of the amygdala to the vagal nuclei. Peptides 4: 657-662.

Hilton, S.M., and K.M. Spyer (1971) Participation of the anterior hypothalamus in the baroreceptor reflex. J. Physiol (Lond.) 218: 271-293.

Hilton, S.M., and A.W. Zbrozyna (1963) Amygdaloid region for defence reactions and its efferent pathway to the brainstem. J Physiol (Lond) 165: 160-173.

Hokfelt, T., R. Elde, O. Johansson, L. Terenius, and L. Stein (1977) The distribution of enkephalin-immunoreactive cell bodies in the rat central nervous system. Neurosci Lett 5: 25-31.

Hokfelt, T., B.J. Everitt, E. Theodorsson-Norheim, and M. Goldstein (1984) Occurrence of neurotensinlike immunoreactivity in subpopulations of hypothalamic, mesencephalic, and medullary catecholamine neurons. J Comp Neurol 222: 543-559.

Hokfelt, T., K. Fuxe, M. Goldstein, and O. Johansson (1973) Evidence for adrenaline neurons in the rat brain. Acta Physiol Scand 89: 286-288.

Hokfelt, T., K. Fuxe, M. Goldstein, and O. Johansson (1974) Immunohistochemical evidence for the existence of adrenaline neurons in the rat brain. Brain Res 66: 235-251.

Holmgren, N. (1925) Points of view concerning forebrain morphology in higher vertebrates. Acta Zool (Stockh) 6: 415-477.

Holstege, G., L. Meiners, and K. Tan (1985) Projections of the bed nucleus of the stria terminalis to the mesencephalon, pons, and medulla oblongata in the cat. Exp Brain Res 58: 379-391.

Hopkins, D.A. (1975) Amygdalotegmental projections in the rat, cat, and rhesus monkey. Neurosci Lett 1: 263-270.

Hopkins, D.A., and G. Holstege (1978) Amygdaloid projections to the mesencephalon, pons and medulla oblongata in the cat. Brain Res 78: 529-547.

Howe, P.R.C., M. Costa, J.B. Furness, and J.P. Chalmers (1980) Simultaneous demonstration of phenylethanolamine N-methyltransferase immunofluorescent and catecholamine fluorescent nerve cell bodies in the rat medulla oblongata. Neuroscience 5: 2229-2238.

Humphrey, T. (1936) The telencephalon of the bat. I. The non-cortical nuclear masses and certain pertinent fiber connections. J Comp Neurol 65: 603-711.

Humphrey, T. (1968) The development of the human amygdala during early embryonic life. J Comp Neurol 132: 135-165.

Jackson, A., and A.R. Crossman (1981) Basal ganglia and other afferent projections to the peribrachial area in the rat: A study using retrograde and anterograde transport of horseradish peroxidase. Neuroscience 6: 1537-1549.

Jacobs, B.L., and D.J. McGinty (1971) Amygdala unit activity during sleep and waking. Exp Neurol 33: 1-15.

Jeffries, J.J., and J. Levene (1985) All about schizophrenia. In M.N. Menuck and M.V. Seeman (eds): New Perspectives in Schizophrenia. New York: Macmillan Publishing Company, pp. 175-186.

Jellestad, F.K., and H.K. Bakke (1985) Passive avoidance after ibotenic acid and radio frequency lesions in the rat amygdala. Physiol Behav 34: 299-305.

Jellestad, F.K., A. Markowska, H.K. Bakke, and B. Walther (1986) Behavioral effects after ibotenic acid, 6-OHDA and electrolytic lesions in the central amygdala nucleus of the rat. Physiol Behav 37:

855-862.

Jennes, L., W.E. Stumpf, and P.W. Kalivas (1982) Neurotensin: topographical distribution in rat brain by immunohistochemistry. J Comp Neurol 210: 211-224.

Johnston, J.B. (1923) Further contributions to the study of the evolution of the forebrain. J Comp Neurol 35: 337-428.

Kaada, B.R. (1951) Somato-motor, autonomic and electrocorticographic responses to electrical stimulation of rhinencephalic and other structures in primates, cat and dog:A study of responses from the limbic, subcall osal, orbito-insular, piriform and temporal cortex, and amygdala. Acta Physiol Scand 24 S.83: 1-285.

Kaada, B.R. (1972) Stimulation and regional ablation of the amygdaloid complex with reference to functional representations. In B.F. Eleftheriou (ed): The Neurobiology of the Amygdala. New York: Plenum Press, pp. 205-281.

Kalia, M., K. Fuxe, and M. Goldstein (1985a) Rat medulla olongata.II. Dopaminergic, noradrenergic (A1 and A2) and adrenergic neurons, nerve fibers, and presumptive terminal processes. J Comp Neurol 233: 308-332.

Kalia, M., K. Fuxe, and M. Goldstein (1985b) Rat medulla oblongata. III. Adrenergic (C1 and C2) neurons, nerve fibres and presumptive terminal processes. J Comp Neurol 233: 333-349.

Kalia, M., and M.M. Mesulam (1980) Brain stem projections of sensory and motor components of the vagus complex in the cat: II. Laryngeal, tracheobronchial, pulmonary, cardiac, gastrointestinal branches. J Comp Neurol 193: 467-508.

Kalia, M.P. (1981) Localization of aortic and carotid baroreceptor and chemoreceptor primary afferents in the brain stem. In J.P. Buckley and C.M. Ferrario (eds): Central Nervous System Mechanisms in Hypertension. New York: Raven Press, pp. 9-24.

Kalia, M.P., and J.M. Sullivan (1982) Brainstem projections of sensory and motor components of the vagus nerve in rat. J Comp Neurol 211: 248-264.

Kalivas, P.W., B.A. Gau, C.B. Nemeroff, and A.J. Prange (1982) Antinoception after microinjection of neurotensin into the central amygdaloid nucleus of the rat. Brain Res 243: 279-286.

Kapp, B.S., R.C. Frysinger, M. Gallagher, and J.R. Haselton (1979) Amygdala central nucleus lesions: effect on heart rate conditioning in the rabbit. Physiol Behav 23: 1109-1117.

Kapp, B.S., M. Gallagher, R.C. Frysinger, and C.A. Applegate (1981) The amygdala, emotion, and cardiovascular conditioning. In Y. Ben-Ari (ed): The Amygdaloid Complex. Amsterdam: Elsevier/North Holland Biomedical, pp. 355-366.

Kapp, B.S., M. Gallagher, M.D. Underwood, C.L. McNall, and D. Whitehorn (1982) Cardiovascular responses elicited by electrical stimulation of the amygdala central nucleus in the rabbit. Brain Res 234: 251-262.

Kappers, C.U.A., G.C. Huber, and E.C. Crosby (1936) The submammalian telencephalon and the mammalian telencephalon exclusive of the non-olfactory cortex. In (ed): The Comparative Anatomy of the Nervous System of Vertebrates, Including Man. New York: The Macmillan Company, pp. 1240-1325.

Kawai, Y., H. Takagi, and M. Tohyama (1988) Co-localization of neurotensin- and cholecystokinin-like immunoreactivities in catecholamine neurons in the rat dorsomedial medulla. Neuroscience 24: 227-236.

Kawai, Y.S., S. Inagaki, S. Shiosaka, E. Senba, Y.-.B. Hara, M. Sakanaka, K. Takatsuki, and M. Tohyama (1982) Long descending projections from the amygdaloid somatostatin-containing cells to the lower brain stem. Brain Res 239: 603-607.

Kawai, Y.S., K. Takami, S. Shiosaka, P.C. Emson, C.J. Hillyard, S. Girgis, I. MacIntyre, and M. Tohyama (1985) Topographic localization of calcitonin gene-related peptide in the rat brain: an immunohistochemical analysis. Neuroscience 15: 747-763.

Kawakami, F., K. Fukui, H. Okamura, N. Morimoto, N. Yanaihara, T. Nakajima, and Y. Ibata (1984) Influence of ascending noradrenergic fibers on the neurotensin-like immunoreactive perikarya and evidence of direct projection of ascending neurotensin-like immunoreactive fibers in the rat central nucleus of the amygdala. Neurosci Lett 51: 231-234.

Kent, G.C. (1973) Comparative Anatomy of the Vertebrates. St. Louis: C.V. Mosby, pp. 349-365.

Khachaturan, H., M.E. Lewis, and S.J. Watson (1983) Enkephalin systems in diencephalon and brainstem of the rat. J Comp Neurol 220: 310-320.

Khachaturian, H., S.J. Watson, M.E. Lewis, D. Coy, A. Goldstein, and H. Akil (1982) Dynorphin immunocytochemistry in the rat central nervous system. Peptides 3: 941-954.

Kita, H., and Y. Oomura (1982a) An HRP study of the afferent connections to the rat medial hypothalamic region. Brain Res Bull 8: 53-62.

Kita, H., and Y. Oomura (1982b) An HRP study of the afferent connections to the rat lateral hypothalamic region. Brain Res Bull 8: 63-71.

Koepke, J.P., S. Jones, and G.F. DiBona (1987) Alpha2-adrenoceptors in amygdala control renal sympathetic nerve activity and renal function in conscious spontaneously hypertensive rats. Brain Res 404: 80-88.

Koikegami, H., S. Fuse, T. Yokoyama, T. Watanabe, and H. Watenabe (1955) Contributions to the comparative anatomy of the amygdaloid nuclei of mammals with some experiments of their destruction or stimulation. Folia Psych Neurol Japonica 8: 336-370.

Kolliker, A. (1896) Handbuch der Gewebelehre des Menschen. Leipzig: W Englemann.

Krettek, J.E., and J.L. Price (1978a) A description of the amygdaloid complex in the rat and cat with obsevations on intra-amygdaloid axonal connections. J Comp Neurol 178: 255-280.

Krettek, J.E., and J.L. Price (1978b) Amygdaloid projections to subcortical structures within the basal forebrain and brainstem in the rat and cat. J Comp Neurol 178: 225-254.

Krieger, M.S., L.C. Conrad, and D.W. Pfaff (1979a) An autoradiographic study of the effernt connections to the ventromedial nucleus of the hypothalamus. J Comp Neurol 183: 785-816.

Krieger, M.S., L.C. Conrad, and D.W. Pfaff (1979b) An autoradiographic study of the efferent projections to the ventromedial nucleus of the hypothalamus. J Comp Neurol 183: 785-816.

Kubota, Y., I. Inagaki, S. Shiosaka, H.J. Cho, K. Tateishi, E. Hashimura, T. Hamaoka, and M. Tohyama (1983) The distribution of cholecystokinin octapeptide-like structures in the lower brain stem of the rat: an immunohistochemical analysis. Neuroscience 9: 587-604.

Kunos, G., C. Farsang, and M.D. Ramirez-Gonzalez (1981) Beta-endorphin: possible involvement in the antihypertensive effect of central alpha receptor activation. Science 211: 82-85.

Kupfermann, I. (1981) Peptidergic neurons, homeostasis, and emotional behavior. In E.R. Kandel and J.H. Schwartz (eds): Principles of Neural Science. New York: Elsevier, pp. 433-449.

Lawler, J.E., R.H. Cox, J.W. Hubbard, V.P. Mitchell, G.F. Barker, W.P. Trainor, and B.J. Sanders (1985) Blood pressure and heart rate responses to environmental stress in the spontaneously hypertensive rat. Physiol Behav 34: 973-976.

Lechan, R.M., and I.M.D. Jackson (1982) Immunohistochemical localization of thyrotropin-releasing hormone in the rat hypothalamus and pituitary. Endocrinology 111: 55-65.

Lechan, R.M., M.E. Molitch, and I.M.D. Jackson (1983) Distribution of immunoreactive human growth hormone-like material and thyrotropin-releasing hormone in the rat central nervous system: evidence for the coexistance in the same neurons. Endocrinology 112: 877-884.

LeDoux, J.E. (1987) Emotion. In V.B. Mountcastle, F. Plum, and S.R. Geiger (eds): Handbook of Physiology. Section 1: The Nervous System. Bethesda: American Physiological Society, pp. 419-459.

LeDoux, J.E., A. Sakaguchi, and D.J. Reis (1984) Subcortical efferent projections of the medial geniculate nucleus mediate emotional responses conditioned to acoustic stimuli. J Neurosci 4: 683-698.

Lee, H.S., and A.I. Basbaum (1984) Immunoreactive pro-enkephalin and pro-dynorphin products are differentially distributed within the nucleus of the solitary tract of the rat. J Comp Neurol 230: 614-619.

Lind, R.W., and L.W. Swanson (1984) Evidence for corticotropin releasing factor and leu-enkephalin in the neural projection from the lateral parabrachial nucleus to the median preoptic nucleus: a retrograde transport, immunohistochemical double-labeling study in the rat. Brain Res 321: 217-224.

Lind, R.W., L.W. Swanson, and D. Ganten (1984) Organization of angiotensin II immunoreactive cells and fibers in the rat central nervous system. Neuroendocrinology 40: 2-24.

Lind, R.W., G.W. VanHoesen, and A.K. Johnson (1982) An HRP study of the connections of the subfornical organ of the rat. J Comp Neurol 210: 265-277.

Ljungdahl, A., T. Hokfelt, and G. Nilsson (1978) Distribution of substance P-like immunoreactivity in the central nervous system rat-I. Cell bodies and nerve terminals. Neuroscience 3: 861-943.

Loren, I., R. Alumets, R. Hakanson, and F. Sundler (1979) Distribution of gastrin and CCK-like peptides in rat brain. Histochemistry 59: 249-257.

Luiten, P.G.M., and P. Room (1980) Interrelations between lateral, dordomedial and ventromedial hyothalamic nuclei in the rat. An HRP study. Brain Res 190: 321-332.

Luiten, P.G.M., G.J. TerHorst, and A.B. Steffens (1987) The hypothalamus, intrinsic connections and outflow pathways to the endocrine system in relation to the control of feeding and metabolism. Prog Neurobiol 28: 1-54.

Luskin, M.B., and J.L. Price (1983) The topographic organization of associational fibers of the olfactory system in tha rat, including centrifugal fibers to the olfactory bulb. J Comp Neurol 216: 264-291.

MacLean, P.D., and J.M.R. Delgado (1953) Electrical and chemical stimulation of forntotemporal portion of limbic system in the waking animal. Electroencephalog Clin Neurophysio 5: 91-100.

Mantyh, P.W., and S.P. Hunt (1984) Neuropeptides are present in projection neurones at all levels in visceral and taste pathways: from periphery to sensory cortex. Brain Res 299: 297-311.

McAllen, R.M., and K.M. Spyer (1975) The origin of cardiac vagal efferent neurones in the medulla of the cat. J Physiol (Lond) 244: 83-83P.

McAllen, R.M., and K.M. Spyer (1976) The location of cardiac vagal preganglionic motorneurones in the medulla of the cat. J Physiol (Lond) 258: 187-204.

McAllen, R.M., and K.M. Spyer (1978) Two types of vagal preganglionic motorneurones projecting to the heart and lungs. J Physiol (Lond) 282: 353-364.

McDonald, A.J. (1982) Cytoarchitecture of the central amygdaloid nucleus of the rat. J Comp Neurol 208: 401-418.

McDonald, A.J. (1983) Neurons of the bed nucleus of the stria terminalis: A Golgi study in the rat. Brain Res Bull 10: 111-120.

McEwen, B.S., E.R. DeKloet, and W. Rostene (1986) Adrenal steriod receptors and actions in the nervous system. Physiol Rev 66: 1121-1179.

Mehler, W.R. (1980) Subcortical afferent connections of the amygdala in the monkey. J Comp Neurol 190: 733-762.

Merchenthaler, I., S. Vigh, P. Petrusz, and A.V. Schally (1982) Immunocytochemical localization of corticotropin-releasing factor (CRF) in the rat brain. Am J Anat 165: 385-396.

Micco, D.J. (1974) Complex behaviors elicited by stimulation of the dorsal pontine tegmentum. Brain Res 75: 172-176.

Millhouse, O.E., and J. DeOlmos (1983) Neuronal configurations in the lateral and basolateral amygdala. Neuroscience 10: 1269-1300.

Milner, T.A., T.H. Joh, R.J. Miller, and V.M. Pickel (1984) Substance P, enkephalin, and catecholamine-synthesizing enzymes: light microscopic localizations compared with autoradiographic label in solitary efferents to the rat parabrachial region. J Comp Neurol 226: 434-447.

Milner, T.A., and V.M. Pickel (1986) Ultrastructural localization and afferent sources of substance P in the rat parabrachial region. Neuroscience 17: 687-707.

Miselis, R.R. (1981) The efferent projections of the subfornical organ of the rat: a circumventricular organ within a neural network subserving water balance. Brain Res 230: 1-23.

Mitchell, R.A., and A.J. Berger (1981) Neural regulation of respiration. In A.L. Bianchi and M. Denavit-Saubie (eds): Neurogenesis of Central Respiratory Rhythm. Lancaster: MTP Press Ltd., pp. 191-197.

Miura, M., and K. Takayama (1986) The functional subdivisions of the nucleus tractus solitarii of the cat in relation to the carotid sinus nerve reflex. J Auton Nerv Syst 15: 79-92.

Mizuno, N., O. Takahashi, T. Satoda, and R. Matsushima (1985) Amygdalospinal projections in the macaque monkey. Neurosci Lett 53: 327-330.

Moga, M.M., and T.S. Gray (1985) Evidence for corticotropin-releasing factor, neurotensin, and somatostatin in the neural pathway from the central nucleus of the amygdala to the parabrachial nucleus. J Comp Neurol 241: 275-284.

Moga, M.M., K.M. Hurley-Gius, D.F. Cechetto, T.S. Gray, and C.B. Saper (1986) Distribution of forebrain afferents to the parabrachial nucleus in the rat. Soc Neurosci Abstr 12: 1054.

Moga, M.M., C.B. Saper, and T.S. Gray (1989) The bed nucleus of the stria terminalis: cytoarchitecture, immunohistochemistry an projection to the parabrachial nucleus in the rat. J Comp Neurol : In press.

Mogenson, G.J., and F.R. Calaresu (1973) Cardiovascular responses to electrical stimulation of the amygdala in the rat. Exp Neurol 39: 166-180.

Mohring, J., J. Schoun, J. Kintz, and R. McNeill (1980) Decreased vasopressin content in brainstem of rats with spontaneous hypertension. Naunyn-Schmiedeberg's Arch Pharmacol 315: 83-84.

Moore, S.D., and P.G. Guyenet (1983) An electrophysiological study of the forebrain projection of nucleus commissuralis: preliminary identification of presumed A2 catecholaminergic neurons. Brain Res 263: 211-222.

Morishima, Y., H. Takagi, F. Akai, M. Tohyama, P.C. Emson, C.J. Hillyard, S.I. Girgis, and I. MacIntyre (1985) Light and electron microscopic studies of calcitonin gene-realted peptide-like immunoreactive neurons and axon terminals of the nucleus of the tractus solitarius of the rat. Brain Res 344: 191-195.

Morley, J.E., A.S. Levine, G.K. Yim, and M.T. Lowy (1983) Opioid modulation of appetite. Neurosci Behav Rev 7: 281-305.

Morrell, J.L., L.M. Greenberg, and D.W. Pfaff (1981) Hypothalamic, other diencephalic, and telencephalic neurons that project to the dorsal midbrain. J Comp Neurol 201: 589-620.

Morris, M., J.A. Wren, and D.A. Sundberg (1981) Central neural peptides and catecholamines in spontaneous and DOCA salt hypertension. Peptides 2: 207-211.

Mraovitch, S., M. Kumada, and D.J. Reis (1982) Role of the nucleus parabrachialis in cardiovascular regulation in the cat. Brain Res 232: 57-75.

Murakami, S., H. Okamura, G. Pelletier, and Y. Ibata (1989) Differential colocalization of neuropeptide Y- and methionine-enkephalin-arg6-gly7-leu8-like immunoreactivity in catecholaminergic neurons in the rat brain stem. J Comp Neurol 281: 532-544.

Nachman, M., and J.H. Ashe (1974) Effects of basolateral amygdala lesions on neophobia, learned taste aversions, and sodium appetite in rats. J Comp Physiol Psychol 4: 622-643.

Nitecka, L., L. Amerski, and C. Narkiewicz (1981) Intraamygdaloid connections in the rat studied by the horseradish peroxidase method. Neurosci Lett 26: 1-4.

Norgren, R. (1974) Gustatory afferents to ventral forebrain. Brain Res 81: 285-295.

Norgren, R. (1976) Taste pathways to hypothalamus and amygdala. J Comp Neurol 166: 17-30.

Norgren, R. (1978) Projections from the nucleus of the solitary tract in the rat. Neuroscience 3: 207-218.

Norgren, R., and H.J. Grill (1976) Efferent distribution from the cortical gustatory area in rats. Soc Neurosci Abstr 6: 124.

Norgren, R., and C.M. Leonard (1973) Ascending central gustatory pathways. J Comp Neurol 207: 157-176.

Norgren, R., and C. Pfaffman (1975) The pontine taste area in the rat. Brain Res 91: 99-117.

Nosaka, S., and S.C. Wang (1972) Carotid sinus baroreceptor function in the spontaneously hypertensive rat. Am J Physiol 222: 1079-1094.

O'Donohue, T.L., R.L. Miller, and D.M. Jacobowitz (1979) Identification, characterization and stereotaxic mapping of intraneuronal alpha-melanocyte stimulating hormone-like immunoreactive peptides in discrete regions of the rat brain. Brain Res 176: 101-123.

Ohman, L.E., and A.K. Johnson (1986) Lesions in lateral parabrachial nucleus enhance drinking to angiotensin II and isoproternol. Am J Physiol (Regulatory Integrative Comp Physiol) 251: R504-R509.

Ohta, M. (1984) Amygdaloid and cortical facilitation or inhibition of trigeminal motorneurons in the rat. Brain Res 291: 39-48.

Olschowka, J.A., T.L. O'Donohue, G.P. Mueller, and D.M. Jacobowitz (1982) The distribution of corticotropin releasing factor-like immunoreactive neurons in rat brain. Peptides 3: 995-1015.

Onai, T., K. Takayama, and M. Miura (1987) Projections to areas of the nucleus tractus solitarii related to circulatory and respiratory responses in cats. J Auton Nerv Syst 18: 163-175.

Ottersen, O.P. (1981) Afferent connections to the amygdaloid complex of the rat with some observations in the cat. III. Afferents from the lower brain stem. J Comp Neurol 202: 335-356.

Ottersen, O.P. (1982) Connections of the amygdala of the rat. IV: Corticoamygdaloid and intraamygdaloid connections as studied with axonal transport of horseradish peroxidase. J Comp Neurol 205: 30-48.

Otterson, O.P. (1980) Afferent connections to the amygdaloid complex of the rat and cat. II. Afferents from the hypothalamus and the basal telencephalon. J Comp Neurol 194: 267-289.

Otterson, O.P., and Y. Ben-Ari (1978) Pontine and mesencephalic afferents to the central nucleus of the amygdala of the rat. Neurosci Lett 8: 329-334.

Otterson, O.P., and Y. Ben-Ari (1979) Afferent connections to the amygdaloid complex of the rat and cat. I. Projections from the thalamus. J Comp Neurol 187: 401-424.

Paintal, A.S. (1973) Vagal sensory receptors and their reflex effects. Physiol Rev 53: 159-227.

Palkovits, M., J. Epelbaum, and C. Gros (1981) Met-enkephalin concentrations in individual brain nuclei of ansa lenticularis and stria terminalis transected rats. Brain Res 216: 203-209.

Panksepp, J. (1980) Hypothalamic integration of behavior. In P.J. Morgane and J. Panksepp (eds): Handbook of the Hypothalamus: Behavioral Studies of the Hypothalamus. New York: Marcel Dekker Inc., pp. 289-431.

Panksepp, J. (1982) Toward a general psychobiological theory of emotions. The Behavioral and Brain Sciences 5: 407-467.

Papez, J.W. (1937) A proposed mechanism of emotion. Arch Neurol Psychiatry 38: 725-743.

Pascoe, J.P., and B.S. Kapp (1985) Electrophysiological characteristics of amygdaloid central nucleus neurons during Pavlovian fear conditioning in the rabbit. Behav Brain Res 16: 117-133.

Paxinos, G., and C. Watson (1986) The Rat Brain in Stereotaxic Coordinates. New York: Academic Press.

Pelletier, G., and R. LeClerc (1979) Immunohistochemical localization of adrenocorticotropin in the rat brain. Endocrinology 104: 1426-1433.

Peselow, E., B. Angrist, A. Sudilovsky, J. Corwin, J. Siekierski, F. Trent, and J. Rotrosen (1987) Double blind controlled trials of cholecystokinin octapeptide in neuroleptic-refractory schizophrenia. Psychopharm 91: 80-84.

Petty, M.A., and J.L. Reid (1977) Changes in noradrenaline concentration in the brain stem and hypothalamic nuclei during the development of renovascular hypertension. Brain Res 136: 376-380.

Pfaffman, C., R. Norgren, and H.J. Grill (1977) Sensory affect and motivation. Ann NY Acad Sci 290: 18-34.

Phelix, C., Z. Liposits, and W. Paull (1986) Distribution and interrelationship of ctecholaminergic fibres and corticotropin releasing factor (CRF) immunoreactive neurons located in the bed nucleus of the stria terminalis. Anat Rec 214: 101A.

Piekut, D.T. (1987) Interactions of immunostained ACTH1-39 fibers and CRF neurons in the paraventricular nucleus of rat hypothalamus: application of avidin-glucose to dual immunostaining procedures. J Histochem Cytochem 35: 261-265.

Pieribone, V.A., and G. Aston-Jones (1988) The iontophoretic application of Fluoro-Gold for the study of afferents to deep brain nuclei. Brain Res 475: 259-271.

Pretorius, J.K., K.D. Phelan, and W.R. Mehler (1979) Afferent connections of the amygdala in rat. Anat Rec 193: 657.

Price, J.L., and D.G. Amaral (1981) An autoradiographic study of the projections of the central nucleus of the monkey amygdala. J Neurosci 1: 1242-1259.

Price, J.L., F.T. Russchen, and D.G. Amaral (1987) The limbic region. II: The amygdaloid complex. In A. Bjorkland, T. Hokfelt, and L.W. Swanson (eds): Handbook of Chemical Neuroanatomy. Amsterdam: Elsevier Science, pp. 279-388.

Randich, A., and W. Maixner (1984) Interactions between cardiovascular and pain regulatory systems. Neurosci Behav Rev 8: 343-367.

Ray, A., P.G. Henke, and R. Sullivan (1987) The central amygdala and immobilization stress-induced gastric pathology in rats: neurotensin and dopamine. Brain Res 409: 398-402.

Redgate, E.S., and E.E. Fahringer (1973) A comparision of the pituitary adrenal activity elicited by electrical stimulation of preoptic, amygdaloid and hypothalamic sites in the rat brain. Neuroendocrinology 12: 334-343.

Reis, D.J., and N. Doba (1974) The central nervous system and neurogenic hypertension. Prog Cardiovasc Dis 17: 51-71.

Reis, D.J., T.H. Joh, M.A. Nathan, B. Renaud, D.W. Synder, and W.T. Talman (1978) Nucleus tractus solitarii: catecholaminergic innervation in normal and abnormal control of arterial pressure. In P. Meyer and H. Schmitt (eds): Nervous System and Hypertension. Paris/New York: Wiley-Flammarion, pp. 147-164.

Reis, D.J., and P.R. McHugh (1968) Hypoxia as a cause of bradycardia during amygdala stimulation in monkey. Am Physiol Soc 214: 601-610.

Reis, D.J., and M.C. Oliphant (1964) Bradycardia and tachycardia following electrical stimulation of the amygdaloid region in monkey. J Neurophysiol : 893-912.

Renaud, L.P., and D.A. Hopkins (1977) Amygdala afferents from the mediaobasal hypothalamus: an electrophysiological and neuroanatomical study in the rat. Brain Res 121: 201-213.

Ricardo, J.A., and E.T. Koh (1978) Anatomical evidence of direct projections from the nucleus of the solitary tract to the hypothalamus, amygdala, and other forebrain structures in the rat. Brain Res 153: 1-26.

Richardson, J.S., and E.K.Y. Chiu (1983) The regulation of cardiovascular functions by monoamine neurotransmitters in the brain. Intern J Neuroscience 20: 103-148.

Riley, A.L., D.A. Zellner, and H.J. Duncan (1980) The role of endorphins in animal learning and behavior. Neurosci Biobehav Rev 4: 69-76.

Riolobas, A.S., and A.I.M. Garcia (1987) Open field activity and passive avoidence responses in rats after lesion of the central amygdaloid nucleus by elctrocoagulation and ibotenic acid. Physiol Behav 39: 715-720.

Roberts, G.W., I.N. Ferrier, Y. Lee, T.J. Crow, E.C. Johnstone, D.G.C. Owens, A.J. Bacarese-Hamilton, and G. McGregor (1983) Peptides, the limbic lobe and schizophrenia. Brain Res 288: 199-211.

Roberts, G.W., P.L. Woodhams, M.G. Bryant, T.J. Crow, S.L. Bloom, and J. M. Polak (1980) VIP in the rat brain: evidence for a major pathway linking the amygdala and hypothalamus via the stria terminalis. Histochemistry 65: 103-119.

Roberts, G.W., P.L. Woodhams, J.M. Polak, and T.J. Crow (1982) Distribution of neuropeptides in the limbic system of the rat: The amygdaloid complex. Neuroscience 7: 99-131.

Rogers, R.C., and D.L. Fryman (1988) Direct connections between the central nucleus of the amygdala and the nucleus of the solitary tract: an electrophysiological study in the rat. J Auton Nerv Syst 22: 83-87.

Rokaeus, A., T. Melander, T. Hokfelt, J.M. Lundberg, K. Tatemoto, M. Carlquist, and V. Mutt (1984) A galanin-like peptide in the central nervous system and intestine of the rat. Neurosci Lett 47: 161-166.

Roldan, E., R. Alvarez-Pelaez, and F. DeMolina (1974) Electrographic study of the amygdaloid defense response. Physiol Behav 13: 779-787.

Rolls, B.J., and E.T. Rolls (1973) Effects of lesions in the basolateral amygdala on fluid intake in the rat. J Comp Physiol Psychol 83: 240-247.

Rolls, E.T., and B.J. Rolls (1973) Altered food preferences after lesions in the basolateral region of the amygdala in the rat. J Comp Physiol Psychol 83: 248-259.

Rosenfeld, M.G., J.J. Mermod, S.A. Amara, L.W. Swanson, P.E. Sawchenko, J. Rivier, W.E. Vale, and R.M. Evans (1983) Production of a novel neuropeptide encoded by the calcitonin gene via tissue-specific RNA processing. Nature 304: 129-135.

Ross, C.A., D.A. Ruggiero, T.H. Joh, D.H. Park, and D.J. Reis (1983) Adrenaline synthesizing neurons in the rostral ventrolateral medulla: a possible role in tonic vasomotor control. Brain Res 273: 356-361.

Ross, C.A., D.A. Ruggiero, D.H. Park, T.H. Joh, A.F. Sved, J. Fernandez-Pardal, J.M. Saaverdra, and D.J. Reis (1983) Tonic vasomotor control by the rostral ventrolateral medulla: Effect of electrical or chemical stimulation of the area containing C1 adrenaline neurons on arterial pressure, heart rate, and plasma catecholamines and vasopressin. J Neurosci 4: 474-494.

Ruggiero, D.A., C.A. Ross, M. Anwar, D.H. Park, T.H. Joh, and D.J. Reis (1985) Distribution of neurons containing phenylethanolamine N-methyltransferase in medulla and hypothalamus of rat. J Comp Neurol 239: 127-154.

Russchen, F.T. (1982) Amygdalaopetal connections in the cat: II. Subcortical afferent connections. A study with retrograde tracing techniques. J Comp Neurol 207: 157-176.

Russchen, F.T., and A.H.M. Lohman (1979) Afferent connections of the amygdala in the cat. Acta Anat Iugoslavica Sup. 9: 57-63.

Russchen, F.T., and J.L. Price (1984) Amygdalaostriatal projections in the rat. Topographical organization and fiber morphology shown using the lectin PHA-L as an anterograde tracer. Neurosci Lett 47: 15-22.

Saavedra, J.M. (1981) Central biogenic amines and neuropeptides in genetic hypertension. In J.P. Buckly and C.M. Ferrario (eds): Central Nervous System Mechanisms in Hypertension. New York: Raven Press, pp. 129-139.

Saavedra, J.M., M. Palkovits, M.J. Brownstein, and J. Axelrod (1974) Localisation of phenylethanolamine N-methyl transferase in the rat brain nuclei. Nature 248: 695-696.

Saper, C.B. (1982) Convergence of autonomic and limbic connections in the insular cortex of the rat. J Comp Neurol 210: 163-173.

Saper, C.B. (1984) Organization of cerebral cortical afferent systems in the rat. II. Magnocellular basal nucleus. J Comp Neurol 222: 313-342.

Saper, C.B., and D. Levisohn (1983) Afferent connections of the median preoptic nucleus in the rat: anatomical evidence for a cardiovascular integrative mechanism in the anterolateral third ventricle (AV3V) region. Brain Res 288: 21-31.

Saper, C.B., and A.D. Lowey (1980) Efferent connections of the parabrachial nucleus in the rat. Brain Res 197: 291-317.

Saper, C.B., L.W. Swanson, and W.M. Cowan (1976) The efferent connections of the ventromedial nucleus of the hypothalamus of the rat. J Comp Neurol 169: 409-442.

Sar, M., W.E. Stumpf, R.J. Miller, K.J. Chang, and P. Cuatrecasas (1978) Immunohistochemical localization of enkephalin in rat brain and spinal cord. J Comp Neurol 182: 17-38.

Sarter, M., and H.J. Markowitsch (1985) Involvement of the amygdala in learning amd memory: a critical review, with emphasis on anatomical relations. Behav Neurosci 99: 342-380.

Sawchenko, P.E., and L.W. Swanson (1981) A method for tracing biochemically defined pathways in the central nervous system using combined fluorescence retrograde transport and immunohistochemical techniques. Brain Res 210: 31-51.

Sawchenko, P.E., and L.W. Swanson (1982) The organization of noradrenergic pathways from the brainstem to the paraventricular and supraoptic nucleus in the rat. Brain Res Rev 4: 275-325.

Scalia, F., and S.S. Winans (1975) The differential projections of the olfactory bulb and accessory olfactory bulb in mammmals. J Comp Neurol 1: 31-56.

Schlor, K.H., H. Stumpf, and G. Stock (1984) Baroreceptor reflex during arousal induced by electrical stimulation of the amygdala or by natural stimuli. J Auton Nerv Syst 10: 157-165.

Schmitt, H., and M. Laubie (1980) Destruction of the nucleus tractus solitarii in dogs: acute effects on blood pressure and haemodynamics, chronic effects on blood pressure. Importance of the nucleus for the effects of drugs. In D.S. Davies and J.L. Reid (eds): Central Action of Drugs in Blood pressure Regulation. Baltimore: Univ. Park Press, pp. 173-201.

Schmued, L.C., and J.H. Fallon (1986) Fluoro-Gold: a new fluorescent tracer with numerous unique properties. Brain Res 377: 147-154.

Schwaber, J.S. (1986) Neuroanatomical substrates of cardiovascular and emotional - autonomic regulation. In A. Magro, W. Osswald, D. Reis, and P. Vanhoutte (eds): Central and Peripheral Mechanisms of Cardiovascular Regulation. New York: Plenum Publishing Corporation, pp. 353-384.

Schwaber, J.S., B.S. Kapp, and G. Higgins (1980) The origin and extent of direct amygdala projections to the region of the dorsal motor nucleus of the vagus and nucleus of the solitary tract. Neurosci Lett 20: 11-14.

Schwaber, J.S., B.S. Kapp, G.A. Higgins, and P.R. Rapp (1982) Amygdaloid and basal forebrain direct connections with the nucleus of the solitary tract and the dorsal motor nucleus. J Neurosci 2: 1424-1438.

Schwaber, J.S., C. Sternini, N.C. Brecha, W.T. Rogers, and J.P. Card (1988) Neurons containing calcitonin gene-related peptide in the parabrachial nucleus project to the central nucleus of the amygdala. J Comp Neurol 270: 416-426.

Schwaber, J.S., S. Wray, G.A. Higgins, and G.E. Hoffman (1981) The central nucleus of the amygdala: descending autonomic connections and neuropeptide systems in the rat. Anat Rec 199: 228A.

Schwartz, G.E. (1977) Psychosomatic disorders and biofeedback: A psychobiological model of disregulation. In J.D. Maser and M.E.P. Seligman (eds): Psychopathology:Experimental Models. San Francisco: W. H. Freeman.

Schwartzbaum, J.S. (1983) Electrophysiology of taste-mediated functions in parabrachial nuclei of behaving rabbit. Brain Res Bull 11: 61-89.

Seeman, P. (1985) Brain dopamine receptors in schizophrenia. In M.N. Menuck and M.V. Seeman (eds): New Perspectives in Schizophrenia. New York: Macmillan Publishing Company, pp. 71-79.

Shapiro, R.E., and R.R. Miselis (1985) The central organization of the vagus nerve innervating the stomach of the rat. J Comp Neurol 238: 473-488.

Shimada, S., S. Shiosaka, P.C. Emson, C.J. Hillyard, S. Girgis, I. MacIntyre, and M. Tohyama (1985) Calcitonin gene-related peptidergic projection from the parabrachial area to the forebrain and diencephalon in the rat: an immunohistochemical analysis. Neuroscience 16: 607-616.

Shioska, S.M., H. Tohyama, Y. Takagi, Y. Takahashi, T. Saitoh, H. Sakumoto, T. Nakagawa, and N. Shimizu (1980) Ascending and descending components of the median forebrain bundle in the rat as demonstrated by the horseradish peroxidase-blue reaction. Exp Brain Res 39: 377-388.

Sieck, G.C., and R.M. Harper (1980) Discharge of neurons in the parabrachial pons related to the cardiac cycle: changes in different sleep-waking states. Brain Res 199: 385-399.

Silverman, A.J., D.L. Hoffman, and E.A. Zimmerman (1981) The descending afferent connections of the paraventricular nucleus of the hypothalmus (PVN). Brain Res Bull 6: 47-61.

Sims, K.B., D.L. Hoffman, S.I. Said, and E.A. Zimmerman (1980) Vasoactive intestinal polypeptide (VIP) in mouse and rat brain: an immunocytochemical study. Brain Res 186: 165-183.

Skirboll, L., T. Hokfelt, G. Norell, O. Phillipson, H.G.J.M. Kuypers, M. Bentivoglio, C.E. Catsman-Berrevoets, and T.J. Visser (1984) A method for specific transmitter identification of retrogradely labeled neurons: immunofluorescence combined with fluorescence tracing. Brain Res Rev 8: 99-127.

Skofitsch, G., and D.M. Jacobowitz (1985) Calcitonin gene-related peptide: detailed immunohistochemical distribution in the central nervous system. Peptides 6: 721-745.

Smith, B.S., and O.E. Millhouse (1985) The connections between the basolateral and central amygdaloid nuclei. Neurosci Lett 56: 307-309.

Smith, O.A., and J.L. DeVito (1984) Central neural integration for the control of autonomic responses associated with emotion. Ann Rev Neurosci 6: 269-325.

Sofroniew, M.V. (1983) Direct reciprocal connections between the bed nucleus of the stria terminalis and dorsomedial medulla oblongata: evidence from immunohistochemical detection of tracer proteins. J Comp Neurol 213: 399-405.

Squire, L.R. (1987) Memory: neural organization and behavior. In V.B. Mountcastle, F. Plum, and S.R. Geiger (eds): Handbook of Physiology. Section 1: The Nervous System. Bethesda: American Physiological Society, pp. 295-371.

Standaert, D.G., P. Needleman, and C.B. Saper (1986) Organization of atriopeptin-like immunoreactive neurons in the central nervous system of the rat. J Comp Neurol 253: 315-341.

Stein, L., and C.D. Wise (1969) Release of norepinephrine from hypothalamus and amygdala by rewarding forebrain bundle stimulation and amphetamine. J Comp Physiol Psychol 67: 189-198.

Stock, G., K.H. Schlor, H. Heidt, and J. Buss (1978) Psychomotor behaviour and cardiovascular patterns during stimulation of the amygdala. Eur J Physiol 376: 177-184.

Swanson, L.W. (1976) An autoradiographic study of the efferent connections of the preoptic region in the rat. J Comp Neurol 167: 227-256.

Swanson, L.W., and W.M. Cowan (1979) The connections of the septal region in the rat. J Comp Neurol 186: 621-656.

Swanson, L.W., and B.K. Hartman (1976) The central adrenergic system. An immunofluorescence study of the location of cell bodies and their efferent connections in the rat dopamine-B-hydroxylase as a marker. J Comp Neurol 163: 467-506.

Swanson, L.W., and R.W. Lind (1986) Neural projections subserving the initiation of a specific motivated behavior in the rat: new projections from the subfornical organ. Brain Res 379: 399-403.

Swanson, L.W., and G.J. Mogenson (1981) Neural mechanisms for the functional coupling of autonomic, endocrine and somatomotor responses in adaptive behavior. Brain Res Rev 3: 1-34.

Swanson, L.W., G.J. Mogenson, C.R. Gerfen, and P. Robinson (1984) Evidence for a projection from the lateral preoptic area and substantia innominata to the "mesencephalic locomotor region" in the

rat. Brain Res 295: 161-178.

Swanson, L.W., P.E. Sawchenko, J. River, and W. Vale (1983) Organization of ovine corticotropin-releasing factor immunoreactive cells and fibers in the rat brain: an immunohistochemical study. Endocrinology 36: 165-186.

Swanson, L.W., and L.G. Sharpe (1973) Centrally induced drinking: comparision of angiotensin II- and carbachol-sensitive sites in rats. Am J Physiol 225: 566-573.

Switzer, R.C., J.D.e. Olmos, and L. Heimer (1985) Olfactory system. In G. Paxinos (ed): The Rat Nervous System: Forebrain and Midbrain. Orlando: Academic Press, pp. 1-36.

Tanaka, J., and K. Seto (1988) Neurons in the nucleus of the solitary tract with ascending projections to the subfornical organ in the rat. Neurosci Lett 89: 152-155.

Thames, M.D. (1984) Arterial baroreflexes in hypertension. In G.P. Guthrie and T.A. Kotchen (eds): Hypertension and the Brain. Mt. Kisco: Futura Pub. Co., pp. 49-62.

Thames, M.D., C.L. Eastman, and M.L. Marcus (1981) Baroreflex control of heart interval in conscious renal hypertensive dogs. Amer J Physiol 241: H332-H336.

Thompson, R.L., and M.D. Cassell (1989) Differential distribution and non-collateralization of central amygdaloid neurons projecting to different medullary regions. Neurosci Lett 97: 245-251.

Titus, J.A., R. Haugland, S.O. Sharrow, and D.M. Segal (1982) Texas Red, a hydrophilic, red emitting fluroprobe for use with fluorescein in dual parameter flow microfluorometric and fluorescence microscopic studies. J Immuno Meth 50: 193-204.

Tucker, D.C., C.B. Saper, D.A. Ruggiero, and D.J. Reis (1987) Organization of central adrenergic pathways: I. Relationships of ventrolateral medullary projections to the hypothalamus and spinal cord. J Comp Neurol 259: 591-603.

Turner, B.H., and J. Zimmer (1984) The architecture and some of the interconnections of the rat's amygdala and lateral periallocortex. J Comp Neurol 227: 540-557.

Turton, W.E., J. Ciriello, and F.R. Calaresu (1986) Changes in forebrain hexokinase activity after aortic baroreceptor denervation. Am J Physiol (Reg Integrative Comp Physiol) 251: R274-R281.

Tyrer, P., and A. MacKay (1986) Schizophrenia: no longer a functional psychosis. Trends in Neurosci 9: 537-538.

Uchida, Y. (1950) A contribution to the comparitive anatomy of the amygdaloid nuclei in mammals, especially in rodents. Part I: Rat and mouse. Folio Psychiat Neurol Jap 4: 91-107.

Uhl, G.R., R.R. Goodman, and S.H. Snyder (1979) Neurotensin-containing cell bodies, fibers and nerve terminals in the brain stem of the rat: immunohistochemical mapping. Brain Res 167: 77-91.

Uhl, G.R., M.J. Kuhar, and S.H. Snyder (1978) Enkephalin containing pathway: amygdalaloid efferents in the stria terminalis. Brain Res 149: 223-228.

Uhl, G.R., and S.H. Snyder (1979) Neurotensin: a neuronal pathway projecting from the amygdala through the stria terminalis. Brain Res 161: 522-526.

Unger, J.W., T.H. McNeill, L.L. Lapham, and R.W. Hamill (1988) Neuropeptides and neuropathology in the amygdala in Alzheimer's disease: relationship between somatostatin, neuropeptide Y and

subregional distribution of neuritic plaques. Brain Res 452: 293-302.

Van der Kooy, D., L.Y. Koda, J.F. McGinty, C.R. Gerfen, and F.E. Bloom (1984) The organization of projections from the cortex, amygdala, and hypothalamus to the nucleus of the solitary tract in rat. J Comp Neurol 224: 1-24.

Van Praag, H.M., and W.M.A. Vrhoeven (1981) Endorphin research in schizophrenic psychoses. Compr Psychiatry 22: 135-146.

Vanderhaeghen, J.J., F. Lotstra, J. DeMey, and C. Gillies (1980) Immunohistochemical localization of cholecystokinin- and gastrin-like peptides in the brain and hypophysis of the rat. Proc Nat Acad Sci (USA) 77: 1190-1194.

Veening, J., L.W. Swanson, and P.E. Sawchenko (1984) The organization of projections from the central nucleus of the amygdala to brainstem sites involved in central autonomic regulation: a combined retrograde-transport immunohistochemical study. Brain Res 303: 337-357.

Veening, J.G. (1978) Subcortical afferents of the amygdaloid complex in the rat: an HRP study. Neurosci Lett 8: 197-202.

Veening, J.G., L.W. Swanson, W.M. Cowan, R. Nieuwenhuys, and L.M. Geeraedts (1982) The medial forebrain bundle of the rat. II. An autoradiographic study of the major descending and ascending components. J Comp Neurol 206: 82-108.

Versteeg, D.H.G., M. Palkovits, J. Van der Gugen, H.L.J.M. Wijnen, G.W.M. Smeets, and W. DeJong (1976) Catecholamine content of individual brain regions of spontaneously hypertensive rats (SH-rats). Brain Res 112: 429-434.

Volsch, M. (1906) Zur vergleichenden Anatomie des Manddelkerns und seiner Nachbargebilde. I Teil. Arch Mikrosk Anat Entwicklungsmech 68: 573-683.

Volsch, M. (1910) Zur vergleichenden Anatomie des mandelkerns und seiner Marchbargebilde. II Teil. Arch Mikrosk Anat Entwicklungsmech 76: 373-523.

Voshart, K., and D. Van der Kooy (1981) The organization of efferent projections of the parabrachial nucleus to the forebrain in the rat: a retrograde fluorescent double-labeling study. Brain Res 212: 271-286.

Wallace, D.M., D.J. Magnuson, and T.S. Gray (1989) The amygdalo-brainstem pathway: selective innervation of dopaminergic, noradrenergic and adrenergic cells in the rat. Neurosci Lett 97: 252-258.

Weller, K.L., and D.A. Smith (1982) Afferent connections to the bed nucleus of the stria terminalis. Brain Res 232: 255-270.

Werka, T., J. Skar, and H. Ursin (1978) Exploration and avoidance in rats with lesions in amygdala and piriform cortex. J Comp Physiol Psych 92: 672-681.

Wijnen, H.J.L.M., M. Palkovits, W. DeJong, and D.H.G. Versteeg (1978) Elevated adrenaline content in nuclei of the medulla oblongata and hypothalamus during the development of spontaneous hypertension. Brain Res 157: 191-195.

Williams, R.G., and G.J. Dockray (1983) Distribution of enkephalin-related peptides in rat brain: immunohistochemical studies using antisera to met-enkephalin and met-enkephalin arg-6-phe-7. Neuroscience 9: 563-586.

Witter, M.P., and H.J. Groenewegen (1986) The connections of the parrahippocampal cortex in the cat. IV. Subcortical efferents. J Comp Neurol 252: 51-77.

Woodhams, P.L., G.W. Roberts, J.M. Polak, and T.J. Crow (1983) Distribution of neuropeptides in the limbic system of the rat: The bed nucleus of the stria terminalis, septum and preoptic area. Neuroscience 8: 677-703.

Wouterlood, F.G., and H.J. Groenewegen (1985) Neuroanatomical tracing by use of Phaseolus vulgaris-leucoagglutinin (PHA-L): electron microscopy of PHA-L-filled neuronal somata, dendrites, axons and axon terminals. Brain Res 326: 188-191.

Wray, S., and G.E. Hoffman (1983) Organization and interrelationship of neuropeptides in the central amygdaloid nucleus of the rat. Peptides 4: 525-541.

Yamamoto, T., S. Azuma, and Y. Kawamura (1980) The pontine taste are in the rabbit. Neurosci Lett 16: 5-9.

Yamamoto, T., S. Azuma, and Y. Kawamura (1984) Functional relations between the cortical gustatory area and the amygdala: electrophysiological and behavioral studies in rats. Exp Brain Res 56: 23-31.

Yamazoe, M., S. Shiosaka, P.C. Emson, and M. Tohyama (1985) Distribution of neuropeptide y in the lower brainstem: an immunohistochemical analysis. Brain Res 335: 109-120.

Yamono, M., C.J. Hillyard, S. Girgis, I. MacIntyre, P.C. Emson, and M. Tohyama (1988) Presence of a substance P-like immunoreactive neurone system from the parabrachial area to the central amygdaloid nucleus of the rat with refernce to coexistence with calcitonin gene-related

peptide. Brain Res 451: 179-188.

Yang, H.-.Y.T., and E. Costa (1982) Neuronal localization of the bombesin-like immunoreactivity in the central nervous system of the rat. Regul Peptides 4: 275-283.

Young, M.W. (1936) The nuclear pattern and fiber connections of the noncortical centers of the telencephalon in the rabbit (Lepus cuniculus). J Comp Neurol 65: 295-401.

Zaborsky, L., C. Leranth, and L. Heimer (1984) Ultrastructural evidence of amygdalofugal axons terminating on cholinergic cells of the rostral forebrain. Neurosci Lett 52: 219-225.

Zaborszky, L., G.F. Alheid, M.C. Beinfeld, L.E. Eiden, L. Heimer, and M. Palkovits (1985) Cholecystokinin innervation of the ventral striatum: A morphological and radioimmunological study. Neuroscience 14: 427-453.

Zaborszky, L., C. Leranth, and L. Heimer (1984) Ultrastructural evidence of amygdalofugal axons terminating on cholinergic cells of the rostral forebrain. Neurosci lett 52: 219-225.

Zardetto-Smith, A.M., and T.S. Gray (1986a) Peptidergic projections from the nucleus tractus solitarius to the central nucleus of the amygdala in the rat. Anat Rec 214: 150A.

Zardetto-Smith, A.M., and T.S. Gray (1986b) Peptidergic efferents from the parabrachial nucleus to the central nucleus of the amygdala in the rat. Soc Neurosci Abstr 12: 1054.

Zardetto-Smith, A.M., and T.S. Gray (1987) Efferent projections of the nucleus of the solitary tract to the amygdala, bed nucleus of the stria terminalis and subfornical organ in the rat examined using the PHA-L anterograde tracing method. Soc Neurosci Abstr 13: 386.

Zardetto-Smith, A.M., and T.S. Gray (1988) Catecholaminergic cells of the ventrolateral medulla and nucleus of the solitary tract innervate the central nucleus of the amygdala in the rat. Soc Neurosci Abstr 14: 1318.

Zardetto-Smith, A.M., D.J. Magnuson, and T.S. Gray (1989) Efferent projections from the bed nucleus of the stria terminalis to the nucleus of the solitary tract and ventrolateral medulla in the rat. Soc Neurosci Abstr : Submitted.

Zardetto-Smith, A.M., S.J. Watson, and T.S. Gray (1984) The distribution of dynorphin and proenkephalin (BAM-22-P) immunoreactivity within the central nucleus of the amygdala. Soc Neurosci Abstr 10: 410.

Zawoiski, E.J. (1967) Gastric secretory response of the unrestrained cat following electrical stimulation of the hypothalamus, amygdala and basal ganglia. Exp Neurol 16: 128-139.

Zech, M., G.W. Roberts, B. Bogerts, T.J. Crow, and J.M. Polak (1986) Neuropeptides in the amygdala of controls, schizophrenics and patients suffering from Huntington's chorea: an immunohistochemical study. Acta Neuropathol (Berl) 71: 259-266.

Zhang, J.-.X., R.M. Harper, and H. Ni (1986) Cryogenic blockade of the central nucleus of the amygdala attenuates aversely conditioned blood pressure and respiratory responses. Brain Res 386: 136-145.

APPROVAL SHEET

The dissertation submitted by Andrea M. Zardetto-Smith has been read and approved by the following committee:

Dr. Thackery S. Gray, Director
Associate Professor, Anatomy, Loyola

Dr. Anthony J. Castro
Professor, Anatomy, Loyola

Dr. Edward J. Neafsey
Associate Professor, Anatomy, Loyola

Dr. Robert D. Wurster
Professor, Physiology, Loyola

Dr. Clifford B. Saper
Professor, Pharmacological and Physiological Sciences
University of Chicago
Chicago, Illinois

The final copies have been examined by the director of the dissertation and the signature which appears below verifies the fact that any necessary changes have been incorporated and the dissertation is now given final approval by the committee with reference to content and form.

The dissertation is therefore accepted in partial fulfillment of the requirements for the degree of Doctor of Philosophy.

6-23-89
Date

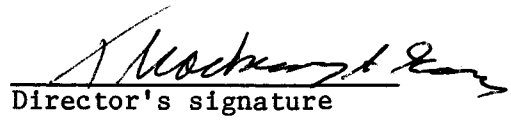
Director's signature